Preparation of new rhodium and cobalt complexes as catalysts for hydroformylation studies

by

Arno Neveling

Dissertation for the degree

of

DOCTOR in PHILOSOPHY

at the

UNIVERSITY of STELLENBOSCH.

Promoter: Prof. H.G. Raubenheimer

December 2003

Declaration

I, the undersigned, hereby declare that the work contained in this dissertation is my own original work and that I have not previously in its entirety or in part submitted it at any university for a degree.

Signature:

Date:

Abstract

Organometallic chemistry offers the opportunity for the preparation of tailor-made, active and selective complexes for specific catalytic purposes. Ionic liquids present novel, benign reaction media both for a cleaner environment and more efficient product separation. In this dissertation new compound preparation and characteristics related to hydroformylation as well as the effectivity of the hydroformylation process itself, were investigated.

Certain cobalt and rhodium complexes were targeted. The search for a compound that could be immobilised in chosen ionic liquids prompted the use of various heterocyclic ligands that are related to the cations of the ionic liquids. The recent successes of *N*-heterocyclic carbene ligands in homogeneously catalysed processes, made this class of ligands one obvious choice for this study.

The pursuit of stable cobalt carbene complexes of the type $[Co(CO)_3L]_2$ (L = *N*-heterocyclic carbene), analogous to well-known phosphine complexes, were unsuccessful due to the instability of the complexes prepared from free carbenes. Attempts to prepare cobalt carbene complexes utilising consecutive transmetallation and alkylation only yielded classical cobalt(II) coordination compounds such as $[CoBr_2(\overline{NCBrSCHCH})_2]$, **37,** $[CoBr_2(OPPh_3)_2]$, **38**, and $[Co(SO_3CF_3)_2(OPPh_3)_2(\overline{NCHSCHCH})_2]$, **39**, by unknown mechanisms.

N-heterocyclic carbenes, heterocyclic thiones, imines and a phosphine ligand that contains five-membered azoles were used for further diversification of known rhodium(I) compounds. Thirty-one new rhodium(I) complexes were prepared from the commercially available precursor rhodium(I) compounds, $[RhCl(cod)]_2$ and $[RhCl(CO)_2]_2$. Both the ^1H and ^{13}C NMR spectra of the carbene complexes, *e.g.* chloro(η^4-1,5-cyclooctadiene)(1,3-diisopropyl-4,5-dimethyl-2,3-dihydro-1*H*-imidazol-2-ylidene)rhodium(I), **1**, chloro(η^4-1,5-cyclooctadiene)(1-butyl-3-methyl-2,3-dihydro-1*H*-imidazol-2-ylidene)rhodium(I), **3**, chloro(dicarbonyl)(1,3-diisopropyl-4,5-dimethyl-2,3-dihydro-1*H*-imidazol-2-ylidene)rhodium(I), **6**, and chloro(carbonyl)-*trans*-(triphenylphosphine)(1,3-diisopropyl-4,5-dimethyl-2,3-dihydro-1*H*-imidazol-2-ylidene)rhodium(I), **11**, clearly indicated the existence of two different molecular species of all these products in solution. All available spectroscopic evidence suggested that

rotation around the Rh-$C_{carbene}$ bonds is restricted leading to geometric isomerisation. The existence of these pairs indicate that each complex has a completely different structure in solution than in the solid state.

Certain thione complexes, chloro(η^4-1,5-cyclooctadiene)(1,3-diisopropyl-4,5-dimethyl-2,3-dihydro-1*H*-imidazol-2-thione)rhodium(I), **16**, chloro(η^4-1,5-cyclooctadiene)(1,3,4,5-tetramethyl-2,3-dihydro-1*H*-imidazol-2-thione)rhodium(I), **17**, and chloro(carbonyl)-*trans*-bis(1,3-diisopropyl-4,5-dimethyl-2,3-dihydro-1*H*-imidazol-2-thione)rhodium(I), **24**, also appeared as isomers at room temperature, probably due to slow coordination exchange on the S donor atom that contains two lone pairs.

Crystal structure determinations have been performed on five different complexes, [(η^4-1,5-cyclooctadiene)-*cis*-(1,1′-propylene-3,3′-dimethyl-2,3,2′,3′-tetrahydro-1,1′-*H*-diimidazol-2,2′-diylidene)rhodium(I)][hexafluorophosphate], **4**, *cis*-[(η^4-1,5-cyclooctadiene)bis(1,3,4,5-tetramethyl-2,3-dihydro-1*H*-imidazol-2-ylidene)rhodium(I)]chloride, **5**, chloro(η^4-1,5-cyclooctadiene)(1,3,4,5-tetramethyl-2,3-dihydro-1*H*-imidazol-2-thione)rhodium(I), **17**, chloro(η^4-1,5-cyclooctadiene)(*N*,*N*-dimethylthioformamide)rhodium(I), **18**, and chloro(carbonyl)-*trans*-(triphenylphosphine)(1,3-diisopropyl-4,5-dimethyl-2,3-dihydro-1*H*-imidazol-2-thione)rhodium(I), **22**. The average Rh-$C_{carbene}$ bond length [2.030(4) Å] in the chelating biscarbene complex, **4**, is significantly shorter than the bond lengths reported for other biscarbene rhodium complexes.

All but one of the new complexes proved to be active hydroformylation catalysts under the chosen conditions: 80 °C, 8 MPa CO/H_2 (1:1), 16 hours, 1:1000 catalyst to 1-hexene ratio. Initial 1-hexene isomerisation occurred, but the formed isomers were generally quantitatively hydroformylated. A higher linearity of aldehydes was obtained when additional phosphine was added to the three complexes, **1**, **6** and **22**, while the opposite occurred with another complex, **11**. The carbene complexes, excluding **1**, **3**, **4** and **6**, produced aldehydes without any *iso*-aldehyde formed from the isomerised 1-hexene, whereas the carbene complexes **1**, **3**, **4** and **6**, as well as all the thione and imine complexes produced the three possible aldehyde products, including the *iso*-aldehyde derived from isomerised 1-hexene. Performing hydroformylation reactions in both toluene and dodecane proved the solvent dependence of

the catalysts. The activity and selectivity of the catalysts are also dependent on the pressure of synthesis gas used.

Complex **6** exhibited the highest average TOF (118 h^{-1}) of all the carbene complexes while the most active thione complex, chloro(dicarbonyl)(1,3-diisopropyl-4,5-dimethyl-2,3-dihydro-1*H*-imidazol-2-thione)rhodium(I), **19**, displayed an even higher average TOF of 167 h^{-1}. Using different reaction times for the hydroformylation reaction, it was found that the activity of the catalysts increases with time. The carbene complex **1** was used successfully in two consecutive hydroformylation reactions without significant loss of activity. Unfortunately the catalytic investigations conducted in ionic liquids proved somewhat disappointing since either the catalyst leached into the organic phase or no hydroformylation occurred. This is in line with recent results in our laboratory when cobalt carbonyl phosphine complexes afforded no hydride formation under hydroformylation conditions in ionic liquids.

Opsomming

Organometaalchemie bied die geleentheid om aktiewe en selektiewe komplekse vir spesifieke katalitiese prosesse te beplan en berei. Ioniese vloeistowwe is nuwe oplosmiddels vir 'n beter skeiding van produkte en wat terselfdertyd ongewingsvriendelik is. In hierdie proefskrif word die bereiding en eienskappe van nuwe komplekse vir hidroformilering asook die effektiwiteit van die hidroformileringsproses self, bestudeer.

Sekere kobalt- en rodiumkomplekse is in die studie ingesluit. Die soektog na 'n kompleks wat in ioniese vloeistowwe geïmmobiliseer kan word, het gelei tot die ondersoek van verskeie heterosikliese ligande waarin die strukture vergelykbaar is met dié van katione in die ioniese vloeistowwe. Die onlangse sukses van *N*-heterosikliese karbeenligande in homogeen-gekataliseerde prosesse, maak hierdie klas van ligande 'n amper vanselfsprekende keuse.

Die soektog na stabiele karbeenkomplekse van kobalt van die tipe $[Co(CO)_3L]_2$ (L = *N*-heterosikliese karbeen), struktuuranaloë van welbekende fosfienkomplekse, was onsuksesvol as gevolg van die termodinamiese onstabiliteit van die komplekse. Pogings om kobaltkarbeenkomplekse te berei deur transmetallering gevolg deur alkilering, lei slegs tot die vorming van klassieke kobalt(II)koordinasiekomplekse soos $[CoBr_2(\overline{NCBrSCHCH})_2]$, **37**, $[CoBr_2(OPPh_3)_2]$, **38**, en $[Co(SO_3CF_3)_2(OPPh_3)_2(\overline{NCHSCHCH})_2]$, **39**, volgens onbekende reaksieroetes.

N-heterosikliese karbene, heterosikliese tione, imiene en 'n fosfien wat vyflid asoliele bevat, is gebruik om bekende rodium(I)komplekse te diversifiseer. Een-en-dertig nuwe rodium(I) verbindings is vanaf die kommersieël-beskikbare rodium(I) uitgangstowwe $[RhCl(cod)]_2$ en $[RhCl(CO)_2]_2$ berei. Sowel ^1H- as ^{13}C-KMR-spektra van die karbeenkomplekse chloro(η^4-1,5-siklo-oktadieen)(1,3-di-isopropiel-4,5-dimetiel-2,3-dihidro-1*H*-imidasol-2-ilideen)rodium(I), **1**, chloro(η^4-1,5-siklo-oktadieen)(1-butiel-3-metiel-2,3-dihidro-1*H*-imidasol-2-ilideen)rodium(I), **3**, chloro(dikarboniel)(1,3-di-isopropiel-4,5-dimetiel-2,3-dihidro-1*H*-imidasol-2-ilideen)rodium(I), **6**, en chloro(karboniel)-*trans*-(trifenielfosfien)(1,3-di-isopropiel-4,5-dimetiel-2,3-dihidro-1*H*-imidasol-2-ilideen)rodium(I), **11**, toon die bestaan van twee verskillende molekulêre strukture van al hierdie komplekse in oplossing.

Die spektroskopiese gegewens dui daarop dat die rotasie om die Rh-$C_{karbeen}$ binding beperk is en aanleiding gee tot geometriese isomere. Die bestaan van hierdie molekulêre pare in oplossing, beteken dat die kompleks verskillende strukture in oplossing en in die vaste toestand het.

Sekere tioonkomplekse, chloro(η^4-1,5-siklo-oktadieen)(1,3-di-isopropiel-4,5-dimetiel-2,3-dihidro-1*H*-imidasol-2-tioon)rodium(I), **16**, chloro(η^4-1,5-siklo-oktadieen)(1,3,4,5-tetrametiel-2,3-dihidro-1*H*-imidasol-2-tioon)rodium(I), **17**, en chloro(karboniel)-*trans*-bis(1,3-di-isopropiel-4,5-dimetiel-2,3-dihidro-1*H*-imidasol-2-tioon)rodium(I), **24**, blyk ook as isomere in oplossing voor te kom, moontlik as gevolg van koördinasie-uitruiling deur die alleenpare van die S atoom.

Kristalstruktuurbepalings van vyf komplekse is uitgevoer: [(η^4-1,5-siklo-oktadieen)-*cis*-(1,1′-propileen-3,3′-dimetiel-2,3,2′,3′-tetrahidro-1,1′-*H*-di-imidasol-2,2′-di-ilideen)rodium(I)][heksafluorofosfaat], **4**, *cis*-[(η^4-1,5-siklo-oktadieen)bis(1,3,4,5-tetrametiel-2,3-dihidro-1*H*-imidasol-2-ilideen)rodium(I)]chloried, **5**, chloro(η^4-1,5-siklo-oktadieen)(1,3,4,5-tetrametiel-2,3-dihidro-1*H*-imidasol-2-tioon)rodium(I), **17**, chloro(η^4-1,5-siklo-oktadieen)(*N*,*N*-dimetieltioformamied)rodium(I), **18**, en chloro(carbonyl)-*trans*-(trifenielfosfien)(1,3-di-isopropiel-4,5-dimetiel-2,3-dihidro-1*H*-imidasol-2-tioon)rodium(I), **22**. Die gemiddelde Rh-$C_{karbeen}$ bindingslengte [2.030(4) Å] van die biskarbeen-bevattende chelaat, **4,** is betekenisvol korter as die bindingslengtes van bekende biskarbeenkomplekse van rhodium(I).

Al die komplekse, op 'n enkele uitsondering na, is aktief as katalisatore in die hidroformileringsreaksie onder 'n stel gekose reaksiekondisies van 80 °C, 8 MPa CO/H_2 (1:1), 16 uur, 1:1000 katalisator tot 1-hekseen verhouding. Aanvanklik vind isomerisasie van die 1-hekseen plaas, maar met verloop van tyd word die isomere kwantitatief gehidroformileer. Die lineariteit van die aldehiedprodukte kan verhoog word deur additionele fosfien by die komplekse **1**, **6** en **22**, te voeg, terwyl die teenoorgestelde met kompleks **11** gebeur. Geen *iso*-aldehied gevorm van die geïsomeriseerde hekseen word verkry wanneer die karbeenkomplekse, behalwe **1**, **3**, **4** en **6**, as katalisatore gebruik word nie. Hierteenoor gee al die tioon- en imienkomplekse, asook **1**, **3**, **4** en **6**, ook die derde aldehied as produk. Die aktiwiteit en selektiwiteit van die katalisatore is oplosmiddel-afhanklik (bewys deur die

reaksies in tolueen sowel as dodekaan te doen), sowel as afhanklik van die druk van die sintesegas.

Die karbeenkompleks, **6**, toon die hoogste aktiwiteit met 'n omsettingsfrekwensie van 118 h^{-1}. Die mees aktiewe tioonkompleks, chloro(dikarboniel)(1,3-di-isopropiel-4,5-dimetiel-2,3-dihidro-1*H*-imidasol-2-tioon)rodium(I), **19**, is selfs meer aktief (167 h^{-1}). 'n Verskeidenheid reaksietye is gebruik om vas te stel hoe die aktiwiteit van die katalisatore met verloop van tyd verander. 'n Merkwaardige toename in aktiwiteit is gevind. Geen noemenswaardige afname in aktiwiteit is waargeneem in twee opeenvolgende hidroformileringsreaksies met die karbeenkompleks **1** as katalisator nie. Die hidroformileringsreaksies wat in ioniese vloeistowwe uitgevoer is, was ongelukkig teleurstellend aangesien óf geen hidroformilering voorgekom het nie óf die katalisator in die organiese fase geloog het. Hierdie resultate is soortgelyk aan resultate wat onlangs met kobalt fosfienkarbonielkomplekse in ons laboratorium verkry is.

To Leonie

Acknowledgements

During any piece of work such as this, there are a lot of people to thank for inspiration, motivation, ideas and help. I have to start with my parents because my interest in science is largely due to them. Thank you for the exposure to so many things and the motivation and enthusiasm for my studies. My eternal thanks to Leonie, my wife, for the love, understanding and motivation, especially during the last few months.

I would like to express my gratitude towards Professor Raubenheimer. It was a pleasure and honour to work in his laboratory for the past five years. Thank you for your inspiration and time as well as the exposure to so many things, not just the chemistry. Stephanie has always been the one to help, no matter what the problem. Thank you for all your help and ideas. Without your assistance it would have been only an uphill battle.

The time spent in the laboratory was made enjoyable thanks to the pleasant attitude of all the people in the lab. I have to thank my lab colleagues of the past three years, Gerrit, Matthias, Oleg, Jin, Aletta, Marietjie, William, Uli, Elzet, Karolien, Greta, Madelein, Anne and Maggel, for doing their part in the team. I have to thank Gerrit especially, since without him my research would have been much more difficult. I enjoyed working with you, and your assistance and motivation really helped me, especially during the times we struggled together. Another person that assisted in a big way was Bertie. Without you I would not have been able to finish my research in time. Another word of thanks must go to the other people in the building, mr. Ward, Tommie, Nazier, mr. Wagner and Elsa, that assisted me during my studies.

My visit to Wuerzburg in Germany was a very pleasant experience, thanks to the amount of trouble Giuseppe went to show me around. I would like to thank Professor H. Werner for letting me work in his lab as well as for his financial support.

Many other people have to be thanked for their help in the research. The people in the NMR laboratory did a lot of work for my research. I would like to express my gratitude towards Elisna, Elsa and Jean for all their help. I am also in debt to Jean for reading my thesis and

helping me with my 'Karoo' English. I also want to thank Jaco and dr. Van der Merwe for their help in MS analysis and Matthias and Catharine for crystal structure determinations. Valerie and Nyambeni also did a lot of work for me, for which I am very grateful.

I am very grateful for the financial support I received from Sasol, without whom I would not have been able to study.

Table of contents

Abbreviations

Å	Ångstrom (10^{-10} m)
BMIM	1-butyl-3-methylimidazolium
b.p.	boiling point
^{n}Bu	normal butyl
^{t}Bu	tertiary butyl
EMIM	1-ethyl-3-methylimidazolium
Et	ethyl
gHSQC	gradient Heteronuclear Single Quantum Coherence
HOMO	highest occupied molecular orbital
IR	Infrared spectroscopy
LUMO	lowest unoccupied molecular orbital
m.p.	melting point
MS	Mass Spectrometry
NHC	*N*-heterocyclic carbene
NMR	Nuclear Magnetic Resonance spectroscopy
Ph	phenyl
^{i}Pr	isopropyl
THF	tetrahydrofuran
TON	Turn over number
TOF	Turn over frequency (h^{-1})

NMR

δ	chemical shift (ppm)
d	doublet
dd	doublet of doublets
J	coupling constant (Hz)
m	multiplet
s	singlet
t	triplet

MS

M	molecular ion

IR

m	medium
s	strong
sh	shoulder
vs	very strong
w	weak

Chapter 1

Organometallic chemistry in homogeneous catalysis

1 Introduction

The production of fuels, pharmaceuticals, commodity chemicals, and fine chemicals is heavily dependent on catalysis. Ninety percent of all industrial chemical conversions are based on a catalytic process.[1(See page 20)] According to a lecture by Halpern[2] at the XIXth International Conference on Organometallic Chemistry in Shanghai during July 2000, catalysis is one of the six most notable recent advances and promising areas in organometallic chemistry along with theoretical studies, mechanistic studies, "unconventional" media, materials and supramolecular assemblies, and bioorganometallic chemistry. The fact that the 2001 Nobel Prize in Chemistry (discussed later in this chapter) was awarded for research in catalysis, is an illustration of the importance of this field.

Otto Roelen's discovery of hydroformylation in 1938[3,4] was the beginning of extensive research into homogeneous catalysis, its industrial application being the success story of organometallic chemistry.[5] Since the 1950's homogeneous catalysis has had such a huge impact on industrial process technology that organometallic chemistry has expanded dramatically.[6]

The evolution of organometallic chemistry has led to new knowledge regarding the structure and reactivity of organometallic complexes. This in turn has helped refine the numerous homogeneously catalysed processes as well as introducing new industrial processes.[6]

Despite the significant growth of homogeneous catalysis, heterogeneous catalysis still strongly dominates the industrial scene. In 1997 an estimated 85 % of known industrial catalytic processes still used heterogeneous catalysts.[6] A general comparison of the properties associated with homogeneous and heterogeneous catalysts is summarised below (Table 1.1.1).

Table 1.1.1 *Homogeneous vs. heterogeneous catalysts*[7,8]

	Homogeneous catalysts	Heterogeneous catalysts
Activity	High	Variable
Selectivity	High	Variable
Reaction conditions	Mild	Harsh
Service life of catalyst	Variable	Long
Sensitivity toward catalyst poisons	Low	High
Diffusion problems	None	Can be very important
Catalyst recycling	Expensive	Simple
Variability of steric and electronic properties of catalyst	Possible	Not possible
Mechanistic understanding	Plausible under random conditions	Poorly understood, almost impossible[a]

[a] *Indirect mechanistic conclusions are possible via single-site catalysts.*

Heterogeneous catalysis remains preferred for industrial processes because of the robustness of the catalyst and easy separation procedures. Homogeneous catalysis, however, has some unassailable advantages over heterogeneous catalysis, such as the clearly defined molecular structure of the catalyst and the possibility to vary this structure. The greatest advantage of homogeneous catalysts over heterogeneous catalysts is their greater activity with another major benefit being that high selectivities can be achieved.[9] This high selectivity is presumably due to the fact that the active catalysts have only one reaction site available. Unfortunately high selectivity is usually achieved at the expense of reaction rate. Two of the major disadvantages of homogeneous processes are the difficulties in catalyst recycling and product separation.

Homogeneous catalysts are potentially cheaper since all metal atoms are used rather than only an unknown and possibly small fraction in heterogeneous catalysis.[10] Homogeneous catalysts can also be modified in a controlled manner by variation of one or more parameters, such as the central metal, the ligands or the solvent.[11] Some of the foremost homogeneously catalysed processes and their scale of operation are summarised in Table 1.1.2 below.

Table 1.1.2 *Production of selected commodity chemicals using homogeneous catalysis*[12]

Chemicals produced by homogeneous catalysis	Million tons per year
Terephthalic acid and poly(ethylene terephthalate)	9.0
Acetic acid and acetyl chemicals	7.0
Aldehydes and alcohols via hydroformylation	6.0
Adiponitrile via buta-1,3-diene hydrocyanation	1.0
Detergent-range alkenes via Shell Higher Olefins Process	1.0
Total fine chemicals manufactured, including asymmetric catalysis	< 1.0
Alkene polymerisation (*ca.* 60% production capacity uses Ziegler-Natta type catalysts)	60

The three "battleships" of homogeneous catalysis, according to Herrmann and Cornils, are hydroformylation, olefin polymerisation, and acetaldehyde synthesis.[13] In this study the focus falls on hydroformylation, one of the largest homogeneously catalysed processes. Not only are catalysis and associated catalyst design described, but also the application of an "unconventional" medium, mentioned by Halpern. The two main features of catalysts that can be changed are the central atom and the ligands. Rhodium, and to a lesser extent cobalt, are the metals used in the study of the hydroformylation reaction. The main aim of this work is the preparation of novel complexes with different ligand types and the testing of these complexes for catalytic activity.

Research in the field of catalysis won W.S. Knowles, R. Noyori, and K.B. Sharpless the 2001 Nobel Prize for Chemistry, emphasising the importance of ligands in catalysis.[14] The former two received the prize for developing chiral catalysts for hydrogenation reactions. Research done by Knowles led to the industrial process for the production of the L-DOPA drug that is used in the treatment of Parkinson's disease. Work by Noyori has furthered the development of this process. His discovery of the atropisomeric chiral diphosphine, BINAP, and the ensuing discovery of the BINAP-Ru(II) complex catalysts, was a major advance in stereoselective organic synthesis (Figure 1.1.1). Sharpless shared the prize for his work in developing chiral catalysts for oxidation reactions, which was achieved through ligand synthesis. The Sharpless reaction accomplishes the epoxidation of allylic alcohols with excellent stereoselectivity. These epoxy alcohols are versatile building blocks for the synthesis of a variety of chiral molecules.

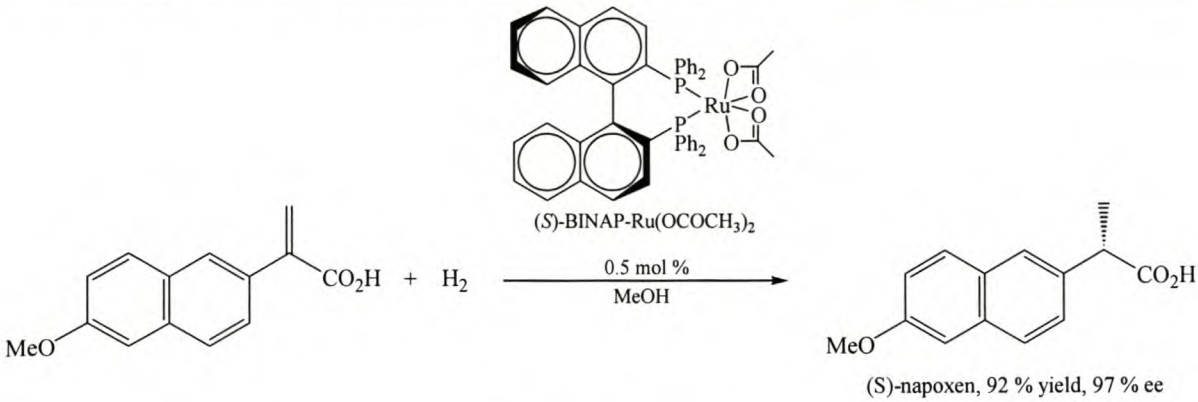

Figure 1.1.1 *The anti-inflammatory agent (S)-naproxen is produced using Noyori's catalyst*

A large number of parameters can be changed and controlled in homogeneous catalysis. One of the current hot research topics is the reaction medium, where ionic liquids are under investigation as potentially environmentally benign, "green" solvents. Catalyst development still plays a very important role in the progress of homogeneous catalysis. Ligand design was, and still is, one of the most important and versatile areas of research. In the following sections ionic liquids, a possible substitute for organic solvents as reaction media, and one of the most important homogeneous catalytic processes, hydroformylation, are discussed.

2 Ionic liquids as solvents

In recent years, the possibility of applying room temperature ionic liquids in catalysis has revealed a new area to be investigated. Ionic liquids, salts that are in the liquid phase at room temperature. They may consist of organic nitrogen-containing heterocyclic cations and counterions that can be inorganic anions or triflates, alkyl sulfates, triflimides, etc. (Table 1.2.1). Recent reviews[15,16,17,18] and a book[19] provide extensive information about ionic liquids as well as their application in various kinds of catalysis. Ionic liquids exhibit certain advantages over conventional solvents, making their use in catalytic processes promising. However, various disadvantages still have to be overcome.

A wide range of organic and inorganic materials are soluble in ionic liquids. Due to their immiscibility with numerous other conventional organic solvents, they are good polar alternatives to water for biphasic systems. They also have the potential to be reused and recycled like water in biphasic systems, where poor solubility of organic substances in water

usually results in low reaction rates. Another disadvantage of water is that it coordinates to the catalysts.

Table 1.2.1 *Typical cation/anion combinations in ionic liquids*[18]

Cations (R = alkyl)	Anions	Coordination ability of anions
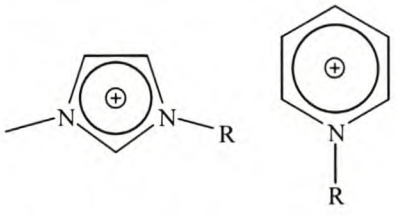	$[BF_4]^-$, $[PF_6]^-$, $[SbF_6]^-$, $[CF_3SO_3]^-$, $[CuCl_2]^-$, $[AlCl_4]^-$, $[AlBr_4]^-$, $[AlI_4]^-$, $[AlCl_3Et]^-$, $[NO_3]^-$, $[NO_2]^-$, $[SO_4]^{2-}$	Weak (neutral)
PR_4^+, SR_4^+, NR_4^+	$[Cu_2Cl_3]^-$, $[Cu_3Cl_4]^-$, $[Al_2Cl_7]^-$, $[Al_3Cl_{10}]^-$	None (acidic)

Ionic liquids can play an important role in green chemistry, i.e. environmentally benign processes.[18] A very important advantage from an environmental perspective is that the solvent, i.e. ionic liquid, can be recycled after simple separation of product and solvent. Benign catalytic processes include higher reaction specificity that translates to higher conversions, higher selectivity, higher catalyst activity, and shorter reaction routes. Replacing conventional organic solvents with ionic liquids could help in achieving a "greener" chemical environment. Replacing organic solvents with ionic liquids can also have important advantages in catalytic reactions. Many studies have shown that reaction rate, conversion, and selectivity in certain reactions are enhanced when an ionic liquid is used as the solvent. Reasons for this is still unclear and extensive research is required.[18]

Ionic liquids can be optimised for a specific application by varying the physical and chemical properties *via* the selection of both cation and anion. A low melting point is preferable for ionic liquids to be useful in catalysis. Both the cation and the anion have a significant influence on the melting point which can be illustrated by a few examples. The melting points of the chloride salts of 1-butyl-3-methylimidazolium (BMIM) and 1-ethyl-3-methylimidazolium (EMIM) differ by more than 20 °C (65 °C and 87 °C respectively), whereas $[EMIM]CF_3SO_3$ melts at –9 °C. An advantage of ionic liquids is that they usually have a wide liquid range of about 300 °C.[17]

A further major advantage of ionic liquids is that they have no measurable vapour pressure. This means that product isolation by distillation of the reaction mixture is possible. Azeotrope formation between solvent and product is also not a problem. The only potential drawback is the thermal instability of the ionic liquid, however, this can be overcome by choosing the right combination of anion and cation. For instance, [EMIM][$(CF_3SO_2)_2N$] is stable up to 400 °C.[20] Density and viscosity can also be varied by changing the anion or cation.

Another key advantage of ionic liquids is that they can be altered to achieve better solubility of the catalyst and the reactants. In a study by Wasserscheid and Keim the influence of the cation was tested in different tosylate melts.[17] The results showed that the solubility of 1-octene increases with the nonpolar character of the cation. Acidity and coordination properties are essentially determined by the nature of the anion and vary from "strongly basic/strongly coordinating" to "strongly acidic/practically non-coordinating" (Table 1.2.2).

Table 1.2.2 *Coordination characteristics of various anions*[18]

basic/strongly coordinating	neutral/weakly coordinating	acidic/non-coordinating
Cl^-	$AlCl_4^-$	$Al_2Cl_7^-$
Ac^-	$CuCl_2^-$	$Al_3Cl_{10}^-$
NO_3^-	SbF_6^-	
SO_4^{2-}	BF_4^-	$Cu_2Cl_3^-$
	PF_6^-	$Cu_3Cl_4^-$

In order to obtain the highest conversions in homogeneous catalysis, the solvent must not react with the metal centre. The solvent plays an import role in dissolving and stabilising all the reactants as well as the active catalytic species. Multi-site coordination is an important characteristic of homogeneous catalysis, and the solvent must not compete for any of these sites. In certain instances ionic liquid based solvents may act as carbene sources, leading to complications.

A disadvantage of organic solvents is the difficulty involved in separating the solvent and catalyst from the product and unused reagents. Ionic liquids offer the opportunity for easy separation if no catalyst leaching to the organic products occurs. Methods to prevent this leaching are currently being investigated. *N*-heterocyclic carbene ligands pose a possible

solution to this problem, especially since they can be tailored to have the exact same structure as the ionic liquid. Ionic liquids (imidazolium salts) are precursors for *N*-heterocyclic carbene ligands and can be obtained by simple deprotonation of the imidazolium cation as shown in Figure 1.2.1.[21]

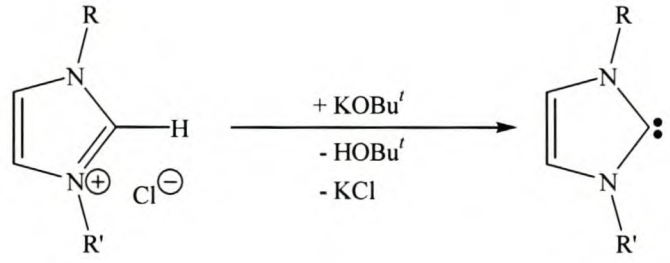

Figure 1.2.1 *Deprotonation of an imidazolium salt yields a free carbene*

The answer lies in the modification of the ionic liquids themselves to achieve optimal solubility of catalyst precursors, α-olefins, hydrogen and CO while minimising catalyst leaching.

3 Hydroformylation

Hydroformylation is the reaction between synthesis gas (mixture of hydrogen and carbon monoxide) and olefinic double bonds in the presence of rhodium or cobalt catalysts to produce aldehydes and in some cases alcohols (Figure 1.3.1). Hydroformylation was discovered in 1938 by Roelen at Ruhrchemie while investigating the recycling of olefins in the heterogeneously-catalysed Fischer-Tropsch synthesis.

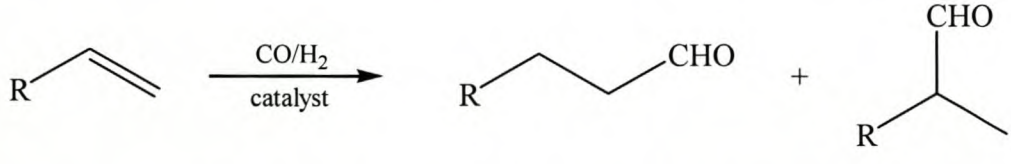

Figure 1.3.1 *The general hydroformylation reaction*

The rapid growth of the petrochemical industry and the emergence of the detergent industry and PVC markets were the main contributors to the progress made in hydroformylation. Aldehydes, the products of the hydroformylation reaction, are useful building blocks for the production of a wide range of chemicals (Figure 1.3.2).[22]

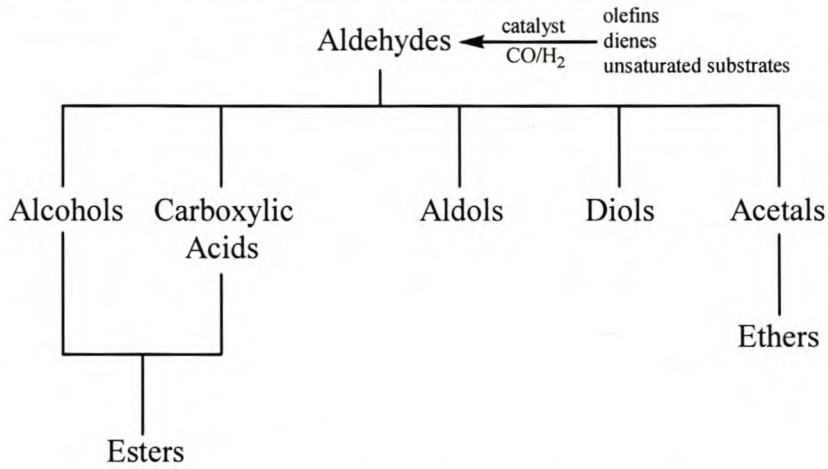

Figure 1.3.2 *Chemicals obtained from aldehydes*

The first generation of hydroformylation catalysts consisted solely of catalysts which contained cobalt as the metal centre. Harsh reaction conditions were required for these catalysts (200 to 350 bar and 150 to 180 °C). Research at Shell led to the discovery that phosphines can replace carbon monoxide as electron donating ligands, resulting in an increase in stability of metal carbonyls (catalysts) and, eventually, reduced CO pressure. The second-generation catalysts combined the advantage of this ligand modification with a change to a rhodium catalyst centre; it operates under moderate conditions. Transferral of the hydroformylation reaction into an aqueous phase was achieved by applying a water-soluble phosphine as a ligand. This can be called the third-generation of hydroformylation catalysts. This biphasic, but homogeneous, system has distinct advantages over the conventional one-phase process, such as easier product separation and catalyst recycling.[23]

3.1 The central atom

The generally accepted order of hydroformylation activity for monometallic catalysts is:[24,25]

$$Rh >> Co > Ir, Ru > Os > Pt > Pd > Fe > Ni$$

Most of the current research on hydroformylation is focussed on cobalt, rhodium, platinum, and ruthenium complexes, but industrial plants use almost exclusively rhodium and cobalt catalysts. These two were also the metals of choice for the current research project.

The two metals have different advantages. Cobalt is much cheaper than rhodium, but the required ratio of metal complex to olefin is much lower for rhodium. Cobalt complexes need high pressure and temperature to stabilise the active catalyst and prevent decomposition,[26] whereas low pressure is required for rhodium catalysts, saving a significant amount of energy. On the other hand, cobalt catalysts are more robust and show higher stability towards impurities. Rhodium catalysts yield almost exclusively aldehydes, whereas cobalt catalysts produce alcohols as well. Table 1.3.1 shows a comparison between commercial processes that use cobalt and rhodium complexes as catalysts.

Table 1.3.1 *Comparison of reaction conditions and process parameters for commercial hydroformylation processes*[27]

Process	Rh/P	Rh/P (biphasic)	Co	Co/P
Catalyst precursor	$HRh(CO)(PPh_3)_3$	$HRh(CO)(PR_3)_3$ R = *m*-$C_6H_4SO_3Na$	$Co_2(CO)_8$ or Co salts	$Co_2(CO)_8/PR_3$ R = Bu^n, other
Phosphine : metal ratio	50:1 – 100:1	50:1 – 100:1	-	2:1
Pressure (bar)	15 – 20	40 – 60	200 – 300	50 – 100
Temperature (°C)	80 – 120	110 – 130	110 – 160	160 – 200
Catalyst concentration (% metal/olefin)	0.01 – 0.05	0.001 – 1.0	0.1 – 1.0	0.6
n/i product ratio	8:1 – 16:1	7:1 – 19:1	4:1	7:1
Hydrogenation (%)	5	< 2	< 2	15
High boiling products (%)	2	< 0.5	5	5
Catalyst recovery and recycling	Simple only for C_3 and C_4 olefins	Facile	Difficult	Simpler

3.2 The ligand

The structure and properties of the catalyst ligands play a very important role in the hydroformylation reaction. Steric and electronic properties of a ligand can drastically influence the rate and selectivity of the reaction. The favourable effects of phosphorus ligands in homogeneous catalysis have been known for the last 50 years. Reppe was one of the first researchers to report the use of a catalyst containing a phosphine ligand in the reaction of alkynes, alcohols and carbon monoxide to make acrylic esters.[28] An early example of the implementation of phosphorus-donor ligand catalysts was seen in the sixties with the Shell

process for alkene hydroformylation, which utilised an alkylphosphine and cobalt complexes.[29]

3.2.1 Phosphorus ligands in hydroformylation

Many industries started using phosphine ligands after the above-mentioned discovery by Shell in the 1960's. However, alkylphosphine ligands result in slow catalysis in the case of rhodium complexes. Work by Wilkinson showed that arylphosphines should rather be used as ligands for rhodium catalysts, and that very active catalysts can then be obtained at very low temperatures.[30]

The first industrial catalysts contained triphenylphosphine ligands. Since then much research has dealt with ligand design which has eventually led to the development of the water-soluble ligand TPPTS [tri(m-sulfonyl)triphenylphosphine trisodium salt], based on the ideas of Kuntz.[31,32] TPPTS is used in the so-called Ruhrchemie/Rhône-Poulenc process.[33] This system has advantages over other systems for product separation. The TPPTS ligand ensures the water-solubility of the catalyst facilitating a biphasic system in which the aldehyde products remain in the organic phase and can be easily separated from the catalyst in the water phase.

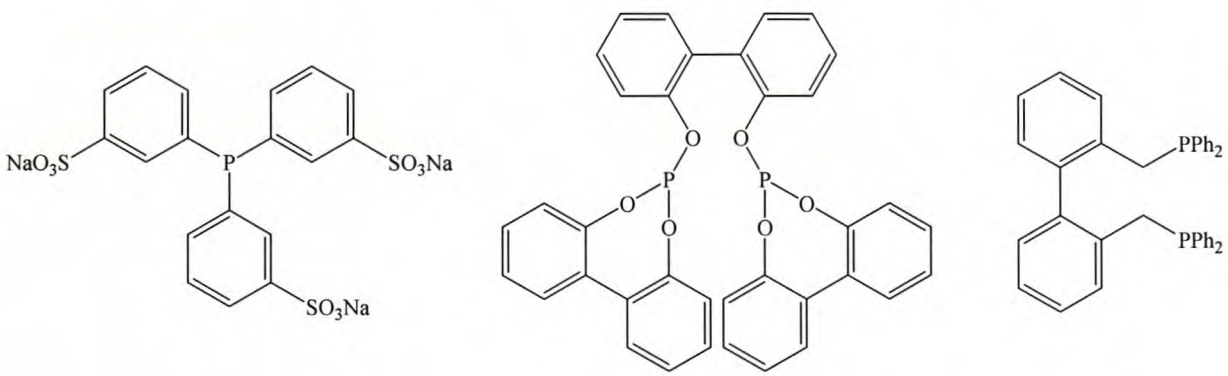

A **B** **C**

Figure 1.3.3 *The TPPTS ligand (**A**) used in the Ruhrchemie/Rhône-Poulenc process, a typical diphosphite from Union Carbide Corporation (**B**), and Texas Eastman's BISBI (**C**)*

Although the study of phosphites also showed promise in the 1960's, triphenylphosphine was still preferred as a ligand. Recently Van Leeuwen and co-workers showed that bulky phosphites also give very high reaction rates, resulting in a renewed interest in phosphite

ligands.[34,35,36] Although Union Carbide developed some bulky phosphite ligands, their focus changed to diphosphites. Currently the only commercial application where monophosphites are used as ligands is the hydroformylation of 3-methylbut-3-en-1-ol, developed by Kuraray.[37]

Diphosphines have also been very popular ligands for the last 15 years. Devon and co-workers from Texas Eastman developed a new diphosphine ligand, BISBI (see Figure 3.3), in 1987.[38] This ligand, and modifications thereof, show very high regioselectivity for the formation of linear aldehydes. It's use in the hydroformylation of propene yields aldehydes with high linearity (*n:i* = 30). Extensive research on bidentate phosphine ligands has led to the speculation that ligands with wider bite angles may have an advantageous effect on the *n:i* ratio in the hydroformylation of 1-alkenes. The subject of bite angles and diphosphine ligands is thoroughly discussed in recent publications[39] but is not of any importance in this work and will, therefore, not be discussed further.

It is also necessary to take a look at ligand parameters that are important. Tolman has studied a variety of ligand effects[40,41] and published a review on the subject.[42] The electronic parameter χ is a measure for the overall effect of electron donating (basic) and electron accepting (acidic) properties of the ligand L and can be written as a ratio ($\pi_{acceptor}/\sigma_{donor}$). A high χ-value means L is a strong π-acceptor and/or a weak σ-donor, and *vice versa* for a low χ-value. This is illustrated in the figure below (Figure 1.3.4).

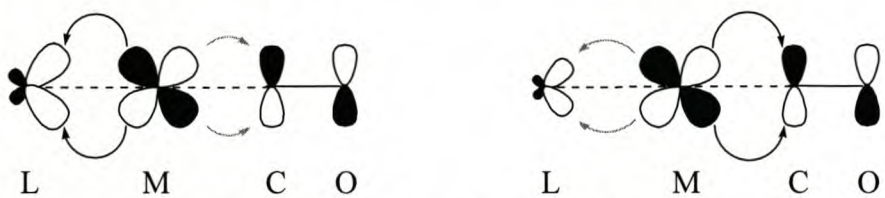

Figure 1.3.4 *Illustration of the effect of χ. The diagram on the left (high χ-value for L) shows weak back-donation to the CO leading to a high C-O stretching frequency, and the picture on the right (low χ-value) indicate strong back-donation to the CO leading to low a C-O stretching frequency*[43]

Over the years numerous studies have shown that steric effects are as important as electronic effects, and can even be dominant in terms of the stability of complexes. The steric parameter is the cone angle θ. For monodentate phosphorus-donor ligands the cone angle, θ, is defined

as the inner angle of a cylindrical cone that is centered at 2.28 Å from the centre of the phosphorus atom, with the sides of the cone touching the outmost atoms of the R-groups of PR_3 (for different R-groups the average is used).[43] This is illustrated in Figure 1.3.5. The influence of the cone angle, or the bite angle - which is relevant for diphosphine ligands - will not be discussed further. However, it is important to know that these factors have been thoroughly investigated in order to improve ligands.

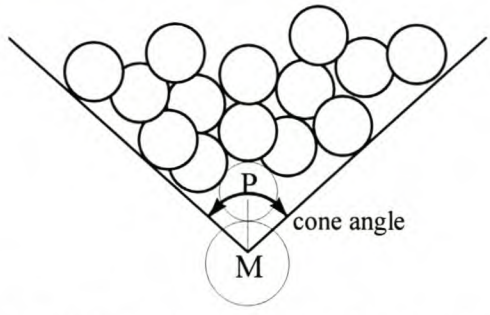

Figure 1.3.5 *An illustration of the cone angle, θ*

The electronic-, steric- and *trans*-effects of ligands are important in the catalytic cycle because they can influence the reaction rate by stabilising or destabilising one or more of the initial, transition or final states of the catalyst, as well as have an influence on the structure of the product (*n:i* ratio).

Although phosphine ligands have dominated homogeneous catalysis, some S-donor, N-donor and carbene ligands have also been investigated. These ligands have certain similarities to phosphines making them potential ligands for active catalysts. This suggests the possibility of new catalysts with completely different properties. All these ligands have an electron pair available for donation to a metal, have strong σ-donating properties, and are relatively weak π-acceptors.

3.2.2 Sulfur-donor ligands in hydroformylation

Transition metal complexes containing sulfur-donor ligands are active catalysts in a considerable number of homogeneously catalysed reactions, for example hydrogenation, isomerisation, hydroformylation, the Heck reaction, and polymerisation to name just a few.[44] Despite their known activity, they have been investigated less thoroughly than ligands containing phosphorus-donor atoms.

Marko has reported the use of thioether ligands with cobalt in the hydroformylation of alkenes.[45] Me_2S was added in large excess to solutions of $[Co_2(CO)_8]$ and $[Co_4(CO)_{12}]$ to obtain $[Co_4(CO)_{11}(SMe_2)]$, characterised by infrared spectroscopy. Using SBu_2 instead of SMe_2 impairs the activity compared to the unmodified cobalt, but the problem can be overcome by an increase in CO pressure.

Binuclear rhodium thiolato-bridged complexes, $[Rh_2(CO)_2(PR_3)_2(\mu\text{-}SR')_2]$ have been found to be effective hydroformylation catalysts at low temperatures and pressures.[46] An advantage of this class of complexes is that it can be modified at the thiolato bridge as well as at the phosphine ligand. For R = OPh and R′ = ^{t}Bu, high activity was noted at a pressure of 5 bar and a temperature of 80 °C. However, in the absence of the phosphine ligand no catalytic activity was found under the same conditions. For thiolato bridged complexes the auxiliary phosphine ligands are essential to obtain hydroformylation catalyst activity.[44]

Research has also been carried out on catalyst recovery. The two main approaches were to anchor the catalyst through the sulfur-donor ligand or the auxiliary phosphine ligand. The rhodium complex $[Rh_2(\mu\text{-}Cl)(\mu\text{-}SR)(CO)_2(PR_3)_2]$ functionalised at the thiolato ligand [R = $(CH_2)_nSi(OEt)_3$] and anchored to silica or alumina, proved to be active for the hydroformylation of olefins and could be recycled more than 10 times without change in performance.[47] Supported complexes of rhodium(I) have been prepared by the reaction of thiourea-functionalised siloxane materials with rhodium(I) species (Figure 1.3.6). These complexes are very active and easily recovered. Non-siloxanised thioureas have been used to prepare rhodium(I) complexes, e.g. [RhCl(COD){PhNHC(S)NHPh}] to use as models for a study of the supported catalysts.[48,49]

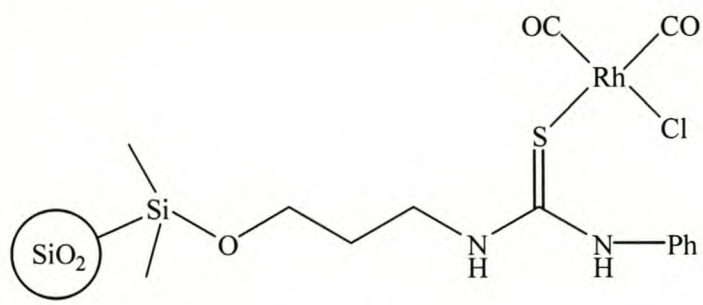

Figure 1.3.6 *An immobilised thiourea rhodium complex*

Dithiolato ligands are another class of ligands with sulfur-donor atoms that have been used in the preparation of hydroformylation catalysts. In 1993 Claver and co-workers reported the first use of chiral sulfur-donor ligands in rhodium catalysed asymmetric hydroformylation.[50] Enantiopure binasH_2 (Figure 1.3.7) was used as a bridging ligand to obtain the complex [Rh_2(μ-binas)(COD)$_2$]. This complex, in the presence of PPh_3, showed good activity in the hydroformylation of styrene. The branched aldehyde product was obtained in high yield with a regioselectivity of greater than 90 %. Though the complex maintained some of its catalytic activity without PPh_3, its stereoselectivity was higher.

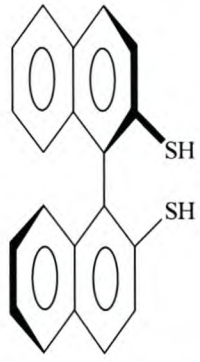

Figure 1.3.7 *BinasH_2 that acts as a bridging ligand*

3.2.3 *N*-heterocyclic carbene ligands

The study of *N*-heterocyclic carbene ligands started in 1962 with an article by Wanzlick entitled *'Aspects of Nucleophilic Carbene Chemistry'*.[51] Öfele later reported the metal coordination chemistry of *N*-heterocyclic carbenes[52] and with Lappert was responsible for developments in synthetic methodology.[53] Since the discovery of stable free carbenes by Arduengo,[21,54] *N*-heterocyclic carbenes have received an enormous amount of attention.[55,56,57,58]

The striking similarities between phosphine ligands and *N*-heterocyclic carbenes in their transition metal coordination chemistry, ligand properties and complex synthesis have been noted by many authors but best articulated by Herrmann.[59,60,61] Both ligand types are strong σ-donors with only a small amount of π-backbonding character. Spectroscopic studies have also shown the similarities between phosphorus ligands and *N*-heterocyclic carbenes.[62,63] Before discussing *N*-heterocyclic carbenes in catalysis, the properties that describe the stability of

carbenes and the strong bond between a metal atom and carbene carbon atom will be considered.

In an *N*-heterocyclic carbene the two nitrogen atoms bonded to the carbene carbon render the originally degenerate orbitals on carbon unequal in energy, consequently enhancing the thermodynamic stability and the nucleophilicity of the carbon atom. Singlet carbenes have a pronounced energy difference between their HOMO and LUMO.[56] Two electronic effects, the inductive effect and the mesomeric effect, are used to explain the influence of substituents on the ground-state multiplicity of the carbene carbon (Figure 1.3.8).[57]

Inductive effect: It is now well established that the singlet state is favoured above the triplet state when the substituents are σ-electron withdrawing. The σ-electron withdrawing substituents inductively stabilise the σ-nonbonding orbital by increasing its s-character and leaving the p_π-orbitals unchanged. The singlet state is favoured by the resulting increase in the σ-p_π gap.

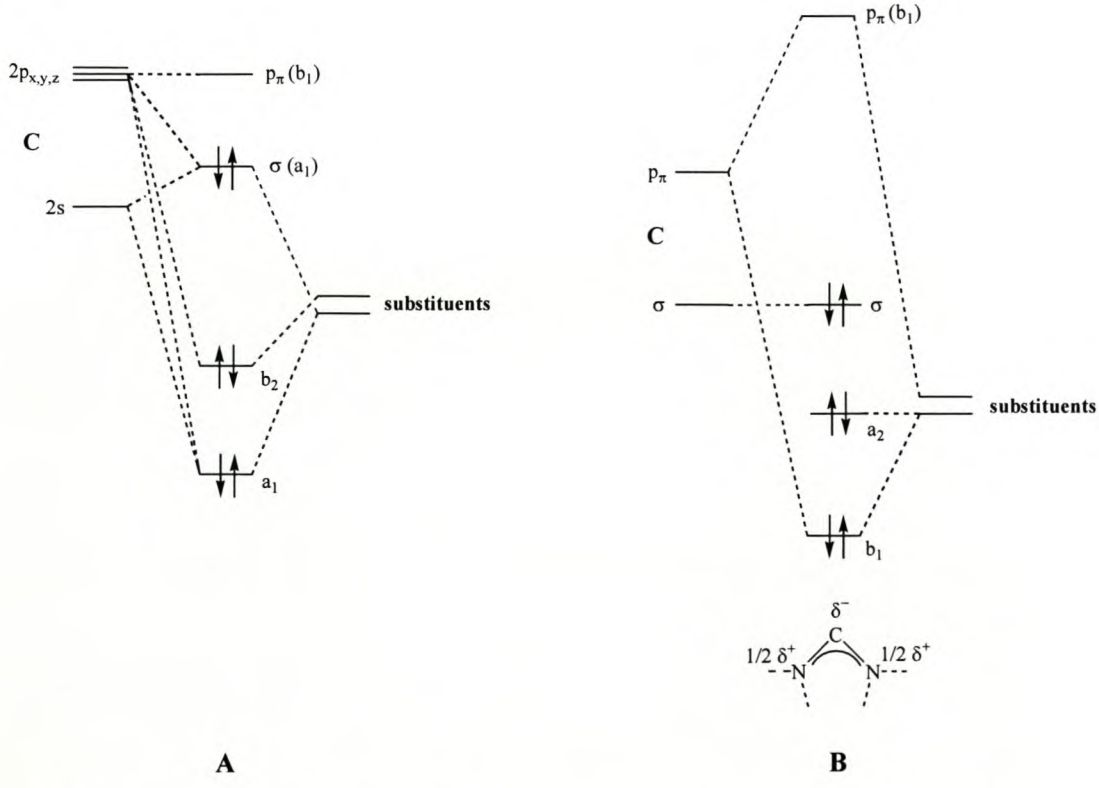

Figure 1.3.8 *Orbital diagrams showing the influence of (**A**) the inductive effect (σ-electron withdrawing substituents) and (**B**) the mesomeric effect (π-electron-donating substituents)*[57]

Mesomeric effect: The mesomeric effect can play an even more significant role than the inductive effect. For π-donating groups (such as $-NR_2$) the singlet state is also favoured. Whereas the σ-orbital remains almost unchanged, the energy of the p_π-orbitals is increased by the interaction with the symmetric combination of the lone pairs (b_1) of the substituents. The donation of the substituent lone pairs results in a polarised four-electron three-centre π-system. Thus, the C-substituent bond has some multiple bond character, implying that the carbene can be best described by the superposition of two zwitterionic structures with a negative charge at the carbene carbon.

Although steric hindrance and the aromatic character of the 6 π-electron five-membered ring also have stabilising effect, they are not sufficient to obtain a stable, free carbene. Most important is the interaction between the carbene carbon and the π-donating, σ-attracting *N*-substituents, as indicated by the isolation of the free carbene compound bis(diisopropylamino)carbene.[64]

N-heterocyclic carbenes bond to transition metals mainly through σ-donation, with π-back-donation being negligible. The very high energy of the p_π-orbital of the carbene carbon, as described above, is the reason for the unusual bonding properties of carbene ligands. The essentially pure σ-donating character of *N*-heterocyclic carbenes has also been revealed by X-ray diffraction studies.[56] In metal-carbene complexes the exceptionally high stability of the bond between the metal and the carbene carbon results in high thermal and hydrolytic stability. It also means these complexes are easily accessible synthetically and there is no need of excess ligand in catalysis.[65] All this implies that the electronic parameter χ ($\pi_{acceptor}/\sigma_{donor}$) for *N*-heterocyclic carbenes is very small.

It has been shown that 2,3-dihydro-1*H*-imidazol-2-ylidene ligands coordinate to transition metals of low and high oxidation states and even to metals that exhibit weak π-backbonding properties.[60,61,62] Zerovalent iron,[60] tetravalent titanium[61] and heptavalent rhenium[61] carbene complexes were prepared and characterised. Furthermore, the extraordinarily small beryllium cation Be^{2+} could form the cationic complex seen in Figure 1.3.9.

This beryllium complex shows that the planar, five-membered heterocyclic carbenes are not sterically very demanding in contrast to the bulky phosphines that are generally used in homogeneous catalysis.

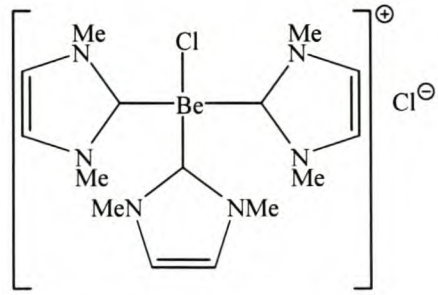

Figure 1.3.9 *Three carbene ligands bonded to beryllium*

N-heterocyclic carbene ligands are, therefore, excellent alternatives for the time-honoured phosphine ligands in homogeneous catalysts. Many publications about *N*-heterocyclic carbene ligands as alternatives to phosphine ligands in homogeneous catalysts have appeared in the past decade as well as in a recent review article.[65] One of the first examples reported was for the Heck coupling of aryl bromides and aryl chlorides using palladium biscarbene complexes.[66] A low concentration of catalyst (1:5000 ratio for catalyst to substrate) is needed to obtain yields of up to 99%.

The excellent properties of *N*-heterocyclic carbenes in catalysis are best demonstrated by olefin metathesis reactions.[67] In the past decade ruthenium catalysts have been extensively investigated. Early systems such as $[(PPh_3)_2Cl_2Ru(=CHCH=CPh_2)]$, employing no *N*-heterocyclic carbene ligands, were only active in ring-opening metathesis polymerisation (ROMP). The use of a more bulky and electron-donating phosphine (PCy_3) yielded active catalysts for ring-closing metathesis (RCM), cross-metathesis (CM) and ROMP. These catalysts, however, were limited to olefins that were not sterically hindered or did not have functionality in the α-position. The limitations were overcome by the introduction of second generation Grubbs ruthenium catalysts containing *N*-heterocyclic carbene ligands (examples in Figure 1.3.10).[68,69,70,71]

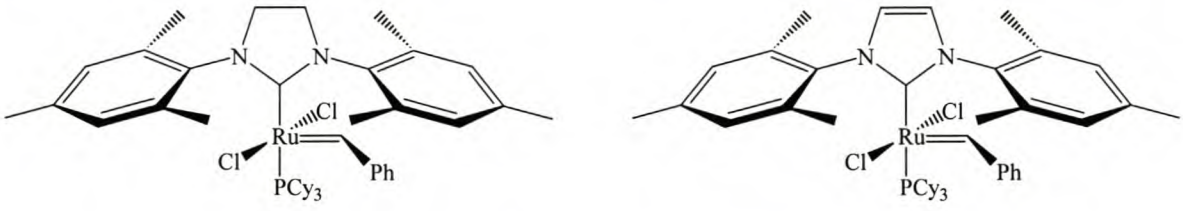

Figure 1.3.10 *Second-generation ruthenium alkylidenes*

Mechanistic studies of these ruthenium carbene complexes revealed that the auxiliary ligands could have a dramatic effect on the reaction rates of the initiation and propagation steps in olefin metathesis reactions. Studies into new ligand systems, such as labile pyridine ligands, have recently been published by Grubbs.[72]

Apart from the above mentioned Heck-reaction and metathesis a host of other catalytic reactions have also been performed with *N*-heterocyclic carbene ligands. These include ethylene/carbon monoxide copolymerisation, hydrosilylation, aryl amination, and metathesis cross coupling.[65] Work by Nolan and co-workers showed that carbene complexes are very promising in ruthenium hydrogenation catalysis. High turn over numbers (2.4×10^5) were achieved at low pressure (4 bar) and a temperature of only 100 °C with ruthenium catalysts.[73]

In 2000 Crudden and co-workers published the results of the hydroformylation of styrene using two novel rhodium carbene complexes.[74] Branched-to-linear ratios of up to 98:2 were reported in high yield. Unfortunately, the reported activities were low (TOF $< 10\ h^{-1}$). The reduced activity of the carbene complexes can be attributed to the increase in electron density at the metal centre caused by the nucleophilic *N*-heterocyclic carbene.

In metal-carbene complexes carbene ligands do not undergo dissociation from the metal centre, making immobilisation and subsequent recycling of the catalyst possible by linking the 2,3-dihydro-1*H*-imidazol-2-ylidene ligand to a polymer. This means that a ligand containing reactive functional groups are required. Another option for recycling the catalyst is based on a two-phase system where the catalyst is dissolved in one of two phases in a biphasic reaction with water or an ionic liquid as the second phase. Herrmann *et. al.* were able to prepare and characterise stable water-soluble *N*-heterocyclic carbene complexes of rhodium

(Figure 1.3.11).[75] This means that carbene complexes of rhodium can potentially be used in biphasic reaction systems like the Ruhrchemie/Rhône-Poulenc process.

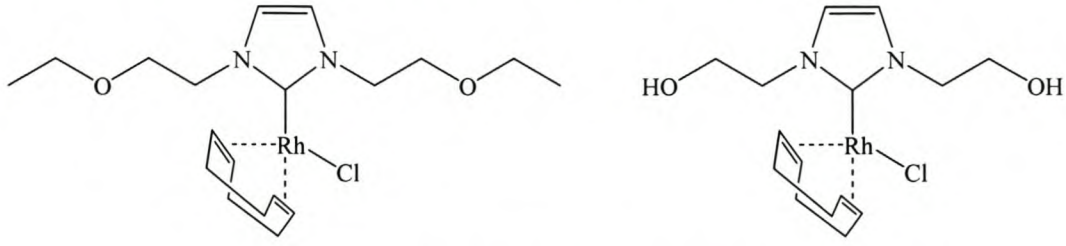

Figure 1.3.11 *Stable water-soluble rhodium carbene complexes*

4 Aims of this study

The main aim of this study was to prepare and characterise novel complexes of cobalt and rhodium as possible catalysts in the hydroformylation reaction.

In order to produce complexes that are well soluble in ionic liquids, it was decided to use ligand systems that contain a heterocyclic ring similar in structure to those employed in ionic liquids. Heterocyclic carbenes, being a relatively new ligand type in catalysis, is an obvious choice. Since very few cobalt carbene complexes are known, it was foreseen that different synthetic methods would have to be investigated. It was planned to prepare rhodium pre-catalysts that contain Arduengo-type carbenes as ligands. Phosphine ligands were always preferred in most catalyst systems. S-donating ligands offered many unexplored opportunities. Therefore, synthetic methods had to be developed to combine carbene and thione ligands in complexes as phosphine-free alternatives.

5 References

1 R. Whyman, in *Applied Organometallic Chemistry and Catalysis*, Oxford University Press, New York, 2001, p. 1.

2 J. Halpern, *IUPAC, Pure and applied chemistry*, 2001, **73**, 209.

3 C.D. Frohning, C.W. Kohlpainter, in *Applied Homogeneous Catalysis with Organometallic Compounds*, Eds. W.A. Herrmann, B. Cornils, Wiley-VCH, Weinheim, 1996, Vol. 1, p. 29.

4 G.W. Parshall, S.D. Ittel, in *Homogeneous Catalysis*, *Second Edition*, John Wiley & Sons, Inc., New York, 1992, p. 107.

5 W.A. Herrmann, B. Cornils, in *Applied Homogeneous Catalysis with Organometallic Compounds*, Eds. W.A. Herrmann, B. Cornils, Wiley-VCH, Weinheim, 1996, Vol. 1, p. 3.

6 W. Herrmann, B. Cornils, *Angew. Chem., Int. Ed. Engl.*, 1997, **36**, 1048.

7 Ref. 5, p. 5.

8 Ref. 1, p. 3.

9 Ref. 1, p. 5.

10 Ref. 1, p. 6.

11 Ref. 1, p. 5.

12 Ref. 1, p. 7.

13 W.A. Herrmann, B. Cornils, in *Applied Homogeneous Catalysis with Organometallic Compounds*, Eds. W.A. Herrmann, B. Cornils, Wiley-VCH, Weinheim, 1996, Vol. 2, p. 1167.

14 Press Release: The 2001 Nobel Prize in Chemistry, www.nobel.se/chemistry/laureates/2001/press.html.

15 J.D. Holbrey, K.R. Seddon, *Clean Prod. Process.*, 1999, **1**, 223.

16 T. Welton, *Chem. Rev.*, 1999, **99**, 2071.

17 P. Wasserscheid, W. Keim, *Angew. Chem., Int. Ed. Engl.*, 2000, **39**, 3772.

18 D. Zhao, M. Wu, Y. Kou, E. Min, *Cat. Today*, 2002, **74**, 157.

19 *Ionic Liquids in Synthesis*, Eds. P. Wasserscheid, T. Welton, Wiley-VCH, Weinheim, 2003.

20 P. Bonhôte, A.-P. Dias, N. Papageorgiou, K. Kalyanasundaram, M. Grätzel, *Inorg. Chem.*, 1996, **35**, 1168.

21 A.J. Arduengo, III, R.L. Harlow, M. Kline, *J. Am. Chem. Soc.*, 1991, **113**, 361.

22 A.M. Trzeciak, J.J. Ziolkowski, *Coord. Chem. Rev.*, 1999, **190 – 192**, 883.

23 Ref. 3, p. 30-32.

24 M. Beller, B. Cornils, C.D. Frohning, C.W. Kohlpainter, *J. Mol. Cat. A*, 1995, **104**, 17.

25 Ref. 3, p. 33.

26 Ref. 4, p. 107.

27 Ref. 1, p. 21.

28 P.W.N.M. van Leeuwen, in *Rhodium catalysed Hydroformylation*, Eds. P.W.N.M. van Leeuwen, C. Claver, Kluwer Academic Publishers, Dordrecht, 2000, p. 1.

29 L.H. Slaugh, R.D. Mullineaux, Shell, *U.S. Pat.*, 3,239,569 and 3,239,570, 1966.

30 J.F. Young, J.A. Osborn, F.H. Jardine, G. Wilkinson, *J. Chem. Soc., Chem. Comm.*, 1965, 131.

31 E.G. Kuntz, *CHEMTECH*, 1987, **17**, 570.

32 B. Cornils, E.G. Kuntz, *J. Organomet. Chem.*, 1995, **502**, 177.

33 Ref. 3, p. 80.

34 P.W.N.M. van Leeuwen, C.F. Roobeck, *J. Organomet. Chem.*, 1983, **258**, 343.

35 T. Jongsma, G. Challa, P.W.N.M. van Leeuwen, *J. Organomet. Chem.*, 1991, **421**, 121.

36 A. van Rooy, E.N. Orij, P.C.J. Kramer, P.W.N.M. van Leeuwen, *Organometallics*, 1995, **14**, 34.

37 Ref. 27, p. 7.

38 T.J. Devon, G.W. Phillips, T.A. Puckette, J.L. Stavinoha, J.J. Vanderbilt, Texas Eastman, *U.S. Pat.*, 4694109, 1987.

39 *Rhodium catalysed Hydroformylation*, Eds. P.W.N.M. van Leeuwen, C. Claver, Kluwer Academic Publishers, Dordrecht, 2000.

40 C.A. Tolman, *J. Am. Chem. Soc.*, 1970, **92**, 2953.

41 C.A. Tolman, *J. Am. Chem. Soc.*, 1970, **92**, 2956.

42 C.A. Tolman, *Chem. Rev.*, 1977, **77**, 313.

43 Ref. 27, p. 9.

44 J.C. Bayón, C. Claver, A.M. Masdeu-Bultó, *Coord. Chem. Rev.*, 1999, **193-195**, 73.

45 L. Marko, *Acta Chim.*, 1969, **59**, 367.

46 P.H. Kalck, J.M. Frances, P.M. Pfister, T.G. Southern, A. Thorez, *J. Chem. Soc., Chem. Comm.*, 1983, 510.

47 M. Eisen, T. Bernstein, J. Blum, H. Schumann, *J. Mol. Catal.*, 1987, **43**, 199.

48 D. Cauzzi, M. Lanfranchi, G. Marzolini, G. Predieri, A. Tiripicchio, M. Costa, R. Zanoni, *J. Organomet. Chem.*, 1995, **488**, 115.

49 D. Cauzzi, M. Costa, L. Gonsalvi, M.A. Pellinghelli, G. Predieri, A. Tiripicchio, R. Zanoni, *J. Organomet. Chem.*, 1997, **541**, 377.

50 C. Claver, S.Castillón, N. Ruiz, G. Delogu, D. Fabbri, S. Gladiali, *J. Chem. Soc., Chem. Comm.*, 1993, 1833.

51 H.W. Wanzlick, *Angew. Chem., Int. Ed. Engl.*, 1962, **2**, 75.

52 K. Öfele, *J. Organomet. Chem.*, 1968, **12**, P42.

53 M.F. Lappert, *Chem. Rev.*, 1972.

54 A.J. Arduengo, III, M. Kline, J.C. Calabrese, F. Davidson, *J. Am. Chem. Soc.*, 1991, **113**, 9704.

55 M. Regitz, *Angew. Chem., Int. Ed. Engl.*, 1996, **35**, 725.

56 W.A. Herrmann, C. Köcher, *Angew. Chem., Int. Ed. Engl.*, 1997, **36**, 2162.

57 D.Bourissou, O. Guerret, F.P. Gabbaï, G. Bertrand, *Chem. Rev.*, 2000, **100**, 39.

58 T. Weskamp, V.P.W. Böhm, W.A. Herrmann, *J. Organomet. Chem.*, 2000, **600**, 12.

59 W.A. Herrmann, D. Mihalios, K. Öfele, P. Kiprof, F. Belmedjahed, *Chem. Ber.*, 1992, **125**, 1795.

60 K. Öfele, W.A. Herrmann, D. Mihalios, M. Elison, E. Herdtweck, W. Scherer, J. Mink, *J. Organomet. Chem.*, 1993, **459**, 177.

61 W.A. Herrmann, K. Öfele, M. Elison, F.E. Kühn, P.W. Roesky, *J. Organomet. Chem.*, 1994, **480**, C7.

62 W.A. Herrmann, O. Runte, G.R.J. Artus, *J. Organomet. Chem.*, 1995, **501**, C1.

63 K. Öfele, W.A. Herrmann, D. Mihalios, M. Elison, E. Herdtweck, T. Priermeier, P. Kiprof, *J. Organomet. Chem.*, 1995, **498**, 1.

64 R.W. Alder, P.R. Allen, M. Murray, A.G. Orpen, *Angew. Chem., Int. Ed. Engl.*, 1996, **35**, 1121.

65 W.A. Herrmann, *Angew. Chem. Int. Ed.*, 2002, **41**, 1291.

66 W.A. Herrmann, M. Elison, J. Fischer, C. Köcher, G.R.J. Artus, *Angew. Chem., Int. Ed. Engl.*, 1995, **34**, 2371.

67 L. Jafarpour, S.P. Nolan, *J. Organomet. Chem.*, 2001, **617-618**, 17.

68 T. Weskamp, W.C. Schattenmann, M. Speigler, W.A. Herrmann, *Angew. Chem., Int. Ed. Engl.*, 1998, **37**, 2490.

69 T. Weskamp, F.J Kohl, W. Hieringer, D. Gleish, W.A. Herrmann, *Angew. Chem., Int. Ed. Engl.*, 1999, **38**, 2416.

70 J. Huang, E.D. Stevens, S.P. Nolan, J.L. Peterson, *J. Am. Chem. Soc.*, 1999, **121**, 2674.

71 M. Scholl, S. Deng, C.W. Lee, R.H. Grubbs, *Org. Lett.*, 1999, **1**, 953.

72 M.S. Sanford, J.A. Love, R.H. Grubbs, *Organometallics*, 2001, **20**, 5314.

73 H.M Lee, D.C. Smith Jr., Z. He, E.D. Stevens, C.S. Yi, S.P. Nolan, *Organometallics*, 2001, **20**, 794.

74 A.C. Chen, L. Ren, A. Decken, C.M. Crudden, *Organometallics*, 2000, **19**, 3459.

75 W.A. Herrmann, L.J. Goossen, M. Spiegler, *J. Organomet. Chem.*, 1997, **547**, 357.

Chapter 2

Rhodium complexes as hydroformylation catalysts

Rhodium catalysed hydroformylation is one of the most widely used homogeneously catalysed reactions in industry today, a reaction responsible for 6 million tons of products each year.[1(See page 176)] Research into homogeneously catalysed hydroformylation has undergone drastic changes since rhodium partly replaced cobalt in industrial processes. Recent advances have created new problems and set new targets for future research. A recently published summary about rhodium compounds in hydroformylation[2] provides a good introduction to the plethora of literature available on this subject. A short introduction to this research field will be given in the following pages.

One of the intentions of this study was to develop and test new rhodium complexes for the hydroformylation of α-olefins. Current interest in ionic liquids as a potential reaction medium for catalysis prompted an investigation of heterocyclic ligands having a structure similar to that of the cationic part of an ionic liquid. Such ligands and their corresponding rhodium complexes will be discussed.

1 Rhodium as a catalytic centre in hydroformylation

About 20 years after Roelen's discovery of the oxo-reaction, the first investigations of rhodium-catalysed hydroformylation were carried out.[3,4] Very early on it was clear that rhodium catalysts were much more active than their cobalt analogues. Initially, simple precursors such as $RhCl_3$ and Rh/Al_2O_3 were used.

P-donor ligands play an important role in catalyst performance during the hydroformylation reaction. Research into phosphine modified rhodium catalysts began with the synthesis and characterisation of rhodium-hydride complexes containing triphenylphosphine.[5] An enormous amount of research has been done on a wide range of phosphorus-[6] or sulfur-containing[7] ligands with different electronic and steric characteristics. However, the effects of electronic

and steric parameters of the P-donors on the active rhodium catalysts are not always predictable, thus the development of such ligands has been, and still is, the subject of considerable interest. Development in ligand design led to the creation of the two-phase system of Ruhrchemie/Rhône-Poulenc (see Chapter 1). Utilising water-soluble phosphine ligands this process has solved problems of product separation and recycling of catalysts.

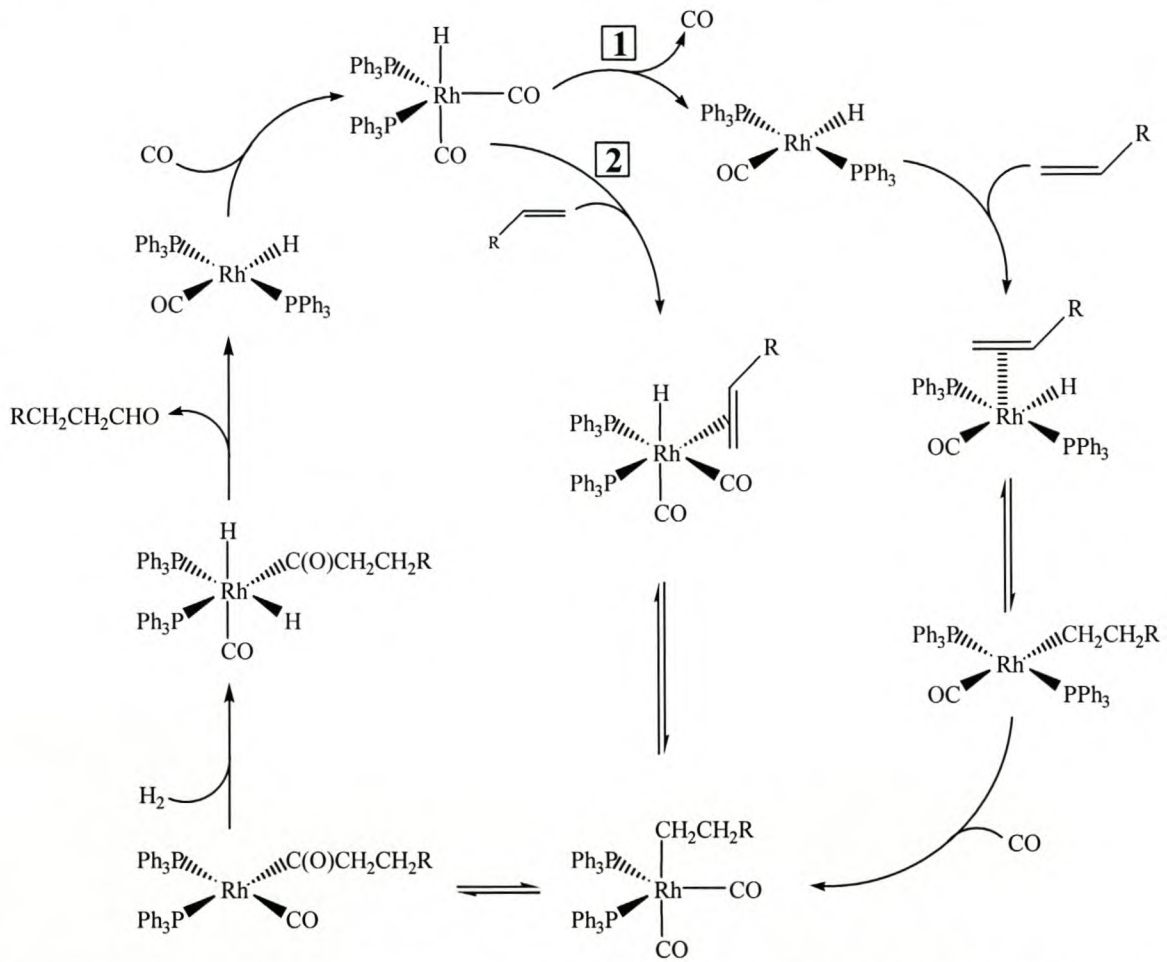

Figure 2.1.1 *The dissociative (**1**) and associative (**2**) mechanisms for the hydroformylation cycle of phosphine modified catalysts*[8]

The presently accepted hydroformylation mechanism for phosphine modified rhodium catalysts follows the Heck-Breslow cycle[9] with a few modifications. In 1968 Wilkinson was the first to introduce the rhodium hydride species $[HRh(CO)(PPh_3)_3]$, believed to be the precursor of the active catalyst, into the hydroformylation scheme. Two possible pathways have been formulated: the associative and the dissociative mechanisms (Figure 2.1.1). The key intermediate and active species is $[HRh(CO)_2(PPh_3)_2]$. The associative mechanism is initiated by the coordination of an olefin to form a six-coordinated complex. This complex

converts irreversibly to an 18 electron alkylrhodium species, $[RRh(CO)_2(PPh_3)_2]$. In the dissociative mechanism this species is generated by the dissociation of carbon monoxide followed by olefin coordination, conversion to the alkylrhodium complex and coordination of carbon monoxide. This species undergoes CO insertion to form the acyl complex, $[RC(O)Rh(CO)(PPh_3)_2]$. Oxidative addition of H_2 to the rhodium centre followed by reductive elimination to form the aldehyde and, finally, carbon monoxide coordination, regenerate the active hydride species and produce the hydroformylated product. The dissociative mechanism is considered to be the major pathway under industrial operating conditions, whereas the associative mechanism is preferred at high concentrations of phosphine and catalyst.[10]

1.1 Recent developments

New hydroformylation catalysts should be highly active, selective and, very importantly, the system should be sustainable. The aqueous biphasic system developed by Ruhrchemie/Rhône-Poulenc is a very good example of an environmentally benign process where the catalyst can be recycled. The latest developments in rhodium hydroformylation catalysis and catalyst/product separation will be discussed in this section.

Bimetallic systems have also enjoyed attention in recent years. Stanley and co-workers reported dinuclear rhodium complexes as active and selective hydroformylation catalysts (*n:i* ratio of up to 27.5:1).[11] The proposed mechanism deviates from the suggested mechanism of Heck and Breslow. A proposal for the existence of an unusual dicationic bimetallic rhodium(II) species is supported by spectroscopic evidence.[12,13] Examples of the ligands used in this work are shown in Figure 2.1.2.

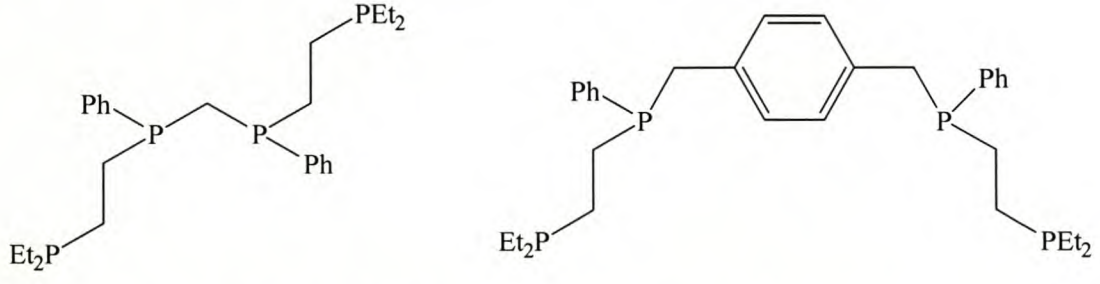

Figure 2.1.2 *Phosphine ligands used by Stanley in bimetallic systems*

There are few examples in the literature that show the cooperative effect of two different metal ions in hydroformylation reactions. The addition of complexes such as $Cp_2Zr(CH_2PPh_2)_2$ or $Cp_2Zr(CH_2PPh_2)Cl$ to rhodium(I) catalyst precursors $Rh(acac)(CO)_2$, $HRhP_4$ or $HRh(CO)P_3$ [P = PPh_3 or $P(OPh)_3$] have produced good aldehyde yields in hydroformylation experiments. These zirconium complexes can be considered as functionalised phosphines.[14]

The majority of recent publications dealing with rhodium and hydroformylation describe ligand development. According to a recent book on homogeneous catalysis, the ligands currently under investigation can be classified into phosphines, phosphites, water-soluble phosphines, *P-N* ligands, and other *N*-containing ligands.[15]

Neibecher, Reau and others introduced phospholes and phosphanorbornadiene (**A** and **B**, Figure 2.1.3) in the late 1980's.[16,17,18] Hydroformylation tests with these ligands produced *n/i* ratios similar to that of triphenylphosphine, and activities of up to five times higher. A sulfonated phosphanorbornadiene (**C**, Figure 2.1.3) was successfully applied in two-phase hydroformylation of propene and 1-hexene.[19] A significant feature of this ligand is that a much lower phosphine/rhodium ratio (13.5:1) is needed than in the commonly used TPPTS systems (80:1) discussed in Chapter 1.

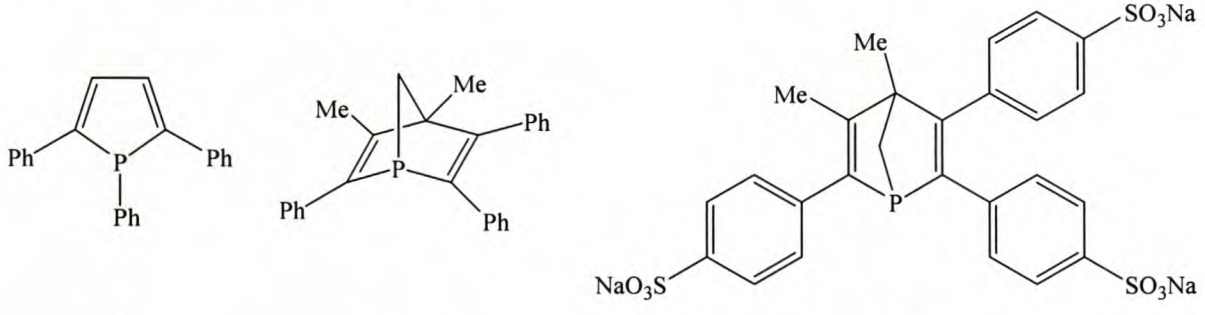

A **B** **C**

Figure 2.1.3 *Examples of a phosphole (**A**), a phosphanorbornadiene (**B**) and the sulfonated phosphanorbornadiene (**C**)*

Modification of triphenylphosphine by placing different heteroatomic groups [$-SCH_3$, $-N(CH_3)_2$, $-OCH_3$, $-CF_3$] in the *ortho* and *para* positions, yielded new phosphine ligands that have been investigated in the hydroformylation of 1-hexene and propene.[20] Selectivity towards aldehyde formation was higher when the substituents occurred in the *para* position.

Variation of the heterodonor atom in the *ortho* position of the ligand led to changes in activity and selectivity.[21] The modified ligands are strong σ-donors and exhibited higher hydroformylation activity than normal triphenylphosphine when used *in situ* with rhodium compounds. The distinct correlation between the catalytic behaviour of complexes and the structures of the ligands led to further studies. Molecular modelling was performed on the ligands to study the effect of the number of substituents on the hydroformylation reaction. Results were discussed in terms of the geometric and electronic properties of the ligands and compared to the actual results of experimental hydroformylation tests.[22] For all the ligands investigated the *n/i* ratio was higher than that obtained with triphenylphosphine due to their greater steric bulk and greater basicity.

Recent work involving triphenylphosphine-thiolate rhodium complexes also yielded good catalytic activity.[23] Different thiol precursors (Figure 2.1.4) were used to determine the correlation between the activity of the catalysts and the donor capacity of the mercaptopyrimidine ligands. An increase in basicity of the ligand corresponds with an increase in reaction rate.

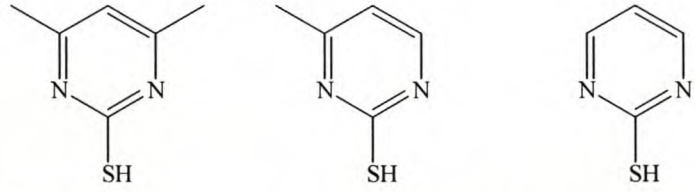

Figure 2.1.4 *Thiol precursors for the preparation of thiolate-rhodium complexes*

Studies on phosphine ligands containing heterocyclic rings were also conducted recently.[24,25] Rhodium-catalysed hydroformylation of 1-hexene was carried out with various pyrrolylphosphines (Figure 2.1.5).[14] Aldehyde yields as high as 91 % were achieved with *n/i* ratios of up to 30:1. The highest *n/i* ratios were obtained at a ligand to metal ratio of 8:1.

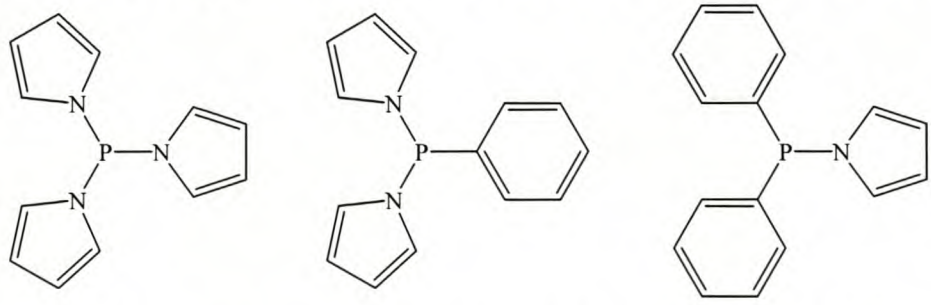

Figure 2.1.5 *Pyrrolylphosphine ligands used in hydroformylation of 1-hexene*

Due to their strong coordination to the metal centre, nitrogen-containing ligands such as amines, amides and isonitriles show lower reaction rates in the hydroformylation reaction.[26] *N*-heterocyclic carbenes are the most promising nitrogen containing ligands at present in the search for more efficient hydroformylation catalysts.

The separation of the catalyst from the products is another important aspect of the hydroformylation process. The number of commercial applications of homogeneously catalysed processes will increase enormously if the separation of the catalyst from the product becomes easier. Some of the latest work on catalyst separation are discussed by Van Leeuwen *et al.* in a recent book.[27] The use of ionic liquids as a reaction medium could solve some of the product separation and catalyst recycling problems encountered thus far. Some results obtained with the hydroformylation of olefins in ionic liquids are discussed in the next section.

1.2 Hydroformylation reactions in ionic liquids

The use of ionic liquids as solvents for cleaner syntheses and as substitutes for organic solvents has received increasing attention in recent years. Several reviews have been published[28,29,30] and a few patents registered.[31,32,33,34] Most of the investigations have concentrated on catalytic conversion with little attention being paid to the chemistry involving the catalyst.

Understanding the behaviour of a catalyst is very important in catalyst design and development. The role of $[RhCl(PPh_3)_3]$ as a catalyst in organic solvents is well understood and, therefore, Mann and Guzman chose to investigate the behaviour of this catalyst in ionic liquids.[35] Dissolving $[RhCl(PPh_3)_3]$ in 1-ethyl-3-methylimidazolium chloroaluminate(III) ionic liquid, one phosphine ligand dissociates from the rhodium centre and is protonated while *cis*-$[RhCl(\mu\text{-}ClAlCl_3)(PPh_3)_2]^-$ forms. Passing a stream of H_2 through a solution of *cis*-$[RhCl(\mu\text{-}ClAlCl_3)(PPh_3)_2]^-$ in the ionic liquid produces the stable species *trans*-$[Rh(H)(\mu\text{-}ClAlCl_3)(PPh_3)_2]^-$. This ionic species is 'fixed' in the ionic liquid resulting in no significant extraction into low polarity organic solvents.

Early studies by Parshall using platinum complexes with low-melting tetraalkylammonium salts,[36] were expanded by Wasserscheid with ionic liquids derived from pyridine.[37]

In 1995 Chauvin showed that the biphasic hydroformylation of 1-pentene with a rhodium catalyst can be achieved in $[BMIM]PF_6$.[38] An advantage of this system is the easy separation of the product form the catalyst and solvent because of the low solubility of hexanals in ionic liquids. A high turn over frequency (TOF = 333 h^{-1}) is achieved with $[Rh(acac)(CO)_2/PPh_3]$, but a small amount of the catalyst is extracted into the organic phase after completion of the reaction. Polar sodium triphenylphosphine salts can be used to prevent leaching of the transition metal catalyst. The use of TPPMS and TPPTS, however, gives rise to lower turnover numbers (59 and 103 h^{-1} respectively).

High-melting phosphonium tosylates (Figure 2.1.6) have the advantage of facilitating easy recovery of the organic product by simple decantation.[39] Hydroformylation of 1-hexene with a rhodium catalyst $[Rh_2(OAc)_4/PPh_3]$ in these tosylate salts gives aldehydes in up to 100 % yield and *n/i* ratios as high as 2.5:1. A remarkable feature is the influence that the substituents attached to the central phosphorus atom of the phosphonium salt have on the performance of the catalyst. For the same set of conditions the phosphonium salt **D** (Figure 2.1.6) affords 100 % conversion with an *n/i* ratio of 2.5:1 whereas the yield for **C** is 66 % with a ratio of 1:4.

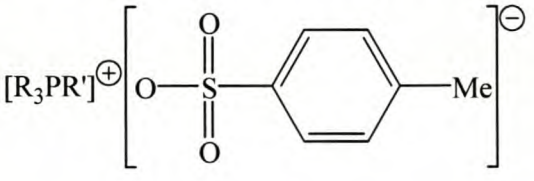

	R	R'
A	Ph	Et
B	Ph	Bu
C	Ph	Octyl
D	Bu	Et

Figure 2.1.6 *Tosylate salts used as solvents in hydroformylation*

Keim and co-workers used $[BMIM]PF_6$ as the solvent in the hydroformylation of methyl-3-pentenoate with $[Rh(acac)(CO)_2]$ and phosphine ligands.[40] Methyl-3-pentenoate and the ionic liquid form a monophasic reaction mixture. The products are isolated by distillation under reaction conditions. A comparative experiment in toluene shows the significant effect that the ionic liquid has on the activity and stability of the catalyst. The catalyst is stabilised by the

ionic liquid under the thermal stress of the distillation process and remains active after 10 hydroformylation experiments, whereas in toluene the catalyst activity is reduced to zero after only four experiments.

A different approach is to use supercritical fluids in continuous flow hydroformylation reactions to transport the substrate, CO and H_2 to the catalyst that is dissolved in an ionic liquid, and extract the product from the reaction mixture. This method of product separation is advantageous when the catalyst is thermally sensitive. In a recent publication supercritical CO_2 was used as a co-solvent with [BMIM]PF_6 in the hydroformylation of 1-octene.[41] The catalyst precursor used in this experiment was $[Rh_2(OAc)_4]$ and [1-propyl-3-methylimidazolium]$_2$[$PhP(C_6H_4SO_3\text{-}3)_2$]. This method of product separation proved to be very effective since only a very small amount of rhodium (< 0.06 % of the Rh loaded) was found in the products.

Although different ionic liquids have been designed and tested in biphasic hydroformylation reactions, ligand design plays an equally important role. Olivier-Bourbigou and co-workers tested a range of different ionic liquids as solvents for the hydroformylation of 1-hexene with rhodium catalysts.[42] The results showed that TOF's, but not the *n/i* ratios, are influenced by the nature of the ionic liquid. Their results include further proof that leaching of the rhodium can be minimised by modification of the phosphorus ligand with cationic (guanidinium or pyridinium) or anionic (sulfonate) groups. The same type of ligands were also used in the hydroformylation of 1-octene in [BMIM]PF_6.[43] The resulting rhodium catalyst proved to be well immobilised in the ionic liquid as only very small amounts of rhodium were found to leach into the organic layer. Activity of the catalyst improves in the third consecutive reaction, probably due to the preformation time needed for the formation of the active catalyst. The results confirm that the modification of phosphine ligands is a very efficient method of immobilisation of the rhodium metal in the ionic liquid.

High catalyst activity, high selectivity and no detectable catalyst leaching was achieved with phosphine substituted cobaltocenium salts as ligands in the rhodium catalysed hydroformylation of 1-octene in [BMIM]PF_6.[44] 1,1′-Bis(diphenylphosphino)cobaltocenium hexafluorophosphate proved to be an especially good ligand, achieving a turn over frequency of higher than 800 h^{-1} when used with $[Rh(acac)(CO)_2]$ in [BMIM]PF_6.

Leaching can also be minimised by the use of ligands bearing a similar structure to the cation of the ionic liquid. Rhodium catalysts with 2-imidazolium phosphine ligands successfully catalyse the hydroformylation of 1-octene in ionic liquids.[45] Two different ligand types (Figure 2.1.7) were used in catalytic tests with $[Rh(acac)(CO)_2]$ in $[BMIM]PF_6$. Ligand **A** gave a TOF of 552 h^{-1} while **B** yielded only 51 h^{-1}. The close proximity of the positive charge to the phosphorus atom is a possible reason for the enhanced catalytic activity achieved with **A**.

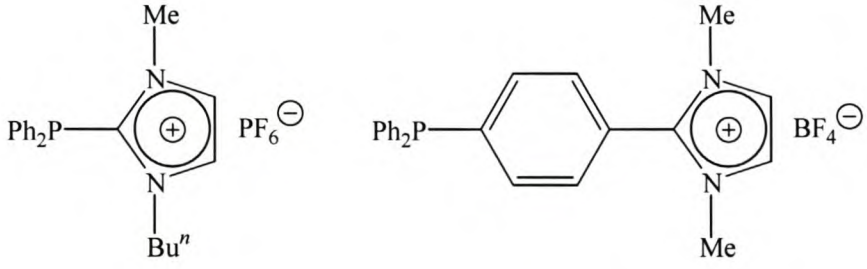

A **B**

Figure 2.1.7 *2-Imidazolium phosphine ligands used in the hydroformylation of 1-octene*

Complexes with other ligand systems have also been tested in ionic liquids. The chiral complex (η^4-1,5-cyclooctadiene)(2-menthyl-4,7-dimethylindenyl)rhodium(I) furnishes the hydroformylation of 1-hexene and 1-dodecene in a range of ionic liquids (Figure 2.1.8).[46] Conversions as high as 100 % and selectivities toward aldehydes of up to 57 % are reported.

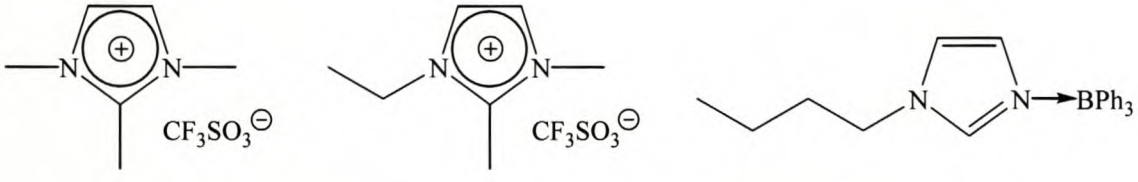

Figure 2.1.8 *Three different ionic liquids used as solvents for hydroformylation reactions*

Heterocyclic ligand types have the potential to facilitate immobilisation of rhodium complexes in ionic liquids. This warrants a discussion of known rhodium(I) complexes with ligands containing heterocyclic units.

2 Carbene complexes of rhodium

In the first chapter *N*-heterocyclic carbenes were discussed and their excellent properties in catalysis mentioned. The similarity between *N*-heterocyclic carbene ligands and ionic liquids was also noted and is illustrated in Figure 2.2.1. A brief discussion of the history of rhodium(I) carbene complex chemistry as well as different synthetic routes to prepare these complexes follows and should serve as an adequate introduction.

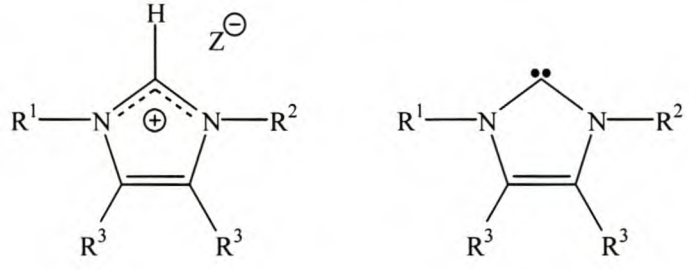

Figure 2.2.1 *Simplified figure of an ionic liquid and an* N*-heterocyclic carbene*

Carbene complexes of almost all transition metals are known. Syntheses of all these complexes are based on three main routes. The most recent route involves the complexation of the free, pre-isolated carbene. The other two routes involve cleavage of an electron rich olefin and the *in situ* deprotonation of ligand precursors. Free carbenes can substitute a range of other ligands such as phosphines or carbon monoxide. The three main synthetic routes as well as other less common synthetic methods, *e.g.* ligand transfer reactions, are summarised in a recent comprehensive review.[47]

The first heterocyclic carbene complexes of rhodium(I) were synthesised by Lappert and co-workers in 1972.[48] The carbene complexes were isolated as the intermediate species in rhodium(I)-catalysed dismutation of electron rich olefins (Figure 2.2.2). The yellow and orange carbene complexes were characterised by infrared and ^{31}P NMR spectroscopy. The complexes were isolated from xylene after refluxing the reaction mixture for two hours. The complexes, containing a carbonyl ligand as well as a phosphine and a carbene ligand, exhibit *trans*-configurations. According to the proposed mechanism the reaction proceeds *via* a rhodium(III) complex.

Lappert continued this work on rhodium carbene complexes and published results about the stereochemistry and mechanism of nucleophilic displacement reactions,[49] restricted rotation

about the Rh-$C_{carbene}$ bond,[50] *cis*-chelating biscarbene complexes,[51] and optically active complexes.[52] Similar carbene complexes, for example [RhCl(cod){CN(Me)CH_2CH_2N(Me)}], were tested as catalysts for hydrogenation and hydrosilylation.[53] From a study comprising the synthesis and characterisation of a wide range of rhodium(I) carbene complexes of seven distinctly different types, including biscarbene complexes and complexes containing both a phosphine and a carbene ligand,[54] Lappert concluded in 1984 that *N*-heterocyclic carbenes have a greater *trans* influence than PPh_3.

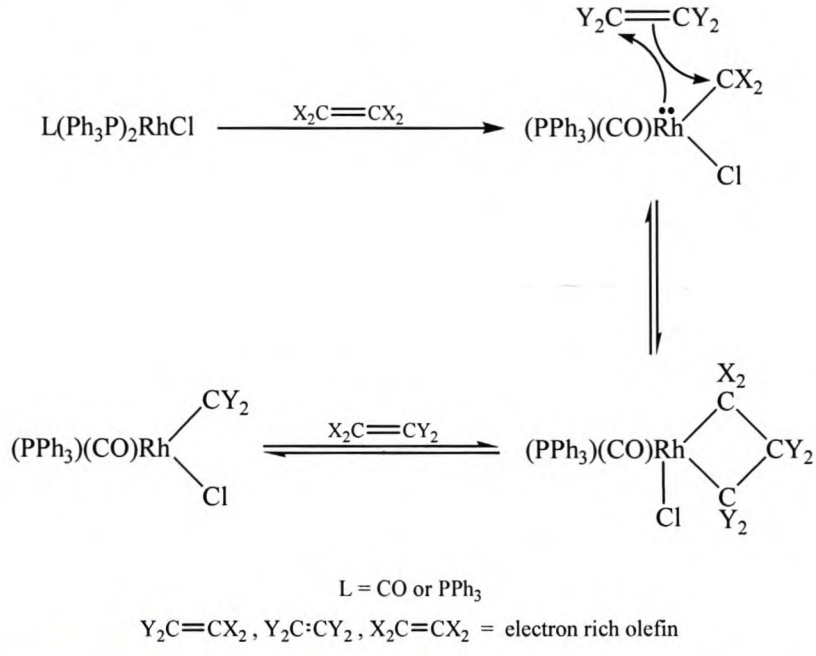

Figure 2.2.2 *Proposed mechanism for rhodium(I) catalysed dismutation of electron rich olefins*

This group was also able to prepare an orange-yellow chelating biscarbene complex (Figure 2.2.3).[51] They further extended their work to the preparation of rhodium(I) complexes containing three carbene ligands [RhCl{CN(R)CH_2CH_2N(R)}$_3$] where R = Et or CH_2Ph.[55] In one instance, with R = CH_2Ph, the researchers succeeded in displacing one carbene ligand with carbon monoxide. This was achieved by passing a stream of carbon monoxide through a dichloromethane solution of the complex at room temperature for a short period of time (5 minutes). The driving force for this substitution reaction is probably the alleviation of steric strain.

Dixneuf and co-workers used the same reaction route in the preparation of rhodium carbene complexes with 2-methoxyethyl substituents on the nitrogen atoms. These complexes proved to be effective catalysts for cyclopropanation of diazoalkane derivatives with styrene, giving yields of up to 91 %.[56] It was the discovery of stable free carbenes, however, that caused a renaissance in carbene coordination chemistry.

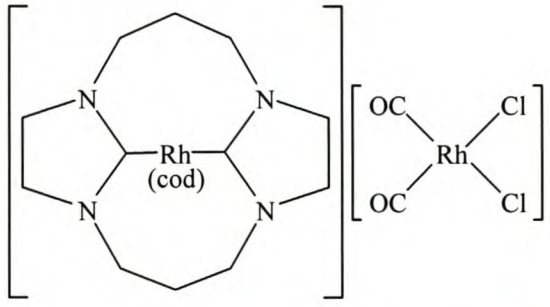

Figure 2.2.3 *The biscarbene rhodium(I) complex synthesised by Lappert*

Arduengo and co-workers realised Wanzlick's dream[57] by preparing and characterising the first electronically stabilised, crystalline, nucleophilic carbene (Figure 2.2.4): simple deprotonation of the corresponding imidazolium salt by either sodium hydride in THF in the presence of a catalytic amount of dimethyl sulfoxide, or *tert*-butoxide in THF, followed by recrystallisation from toluene, affords kinetically and thermodynamically stable colourless crystals. [58]

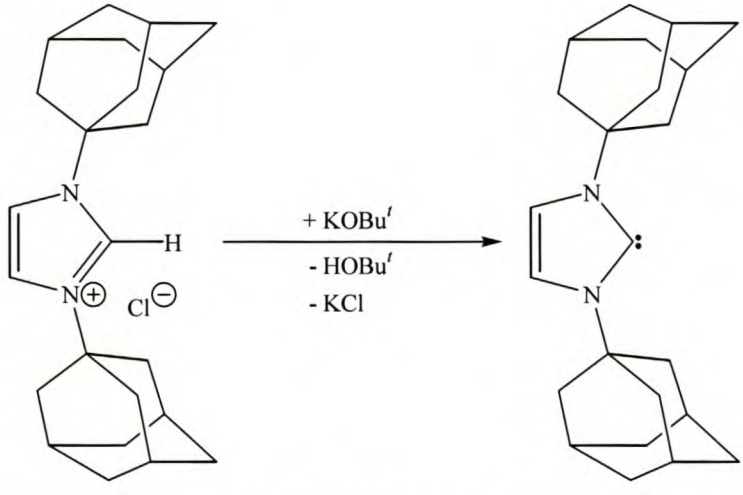

Figure 2.2.4 *Synthesis of the first stable, crystalline carbene*

The synthesis and subsequent electronic and structural information obtained from the isolation of more free carbenes[59] led to discussions about the steric and electronic effects on the stability of carbenes (see Chapter 1).[60,61,62]

Herrmann and co-workers showed that the deprotonation of imidazolium salts occurs much faster when liquid ammonia is used as the solvent.[63,64] Another method for the preparation of carbenes was introduced in 1993 by Kuhn and Kratz.[65] The reaction of 2,3-dihydro-1*H*-imidazol-2-thiones with potassium in boiling THF affords carbenes in yields of more than 90 %. Enders and co-workers reported the preparation of 1,3,4-triphenyl-4,5-dihydro-1*H*-1,2,4-triazol-5-ylidene by the thermal elimination of methanol *in vacuo* (0.1 mbar) at 80 °C.[66]

Since the discovery by Arduengo, a large number of publications on stable carbenes and metal carbene complexes and their activity in catalysis have appeared. This includes a number of review articles.[47,67,68,69,70] For the purpose of this work only the rhodium(I) carbene complexes will be discussed.

The complexation of free carbenes to a metal centre has the advantage that a large variety of metal precursors, without special requirements regarding the ligand sphere and oxidation state, can be used. Nucleophilic *N*-heterocyclic carbenes (NHC's) can cleave dimeric rhodium complexes such as $[RhCl(cod)]_2$ and $[RhCl(CO)_2]_2$ (Figure 2.2.5).[63,64,71,72,73]

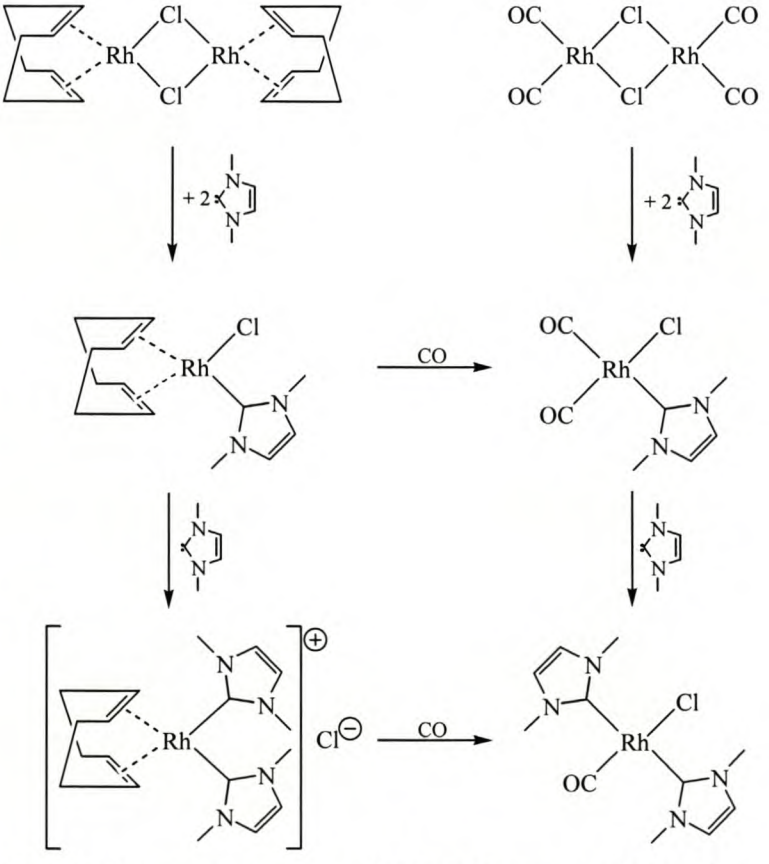

Figure 2.2.5 *Carbene complexes of rhodium(I) prepared from free carbenes*

Ligand exchange also produces carbene complexes. Cationic biscarbene complexes, *cis*-[Rh(cod)(NHC)$_2$]Cl, can be obtained by adding four mole equivalents of carbene to the precursor compound, [RhCl(cod)]$_2$, resulting in the exchange of a chloride for a carbene ligand.[63,74] Addition of two equivalents of carbene ligand to [RhCl(CO)$_2$]$_2$ yields the *trans*-complex, *trans*-[RhCl(CO)(NHC)$_2$], the result of CO displacement.[63] A *cis/trans*-isomerisation is observed when *cis*-[Rh(cod)(NHC)$_2$]Cl is treated with carbon monoxide in methylene chloride to yield *trans*-[RhCl(CO)(NHC)$_2$] (Figure 2.2.5).[63,74] Phosphine ligands can be exchanged for *N*-heterocyclic carbene ligands (Figure 2.2.6). Treatment of Wilkinson's catalyst with an *N*-heterocyclic carbene gives the complex [RhCl(NHC)(PPh$_3$)$_2$]. Passing a stream of CO through a THF solution of the yellow complex [RhCl(IMes)(PPh$_3$)$_2$] yields the pale yellow *trans*-[RhCl(CO)(IMes)(PPh$_3$)] {IMes = 1,3-bis(2,4,6-trimethylphenyl)-2,3-dihydro-1*H*-imidazol-2-ylidene}. A crystal structure determination confirmed that the carbene ligand is situated in the *trans* position relative to the phosphine ligand.[75]

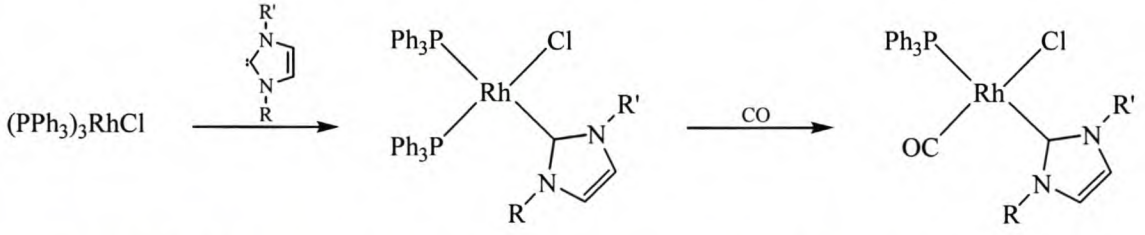

Figure 2.2.6 *Preparation of rhodium(I) carbene complexes by ligand displacement*

In some instances the free carbenes are unstable or difficult to handle. Brønsted-basic anions on the rhodium precursor can lead to *in situ* deprotonation. Coordinating anions of the azolium salts, of which halides are an example, are incorporated into the metal complex. This method was introduced by Wanzlick in the preparation of biscarbene mercury complexes from mercury(II) diacetate.[76] High yields were obtained from the reaction of an imidazolium salt with alkoxide[77] and acetylacetonate[63] rhodium precursor compounds (Figure 2.2.7). Deprotonation of imidazolium salts in the presence of [RhCl(cod)]$_2$ with lithium *tert*-butoxide, or sodium hydride, in THF also yields [RhCl(cod)(NHC)].[68]

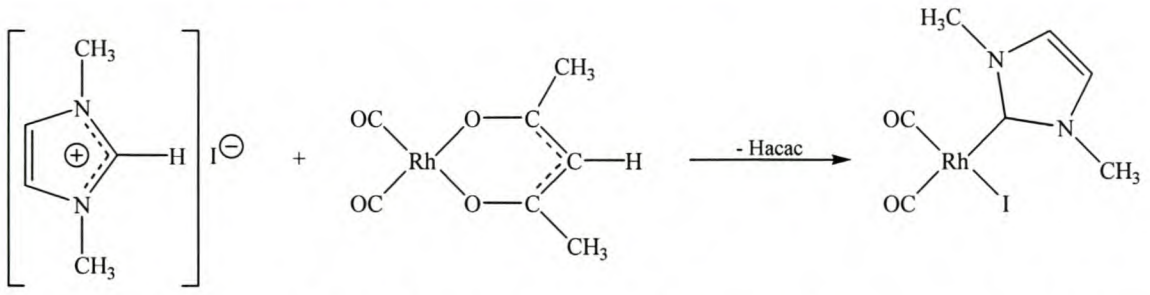

Figure 2.2.7 *Synthesis of a rhodium(I) carbene complex via the elimination of acetylacetone*

A few investigations involving carbene transfer between metal ions to generate new carbene species have been reported. Recent reports show that rhodium(I) carbene complexes can be prepared by ligand transfer reactions in high yields under mild conditions.[78,79] The reaction of pentacarbonyl tungsten carbene complexes with $[RhCl(CO)_2]_2$ yield biscarbene complexes following the substitution of one of the rhodium carbonyl ligands. These complexes in the *trans* configuration were isolated as yellow powders and in one instance a yellow liquid. With *N*-allyl substituents on the carbene ligand, a π-coordinated biscarbene complex was isolated (Figure 2.2.8).

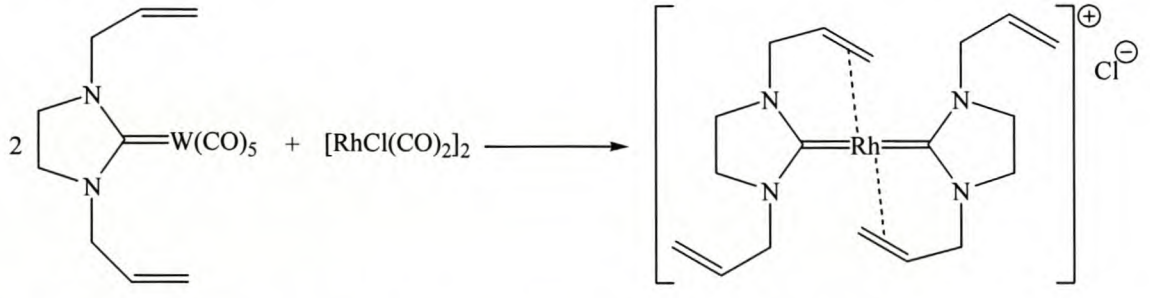

Figure 2.2.8 *Preparation of a π-coordinated biscarbene by a ligand transfer reaction*

N-heterocyclic carbene complexes are promising catalysts because carbene ligands do not easily dissociate from the metal centre and excess ligand is unnecessary for catalytic reactions. Chiral 2,3-dihydro-1*H*-imidazol-2-ylidene complexes can therefore be expected to be suitable catalysts for asymmetric homogeneous catalysis. For this reason Herrmann and co-workers synthesised chiral *N*-heterocyclic carbenes and the corresponding rhodium(I) complexes.[71,72] After two weeks under hydrosilylation reaction conditions, these complexes showed no signs of decomposition. Solutions of rhodium(I) carbene complexes are not oxygen or moisture sensitive, emphasising their potential application in catalysis.

The same group of researchers also studied functionalised *N*-heterocyclic carbenes and their corresponding complexes of rhodium and other transition metals. Although it has been shown that complexes of nickel(II)[80] and chromium[81] can be isolated with chelating di-*N*-heterocyclic carbene ligands, the same type of carbenes yield dinuclear complexes with rhodium(I).[63] Other *N*-functionalised carbenes do have the potential to be chelating ligands (Figure 2.2.9). Of the four different carbene ligands only 2-diethylaminoethyl-3-methyl-2,3-dihydro-1*H*-imidazol-2-ylidene and 2-ethylaminoethyl-3-methyl-2,3-dihydro-1*H*-imidazol-2-ylidene attach successfully to rhodium(I) complexes albeit without chelation.[64]

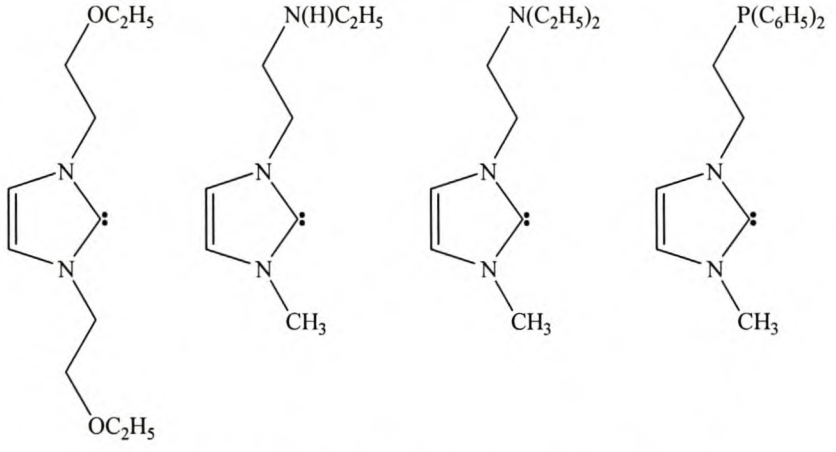

Figure 2.2.9 *Four functionalised carbene ligands*

In 1998 the synthesis of a chiral, *N*-functionalised carbene ligand with an oxazoline substituent was published.[68] This carbene ligand was coordinated to rhodium(I) and the chelating coordination was ensured by removal of the chloride with thallium hexafluorophosphate in THF (Figure 2.2.10).

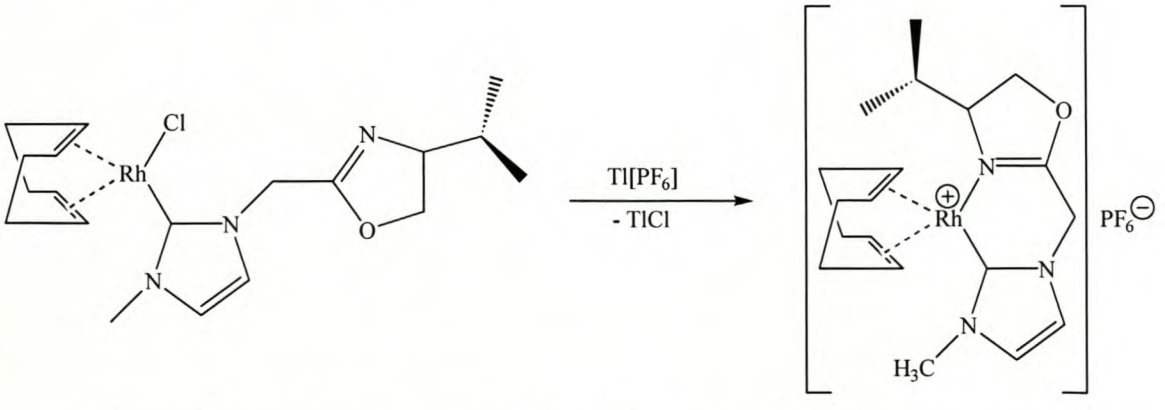

Figure 2.2.10 *Chelating coordination of the oxazoline on the side chain was ensured by the removal of the chloride ligand*

Recently the first example of intramolecular activation of a C-H bond in a functionalised *N*-heterocyclic carbene rhodium complex was reported.[82] Close contact between the rhodium centre and the proton in the 3-position of the pyridine substituent occurs in the crystal structure. Addition of $Na[B\{3,5\text{-}C_6H_3(CF_3)_2\}_4]$ in ether produces the chelating complex in quantitative yield (Figure 2.2.11).

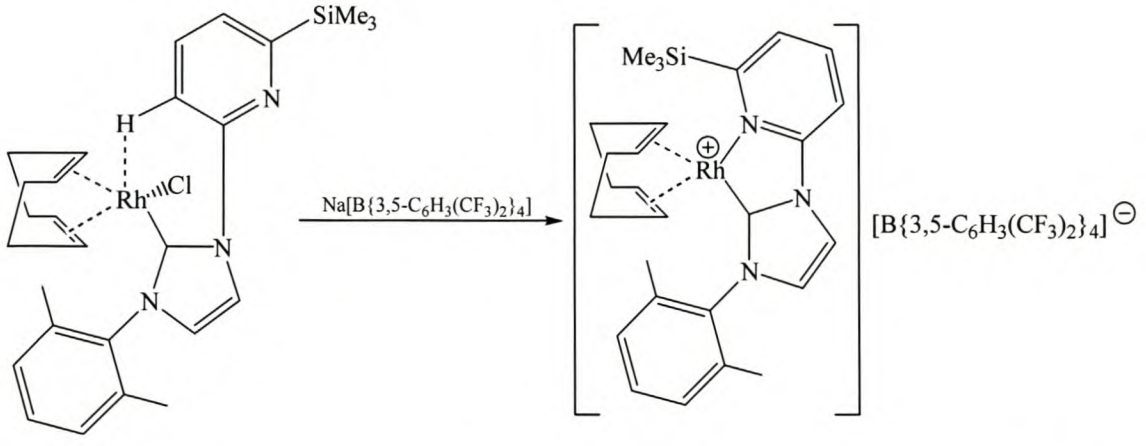

Figure 2.2.11 *C-H activation in an* N*-heterocyclic carbene complex of rhodium*

Novel water soluble *N*-functionalised carbene complexes of rhodium(I) were also prepared (Figure 2.2.12).[77] The metal-carbon bond remains intact when reactions are performed on the side chains. The stability and solubility of these complexes in water can be exploited in biphasic catalysis like the Ruhrchemie/Rhône-Poulenc process.

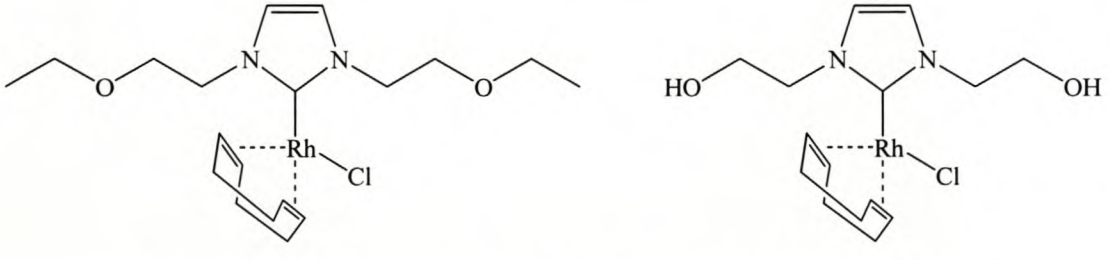

Figure 2.2.12 *Stable water-soluble rhodium carbene complexes*

3 Thiourea complexes of rhodium

In Chapter 1 a short summary of rhodium catalysed hydroformylation with ligands bonded to rhodium through a sulfur atom is given. According to the Pearson classification, rhodium can be classified as a transition metal with soft character.[83] Therefore, ligands containing a soft

donor atom, like sulfur, will form relatively stable complexes with rhodium. Rhodium complexes with thiolate ligands were recently reported as active catalyst precursors for the hydroformylation of 1-heptene.[84] High conversions were noted, but additional phosphine was necessary to increase the aldehyde yield.

This discussion is limited to rhodium complexes with thiourea ligands, as the resulting complexes are similar to the complexes prepared in this investigation. The thiourea ligand is bonded to rhodium by a σ-bond, similar to the rhodium-phosphine bond. Recent work involving rhodium and this ligand type has almost exclusively been concerned with catalyst design, the aim being to combine the easy recovery of solid catalysts with the high activity and selectivity of soluble complexes.

In their search for ancillary ligands for catalytic processes, Tiripicchio and co-workers found that thiourea functionalised xerogels are capable of bonding to rhodium(I).[85] Two benzoylthiourea xerogels, $4.5SiO_2 . SiO_{3/2}(CH_2)_3NHC(S)NHC(O)Ph$ (XGbztu) and $SiO_{3/2}(CH_2)_3NHC(S)NHC(O)Ph$ (XGbztu*), were prepared and bonded to the rhodium(I) species $[RhCl(cod)]_2$ and $[RhCl(CO)_2]_2$. The rhodium composite materials are very active, insoluble and recoverable catalysts for the hydroformylation of styrene. After the first catalytic cycle of the cyclooctadiene complexes, the cyclooctadiene was substituted by two carbonyl ligands. A rhodium complex with the thiourea ligand $CH_3(CH_2)_3NHC(S)NHC(O)Ph$ (Hbztu) was prepared and studied as a model for the anchored complexes (Figure 2.3.1).

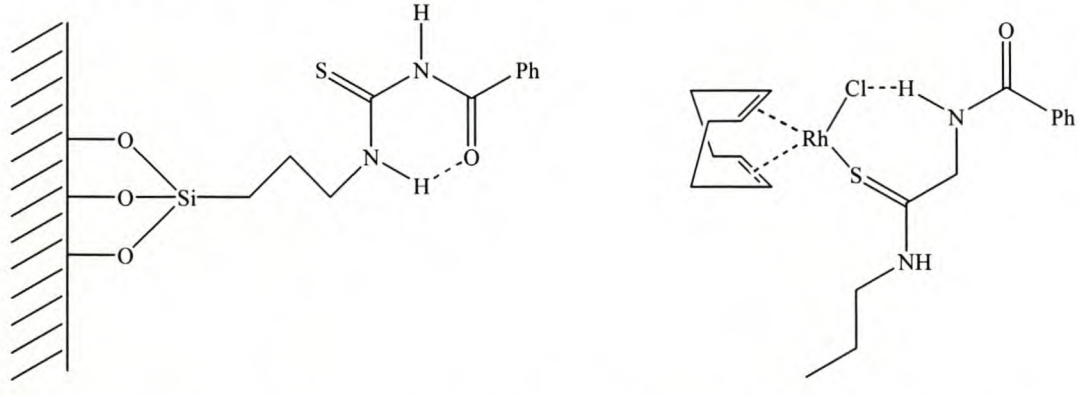

Figure 2.3.1 *A pictorial view of the tethered benzoylthiourea XGbztu and the model complex [RhCl(cod)(Hbztu)]*

Tiripicchio extended the study of the catalytic activity of thiourea-functionalised silica xerogels to hydroformylation reactions.[86] Other siloxane materials, $5SiO_2 . SiO_{3/2}(CH_2)_3NHC(S)NHPh$ (XGpztu), $SiO_{3/2}(CH_2)_3NHC(S)NHPh$ (XGpztu*) and *para*-$\{SiO_{3/2}(CH_2)_3NHC(S)NH\}_2C_6H_4$ (XGphenditu*), were prepared as well as the corresponding rhodium species. Again, the corresponding thiourea complexes served as models for the surface anchored species. Hydroformylation tests were carried out at 80 °C for 10 to 12 hours at a pressure of 60 bar. The conversion of the styrene amounts to approximately 99 % in all the experiments. The *n/i* ratio remains constant in consecutive catalytic runs for the homogeneous rhodium complexes (≈ 0.5), whereas the ratio decreases for the anchored complexes.

In a further expansion of this work, the synthesis of the bifunctional ligand $PhNHC(S)NHCH_2CH_2PPh_2$ (Ptu) that has the potential to be a bidentate ligand was undertaken.[87] The complexes [Rh(cod)(Ptu)]X (X = Cl, PF_6) and $[Rh(cod)(Ptu)]_2[CoCl_4]$ were characterised and used in the hydroformylation of styrene as model systems for the corresponding xerogel anchored complexes. [Rh(cod)(Ptu)]Cl proved to be completely inactive, while the complexes with the non-coordinating anions gave high conversions to aldehydes (at least 96 %).

Another illustration of the strength of the bond between rhodium and thiourea ligands can be observed in the recovery of rhodium-containing catalysts. In a recent publication silica-based chelating ligands with a thione functionality and an *N*-donor atom were tested in the recovery of rhodium and other metals.[88] Stripping the rhodium off the ligands proved to be very difficult, with a variety of stripping agents being used due to the strong Rh-S bond.

Rhodium thiourea complexes have also been used as catalysts in other reactions, for instance the asymmetric reduction of carbonyl complexes.[89] However, ruthenium proved to be a better catalyst both in terms of activity and selectivity. Lemaire and co-workers studied thioureas and a rhodium(I) precursor in the enantioselective hydride transfer reduction of acetophenone.[90] This study proved that thioureas could be suitable ligands in complexes used for asymmetric catalysis. A range of ligands was tested and dithioureas turned out to be the ligands of choice, providing significant enantioselection.[91] The experimental work was followed by theoretical studies in which it was proposed that, of the three possible

coordination modes of a thiourea ligand to a metal (Figure 2.3.2), the metal atom is bonded to a thiourea ligand through the sulfur atom (**B** in Figure 2.3.2).[92] This theoretical proposition is confirmed by the crystal structure of thione complexes such as [RhCl(cod)(Hbztu)].[85]

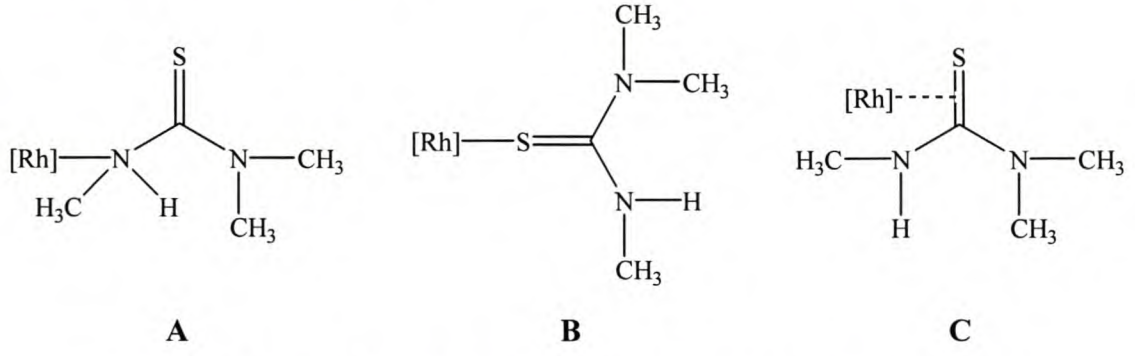

A **B** **C**

Figure 2.3.2 *Possible coordination modes of thiourea ligands to rhodium*

4 Imine complexes of rhodium

Complexes with nitrogen donor ligands have been used as pre-catalysts in numerous catalytic processes.[93] In the vast majority of complexes with nitrogen donor ligands the *N*-donor ligands form part of a chelating ligand system involving other donor atoms such as C, O, P, and S. Very few hydroformylation reactions catalysed by complexes containing nitrogen-donor ligands have been reported.

Rhodium complexes with ligands containing pyrazolato moieties were tested as possible catalyst precursors for the hydroformylation of cyclic and acyclic olefins. Results obtained with monorhodium and dirhodium complexes with pyrazolate and 3,5-dimethylpyrazolate ligands were reported.[94] 1-Dodecane and cyclohexene are converted to the corresponding aldehydes in yields of greater than 95 % at a reaction temperature of 120 °C and CO and H_2 pressures of 28 atmospheres. At lower temperature (70 °C – 90 °C) the monorhodium complexes are substantially less active than the dirhodium complexes. In the hydroformylation of 1-heptene with rhodium complexes containing pyrazolato ligand systems added phosphine improves the selectivity[95] and shortens the induction period[96] of the pyrazolato precursor catalysts.

Although the reaction between $[RhCl(cod)]_2$ and imine ligands was mentioned in a 1975 publication, the resulting mononuclear complexes, [RhCl(cod)(imine)], were not properly

characterised.[97] Eight years later Müller and Stock published results obtained when 1-methylimidazole and 1-vinylimidazole were added to the binuclear $[RhCl(cod)]_2$.[98] Characterisation of the yellow products was difficult because peaks in the proton NMR spectrum exhibited broadening and coalescence, and the products decomposed to the starting compounds when electron impact mass spectrometry was attempted.

In the same year, Siedle and co-workers reported the synthesis of rhodium(I) coordination complexes obtained by cleavage of the halide bridge in $[RhCl(cod)]_2$ and $[RhCl(CO)_2]_2$ with imine ligands. Phenazine and related heterocyclic ligands (Figure 2.4.1) were used.[99] An orange bimetallic complex was obtained in high yield when the same stoichiometric amounts of phenazine and $[RhCl(CO)_2]_2$ were combined.

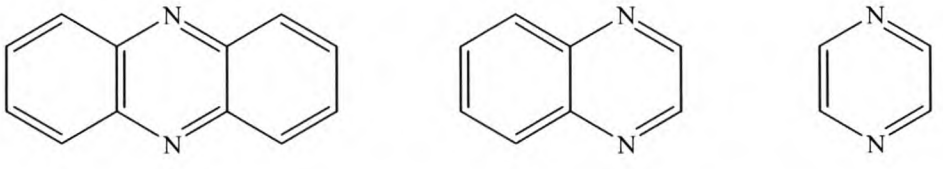

A **B** **C**

Figure 2.4.1 *Phenazine (**A**), quinoxaline (**B**) and pyrazine (**C**)*

Mestroni and co-workers studied rhodium(I) complexes with substituted 1,10-phenanthroline ligands as monodentate and bidentate imine ligand systems.[100] A correlation between the catalytic activity and the pK_a of the ligand exists for the unhindered methyl-substituted species, but not for the hindered species. Infrared studies of the ν(CO) vibrations can serve as a measure of the electron donor-acceptor properties of the ligands in order to discriminate between their steric and electronic properties. A higher value for the A_1 vibration mode corresponds to higher activity of the catalyst.

Other examples of rhodium(I) complexes with imine ligands include the air-stable complexes (chloro)(η^4-1,5-cyclooctadiene)(1-methyl-1*H*-imidazole)rhodium(I) and *cis*-(chloro)(dicarbonyl)(1-methyl-1*H*-imidazole)rhodium(I).[101] The carbonyl complex forms in a yield of 84 % when a stream of carbon monoxide is bubbled through a dichloromethane solution of the cyclooctadiene complex. Cationic complexes with bidentate imine ligands containing benzothiazolyl functionalities were described recently[102] and are tested for activity in hydroformylation reactions in this study.

5 Aims of this study

The preparation and characterisation of novel rhodium(I) complexes with potential hydroformylation activity are two of the major goals for the work described in this chapter. In order to restrict the solubility of catalysts to the ionic liquids in the solvent/substrate-mixture during hydroformylation, it was attempted to prepare complexes bearing ligands with heterocyclic structures similar to that of the cations in ionic liquids.

Heterocyclic carbenes, being a relatively new ligand type for catalyst preparation, were an obvious choice in the light of previous experience in our laboratory. Other heterocyclic ligand systems considered included thiones and phosphine ligands that carry heterocyclic groups. It was also planned to prepare rhodium complexes, to which various combinations of ligands were coordinated, in order to compare the different ligands under similar hydroformylation conditions and also to consider how they mutually influence each other when simultaneously coordinated.

The new complexes should be investigated as pre-catalysts for the hydroformylation of 1-hexene under a chosen set of conditions. Reaction conditions should be varied to determine the influence that such changes have on the catalytic activity of the complexes.

6 Results and discussion

Addition of a donor ligand, L, to the dinuclear rhodium species $[RhCl(cod)]_2$ and $[RhCl(CO)_2]_2$ led to the cleavage of the Rh-Cl bond and the formation of mononuclear rhodium(I) complexes, [RhCl(cod)L] and $[RhCl(CO)_2L]$, respectively. Phosphine ligands like PPh_3, Arduengo-type free carbenes, thiones and imines were found to initiate this type of reaction forming stable products.

6.1 General discussion on the preparation of rhodium(I) complexes

6.1.1 Carbene complexes

The rhodium(I) carbene complexes discussed in this chapter were prepared by either splitting a binuclear rhodium species symmetrically at the $(\mu\text{-}Cl)_2$ bridge, or substituting another ligand

e.g. chloride. Such methods of preparation also used in this study have been described in another context in other published papers or patents.

The free carbenes were prepared either by deprotonation of imidazolium salts with KO^{t}Bu, as previously described by Arduengo,[58] or by the treatment of 2,3-dihydro-1*H*-imidazol-2-thiones with potassium in boiling THF.[65] Known carbene ligands were used in this study to prepare new rhodium complexes. In a few instances carbene ligands with two different substituents at the nitrogen atoms were used in order to obtain a ligand partly mimicking the cation of an ionic liquid.

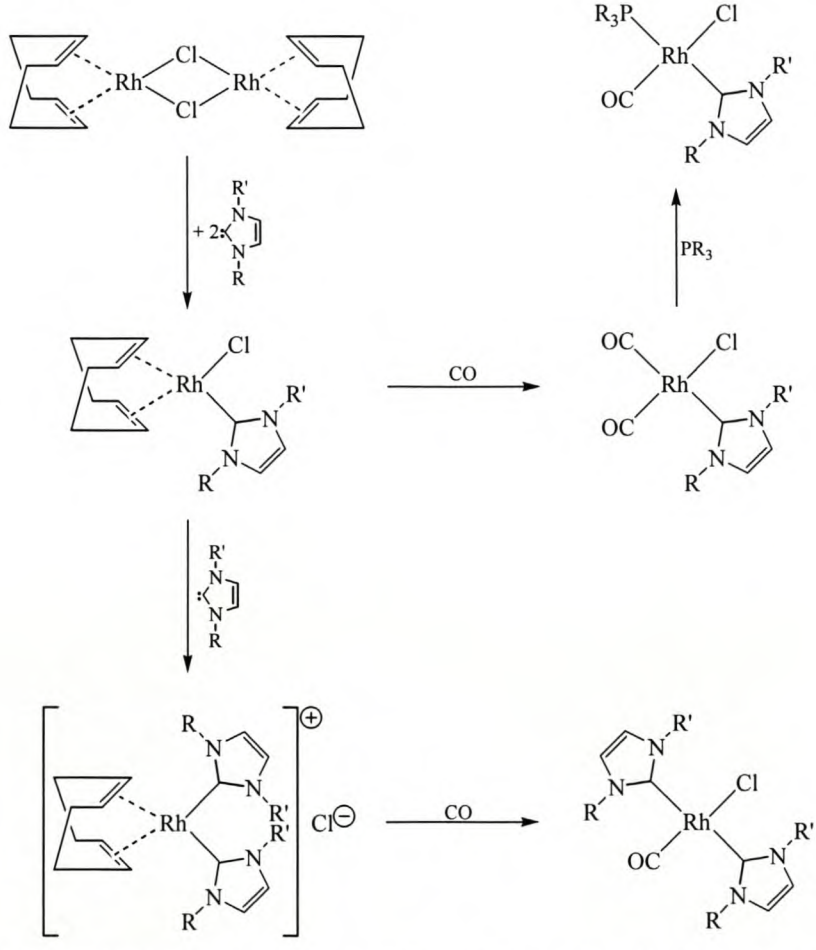

Figure 2.6.1 *Preparation of rhodium(I) carbene complexes from [RhCl(cod)]$_2$*

Compared to the reaction conditions (80 °C to 140 °C) required for the preparation of rhodium(I) carbene compounds from electron-rich olefins,[54] the conditions for the preparation of the free carbene ligand and subsequent synthesis of the rhodium complexes are very mild. In a typical preparation of a rhodium carbene complex, a solution of the free carbene ligand in THF is added to a solution of the rhodium starting material in the same solvent at room

temperature. The products (Figure 2.6.2) were generally purified by flash chromatography on SiO_2.

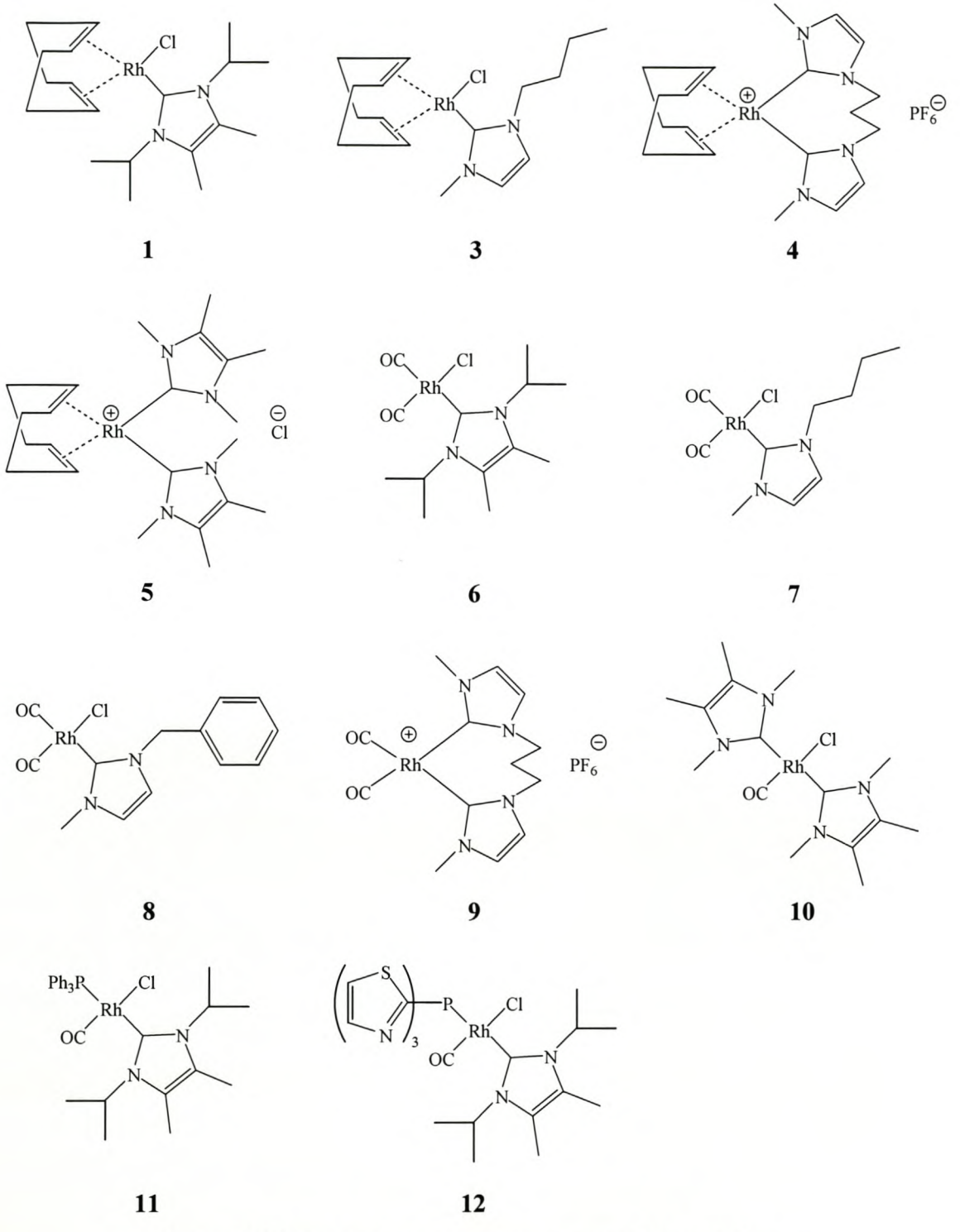

Figure 2.6.2 *New carbene complexes discussed in this chapter*

The two easily accessible starting materials, $[RhCl(cod)]_2$ and $[RhCl(CO)_2]_2$, were prepared using published methods.[103] The cyclooctadiene ligand in the complexes [RhCl(cod)(NHC)]

and $[Rh(cod)(NHC)_2]Cl$ (NHC = heterocyclic carbene, Figure 2.6.1) can be readily substituted with carbon monoxide by bubbling the gas through methylene chloride solutions of the carbene complexes at room temperature, yielding the di- and mono-substituted carbonyl complexes *cis*-$[RhCl(CO)_2(NHC)]$[73] and *trans*-$[RhCl(CO)(NHC)_2]$[74] respectively. The addition of phosphine ligands (PPh_3 or tri{2*H*-thiazol}phosphine[104]) to *cis*-$[RhCl(CO)_2(NHC)]$ produced *trans*-$[RhCl(CO)(NHC)(PR_3)]$ in high yields. The rhodium(I) complexes (Figure 2.6.2) were purified by selective extraction of the starting compounds with either pentane or ether. Interesting NMR results (see Section 6.3.1) prompted the synthesis of (pentacarbonyl)(1,3-diisopropyl-4,5-dimethyl-2,3-dihydro-1*H*-imidazol-2-ylidene)tungsten(0) (**2**) to compare the signals observed for the diisopropyl methyl groups with those observed for chloro(cyclooctadiene)(1,3-diisopropyl-4,5-dimethyl-2,3-dihydro-1*H*-imidazol-2-ylidene)rhodium(I) (**1**).

6.1.2 Thione complexes

Three different thiones were used to prepare this class of complexes. The two heterocyclic thione ligands, 1,3,4,5-tetramethyl-2,3-dihydro-1*H*-imidazol-2-thione and 1,3-diisopropyl-4,5-dimethyl-2,3-dihydro-1*H*-imidazol-2-thione, were prepared as described in the literature.[65] *N*,*N*-dimethylthioformamide, the other thiourea ligand used, was purchased from Aldrich and used without further purification. This ligand was chosen to determine its reactivity in the coordinated form.

Cyclooctadiene rhodium(I) thione complexes were prepared using the same method as was used for the preparation of the carbene complexes mentioned earlier. The thione ligand was added to a solution of the starting compound $[RhCl(cod)]_2$ in THF at room temperature. Displacing the cyclooctadiene ligand with carbon monoxide from the mononuclear thiourea complexes is again possible, but gave very low yields. The use of $[RhCl(CO)_2]_2$ as a starting material with the added thiourea ligand in stoichiometric amounts produced almost quantitative yields at room temperature. The products were purified by either flash chromatography or selective extraction of the starting compounds.

The addition of PPh_3 to a solution of $[RhCl(CO)_2L]$ (L = thiourea) in THF at room temperature produced *trans*-$[RhCl(CO)(PPh_3)L]$ as a yellow complex in high yield. With an

excess of thione, only a very low percentage of $[RhCl(CO)_2L]$ was converted to $[RhCl(CO)L_2]$. The addition of trimethylamine oxide to the reaction mixture in order to affect the expulsion of a carbon monoxide ligand (as CO_2, Figure 2.6.3), followed by stirring for a few days, yielded the desired complexes in satisfactory yields. Trimethylamine oxide and similar compounds affording labile CO substituted products, have been used to remove carbonyl ligands from various metals.[105,106,107,108] The same procedure was followed to prepare [RhCl(CO)(NHC)L] (L = thione).

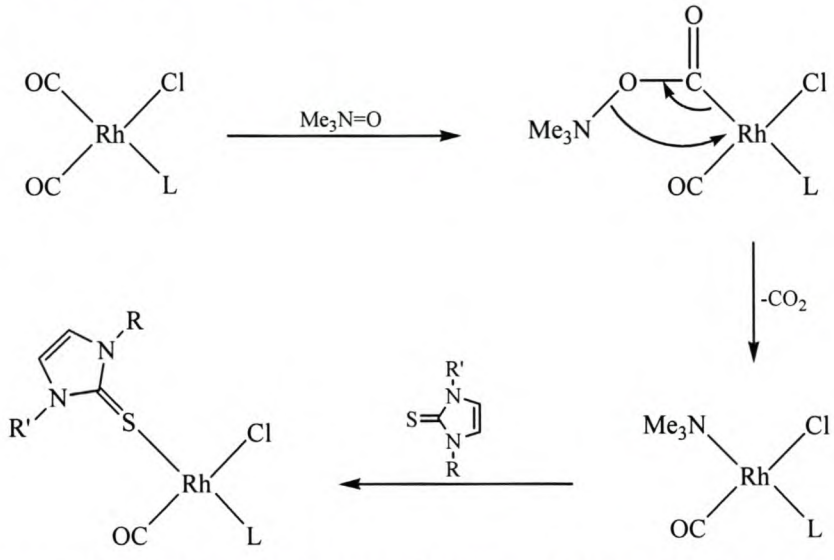

Figure 2.6.3 *Utilising Me_3NO to substitute a CO ligand with a thiourea ligand (L = thiourea or carbene ligand)*

The addition of two equivalents of thiourea ligand for every rhodium atom in $[RhCl(cod)]_2$ in THF at room temperature did not furnish the ionic complex $[Rh(cod)L_2]Cl$ (L = thiourea). Only the mononuclear species [RhCl(cod)L] was isolated from the reaction mixture. Addition of $AgBF_4$ to the reaction mixture afforded disubstitution and the formation of the ionic species *cis*-$[Rh(cod)L_2]BF_4$. Bubbling carbon monoxide through a methylene chloride solution of this complex gave the analogous carbonyl complex *cis*-$[Rh(CO)_2L_2]BF_4$ (Figure 2.6.4). The assignment of a *cis*-configuration for this complex was based on infrared and NMR studies. The same procedure was followed to prepare a complex containing a carbene as well as a thione ligand.

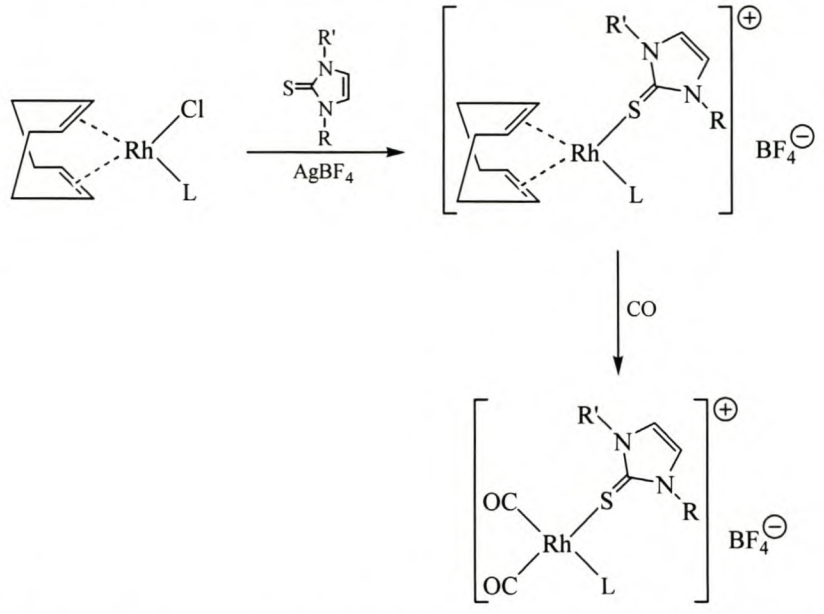

Figure 2.6.4 *Preparation of ionic thiourea complexes (L = thiourea or carbene ligand)*

It has been shown that reaction on the carbene substituents can be performed after the carbene ligand was bonded to rhodium.[77] An attempt was made to do a reaction on a bonded thiourea ligand. An attempt was made to prepare [RhCl(cod)(S=C{SMe}NMe_2)] from [RhCl(cod)(S=CHNMe_2)] (**18**), but led only to the formation of [Rh(SMe)(cod)]$_2$ that was characterised by NMR and MS techniques.

The complexes discussed in this chapter that have both carbene and thione ligands are shown in Figure 2.6.5. Other thione rhodium(I) complexes are illustrated in Figure 2.6.6. The novel cationic complexes with thione ligands appear in Figure 2.6.7.

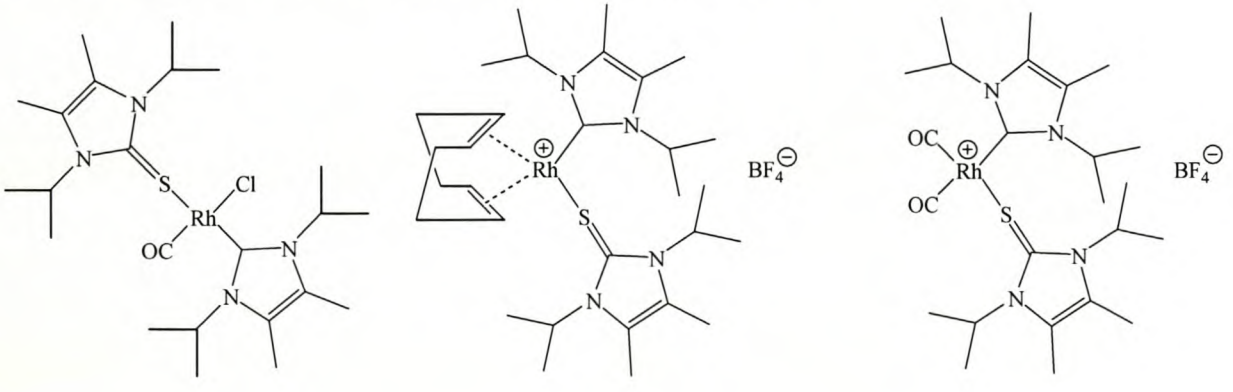

13 **14** **15**

Figure 2.6.5 *Rhodium(I) complexes with thione and carbene ligands*

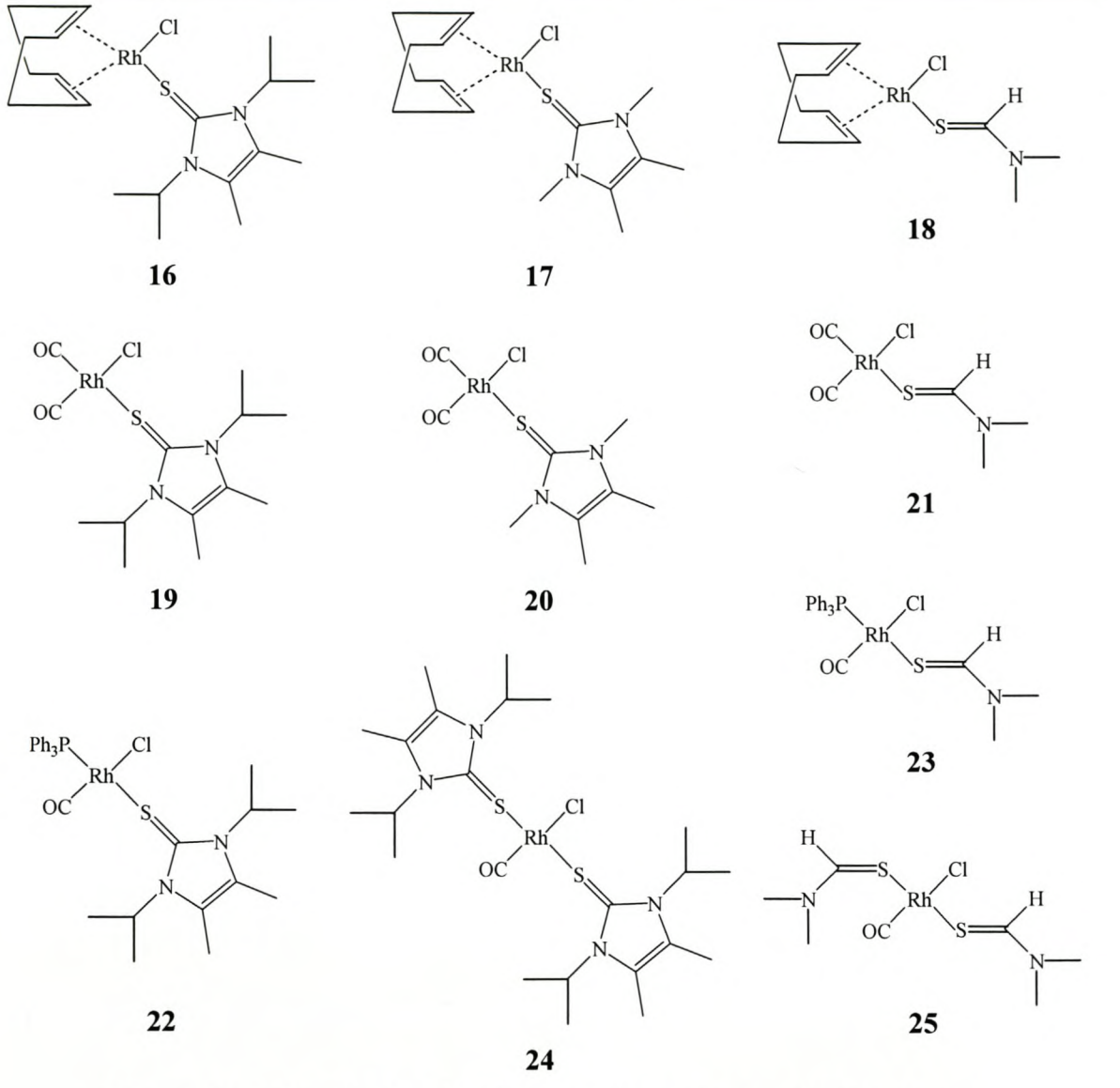

Figure 2.6.6 *New rhodium(I) thione complexes discussed in this chapter*

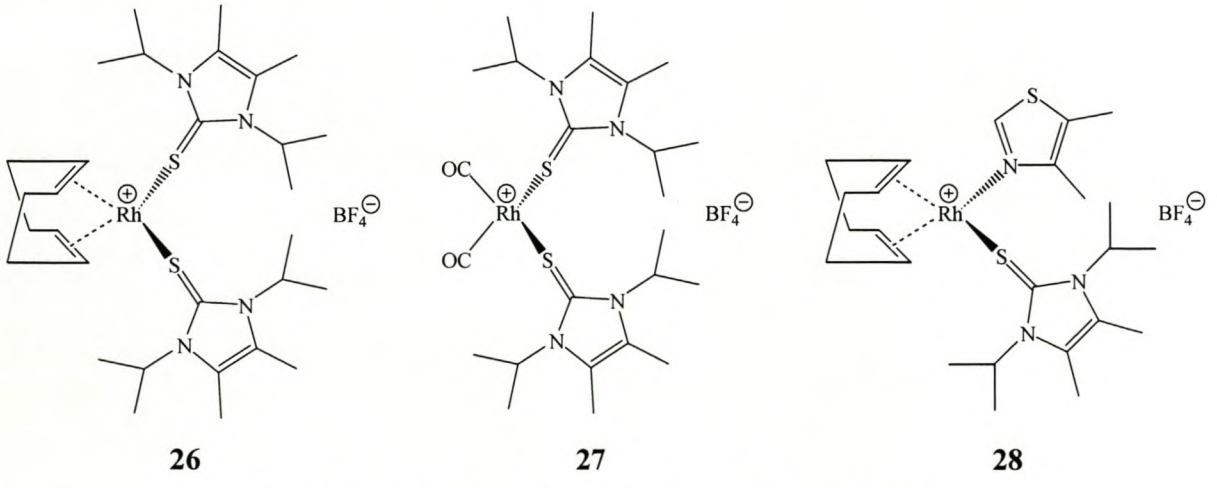

Figure 2.6.7 *Novel cationic rhodium(I) thione complexes*

6.1.3 Imine complexes

The binuclear rhodium complexes $[RhCl(cod)]_2$ and $[RhCl(CO)_2]_2$ can also be cleaved by *N*-donor ligands.[98,109] The addition of 4-methylthiazole and 4,5-dimethylthiazole to $[RhCl(cod)]_2$ and $[RhCl(CO)_2]_2$ in THF at room temperature gave monorhodium complexes with a Rh-N bond.

Only a few imine complexes were prepared to be used in the hydroformylation of 1-hexene in order to compare the effectivity and solubility of the complexes with those that contain carbene and thiourea ligands. The three new rhodium(I) complexes with thiazole ligands are illustrated in Figure 2.6.8.

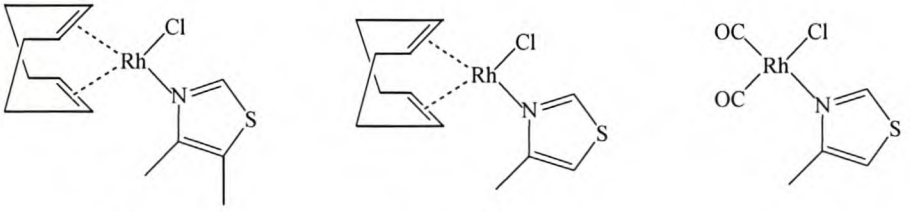

29 **30** **31**

Figure 2.6.8 *New rhodium(I) complexes with thiazole ligands*

6.2 General discussion on the separation, stability and solubility of rhodium(I) complexes

Purification of the complexes sometimes proved to be difficult. In some instances solubility properties were used to extract either the starting compound or the product. In other cases it was necessary to purify the product by SiO_2 flash chromatography. The solvents used on these flash-chromatographic columns include ether, methylene chloride and THF. Specific techniques used to purify each of the complexes are discussed separately in the experimental section.

Almost all the crystalline complexes are extremely stable in air and moisture and no decomposition was observed even after being left in the open for a few weeks. Almost no decomposition was visible when solutions of the complexes were exposed to the atmosphere for a few days.

6.3 Spectroscopic characterisation

The *trans* influences of the various ligands in square planar complexes play an important role in the position of the ligands around the metal centre as well as the chemical shifts observed in the NMR spectra. For this reason the *trans* influences of ligands will be discussed and compared for the different products.

To illustrate the *trans* influence – *i.e.* a weakening of metal-ligand bonding interaction *trans* to a chosen ligand – on the chemical shift in NMR spectroscopy, the coordination of ethylene to a metal centre can be used as a simple example.[110] When a double bond coordinates to a metal the hybridisation of the olefinic carbon atoms changes from sp^2 towards sp^3 in character, resulting in a change in the chemical shifts of these carbons. Weak coordination of the double bond to the metal results in the carbon atoms retaining a strong sp^2 character and a chemical shift close to that of ethylene (δ 123.3; ^{13}C NMR). For very strong coordination, the chemical shift can be compared to that of cyclopropane (δ –2.6). Thus, coordination of a ligand with a strong *trans* influence should lead to weaker coordination of the olefinic carbon atoms *trans* to the ligand and lengthening of the metal-$C_{olefinic}$ bond. Subsequently, the carbon atoms will retain more sp^2 character and the chemical shift of these carbon atoms (and the concomitant hydrogens) will move further downfield. The coupling constant will also be smaller, according to Lappert.[54]

Table 2.6.1 *Pt-Cl bond lengths illustrating the similarity in trans influence of a phosphine and a Fischer-type carbene ligand*

Complex	Bond lengths (Å)	
	Pt-Cl bond length *trans* to carbene ligand	Pt-Cl bond length *trans* to phosphine ligand
cis-$[PtCl_2(PEt_3)\{\overline{CN(Ph)(CH_2)_2N}(Ph)\}]$[111]	2.362(3)	2.381(3)
cis-$[PtCl_2(PEt_3)\{C(OEt)(NHPh)\}]$[112]	2.361(5)	2.367(7)
cis-$[PtCl_2(PMe_3Ph)\{C(OEt)(NH_2Ph)\}]$[113]	2.355(3)	2.375(3)

A comparison of the crystallographic data of platinum(II) complexes (square planar complexes similar to the rhodium(I) complexes discussed later in this section) illustrates the

similarity between phosphine and carbene ligand effects (Table 2.6.1). The Pt-Cl bond lengths are similar for phosphine and carbene ligands, thus showing that the *trans* influences of the two types of ligands are similar.

6.3.1 NMR spectroscopy

NMR spectra were recorded on either a 600 MHz Varian UNITY INOVA spectrometer (600 MHz for ^{1}H, 151 MHz for $^{13}C\{^{1}H\}$ and 243 MHz for $^{31}P\{^{1}H\}$) or a 300 MHz Varian VXR spectrometer (300 MHz for ^{1}H, 75 MHz for $^{13}C\{^{1}H\}$ and 121 MHz for $^{31}P\{^{1}H\}$ NMR). ^{31}P chemical shifts are reported in ppm relative to an 85% H_3PO_4 external standard solution.

*Rhodium(I) carbene complexes (**1 – 12**):*

6.3.1.1 Chloro(η^4-1,5-cyclooctadiene)(1,3-diisopropyl-4,5-dimethyl-2,3-dihydro-1H-imidazol-2-ylidene)rhodium(I) (1)

The ^{1}H NMR and ^{13}C NMR data of complex **1** are summarised in Table 2.6.2. According to published structure determinations the carbene ligand lies perpendicular to the plane that passes through the rhodium centre, the carbene carbon, the chloride ligand, and the centre points of the olefinic bonds of the cyclooctadiene ligand.[63] Thus, the mirror planes present in the complex should contribute to the chemical equivalence of protons H^6 and H^9, the methyl groups of the isopropyl substituents, the methyl groups in the 4 and 5 positions on the carbene ligand, and the olefinic and aliphatic groups of the cyclooctadiene ligand.

In the ^{1}H NMR spectrum, however, the signal for protons H^6 and H^9 appears as a septet at δ 6.10 due to the coupling with the two methyl groups of the isopropyl substituents. This signal is further downfield than the septet observed at δ 5.57 for 1,3-diisopropyl-4,5-dimethyl-2,3-dihydro-1*H*-imidazol-2-thione and the δ 3.95 value in the ^{1}H NMR spectrum of the free carbene 1,3-diisopropyl-4,5-dimethyl-2,3-dihydro-1*H*-imidazol-2-ylidene.[65] A slightly larger coupling constant (7.17 Hz) is observed when the carbene ligand is bonded to the rhodium metal ($^{3}J_{H\text{-}H}$ = 6.8 Hz for the thione and 6.4 Hz for the free carbene). This shift to lower field occurs probably because the carbene ligand experiences the deshielding region of the anisotropic field of the double bonds of the cyclooctadiene ligand.

Table 2.6.2 *NMR data of complex* ***1*** *in CD_2Cl_2 (relative to internal TMS)*

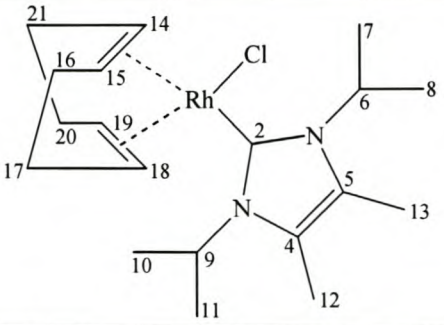

^{1}H NMR assignment	Chemical shift in ppm (number of protons, multiplicity, coupling constant)
H^6/H^9	6.10 (2H, septet, $^3J_{H\text{-}H}$ = 7.17 Hz)
H^{14}/H^{15}	4.81 (2H, m)
H^{18}/H^{19}	3.31 (2H, m)
H^{16}/H^{21}, H^{17}/H^{20} (equatorial)	2.32 (4H, m)
H^{12}/H^{13}	2.10 (6H, s)
H^{16}/H^{21}, H^{17}/H^{20} (axial)	1.87 (4H, m)
H^7/H^8 and H^{10}/H^{11}	1.55 (6H, d, $^3J_{H\text{-}H}$ = 7.17 Hz)
	1.45 (6H, d, $^3J_{H\text{-}H}$ = 7.17 Hz)
^{13}C NMR assignment	Chemical shift in ppm (multiplicity, coupling constant)
C^2	180.7 (d, $^1J_{C\text{-}Rh}$ = 51.5 Hz)
C^4/C^5	126.1 (s)
C^{14}/C^{15}	97.4 (d, $^1J_{C\text{-}Rh}$ = 7.4 Hz)
C^{18}/C^{19}	68.1 (d, $^1J_{C\text{-}Rh}$ = 14.7 Hz)
C^6/C^9	54.4 (s)
C^{16}/C^{21}	33.5 (s)
C^{17}/C^{20}	29.5 (s)
C^7/C^{10} and C^8/C^{11}	22.6 (s) and 22.3 (s)
C^{12}/C^{13}	10.7 (s)

The signals for the two methyl groups of the isopropyl substituents are observed as two separate doublets which both have a coupling constant of 7.17 Hz. This indicates that either the two isopropyl groups are in different chemical environments or that the two methyl groups on each isopropyl substituent are in different chemical environments. The two isopropyl

groups will be in different chemical environments if rotation around the Rh-$C_{carbene}$ bond is restricted and the heterocyclic ring of the carbene ligand lies in the plane containing the rhodium metal, halide atom and the centre of the olefinic cyclooctadiene bonds, and not perpendicular to it, although published crystal structures of related complexes indicate that the heterocyclic ring of the carbene ligand lies perpendicular to this plane as mentioned before.[63] The two methyl groups on each isopropyl substituent will be in different chemical environments if the rotation around the N-C bond is restricted due to steric hindrance or π-delocalisation from the pseudo-aromatic ring. Only one septet is observed for the H^6 and H^9 protons in the proton NMR spectrum. However, if the rotation around the N-C bond were restricted, the two protons would have been observed as a doublet of quartets as a result of the different coupling from the dissimilar methyl groups. From this information it can be concluded that the carbene ligand most probably lies in the plane, as described earlier, and that only the methyl groups of the isopropyl substituents are influenced to such an extent that they are observed at different chemical environments. In the solid state the carbene ligand will be perpendicular to the plane if the crystallisation energy is greater than the barrier of rotation of the carbene ligand around the R-$C_{carbene}$ bond. The inability to obtain crystals of **1** is an indication that the barrier of rotation is greater than the crystallisation energy. The two methyl groups at the 4 and 5 positions on the ring of the carbene ligand are represented by a singlet at δ 2.10. This shift is similar to that of the thione (δ 2.14) but higher than for the free carbene (δ 1.74).

To gain a better understanding of what exactly is responsible for the two sets of doublets, other selected complexes were prepared and analysed. A complex containing a different metal (tungsten, complex **2**, *vide infra*) and the same carbene ligand exhibit no indication of any π-delocalisation from the pseudo-aromatic ring onto the *N*-substituents in the NMR spectra because only one signal is observed for the isopropyl methyl groups in both the ^1H and ^{13}C NMR.

Two different signals were still observed for the isopropyl methyl groups after substituting the cyclooctadiene ligand with two carbonyl ligands (complex **6**), proving that rotation around the Rh-$C_{carbene}$ bond is not necessarily restricted due to sterical interference from the cyclooctadiene ligand. Any possibility of long distance Rh-C coupling can be discarded because the coupling constant changed when the NMR spectra were measured in two

different magnetic fields. Enders and co-workers observed two different signals in the NMR spectra of chiral rhodium(I) triazol-2-ylidene complexes which contain a cyclooctadiene ligand.[114] Calculation of the barrier of rotation about the Rh-$C_{carbene}$ bond yielded an energy of 93 kJ/mol. Similar norbornadiene complexes did not exhibit the same hindrance about the Rh-$C_{carbene}$ bond in the NMR spectra and calculations showed that the barrier of rotation of the norbornadiene complexes is only 58 kJ/mol. The spectrum of a complex that contains a carbene ligand with two different *N*-substituents (complex **3**, *vide infra*) also indicates the existence of more than one isomer in solution.

The multiplets observed for the protons of the cyclooctadiene ligand confirm that complex **1** has a square planar structure similar to results published for other complexes.[63,64] All the protons of the cyclooctadiene are observed as broad multiplets. The multiplets at δ 1.87 and δ 2.32 represent the aliphatic protons. The equatorial aliphatic protons resonate at lower field strength due to the anisoptropic effect of the double bonds.[115] These four protons being in the plane of the double bonds, are deshielded and, therefore, observed at a lower field (δ 2.32). The axial protons are shielded by the anisotropic effect of the double bond and appear at δ 1.87. The olefinic protons of the cyclooctadiene ligands are observed at δ 3.31 and δ 4.81. The difference in chemical shift can be attributed to the stronger *trans* influence of the carbene ligand in comparison to that of the chloride ligand.

Phosphine and carbene ligands both exhibit stronger *trans* influences than the chloride ligand. The bond lengths between the rhodium centre and the olefinic carbon atoms of the cyclooctadiene ligand (Table 2.6.3) illustrate the magnitude of the *trans* influence of the chloride atom compared to that of the carbene and phosphine ligands. It was stated earlier that a ligand with a strong *trans* influence should lead to weaker coordination of the olefinic carbon atoms *trans* to the ligand and lengthening of the metal-$C_{olefinic}$ bond length.

In the ^{13}C NMR spectrum, the signal for the carbene carbon is observed as a doublet at δ 180.7 with a coupling constant of $^{1}J_{C\text{-}Rh}$ = 51.5 Hz. These values are comparable to those found in other examples of similar complexes found in the literature. Published values for the shift of the carbene carbon vary from δ 180 to δ 186, and the ^{1}J coupling constant from 49 to 52 Hz.[63,64,77] The higher degree of deshielding observed for the bonded carbene ligand can be attributed to a delocalisation of electron density via the carbene bond to the rhodium centre.[116]

Due to the symmetry of the molecule, the olefinic carbon atoms of the 2,3-dihydro-1*H*-imidazol-2-ylidene ring are observed as a singlet. The singlet (δ 126.1) is at a slightly lower field than the singlet observed for the thione (δ 121.5) or the free carbene (δ 121.4). The signals of the two methyl groups at the 4 and 5 positions and the signals of the substituents on the nitrogen atoms of the carbene ligand are also observed at lower field when compared to those of the free carbene or the thione. The only interesting observation about the substituents is that the two methyl groups belonging to the isopropyl substituents have different chemical shifts, in accordance with the information obtained from the proton spectrum. Instead of one singlet, two singlets are observed at δ 22.3 and 22.6.

Table 2.6.3 *Rh-$C_{olefinic\ cod}$ bond lengths illustrating the trans influences of phosphine and carbene ligands compared to halide ligands*

Complex	Bond lengths (Å)	
	Rh-C_{cod} bond length *trans* to carbene or phosphorus	Rh-C_{cod} bond length *trans* to halide ligand
[RhCl(cod){P(*p*-$C_6H_4F)_3$}][117]	2.216(6)	2.130(8)
	2.234(7)	2.097(8)
[RhCl(cod){P(Ph)(*m*-py{*o*-OMe}$_2$)$_2$}][118]	2.204(8)	2.121(8)
	2.234(7)	2.144(8)
[RhCl(cod){CN(Me)CHCHN(Me)}][63]	2.205(2)	2.114(2)
	2.175(2)	2.095(2)
[RhBr(cod){CN(R)CHCHN(R)}] (R = $CH_2CO_2CH_3$)[77]	2.226(4)[a]	2.120(3)[a]

[a] *Only one bond length reported*

Two doublets are observed for the olefinic carbons of the cyclooctadiene ligand at δ 97.4 ($^1J_{Rh-C}$ = 7.4 Hz) and δ 68.1 ($^1J_{Rh-C}$ = 14.7 Hz). The different chemical shifts and coupling constants can be attributed to the different *trans* influences of the carbene and chloride ligands. When compared to the dimeric starting compound $[RhCl(cod)]_2$ (δ 79.5, $^1J_{Rh-C}$ = 14.1 Hz) the olefinic carbon atoms *trans* to the carbene ligand show a shift to a lower field as well as a decrease in the rhodium-carbon coupling constant (δ 97.4, $^1J_{Rh-C}$ = 7.4 Hz) as expected. Due to the smaller *cis* influence of the carbene ligand, the signals for the two *cis* olefinic

carbon atoms appear at a higher field with a bigger coupling constant (δ 68.1, $^1J_{Rh\text{-}C}$ = 14.7 Hz). The olefinic carbon atoms of the complex chloro(η^4-1,5-cyclooctadiene)(1,3-dicyclohexyl-2,3-dihydro-1*H*-imidazol-2-ylidene)rhodium(I) have been reported at shifts of δ 97.5 ($^1J_{Rh\text{-}C}$ = 3 Hz) and δ 67.5 ($^1J_{Rh\text{-}C}$ = 15 Hz).[64]

The *trans* and *cis* influences of the carbene and chloride ligands have the same impact on the chemical shifts of the aliphatic carbon atoms of the cyclooctadiene ligand as on the olefinic carbon atoms, δ 33.5 for those *trans* and δ 29.5 for those *cis* to the carbene ligand. Chemical shifts for the signals are similar to those reported for chloro(η^4-1,5-cyclooctadiene)(1,3-dicyclohexyl-2,3-dihydro-1*H*-imidazol-2-ylidene)rhodium(I) mentioned above (δ 34.5 for the aliphatic carbon atoms *trans* and δ 29.2 for the atoms *cis* to the carbene ligand).

6.3.1.2 Pentacarbonyl(1,3-diisopropyl-4,5-dimethyl-2,3-dihydro-1H-imidazol-2-ylidene)tungsten(0) (2)

Complex **2** was prepared in order to determine if there is any π-delocalisation from the pseudo-aromatic ring onto the *N*-substituents. Contrary to the situation in the rhodium complex **1**, the tungsten complex **2** proved to be absolutely symmetrical with respect to the isopropyl groups and only one doublet is observed in the ^{1}H NMR spectrum and only one signal in the ^{13}C NMR spectrum representing the appropriate methyl groups. The ^{1}H and ^{13}C NMR results are summarised in Table 2.6.4.

In the ^{1}H NMR spectrum of **2**, H^6 is observed as a septet, exactly as in **1**. The coupling constant is also of similar size. The two methyl groups attached to positions 4 and 5 on the carbene ring are observed as a sharp singlet at δ 2.22. In contrast to **1** the methyl groups of the isopropyl substituents appear as a single doublet. In the ^{13}C NMR spectrum the four methyl groups of the isopropyl substituents (C^7 and C^8) appear as a single peak at δ 22.1, at a similar chemical shift to the two peaks observed for **1** (δ 22.3 and δ 22.6). All the other carbon atoms of the carbene ligand are observed at the expected chemical shifts. The carbene carbon is observed at δ 178.1, similar to the value δ 176.4, that was observed for pentacarbonyl(1,3-dicyclohexyl-1,3-dihydro-1*H*-imidazol-2-ylidene)tungsten(0).[64] However, the observed carbon-tungsten coupling constant of 50.9 Hz is almost half of the value reported previously (^1J = 99 Hz). The same phenomenon was observed for the *cis* and *trans* carbonyl ligands. The published coupling constants for the carbonyl ligands (^1J = 126 Hz for the *cis* and *trans*

carbonyl ligands) are almost twice the size of the coupling constants observed in **2**, and are probably wrong, while the chemical shifts (δ 201.5 for the *trans* carbonyl ligand and δ 197.7 for the four *cis* carbonyl ligands) are almost the same as those in pentacarbonyl(1,3-dicyclohexyl-1,3-dihydro-1*H*-imidazol-2-ylidene)tungsten(0) (δ 203.2 for the *trans* carbonyl ligand and δ 199.1 for the four *cis* carbonyl ligands).

Table 2.6.4 *NMR data of complex* ***2*** *in CD_2Cl_2 (relative to internal TMS)*

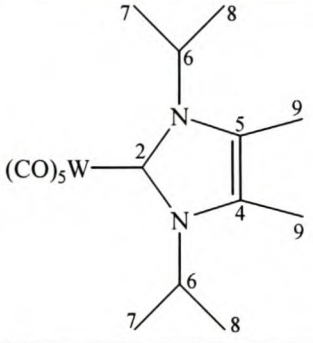

^{1}H NMR assignment	Chemical shift in ppm (number of protons, multiplicity, coupling constant)
H^6	5.52 (2H, septet, $^3J_{H\text{-}H}$ = 7.15 Hz)
H^9	2.22 (6H, s)
H^7/H^8	1.48 (12H, d, $^3J_{H\text{-}H}$ = 7.15 Hz)
^{13}C NMR assignment	Chemical shift in ppm (multiplicity, coupling constant)
CO_{cis}	203.2 (t, $^1J_{C\text{-}W}$ = 66.6 Hz)
CO_{trans}	199.1 (t, $^1J_{C\text{-}W}$ = 62.9 Hz)
C^2	178.1 (t, $^1J_{C\text{-}W}$ = 50.9 Hz)
C^4/C^5	127.6 (s)
C^6	56.4 (s)
C^7/C^8	22.1 (s)
C^9	11.2 (s)

From the NMR data of **2** it is clear that the there is only one complex in solution. In addition there seems to be no restriction on the rotation around the C-N bonds outside the ring. Other methods have to be found to unequivocally determine the reason behind the difference in chemical shifts of the methyl groups on the isopropyl substituents of 1,3-diisopropyl-4,5-dimethyl-2,3-dihydro-1*H*-imidazol-2-ylidene in **1**.

6.3.1.3 Chloro(η^4-1,5-cyclooctadiene)(1-butyl-3-methyl-2,3-dihydro-1H-imidazol-2-ylidene)rhodium(I) (3)

More than one signal were observed for almost all the protons and carbon atoms in the initial ^1H and ^{13}C NMR spectra of **3**. If the multiple signals were due to coupling between different atoms, the coupling constants would be the same regardless of the magnetic field strength used in the experiment. Therefore, two NMR experiments were done: the first on a 300 MHz Varian VXR spectrometer (300 MHz for ^1H, 75 MHz for ^{13}C) and the second on a 600 MHz Varian UNITY INOVA spectrometer (600 MHz for ^1H, 151 MHz for ^{13}C).

The NMR experiments done at the two different magnetic field strengths clearly prove the existence of two distinctly different complexes in solution. Expansions of the NMR spectra showing the signals observed for four different atoms are given in Figure 2.6.9. In some cases the observed sets of signals are very close together, *e.g.* the peak for C^{10}, but there is still no doubt about the presence of two different sets of signals.

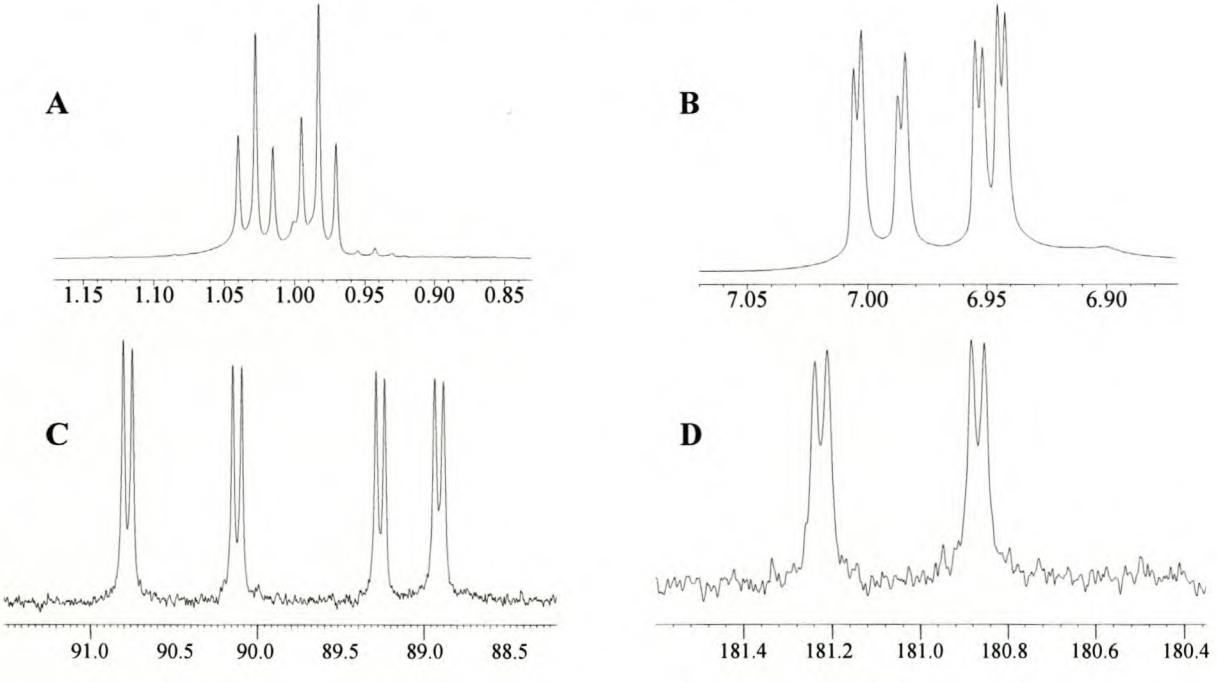

Figure 2.6.9 *Sections of the NMR spectra of **3** (measured with a Varian UNITY INOVA spectrometer, 600 MHz for ^1H, 151 MHz for ^{13}C) that show the two sets of signals. **A** shows the two triplets observed for H^9, **B** the signals observed for H^4 and H^5, **C** the olefinic cyclooctadiene carbons C^{11}/C^{12} and C^{15}/C^{16} and **D** the two doublets observed for the carbene carbon C^2*

The proton NMR data are summarised in Table 2.6.5 and the ^{13}C NMR data in Table 2.6.6. All the observed sets of signals are reported. Two different sets of signals are observed for almost all the protons and carbon atoms. In many cases the two sets of signals are intertwined, rendering the determination of coupling constants in the proton NMR spectrum almost impossible. The presence of the cyclooctadiene ligand also results in a great number of broad peaks, which further complicates the assignment of signals. A COSY ^{1}H-^{1}H correlation experiment was performed in order to fully assign the signals in the proton NMR spectrum.

Table 2.6.5 *Proton NMR data of complex **3** in CD_2Cl_2 (relative to internal TMS)*

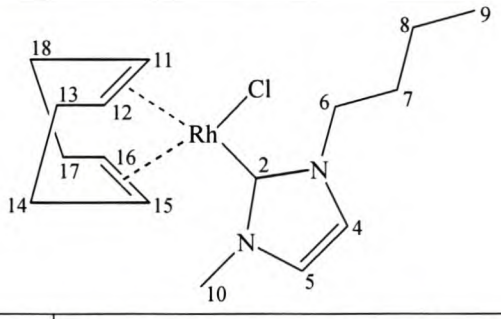

^{1}H NMR assignment	Chemical shift in ppm (number of protons, multiplicity, coupling constant)
H^4/H^5	7.00 (1H, d, $^{3}J_{H\text{-}H}$ = 1.91 Hz) / 6.94 (1H, d, $^{3}J_{H\text{-}H}$ = 1.91 Hz)
	6.99 (1H, d, $^{3}J_{H\text{-}H}$ = 1.91 Hz) / 6.95 (1H, d, $^{3}J_{H\text{-}H}$ = 1.91 Hz)
H^{11}/H^{12}, H^{15}/H^{16}	4.39 (1H, m) and 4.11 (1H, m),
	4.28 (1H, m) and 4.22 (1H, m)
H^{10}	4.04 (3H, s) and 3.98 (3H, s)
H^6	4.01 (2H, m) and 3.99 (2H, m)
H^{13}/H^{18}, H^{14}/H^{17} (equatorial	2.48 (1H, m), 2.45 (1H, m), 2.37 (2H, m), 2.34 (1H, m)
and axial)	2.27 (1H, m) , 2.18 (2H, m) and 2.09 (1H, m)
H^7	1.85 (2H, m) and 1.71 (2H, m)
H^8	1.46 (2H, m) and 1.39 (2H, m)
H^9	1.03 (3H, t, $^{3}J_{H\text{-}H}$ = 7.36 Hz) and
	0.98 (3H, t, $^{3}J_{H\text{-}H}$ = 7.36 Hz)

From the NMR results obtained for **1**, along with the NMR data of **2**, it is clear that there is more than one isomer of the complex present in solution for these types of rhodium carbene complexes. One possible explanation for the presence of 2 compounds is the existence of

rotamers (Figure 2.6.10), but no rotamers can be formed for **1** if the carbene ligand is perpendicular to the plane because of the symmetry of the carbene ligand. Thus, the NMR results of **1** indicate that the existence of rotamers is not the solution to the problem.

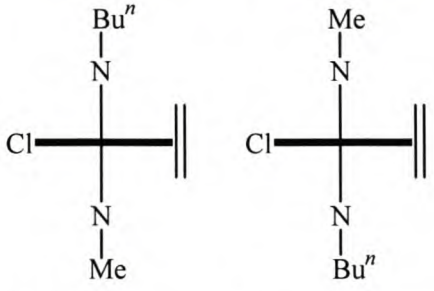

Figure 2.6.10 *An illustration of the possible rotamers of* ***3***

Another possibility is that the rotation around the Rh-$C_{carbene}$ bond is restricted and that the carbene ligand is bonded in two different ways to the rhodium metal, with the carbene ligand either in the plane (aa, Figure 2.6.11) that passes through the rhodium metal, the Cl ligand and the centre of the double bonds of the cyclooctadiene ligand, or perpendicular to this plane. As discussed earlier, the bulky cyclooctadiene ligand could restrict rotation around the Rh-$C_{carbene}$ bond because of steric hindrance. However, if the carbene ligand lies in the plane (aa), two different sets of signals are expected whereas three signals will be expected if the carbene ligand can be both in the plane as well as perpendicular to it. Thus, taking the NMR data of **1** into consideration, it is reasonable to assume that the carbene ligand lies in the plane, with either the methyl substituent or the butyl substituent next to the chloride ligand. However, it is also possible that the carbene ligand lies in the square plane but prefers only one specific configuration (because of the large butyl substituent), as well as perpendicular to the plane, thus leading to the two distinctly different signals for the carbene carbon.

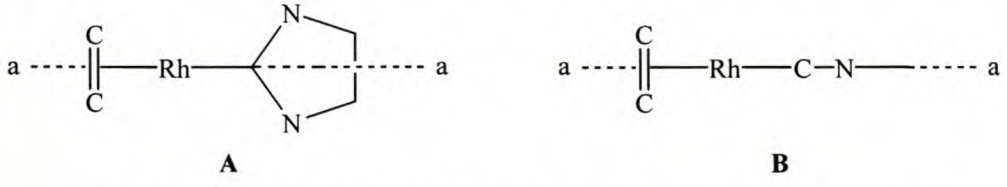

Figure 2.6.11 *An illustration of the carbene ligand bonded to the rhodium* ***(A)*** *perpendicular to the plane (aa) and* ***(B)*** *in the plane*

All the signals in both the ^{1}H NMR and the ^{13}C NMR spectra are observed at expected values when compared to the NMR data of **1** and of [BMIM]BF_4. A COSY experiment was carried

out to identify which ^{1}H peaks belong to each of the two complexes. This was followed by a gHSQC experiment to determine which protons and carbons were attached. Thus the ^{13}C peaks could be assigned as belonging to either of the two complexes. In most instances the signal observed further upfield in the proton NMR spectrum corresponds to a signal further upfield in the ^{13}C spectrum.

Table 2.6.6 *^{13}C NMR data of complex **3** in CD_2Cl_2 (relative to internal TMS)*

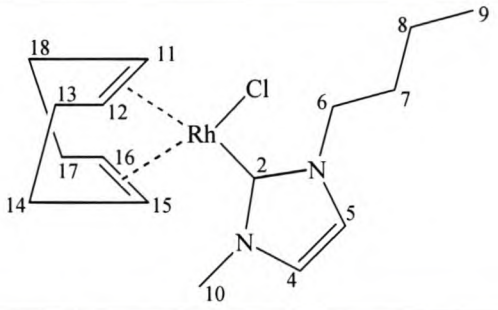

^{13}C NMR assignment	Chemical shift in ppm (multiplicity, coupling constant)
C^2	181.1 (d, $^{1}J_{C\text{-}Rh}$ = 53.7 Hz) and 181.0 (d, $^{1}J_{C\text{-}Rh}$ = 54.1 Hz)
C^4/C^5	124.2 (s) / 124.0 (s) and 121.6 (s) / 121.3 (s)
C^{11}/C^{12}	90.8 (d, $^{1}J_{C\text{-}Rh}$ = 8.1 Hz) and 90.1 (d, $^{1}J_{C\text{-}Rh}$ = 8.2 Hz)
C^{15}/C^{16}	89.3 (d, $^{1}J_{C\text{-}Rh}$ = 7.8 Hz) and 88.9 (d, $^{1}J_{C\text{-}Rh}$ = 7.9 Hz)
C^{10}	51.6 (s) and 51.6 (s)
C^6	39.2 (s) and 39.1 (s)
C^7	33.5 (s) and 33.4 (s)
C^{13}/C^{18}	32.7 (s) and 31.6 (s)
C^{14}/C^{17}	31.6 (s) and 30.4 (s)
C^8	21.0 (s) and 20.8 (s)
C^9	14.4 (s) and 14.3 (s)

Information gathered from these two experiments enabled us to assign the signals for the olefinic cyclooctadiene protons at δ 4.28 (H^{11}/H^{12}) and δ 4.22 (H^{15}/H^{16}) in the proton spectrum and signals for the carbon atoms at δ 90.1 (C^{11}/C^{12}) and δ 89.3 (C^{15}/C^{16}) in the ^{13}C spectrum to one complex, and the signals at δ 4.39 (H^{11}/H^{12}) and δ 4.11 (H^{15}/H^{16}) in the proton spectrum and δ 90.8 (C^{11}/C^{12}) and δ 88.9 (C^{15}/C^{16}) in the ^{13}C spectrum, to the other. Unambiguous assignment of the carbon atoms and protons in the 4 and 5 positions was also

possible. The signals at δ 7.00 and δ 6.94 in the proton spectrum and δ 124.2 and δ 124.0 in the ^{13}C spectrum represent one complex and δ 6.99 and δ 6.95 in the proton NMR and δ 121.6 and δ 121.3 in the ^{13}C spectrum represent the other. All the aliphatic carbon atoms and protons of the cyclooctadiene ligands could not be identified unambiguously. However, it is possible to link the signal at δ 30.4 in the ^{13}C spectrum to the signals at δ 2.34 and δ 2.09 in the proton spectrum, δ 32.7 (^{13}C) to δ 2.48 and δ 2.27 (^{1}H), and δ 31.6 (^{13}C) to δ 2.18, δ 2.37 and δ 2.45 (^{1}H). The two doublets observed at δ 181.1 and δ 181.0 in the ^{13}C spectrum are seen at similar chemical shifts, with similar coupling constants to those observed for analogous complexes like **1**. Unfortunately no conclusive answer can as yet be given for the exact molecular structures of the two geometrical isomers of the complex in solution.

6.3.1.4 [(η^4-1,5-Cyclooctadiene)-cis-(1,1′-propylene-3,3′-dimethyl-2,3,2′,3′-tetrahydro-1,1′-H-diimidazol-2,2′-diylidene)rhodium(I)][hexafluorophosphate] (4)

The ^{1}H NMR and ^{13}C NMR data of complex **4** are summarised in Table 2.6.7. Deuterated acetone was used as the solvent for this compound because a precipitate formed when the complex was dissolved in deuterated methylene chloride. The ^{1}H NMR spectrum of the precursor salt of **4** [1,1′-propylene-3,3′-dimethyl-2,3,2′,3′-tetrahydro-1,1′-*H*-diimidazolium][dihexafluorophosphate] shows a signal at δ 8.93 (in acetone-d_6) for the H^2 proton. This signal is not observed in the ^{1}H spectrum of **4** indicating that the precursor is no longer present, and that a carbene complex has formed.

According to published results,[63] a dinuclear complex was expected, but from the NMR and MS measurements and a structure determination, it was established that a biscarbene monorhodium complex has formed, similar to a complex prepared by Lappert.[51] The two heterocyclic rings of the biscarbene ligand are perpendicular to the plane through the rhodium centre, the two carbene carbons and the centre points of the olefinic bonds of the cyclooctadiene ligand.

Different chemical shifts are seen for H^4 and H^5 in the ^{1}H spectrum, as expected, the two protons being in different chemical environments. A small coupling constant (^{3}J = 1.82 Hz) is observed indicating the two protons are vicinal to each other. For [1,1′-ethylene-3,3′-dimethyl-2,3,2′,3′-tetrahydro-1,1′*H*-diimidazol-2,2′-diylidene]bis[chloro(η^4-1,5-cyclooctadiene)rhodium(I)] small coupling constants are also observed (^{3}J = 1.9 Hz).[63] The

two methyl *N*-substituents of **4** appear as a singlet at δ 4.06, which is practically identical to their chemical shift in the imidazolium salt. The four H^6 atoms appear as two sets of doublets of doublets at δ 5.09 and δ 4.45. One of the protons on each C^6 atom is in the same plane as the heterocyclic carbene rings (equatorial) while the other two are in the axial position. The magnetic anisotropic effect of the semi-aromatic 2,3-dihydro-1*H*-imidazol-2-ylidene rings is responsible for the shielding experienced by the equatorial protons, resulting in a shift to a lower field.[119] The axial protons are deshielded and therefore seen further upfield. The ^2J coupling constant of 14.43 Hz is observed for the geminal coupling between the axial and equatorial H^6 protons. The coupling constants observed for the coupling of the equatorial and axial H^6 atoms with the two H^7 atoms are different (^3J = 11.27 Hz for the equatorial protons and ^3J = 6.39 for the axial protons). The signal for the four H^6 protons of the free imidazolium ligand is observed as a triplet at δ 4.52 (^3J = 7.23). The two H^7 protons of **4** are observed as a multiplet at δ 2.81.

The chemical environments of the protons of the cyclooctadiene ligand are influenced by the different *N*-substituents of the two carbene moieties. On one side of each imidazol-2-ylidene ring is a methyl group and on the other side is the shared propyl chain. The result of the unsymmetrical biscarbene ligand is different chemical shifts for the cyclooctadiene ligand protons. Therefore, the olefinic protons are observed as two multiplets at δ 4.63 and δ 4.08. The aliphatic protons are observed as multiplets at δ 2.55 (equatorial protons) and δ 2.26 (axial protons) due to the anisotropic effect of the cyclooctadiene double bonds, as previously discussed for complex **1**.

The different *N*-substituents only have a small influence on the chemical shifts of the carbon atoms of the cyclooctadiene ligand. The four olefinic carbon atoms are observed as two doublets at δ 91.2 and δ 90.1. The coupling constant for both doublets is 7.9 Hz, almost the same magnitude as the coupling constant of 7.4 Hz observed for the olefinic cyclooctadiene carbon atoms *trans* to the carbene ligand in **1**. The aliphatic carbon atoms of **4** are also clearly in a similar chemical environment (δ = 32.3 and δ 32.1). The two carbene carbons are observed as a single strong doublet at δ 183.8 with a rhodium-carbon coupling constant of 52.5 Hz. The chemical shift and the coupling constant observed for the carbene carbons are comparable to that of other rhodium(I) carbene complexes mentioned in Section 6.3.1.1. The carbon atoms C^4 and C^5 appear to be in the same chemical environment as only one signal is

observed for these carbons at δ 124.6. This is interesting as the protons at these positions resonate at different values. The different *N*-substituents have a significant influence on the chemical environment of the H^4 and H^5 protons, but not on the C^4 and C^5 atoms. The singlets observed for C^6, C^7 and C^8 are at expected positions.

Table 2.6.7 *NMR data of complex* ***4*** *in acetone-d_6 (relative to internal TMS)*

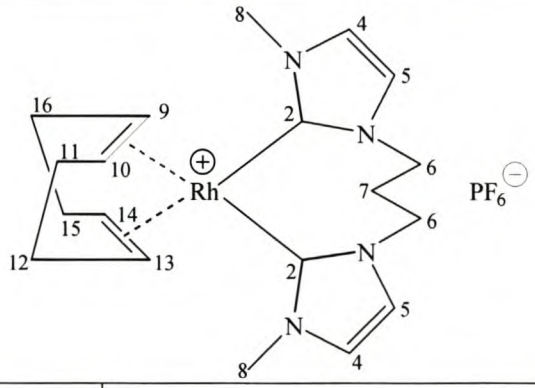

^{1}H NMR assignment	Chemical shift in ppm (number of protons, multiplicity, coupling constant)
H^4/H^5	7.21 (2H, d, $^2J_{H4\text{-}H5}$ = 1.82 Hz) and 7.11 (2H, d, $^2J_{H4\text{-}H5}$ = 1.82 Hz)
H^{6e}	5.09 (2H, dd, $^3J_{H6\text{-}H7}$ = 11.27 Hz, $^2J_{H6e\text{-}H6a}$ = 14.43 Hz)
H^9/H^{14} and H^{10}/H^{13}	4.63 (2H, m) and 4.08 (2H, m)
H^{6a}	4.45 (2H, dd, $^3J_{H6\text{-}H7}$ = 6.39 Hz, $^2J_{H6a\text{-}H6e}$ = 14.43 Hz)
H^8	4.06 (6H, s)
H^7	2.81 (2H, m)
H^{12}/H^{17}, H^{13}/H^{16} (equatorial)	2.55 (4H, m)
H^{12}/H^{17}, H^{13}/H^{16} (axial)	2.26 (4H, m)
^{13}C NMR assignment	Chemical shift in ppm (multiplicity, coupling constant)
C^2	183.8 (d, $^1J_{C\text{-}Rh}$ = 52.5 Hz)
C^4/C^5	124.6 (s)
C^9/C^{14} and C^{10}/C^{13}	91.2 (d, $^1J_{C\text{-}Rh}$ = 7.9 Hz) and 90.1 (d, $^1J_{C\text{-}Rh}$ = 7.9 Hz)
C^8	54.2 (s)
C^6	39.3 (s)
C^7	34.8 (s)
C^{11}/C^{16} and C^{12}/C^{15}	32.3 (s) and 32.1 (s)

6.3.1.5 Cis-[(η^4-1,5-cyclooctadiene)bis(1,3,4,5-tetramethyl-2,3-dihydro-1H-imidazol-2-ylidene)rhodium(I)]chloride (5)

The ^{1}H NMR and ^{13}C NMR data of complex **5** are summarised in Table 2.6.8. In the ^{1}H NMR spectrum the protons of the four *N*-methyl substituents are observed as a singlet at δ 3.84, while a singlet at δ 2.00 represents the four methyl groups (C^8 and C^9) of the two carbene ligands. The signals of the carbene ligand appear at lower field than the signals reported for the free carbene ligand (δ 3.35 and δ 1.59 in C_6D_6,[65] δ 3.48 and δ 2.01 in THF-d_8[59]). It is, however, apparent that the solvent has a strong influence on the chemical shift.

The methyl groups all appear as sharp singlets, an indication of the symmetry of this molecule. Further proof of the C_2 symmetry of this cationic biscarbene rhodium(I) complex is that the olefinic cyclooctadiene protons appear as a single multiplet at δ 4.19. The aliphatic protons are observed as two sets of multiplets representing the equatorial protons (δ 2.39) and the axial protons (δ 2.13) respectively. The NMR data are similar to that of another reported cationic biscarbene rhodium(I) complex, *cis*-[(η^4-1,5-cyclooctadiene)bis(4,5-tetramethyl-2,3-dihydro-1*H*-imidazol-2-ylidene)rhodium(I)]chloride.[74]

In the ^{13}C NMR the carbene carbon C^2 is observed as a doublet at δ 178.7 ($^1J_{C\text{-}Rh}$ = 53.2 Hz), which is similar to the shift of δ 180.5 ($^1J_{C\text{-}Rh}$ = 52.4 Hz) reported for *cis*-[(η^4-1,5-cyclooctadiene)bis(4,5-tetramethyl-2,3-dihydro-1*H*-imidazol-2-ylidene)rhodium(I)]chloride.[74] The four *N*-methyl groups appear at δ 36.7 and the C^8 and C^9 methyl groups at δ 9.6.

Like the ^{1}H NMR signals, the ^{13}C NMR signals for the cyclooctadiene ligand also display the symmetry of the molecule. The four aliphatic carbon atoms of the cyclooctadiene ligand appear in the ^{13}C NMR spectrum as a single peak at δ 31.6, and the olefinic carbons as one doublet at δ 89.3. A comparison of the chemical shifts and coupling constants observed for the olefinic carbon atoms of the cyclooctadiene ligand of the biscarbene complex and the starting compound $[RhCl(cod)]_2$ clearly shows the stronger *trans* influence of the carbene ligand compared to the chloride ligand (δ 89.3 and $^1J_{C\text{-}Rh}$ = 7.3 Hz for the carbene, δ 79.5 and $^1J_{C\text{-}Rh}$ = 14.1 Hz for $[RhCl(cod)]_2$). The *trans* influence of the carbene ligands in the cationic biscarbene complex **5** can also be compared to the *trans* influence of the imine ligands in the cationic imine complex $[Rh(cod)(Hbbtm)]BF_4$.[102] The olefinic carbon atoms of the cyclooctadiene ligand of $[Rh(cod)(Hbbtm)]BF_4$ appear at δ 85.3 with $^1J_{C\text{-}Rh}$ = 12.1 Hz, the

smaller carbon-rhodium coupling constant seen in **5** being proof that carbene ligands have a stronger *trans* influence than imine ligands.

Table 2.6.8 *NMR data of complex* ***5*** *in CD_2Cl_2 (relative to internal TMS)*

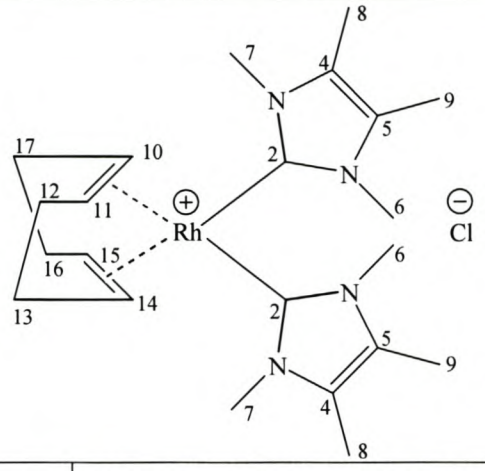

^{1}H NMR assignment	Chemical shift in ppm (number of protons, multiplicity, coupling constant)
H^{10}/H^{11} and H^{14}/H^{15}	4.19 (4H, m)
H^6/H^7	3.84 (12H, s)
H^{12}/H^{17}, H^{13}/H^{16} (equatorial)	2.39 (4H, m)
H^{12}/H^{17}, H^{13}/H^{16} (axial)	2.13 (4H, m)
H^8/H^9	2.00 (12H, m)
^{13}C NMR assignment	Chemical shift in ppm (multiplicity, coupling constant)
C^2	178.7 (d, $^1J_{C\text{-}Rh}$ = 53.2 Hz)
C^4/C^5	126.7 (s)
C^{10}/C^{11} and C^{14}/C^{15}	89.3 (d, $^1J_{C\text{-}Rh}$ = 7.3 Hz)
C^6/C^7	36.7 (s)
C^{12}/C^{17} and C^{13}/C^{16}	31.6 (s)
C^8/C^9	9.6 (s)

6.3.1.6 Chloro(dicarbonyl)(1,3-diisopropyl-4,5-dimethyl-2,3-dihydro-1H-imidazol-2-ylidene)rhodium(I) (6)

The ^{1}H NMR and ^{13}C NMR data of complex **6** are summarised in Table 2.6.9. The septet of the two protons H^{6} and H^{9} in the ^{1}H NMR spectrum appears at δ 5.32, considerably further upfield than the septet of complex **1** (δ 6.10). This confirms the speculation that the carbene ligand was in the deshielding region of the anisotropic field of the cyclooctadiene ligand in **1**, which is not present in **6**. The same tendency, though much smaller, is observed for the signals of the H^{12} and H^{13} methyl groups at δ 2.16. However, as in **1**, two doublets are observed for the methyl groups of the isopropyl substituents.

Table 2.6.9 *NMR data of complex **6** in CD_2Cl_2 (relative to internal TMS)*

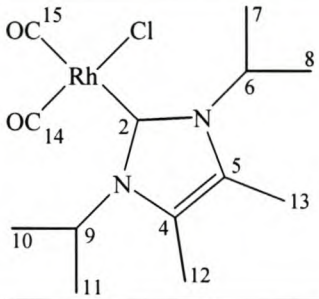	
^{1}H NMR assignment	Chemical shift in ppm (number of protons, multiplicity, coupling constant)
H^{6}/H^{9} H^{12}/H^{13} H^{7}/H^{10} and H^{8}/H^{11}	5.32 (2H, septet, $^{3}J_{H\text{-}H}$ = 7.10 Hz) 2.16 (6H, s) 1.51 (6H, d, $^{3}J_{H\text{-}H}$ = 7.10 Hz) 1.49 (6H, d, $^{3}J_{H\text{-}H}$ = 7.10 Hz)
^{13}C NMR assignment	Chemical shift in ppm (multiplicity, coupling constant)
C^{15} C^{14} C^{2} C^{4}/C^{5} C^{6}/C^{9} C^{7}/C^{8} and C^{10}/C^{11} C^{12}/C^{13}	187.7 (d, $^{1}J_{C\text{-}Rh}$ = 54.3 Hz) 184.4 (d, $^{1}J_{C\text{-}Rh}$ = 75.4 Hz) 170.7 (d, $^{1}J_{C\text{-}Rh}$ = 43.0 Hz) 127.2 (s) 54.7 (s) 22.7 (s) and 22.2 (s) 10.6 (s)

In the absence of the cyclooctadiene ligand, there should be no steric hindrance that could cause a restriction on the rotation around the N-C bonds. High temperature NMR experiments were performed in deuterated toluene in order to determine if there is any restricted rotation. Two sets of doublets in the proton NMR spectrum and two different signals in the ^{13}C NMR spectrum for the methyl groups of the isopropyl substituents are still observed at temperatures as high as 70 °C. It would be expected that at such temperatures restriction on N-C rotation should have been lifted, but clearly the temperature was not increased sufficiently.

Another possible explanation for the observed difference in chemical shifts of the methyl groups of the isopropyl substituents is Rh-C_{methyl} coupling. This possibility was discarded after doing NMR experiments at different magnetic field strengths, showing that there is no distinct coupling constant separating the two doublets. This, as well as the information obtained from the NMR data of complex **3**, indicates that there is probably restriction of rotation around the Rh-$C_{carbene}$ bond. This phenomenon has not been observed before for dicarbonyl rhodium(I) carbene complexes. Unfortunately we can still not give an ambiguous answer about the exact complexes in solution.

In accordance with a published example,[73] the signal of the carbene carbon of the dicarbonyl carbene complex **6** appears at a higher field (δ 170.7) compared to the carbene carbon of the cyclooctadiene complex **1** (δ 180.7). Herrmann reported a similar change in the chemical shift, from δ 185.3 for bromo(η^4-1,5-cyclooctadiene)(1,3-bis{diphenylmethyl}-2,3-dihydro-1*H*-imidazol-2-ylidene)rhodium(I) to δ 177.0 for the corresponding carbonyl complex. The change in coupling constant (from 51.5 Hz to 43.0 Hz) is also comparable to the published results (51.5 Hz and 43.2 Hz). The stronger *trans* influence of the carbene ligand compared to the chloride ligand is observed in the chemical shifts and coupling constants of the two carbonyl ligands. In agreement with the earlier discussion on *trans* influences the peak at δ 187.7 (^1J = 54.3 Hz) was assigned to the carbonyl ligand *trans* to the carbene ligand, while the carbonyl ligand in the *cis* position is observed as a doublet at δ 184.4 with a larger coupling constant (^1J = 75.4 Hz).

However, in one publication of Herrmann[63] the carbene carbon of chloro(dicarbonyl)(1,3-dimethyl-2,3-dihydro-1*H*-imidazol-2-ylidene)rhodium(I) was reported at δ 185.3 with a coupling constant of ^1J = 53 Hz. Since only one carbonyl ligand was reported, it can be

argued that the reported carbene carbon was in fact not the carbene carbon at all. Indeed, the signal at δ 185.3 could be due to the carbonyl ligand *trans* to the carbene ligand. The signals observed for C^4 and C^5, C^6 and C^9, and C^{12} and C^{13} all appear at expected chemical shifts when compared to those observed for **1** and **2**.

6.3.1.7 Chloro(dicarbonyl)(1-butyl-3-methyl-2,3-dihydro-1H-imidazol-2-ylidene)rhodium(I) (7)

The ^{1}H NMR and ^{13}C NMR data of complex **7** are summarised in Table 2.6.10. A comparison of the chemical shifts observed for the imidazolium salt and the carbene ligand bonded to the rhodium shows that all the protons and carbon atoms are observed at lower field for the bonded ligand than in the free ligand. The observed deshielding can be attributed to a delocalisation of electron density to the metal centre via the Rh-$C_{carbene}$ bond. Compared to **3**, the protons of the *N*-substituents of the carbene ligand of **7** appear at higher field in the ^{1}H NMR spectrum. This is an indication that the *N*-substituents of the carbene ligand of **3** are in the deshielding region of the anisotropic field of the cyclooctadiene ligand. The signals observed for the carbene ligand in the proton NMR spectrum are rather broad, but coupling constants could still be determined.

In the ^{13}C NMR spectrum, the two signals observed for each of the carbon atoms C^4, C^5 and C^6 indicate that there is more than one complex in solution. The three sets of doublets observed for the two carbonyl carbons and the carbene carbon appear at chemical shifts that compare well to those observed for **6** and other similar published complexes mentioned earlier. The coupling constants are also in agreement. This compound and complex **3** are the only ones for which 2 sets of signals for each atom in the carbene ligand are observed.

A further ^{1}H NMR experiment was carried out on **7** at –20 °C to confirm the presence of two different compounds in solution. All the signals in the proton NMR became broad signals at this low temperature, collapsing all the fine structure, except for the triplet observed for H^9, rendering the determination of coupling constants impossible. This broadening is another indication of the existence of two distinctly different molecular structures, because if there was only one in solution, the signals should certainly rather have become sharper. This information again indicate one of two possible scenarios, as stated earlier: The carbene ligand

lies in the plane, with either the methyl substituent or the butyl substituent next to the chloride ligand or the carbene ligand lies in the square plane preferring only one specific arrangement, (because of the large butyl substituent), as well as perpendicular to the plane.

Table 2.6.10 *NMR data of complex* ***7*** *in CD_2Cl_2 (relative to internal TMS)*

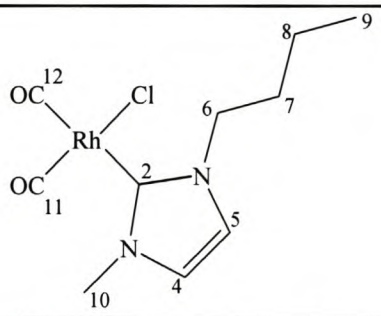

^{1}H NMR assignment	Chemical shift in ppm (number of protons, multiplicity, coupling constant)
H^4 and H^5	7.16 (1H, d, $^3J_{H\text{-}H}$ = 1.95 Hz)
	7.09 (1H, d, $^3J_{H\text{-}H}$ = 1.95 Hz)
H^6	3.88 (2H, t, $^3J_{H\text{-}H}$ = 7.56 Hz)
H^{10}	3.78 (3H, s)
H^7	1.65 (2H, p, $^3J_{H\text{-}H}$ = 7.56 Hz)
H^8	1.29 (2H, sextet, $^3J_{H\text{-}H}$ = 7.56 Hz)
H^9	0.93 (3H, t, $^3J_{H\text{-}H}$ = 7.56 Hz)
^{13}C NMR assignment	Chemical shift in ppm (multiplicity, coupling constant)
C^{12}	187.3 (d, $^1J_{C\text{-}Rh}$ = 55.7 Hz)
C^{11}	180.7 (d, $^1J_{C\text{-}Rh}$ = 77.1 Hz)
C^2	171.2 (d, $^1J_{C\text{-}Rh}$ = 46.4 Hz)
C^4 and C^5	125.11 (s) and 125.08 (s),
	123.13 (s) and 123.08 (s)
C^{10}	51.7 (s)
C^6	39.2 (s)
C^7	33.5 (s)
C^8	20.4 (s)
C^9	14.1 (s)

6.3.1.8 Chloro(dicarbonyl)(1-benzyl-3methyl-2,3-dihydro-1H-imidazol-2-ylidene)rhodium(I) (8)

The NMR data of complex **8** are summarised in Table 2.6.11. Only one signal is observed for the two H^6 protons of **8**, whereas two signals were observed for the same protons of the known cyclooctadiene complex.[120] All the other signals for the protons and of **8** appear at expected chemical shifts when compared to the cyclooctadiene complex and compounds **6** and **7**.

Table 2.6.11 *NMR data of complex **8** in CD_2Cl_2 (relative to internal TMS)*

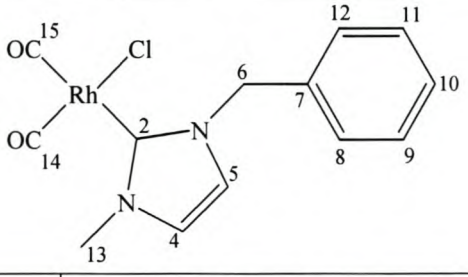

^{1}H NMR assignment	Chemical shift in ppm (number of protons, multiplicity, coupling constant)
Ph	7.34 (5H, m)
H^4 and H^5	7.00 (1H, d, $^3J_{H\text{-}H}$ = 1.51 Hz)
	6.90 (1H, d, $^3J_{H\text{-}H}$ = 1.51 Hz)
H^6	5.48 (2H, s)
H^{13}	3.89 (3H, s)
^{13}C NMR assignment	Chemical shift in ppm (multiplicity, coupling constant)
C^{15}	186.8 (d, $^1J_{Rh\text{-}H}$ = 53.9 Hz)
C^{14}	183.5 (d, $^1J_{Rh\text{-}H}$ = 74.3 Hz)
C^2	Not observed
C^7	136.8 (s)
C^9/C^{11}	129.7 (s)
C^8/C^{12}	129.2 (s)
C^{10}	129.0 (s)
C^4 and C^5	124.1 (s) and 122.3 (s)
C^6	55.5 (s)
C^{13}	39.1 (s)

All the signals and coupling constants observed in the ^{13}C NMR spectrum were also as expected. The signal for the carbene carbon could not be unambiguously assigned, but a very weak, broad signal at δ 174 could possibly be assigned to the expected doublet for the carbene carbon. The absence of two sets of signals in both the proton and the ^{13}C NMR spectra is an indication that there is only one arrangement of the carbene ligand. The carbene ligand lies in the square plane but prefer only one specific configuration, possibly due to the large benzyl substituent.

6.3.1.9 [Dicarbonyl(cis-(1,1'-propylene-3,3'-dimethyl-2,3,2',3'-tetrahydro-1,1'H-diimidazol-2,2'-diylidene)rhodium(I)][hexafluorophosphate] (9)

The proton NMR data for complex **9**, summarised in Table 2.6.12, are very similar to that of complex **4** with no significant difference in either the observed chemical shifts or coupling constants. The ^{13}C NMR data are also summarised in Table 2.6.12. The carbene ligand carbons are observed at expected chemical shifts when compared to **4**. The only significant difference between the spectra of **4** and **9** is that two signals appear for C^4 and C^5 in the ^{13}C NMR spectrum of **9**, while only one signal was observed in the ^{13}C NMR spectrum of **4**. The chemical shift (δ 173.9) and coupling constant ($^1J_{C\text{-}Rh}$ = 44.6 Hz) for the doublet representing the carbene carbon are comparable to the values found for similar dicarbonyl complexes like compound **6**.

As expected, only one doublet is observed for the two carbonyl ligands (δ 189.9) in the ^{13}C NMR spectrum. The coupling constant ($^1J_{C\text{-}Rh}$ = 57.6 Hz) is similar to the coupling constants of carbonyl ligands in the *trans* position relative to the carbene ligand in other rhodium(I) carbene complexes. The strong *trans* influence of the carbene ligands is again illustrated when the coupling constant of the carbonyl ligands is compared to that found for a similar cationic imine complex, $[Rh(CO)_2(Hbbtm)]BF_4$.[102] The carbonyl ligands of this complex are observed as a doublet at δ 182.7 with $^1J_{C\text{-}Rh}$ = 70.1 Hz, the larger coupling constant being an indication of the weaker *trans* influence of the imine ligand.

The relative magnitude of the *trans* influences of the carbene and imine ligands can be illustrated with an example from the literature. A cationic rhodium(I) complex, [(η^4-1,5-cyclooctadiene)(1-[(2*S*)-(4-benzyl-4,5-dihydrooxazolyl)methyl]-3-*tert*-butyl-2,3-dihydro-1*H*-

imidazol-2-ylidene)rhodium(I)][hexafluorophosphate] with both a carbene and an imine ligand bonded to the central rhodium atom was published in 1998 (Figure 2.6.12).[68] A comparison of the bond lengths between the rhodium centre and the olefinic carbon atoms of the cyclooctadiene ligand gives an indication of the relative *trans* influences of the imine and carbene ligands. The average Rh-$C_{olefinic\ cod}$ bond distance *trans* to the carbene ligand is 2.201(6) Å and *trans* to the imine ligand the average bond distance is 2.143(6) Å. The greater average bond distance indicates that the *trans* influence of the carbene ligand is stronger than that of the imine ligand.

Table 2.6.12 *NMR data of complex* ***9*** *in acetone-d_6 (relative to internal TMS)*

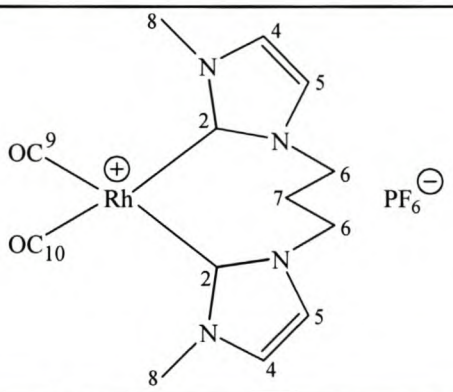

^{1}H NMR assignment	Chemical shift in ppm (number of protons, multiplicity, coupling constant)
H^4/H^5	7.38 (2H, d, $^1J_{H4\text{-}H5}$ = 1.85 Hz) and
	7.31 (2H, d, $^1J_{H4\text{-}H5}$ = 1.85 Hz)
H^{6e}	4.78 (2H, dd, $^3J_{H6\text{-}H7}$ = 11.55 Hz, $^2J_{H6e\text{-}H6a}$ = 14.43 Hz)
H^{6a}	4.50 (2H, dd, $^3J_{H6\text{-}H7}$ = 5.91 Hz, $^2J_{H6a\text{-}H6e}$ = 14.43 Hz)
H^8	3.98 (6H, s)
H^7	2.82 (2H, m)
^{13}C NMR assignment	Chemical shift in ppm (multiplicity, coupling constant)
C^9 and C^{10}	189.9 (d, $^1J_{C\text{-}Rh}$ = 57.6 Hz)
C^2	173.9 (d, $^1J_{C\text{-}Rh}$ = 44.6 Hz)
C^4/C^5	125.9 (s) and 125.7 (s)
C^8	54.5 (s)
C^6	39.7 (s)
C^7	33.6 (s)

Another example illustrating this effect involves the comparison of a rhodium(I) complex with a bidentate imine ligand, $[Rh(bbte)(cod)]BF_4$ (bbte = bis{benzothiazol-2-yl}ethane),[102] and the biscarbene complex [(η^4-1,5-cyclooctadiene)bis(1,3-dimethyl-2,3-dihidro-1*H*-imidazol-2-ylidene)rhodium(I)][chloride].[63] The average Rh-$C_{olefinic\ cod}$ bond length for the former compound is 2.147(2) Å whereas for the biscarbene complex it is 2.189(9) Å.

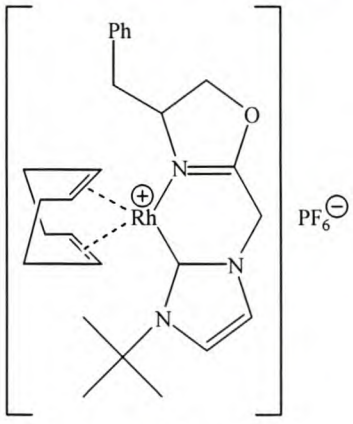

Figure 2.6.12 *Rhodium(I) complex with a chelating carbene and imine ligand*

*6.3.1.10 Chloro(carbonyl)-trans-bis(1,3,4,5-tetramethyl-2,3-dihydro-1*H*-imidazol-2-ylidene)rhodium(I) (10)*

The proton and ^{13}C NMR signals for the carbene ligands in **10**, summarised in Table 2.6.13, are at chemical shifts similar to those observed for the cationic cyclooctadiene biscarbene complex **5**. The differences in chemical shifts are also similar to those of the known complexes, *cis*-[(η^4-1,5-cyclooctadiene)bis(1,3-dimethyl-2,3-dihydro-1*H*-imidazol-2-ylidene)rhodium(I)]chloride and chloro(carbonyl)-*trans*-bis(1,3-dimethyl-2,3-dihydro-1*H*-imidazol-2-ylidene)rhodium(I).[74] As was observed for the published complexes, the signal of the carbene carbons of **10** (δ 182.9, $^1J_{C\text{-}Rh}$ = 40.6 Hz) appears at a lower field with a smaller coupling constant than that of the cyclooctadiene complex **5** (δ 178.7, $^1J_{C\text{-}Rh}$ = 53.2 Hz). The carbonyl ligand of **10** is observed as a doublet at δ 184.4. The magnitude of the coupling constant of the carbonyl ligand ($^1J_{C\text{-}Rh}$ = 82.8 Hz) is similar to that of the carbonyl in the *cis* position relative to the carbene ligand in complex **6** ($^1J_{C\text{-}Rh}$ = 75.4 Hz). The fact that only one set of signals are observed for the methyl *N*-substituents can indicate free rotation around the Rh-$C_{carbene}$ bonds. However, it is also possible that the chemical environments of the substituents are similar, even if the carbene ligands lie in the square plane, explaining the single peaks in the NMR spectra.

Table 2.6.13 *NMR data of complex* ***10*** *in CD_2Cl_2 (relative to internal TMS)*

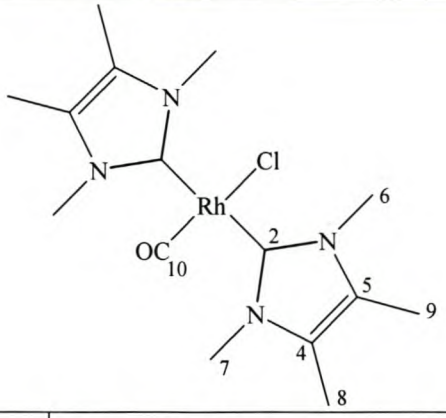

^{1}H NMR assignment	Chemical shift in ppm (number of protons, multiplicity, coupling constant)
H^6/H^7	3.91 (6H, s)
H^8/H^9	2.11 (6H, s)
^{13}C NMR assignment	Chemical shift in ppm (multiplicity, coupling constant)
C^{10}	188.4 (d, $^1J_{C\text{-}Rh}$ = 82.8 Hz)
C^2	182.9 (d, $^1J_{C\text{-}Rh}$ = 40.6 Hz)
C^4/C^5	125.3 (s)
C^6/C^7	36.0 (s)
C^8/C^9	9.7 (s)

6.3.1.11 Chloro(carbonyl)-trans-(triphenylphosphine)(1,3-diisopropyl-4,5-dimethyl-2,3-dihydro-1H-imidazol-2-ylidene)rhodium(I) (11)

Compared to the dicarbonyl complex **6**, all the signals of the carbene ligand in the ^{1}H NMR spectrum (Table 2.6.14) appear further upfield. A similar change in chemical shift was observed for bromo(dicarbonyl)-(1,3-bis{diphenylmethyl}-2,3-dihydro-1*H*-imidazol-2-ylidene)rhodium(I) and the phosphine complex bromo(carbonyl)-*trans*-(triphenylphosphine)(1,3-bis{diphenylmethyl}-2,3-dihydro-1*H*-imidazol-2-ylidene)rhodium(I).[73] The two protons H^6 and H^9 appear as a septet at δ 5.84. The two methyl groups H^{12} and H^{13} as well as the phenyl groups of the triphenylphosphine ligand appear at expected chemical shifts. The methyl groups of the isopropyl substituents appear as two sets of doublets in the proton NMR spectrum, in accordance with the proton NMR spectra of **1**

and **6**, indicating, again, the presence of two different isomers of the complex in solution and, with high probability, a restriction of rotation about the Rh-$C_{carbene}$ bond.

Table 2.6.14 *^1H NMR data of complex **11** in CD_2Cl_2 (relative to internal TMS)*

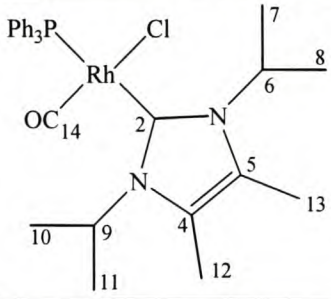

^1H NMR assignment	Chemical shift in ppm (number of protons, multiplicity, coupling constant)
H (Ph)	7.55 (15H, m)
H^6/H^9	5.84 (2H, septet, $^3J_{H-H}$ = 7.15 Hz)
H^{12}/H^{13}	2.19 (6H, s)
H^7/H^{10} and H^8/H^{11}	1.57 (6H, d, $^3J_{H-H}$ = 7.15 Hz)
	1.55 (6H, d, $^3J_{H-H}$ = 7.15 Hz)

In the ^{13}C spectrum the signals observed for C^6 and C^9, and the two methyl carbons C^{12} and C^{13} are at the expected positions (Table 2.6.15). The two olefinic carbon atoms C^4 and C^5 appear as either two different signals or a doublet. The carbene ligand as discussed for **1** can account for the two different signals, whereas a doublet can be attributed to ^4J carbon-phosphorus coupling. Carbon-phosphorus coupling is also observed for the phenyl groups of the phosphine ligand and the signals are assigned according to published results.[46] The signals for the carbonyl and carbene carbons appear as doublets of doublets at chemical shifts similar to published results. Both have moved to lower field when compared to the dicarbonyl complex **6**, which is what is observed for the published compounds bromo(dicarbonyl)-(1,3-bis{diphenylmethyl}-2,3-dihydro-1*H*-imidazol-2-ylidene)rhodium(I) and the phosphine complex bromo(carbonyl)-*trans*-(triphenylphosphine)(1,3-bis{diphenylmethyl}-2,3-dihydro-1*H*-imidazol-2-ylidene)rhodium(I).[73] The coupling constants for the doublets of doublets are approximately of the same magnitude as for the reported complexes. The $^1J_{C-Rh}$ coupling constant of 123.2 Hz for the $C_{carbene}$-Rh coupling is much larger than that seen for the dicarbonyl complex **6** ($^1J_{C-Rh}$ = 43.0 Hz). This is due to the presence of triphenylphosphine in

the *trans* position relative to the carbene ligand. The phosphine ligand has a smaller effect on the $C_{carbonyl}$-Rh coupling constant, which is 78.7 Hz, only 3.3 Hz larger than the 75.4 Hz observed for **6**. In addition to C-Rh coupling, the phosphorus also couples to the carbene carbon and the carbonyl carbon atoms. Rh-P coupling is responsible for the appearance of a doublet (δ 32.8, $^1J_{P\text{-}Rh}$ = 116.3 Hz) in the phosphorus NMR spectrum. These values are similar to those reported for bromo(carbonyl)-*trans*-(triphenylphosphine)(1,3-bis{diphenylmethyl}-2,3-dihydro-1*H*-imidazol-2-ylidene)rhodium(I) (δ 32.2, $^1J_{P\text{-}Rh}$ = 115.5 Hz).[73]

Table 2.6.15 *^{13}C and ^{31}P NMR data of complex **11** in CD_2Cl_2 (relative to internal TMS)*

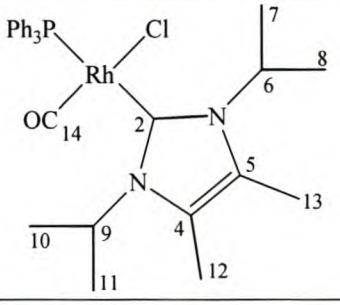

^{13}C NMR assignment	Chemical shift in ppm (multiplicity, coupling constant)
C^{14}	188.4 (dd, $^1J_{C\text{-}Rh}$ = 78.7 Hz, $^2J_{C\text{-}P}$ = 15.6 Hz)
C^2	177.2 (dd, $^1J_{C\text{-}Rh}$ = 123.2 Hz, $^2J_{C\text{-}P}$ = 45.4 Hz)
C_{ipso} (Ph)	135.7 (d, $^1J_{C\text{-}P}$ = 39.1 Hz)
C_{orto} (Ph)	135.6 (d, $^2J_{C\text{-}P}$ = 11.9 Hz)
C_{meta} (Ph)	130.7 (d, $^3J_{C\text{-}P}$ = 1.8 Hz)
C_{para} (Ph)	128.9 (d, $^4J_{C\text{-}P}$ = 9.5 Hz)
C^4/C^5	126.3 (d, $^4J_{C\text{-}P}$ = 3.1 Hz) [or 126.3 (s) and 126.4 (s)]
C^6/C^9	54.4 (s)
C^7/C^8 and C^{10}/C^{11}	22.7 (s) and 22.3 (s)
C^{12}/C^{13}	10.7 (s)
^{31}P NMR assignment	Chemical shift in ppm (multiplicity, coupling constant)
P	32.8 (d, $^1J_{P\text{-}Rh}$ = 116.3 Hz)

According to Lappert, *N*-heterocyclic carbene ligands have a greater *trans* influence than PPh_3, the phosphine of choice in catalyst preparation.[54] The argument is based on the size of the coupling constants $^1J_{C\text{-}Rh}$ and $^1J_{P\text{-}Rh}$ measured in ^{13}C and ^{31}P NMR spectra. As illustrated for platinum(II) complexes,[121] a smaller coupling constant is expected for a ligand with a

larger *trans* influence. In another instance the coupling constant $^1J_{P\text{-}Rh}$ is smaller for *trans*-[RhCl(CO)(L^{Et})(PPh_3)] (112 Hz), where L^{Et} = {CN(Et)CH_2CH_2N(Et)}, than for *trans*-[RhCl(CO)(PPh_3)$_2$] (129 Hz). The same trend is seen in *trans*-[Rh(CO)(L^{Et})$_2$(PPh_3)]Cl (117 Hz) and *trans*-[Rh(CO)(L^{Et})(PPh_3)$_2$]Cl (132 Hz). A coupling constant of the same magnitude has been reported more recently for *trans*-[RhCl(CO){CN($CHPh_2$)CHCHN($CHPh_2$)}(PPh_3)] ($^1J_{P\text{-}Rh}$ = 115.5 Hz).[73] Lappert and co-workers also concluded that the *N*-heterocyclic carbene ligands have smaller *cis* influences than PPh_3. An example of this is seen when comparing [RhCl(PPh_3)$_3$] (142 Hz)[122] and *trans*-[RhCl(IMes)(PPh_3)$_2$] (210 Hz),[75] where IMes is 1,3-bis(2,4,6-trimethylphenyl)-2,3-dihydro-1*H*-imidazol-2-ylidene.

6.3.1.12 Chloro(carbonyl)-trans-(tri{2'H-thiazol}phosphine)(1,3-diisopropyl-4,5-dimethyl-2,3-dihydro-1H-imidazol-2-ylidene)rhodium(I) (12)

The ^{1}H NMR and ^{13}C NMR data of complex **12** are summarised in Table 2.6.16. The patern of the signals for the protons on the carbene ligand in the ^{1}H NMR spectrum are similar to those observed for complex **11**. Two different signals are again observed for the methyl groups of the isopropyl substituents on the carbene ligand. The H^{17} protons of the thiazole groups are observed as a doublet, which is similar to what is seen for the free ligand. The H^{16} protons, however, are observed as a doublet of doublets, differing from the doublet that appears in the ^{1}H NMR spectrum of the free ligand. The coupling constant for the coupling between the H^{16} and H^{17} ($^3J_{H\text{-}H}$ = 3.13 Hz) protons is the same as that observed for the free ligand and selective decoupling experiments were performed to determine the origin of the smaller coupling (Figure 2.6.13).

Selective homonuclear proton decoupling of the H^{17} protons confirms the magnitude of the coupling constant for the coupling between the H^{16} and H^{17} protons. Selective heteronuclear phosphorus decoupling proved that P-C coupling is responsible for the small coupling constant of 1.65 Hz. The phosphorus couples to the H^{16} protons through the sulfur atom. Electron donation to the rhodium metal results in a lower electron density on the phosphorus atom and with the three thiazole substituents possibly leading to a more rigid structure of the thiazole groups and enabling coupling between the phosphorus atom and H^{16}.

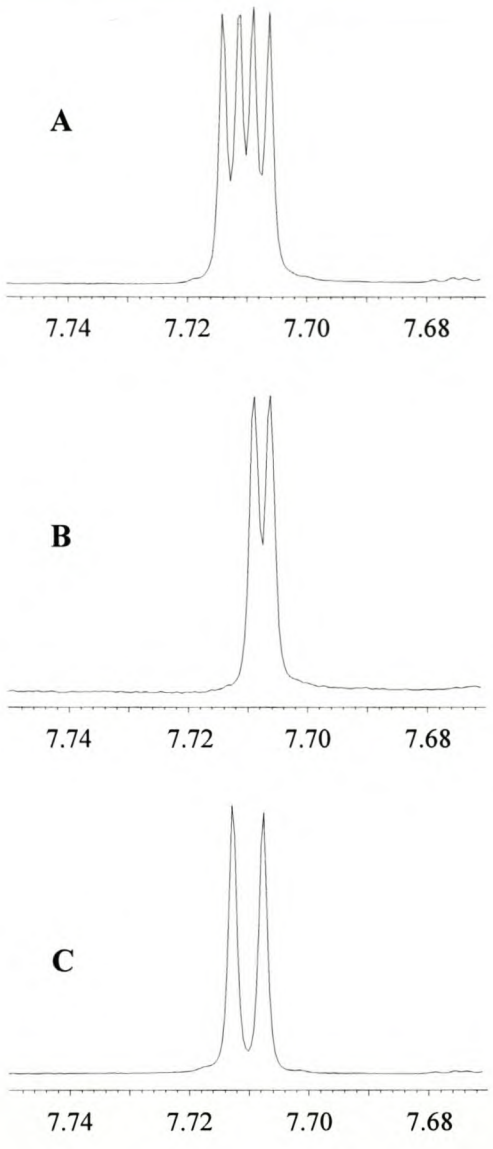

Figure 2.6.13 *The signal of H^{16} observed in the ^1H NMR spectrum (**A**), after selective homonuclear proton-proton decoupling (**B**) and after selective heteronuclear phosphorus decoupling (**C**)*

In the ^{13}C NMR spectrum, the carbene carbon was observed as a doublet of doublets at δ 173.6, when using a pulse delay of 5 seconds. The C-Rh coupling constant ($^1J_{C\text{-}Rh}$ = 137.4 Hz) is larger than the coupling constant for complex **11** ($^1J_{C\text{-}Rh}$ = 123.2 Hz). The C-P coupling constant ($^2J_{C\text{-}P}$ = 46.1 Hz) has almost the same magnitude as the corresponding coupling constant observed for **11** ($^2J_{C\text{-}P}$ = 45.4 Hz). From these results it can be tentatively concluded that the *trans* influence of the tri{2*H*-thiazol}phosphine is comparable to that of triphenylphosphine. The other carbon atoms of the carbene ligand are observed at chemical shifts similar to those of **11**, including the possible C-P coupling observed at the C^4 and C^5

atoms. Another explanation is that the two carbon atoms are in different chemical environments due to the carbene ligand being in the square plane of the complex, as found for complexes **3**, **7**, and **11**.

Table 2.6.16 *NMR data of complex* ***12*** *in CD_2Cl_2 (relative to internal TMS)*

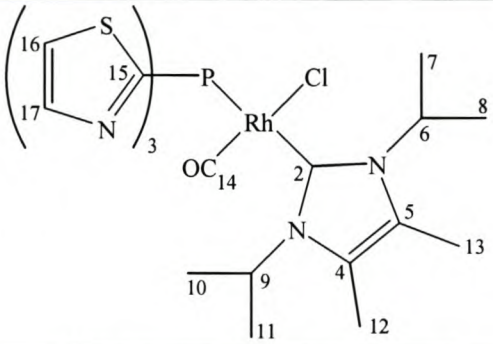

^{1}H NMR assignment	Chemical shift in ppm (number of protons, multiplicity, coupling constant)
H^{17}	8.10 (3H, d, $^3J_{H\text{-}H}$ = 3.13 Hz)
H^{16}	7.71 (3H, dd, $^3J_{H\text{-}H}$ = 3.13 Hz, $^4J_{H\text{-}P}$ = 1.65 Hz)
H^6/H^9	5.77 (2H, septet, $^3J_{H\text{-}H}$ = 7.15 Hz)
H^{12}/H^{13}	2.22 (6H, s)
H^7/H^8	1.60 (6H, d, $^3J_{H\text{-}H}$ = 7.15 Hz)
H^{10}/H^{11}	1.57 (6H, d, $^3J_{H\text{-}H}$ = 7.15 Hz)
^{13}C NMR assignment	Chemical shift in ppm (multiplicity, coupling constant)
C^{14}	186.5 (dd, $^1J_{C\text{-}Rh}$ = 77.1 Hz, $^2J_{C\text{-}P}$ = 15.6 Hz)
C^2	173.6 (dd, $^1J_{C\text{-}Rh}$ = 137.4 Hz, $^2J_{C\text{-}P}$ = 46.1 Hz)
C^{15}	163.7 (d, $^1J_{C\text{-}P}$ = 60.0 Hz)
C^{17}	145.9 (d, $^3J_{C\text{-}P}$ = 17.7 Hz)
C^4/C^5	126.5 (d, $^3J_{C\text{-}P}$ = 3.8 Hz) [or 126.5 (s) and 126.5 (s)]
C^{16}	126.4 (s)
C^6/C^9	54.8 (s)
C^7/C^8 and C^{10}/C^{11}	22.9 (s) and 22.5 (s)
C^{12}/C^{13}	10.9 (s)
^{31}P NMR assignment	Chemical shift in ppm (multiplicity, coupling constant)
P	15.6 (d, $^1J_{P\text{-}Rh}$ = 122.5 Hz)

The doublet of doublets observed for the carbonyl ligand at δ 186.5 ($^1J_{C\text{-}Rh}$ = 77.1 Hz, $^2J_{C\text{-}P}$ = 15.6 Hz) appears at almost the same chemical shift, and with similar coupling constants, as that observed for **11** at δ 188.4 ($^1J_{C\text{-}Rh}$ = 78.7 Hz, $^2J_{C\text{-}P}$ = 15.6 Hz). The phosphorus atom is observed as a doublet at δ 15.6 in the ^{31}P NMR spectrum, at lower field than for the free ligand (δ –31.3 in $CDCl_3$). The phosphorus-rhodium coupling is slightly larger for **12** than for **11** ($^1J_{P\text{-}Rh}$ = 122.5 Hz for **12**, and $^1J_{P\text{-}Rh}$ = 116.3 Hz for **11**).

*Rhodium(I) complexes with carbene and thione ligands (**13 – 15**):*

6.3.1.13 Chloro(carbonyl)-trans-(1,3-diisopropyl-4,5-dimethyl-2,3-dihydro-1H-imidazol-2-thione)(1,3-diisopropyl-4,5-dimethyl-2,3-dihydro-1H-imidazol-2-ylidene)rhodium(I) (13)

For complex **13** the two methyl groups of the isopropyl substituents of the carbene ligand still appear as two sets of doublets (δ 1.45 and δ 1.48) in the ^{1}H NMR spectrum and show two resonances in the ^{13}C NMR spectrum (δ 22.0 and δ 22.1), similar to complexes **1**, **6**, **11** and **12**. The same methyl groups on the thione ligand, somewhat further removed from the rhodium centre, appear as the same methyl groups of the carbene ligand, as one doublet in the ^{1}H NMR spectrum at δ 1.53, which is at a lower field than for the carbene ligand, and at δ 21.2 in the ^{13}C NMR spectrum, at a slightly higher field compared to the signals observed for the carbene ligand. The two methyl groups in the 4 and 5 positions of the carbene ligand and the same methyl groups in the 4′ and 5′ positions of the thione ligand appear very close together in both the ^{1}H NMR and ^{13}C NMR spectra, and no definite assignment to either the carbene ligand or thione ligand can be made.

The septet representing the H^6 and H^9 carbene ligand protons appears at δ 6.21, a chemical shift similar to that observed for **1** (δ 6.10), but at much lower field than the septets observed for **6** (δ 5.32), **11** (δ 5.84) and **12** (δ 5.77). No coupling constant could be determined for the same protons on the thione ligand, $H^{6'}$ and $H^{9'}$, which are observed as a broad peak. This phenomenon is also observed in the other thione complexes, which will be discussed later (**14**, **15**, **16**, **19** and **22**). The signals of the thione ligand are generally broader than the corresponding signals of the carbene ligand, allowing the unambiguous assignment of $C^{6'}$ and $C^{9'}$ (δ 51.5), and C^6 and C^9 (δ 54.3) signals in the ^{13}C NMR spectrum. A comparison with the corresponding signals observed for the carbene complexes (**1**, **6**, **11** and **12**) and the thione

complexes (**15**, **18** and **21**) also provides an indication of which ligand is responsible for which set of signals. In the ^{13}C NMR spectrum the signals of the carbonyl (δ 187.5) and carbene (δ 175.1) carbons are observed at chemical shifts similar to those observed for **11** (δ 188.4 and δ 177.2) and **12** (δ 186.5 and δ 173.6).

Table 2.6.17 *NMR data of complex* ***13*** *in CD_2Cl_2 (relative to internal TMS)*

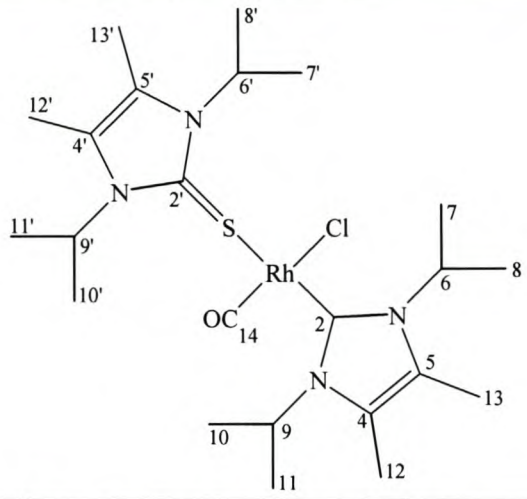

^{1}H NMR assignment	Chemical shift in ppm (number of protons, multiplicity, coupling constant)
H^6/H^9	6.21 (2H, septet, $^3J_{H\text{-}H}$ = 7.15 Hz)
$H^{6'}/H^{9'}$	5.96 (2H, broad signal)
H^{12}/H^{13} and $H^{12'}/H^{13'}$	2.21 (6H, s) and 2.16 (6H, s)
$H^{7'}/H^{8'}$ and $H^{10'}/H^{11'}$	1.53 (12H, d, $^3J_{H\text{-}H}$ = 7.15 Hz)
H^7/H^8 and H^{10}/H^{11}	1.48 (6H, d, $^3J_{H\text{-}H}$ = 7.15 Hz) and 1.45 (6H, d, $^3J_{H\text{-}H}$ = 7.15 Hz)
^{13}C NMR assignment	Chemical shift in ppm (multiplicity, coupling constant)
C^{14}	187.5 (d, $^1J_{C\text{-}Rh}$ = 80.8 Hz)
C^2	175.1 (d, $^1J_{C\text{-}Rh}$ = 54.8 Hz)
$C^{2'}$	157.2 (s)
C^4/C^5 and $C^{4'}/C^{5'}$	125.6 (s) and 124.5 (s)
C^6/C^9	54.3 (s)
$C^{6'}/C^{9'}$	51.5 (s)
C^7/C^8 and C^{10}/C^{11}	22.1 (s) and 22.0 (s)
$C^{7'}/C^{8'}$ and $C^{10'}/C^{11'}$	21.2 (s)
C^{12}/C^{13} and $C^{12'}/C^{13'}$	10.9 (s) and 10.8 (s)

The magnitudes of the coupling constants of the carbonyl carbon doublet are also comparable ($^1J_{C\text{-}Rh}$ = 80.8 Hz for **13**, $^1J_{C\text{-}Rh}$ = 78.7 Hz for **11**, $^1J_{C\text{-}Rh}$ = 77.1 Hz for **12**). The magnitude of the coupling constant observed for the carbene carbon doublet ($^1J_{C\text{-}Rh}$ = 54.8 Hz) is closer to that observed for the cyclooctadiene complex **1** ($^1J_{C\text{-}Rh}$ = 51.5 Hz) or the dicarbonyl complex **6** ($^1J_{C\text{-}Rh}$ = 43.0 Hz) than to the coupling constant observed for **11** ($^1J_{C\text{-}Rh}$ = 123.2 Hz) or **12** ($^1J_{C\text{-}Rh}$ = 137.4 Hz). This information is a clear indication of the weaker *trans* influence of the thione ligand compared to that of the phosphine ligands.

The relative *trans* influence of the thione ligand can also be seen in the crystal structure of another thiourea complex. The average Rh-$C_{olefinic\ cod}$ bond length *trans* to the thiourea ligand in [RhCl(cod)(Phtu)] {Phtu = PhNHC(S)NHPh}[85] is 2.156(15) Å. *Trans* to the chloride ligand the average bond length is 2.129(14) Å. The conclusion from this information is that the *trans* influence of the thiourea ligand is slightly stronger than that of the chloride ligand. This means that the *trans* influence of the thione ligand is greater than that of a halide but smaller than the *trans* influences of phosphine and carbene ligands, which have also been proved to be greater than that of halides.

6.3.1.14 [(η^4-1,5-Cyclooctadiene)(1,3-diisopropyl-4,5-dimethyl-2,3-dihydro-1H-imidazol-2-thione)(1,3-diisopropyl-4,5-dimethyl-2,3-dihydro-1H-imidazol-2-ylidene)rhodium(I)][tetrafluoroborate] (14)

The ^{1}H NMR data of complex **14** are summarised in Table 2.6.18. The signals of the thione and carbene ligands appear at chemical shifts similar to those observed for the same ligands of complex **13**, again with two signals for the methyl groups of the *N*-substituents of the carbene ligand, similar to **1**, **6**, **11**, **12** and **13**. The two sets of multiplets that represent the olefinic protons of the cyclooctadiene ligand appear at δ 3.92 (*trans* to the carbene ligand) and δ 3.75 (*trans* to the thione ligand). The difference is much smaller than was observed for **1** (δ 4.81 *trans* to the carbene ligand and δ 3.31 *trans* to the chloride ligand). This is a further indication that the thione ligand has a stronger *trans* influence than the chloride ligand of **1**. The signals of the equatorial and axial aliphatic protons of the cyclooctadiene ligand appear at almost the same chemical shifts for **14** (δ 2.33 and δ 1.95) as for **1** (δ 2.32 and δ 1.87).

In the ^{13}C NMR spectrum, summarised in Table 2.6.19, the chemical shifts of the signals observed for the thione and carbene ligands are comparable with the chemical shifts observed for the same ligands of **13**. The carbene carbon appears as a doublet at δ 176.5. The coupling constant of this doublet is 50.2 Hz, smaller than the coupling constant observed for **13** ($^1J_{C\text{-}Rh}$ = 54.8 Hz), but similar to that observed for **1** ($^1J_{C\text{-}Rh}$ = 51.5 Hz). The peak that appears for $C^{2'}$ is at δ 152.9, further upfield than the same peak observed for **13** (δ 157.2). This is probably due to the weaker *cis* influence of the carbene ligand compared to the chloride ligand in **13**. More clarity will be obtained when the NMR data of the thione complex **16**, with a structure similar to that of the carbene complex **1**, are being discussed in section 6.3.1.16 later.

Table 2.6.18 *^1H NMR data of complex **14** in CD_2Cl_2 (relative to internal TMS)*

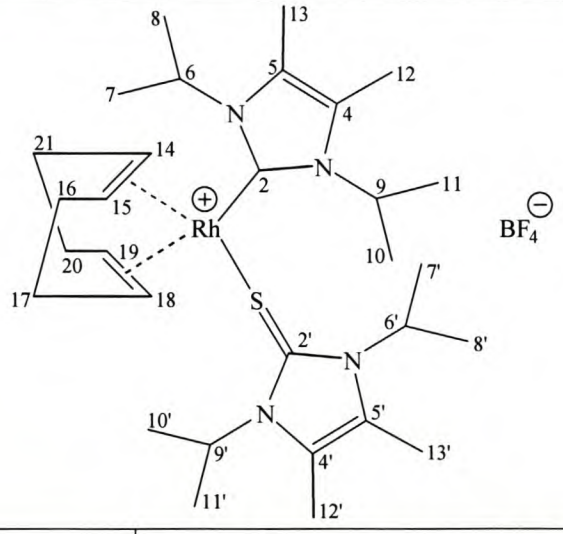

^1H NMR assignment	Chemical shift in ppm (number of protons, multiplicity, coupling constant)
H^6/H^9	5.97 (2H, septet, $^3J_{H\text{-}H}$ = 7.15 Hz)
$H^{6'}/H^{9'}$	5.39 (2H, broad signal)
H^{18}/H^{19}	3.92 (2H, m)
H^{14}/H^{15}	3.75 (2H, m)
H^{16}/H^{21}, H^{17}/H^{20} (equatorial)	2.33 (4H, m)
H^{12}/H^{13} and $H^{12'}/H^{13'}$	2.24 (6H, s) and 2.17 (6H, s)
H^{16}/H^{21}, H^{17}/H^{20} (axial)	1.95 (4H, m)
H^7/H^8 and H^{10}/H^{11}	1.61 (6H, d, $^3J_{H\text{-}H}$ = 7.15 Hz) and 1.56 (6H, d, $^3J_{H\text{-}H}$ = 7.15 Hz)
$H^{7'}/H^{10'}$ and $H^{8'}/H^{11'}$	1.51 (12H, d, $^3J_{H\text{-}H}$ = 7.15 Hz)

The olefinic carbon atoms of the cyclooctadiene ligand *trans* to the carbene ligand, C^{18} and C^{19}, appear at δ 92.7 with a $^1J_{Rh\text{-}C}$ value of 7.4 Hz. This coupling constant is the same magnitude as the coupling constant of the doublet that was observed for the same olefinic carbon atoms *trans* to the carbene ligand of complex **1**. C^{14} and C^{15} are observed as a doublet at δ 75.4 ($^1J_{Rh\text{-}C}$ = 12.1 Hz). This coupling constant is smaller than the coupling constant of the olefinic carbon atoms of the cyclooctadiene ligand *trans* to the chloride atom in **1** ($^1J_{Rh\text{-}C}$ = 14.7 Hz), additional proof of the sequence of *trans* influences proposed earlier.

Table 2.6.19 *^{13}C NMR data of complex **14** in CD_2Cl_2 (relative to internal TMS)*

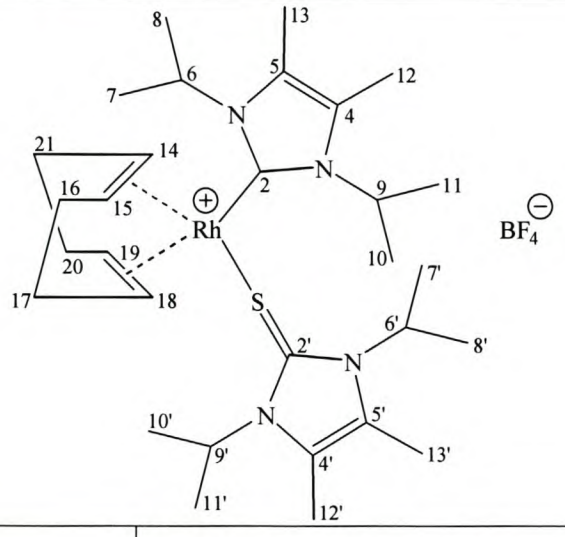

^{13}C NMR assignment	Chemical shift in ppm (multiplicity, coupling constant)
C^2	176.5 (d, $^1J_{Rh\text{-}C}$ = 50.2 Hz)
$C^{2'}$	152.9 (s)
C^4/C^5 and $C^{4'}/C^{5'}$	127.2 (s) and 126.8 (s)
C^{18}/C^{19}	92.7 (d, $^1J_{Rh\text{-}C}$ = 7.4 Hz)
C^{14}/C^{15}	75.4 (d, $^1J_{Rh\text{-}C}$ = 12.1 Hz)
C^6/C^9	54.8 (s)
$C^{6'}/C^{9'}$	52.2 (s)
C^{17}/C^{20}	32.8 (s)
C^{16}/C^{21}	30.0 (s)
C^7/C^8 and C^{10}/C^{11}	22.5 (s) and 22.1 (s)
$C^{7'}/C^{10'}$ and $C^{8'}/C^{11'}$	21.6 (s)
C^{12}/C^{13} and $C^{12'}/C^{13'}$	11.1 (s) and 10.8 (s)

6.3.1.15 [(Dicarbonyl)-cis-(1,3-diisopropyl-4,5-dimethyl-2,3-dihydro-1H-imidazol-2-thione)(1,3-diisopropyl-4,5-dimethyl-2,3-dihydro-1H-imidazol-2-ylidene)rhodium(I)][tetrafluoroborate] (15)

Table 2.6.20 *Proton NMR data of complex* ***15*** *in CD_2Cl_2 [and $CDCl_3$] (relative to internal TMS)*

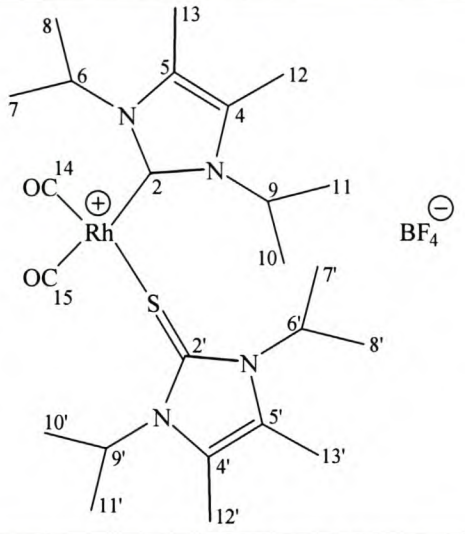

^{1}H NMR assignment	Chemical shift in ppm (number of protons, multiplicity, coupling constant)
$H^{6'}/H^{9'}$	5.36 (2H, broad signal) ; [5.35 (2H, broad signal)]
H^6/H^9	5.30 (2H, septet, $^3J_{H\text{-}H}$ = 7.15 Hz) ; [5.31 (2H, septet, $^3J_{H\text{-}H}$ = 7.15 Hz)]
$H^{12'}/H^{13'}$ and H^{12}/H^{13}	2.29 (s) and 2.22 (s) ; [2.34 (6H, s) and 2.26 (6H, s)]
H^7/H^8 and H^{10}/H^{11}	1.58 (6H, d, $^3J_{H\text{-}H}$ = 7.15 Hz) and 1.56 (6H, d, $^3J_{H\text{-}H}$ = 7.15 Hz) ; [1.61 (6H, d, $^3J_{H\text{-}H}$ = 7.15 Hz) and 1.59 (6H, d, $^3J_{H\text{-}H}$ = 7.15 Hz)]
$H^{7'}/H^{10'}$ and $H^{8'}/H^{11'}$	1.57 (12H, d, $^3J_{H\text{-}H}$ = 7.15 Hz) ; [1.60 (12H, d, $^3J_{H\text{-}H}$ = 7.15 Hz)]

In the ^{1}H NMR spectrum of **15**, summarised in Table 2.6.20, the peak observed for H^6 and H^9 appears at a higher field than the peak observed for $H^{6'}$ and $H^{9'}$, whereas in the ^{1}H NMR spectra of **13** and **14** it is the other way round. This shift of the H^6, H^9 peak to a higher field corresponds to the shift observed in the spectra of **1** (δ 6.10) and **6** (δ 5.32). These protons are in the deshielding region of the anisotropic field of the cyclooctadiene ligand in complexes **1**

and **14**, a field that is not present in the carbonyl complexes **6** and **15**. This anisotropic field does not affect the $H^{6'}$ and $H^{9'}$ protons of the thione ligand, which are probably too far from the metal centre. The signals of the methyl groups of the isopropyl substituents of the thione and carbene ligands appear at the same chemical shift when CD_2Cl_2 is used as the NMR solvent. A better resolution is achieved when $CDCl_3$ is used as the solvent.

Table 2.6.21 *^{13}C NMR data of complex **15** in CD_2Cl_2 [and $CDCl_3$] (relative to internal TMS)*

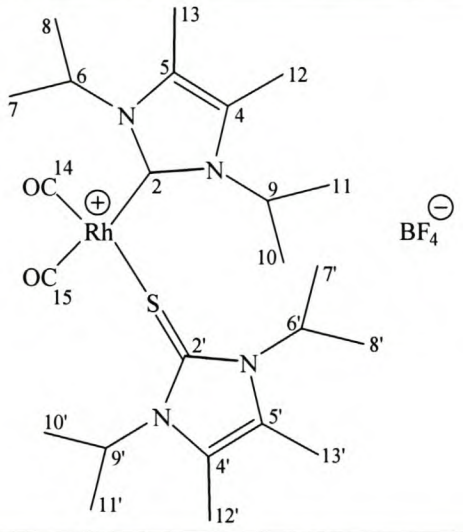

^{13}C NMR assignment	Chemical shift in ppm (multiplicity, coupling constant)
C^{15}	189.2 (d, $^1J_{C\text{-}Rh}$ = 56.7 Hz) ; [188.3 (d, $^1J_{C\text{-}Rh}$ = 57.6 Hz)]
C^{14}	183.6 (d, $^1J_{C\text{-}Rh}$ = 70.6 Hz) ; [182.7 (d, $^1J_{C\text{-}Rh}$ = 70.6 Hz)]
C^{2}	164.9 (d, $^1J_{C\text{-}Rh}$ = 40.9 Hz) ; [164.4 (d, $^1J_{C\text{-}Rh}$ = 41.8 Hz)]
$C^{2'}$	152.2 (s) ; [150.9 (s)]
C^4/C^5 and $C^{4'}/C^{5'}$	128.6 (s) and 127.1 (s) ; [127.7 (s) and 126.4 (s)]
C^6/C^9	55.3 (s) ; [54.5 (s)]
$C^{6'}/C^{9'}$	52.4 (s) ; [51.7 (s)]
C^7/C^8 and C^{10}/C^{11}	22.6 (s) and 22.1 (s) ; [22.0 (s) and 21.5 (s)]
$C^{7'}/C^{10'}$ and $C^{8'}/C^{11'}$	21.1 (s) ; [20.5 (s)]
C^{12}/C^{13} and $C^{12'}/C^{13'}$	10.9 (s) and 10.8 (s) ; [10.3 (s) and 10.2 (s)]

In the ^{13}C NMR spectrum, summarised in Table 2.6.21, the carbene carbon appears as a doublet at δ 164.9, which is much further upfield than for any of the other similar carbene complexes (δ 180.7 for **1**, δ 170.7 for **6**, δ 177.2 for **11**, δ 173.6 for **12**, δ 175.1 for **13** and δ 176.5 for **14**). The magnitude of the coupling constant ($^1J_{C\text{-}Rh}$ = 40.9 Hz) is slightly smaller than the coupling constant observed for the dicarbonyl complex **6** ($^1J_{C\text{-}Rh}$ = 43.0 Hz). The $C^{2'}$ carbon atom appears at δ 152.2, almost the same value as the chemical shift observed for $C^{2'}$ in **14** (δ 152.9). Other signals of the thione and carbene ligands also appear at chemical shifts similar to those observed for **14**.

The presence of two doublets for the two carbonyl carbon atoms confirms that the carbene and thione ligands of **15** are in a *cis* configuration. The magnitude of the chemical shift and coupling constant of the doublet observed for the carbonyl carbon *trans* to the carbene ligand are slightly larger (δ 189.2, $^1J_{C\text{-}Rh}$ = 56.7 Hz) than those observed for **6** (δ 187.7, $^1J_{C\text{-}Rh}$ = 54.3 Hz). The carbonyl carbon C^{14}, *trans* to the thione ligand, is observed as a doublet at δ 183.6 with a coupling constant of 70.6 Hz. The carbonyl ligand *trans* to the chloride ligand in **6** appears as a doublet with a coupling constant of 75.4 Hz. The smaller coupling constant observed for **15** confirms that the *trans* influence of the thione ligand is larger than that of the chloride.

*Rhodium(I) complexes with thione ligands (**16 – 25**):*

6.3.1.16 Chloro(η⁴-1,5-cyclooctadiene)(1,3-diisopropyl-4,5-dimethyl-2,3-dihydro-1H-imidazol-2-thione)rhodium(I) (16)

The NMR data of **16** are summarised in Table 2.6.22. The signals of the thione complex **16** exhibit broadening and coalescence in its ^1H NMR spectrum, a phenomenon also observed by Müller and Stock during the characterisation of cyclooctadiene imine rhodium(I) complexes.[98] The peak for H^6 and H^9 in the ^1H NMR spectrum of the free thione ligand (in CD_2Cl_2) appears as a broad signal, while a sharp singlet is observed for H^{12} and H^{13} (δ 2.12) and a doublet (δ 1.37, $^3J_{H\text{-}H}$ = 7.17 Hz) for H^7/H^{10} and H^8/H^{11}.

Interestingly, two signals appear for the two methyl protons H^{12} and H^{13} of **16** as well as for the methyl groups of the isopropyl substituents. For H^6 and H^9, however, there is only one broad peak as for the free ligand. A solution of **16** in deuterated toluene yielded the same

broad signals, and a change in chemical shifts compared to spectra recorded in a CD_2Cl_2 solution of **16**. At higher temperatures, the signals representing the axial protons of the cyclooctadiene ligand become one sharp singlet at δ 1.92, while the broad signals observed for H^7/H^8 and H^{10}/H^{11} become single, though still somewhat broad (Figure 2.6.14).

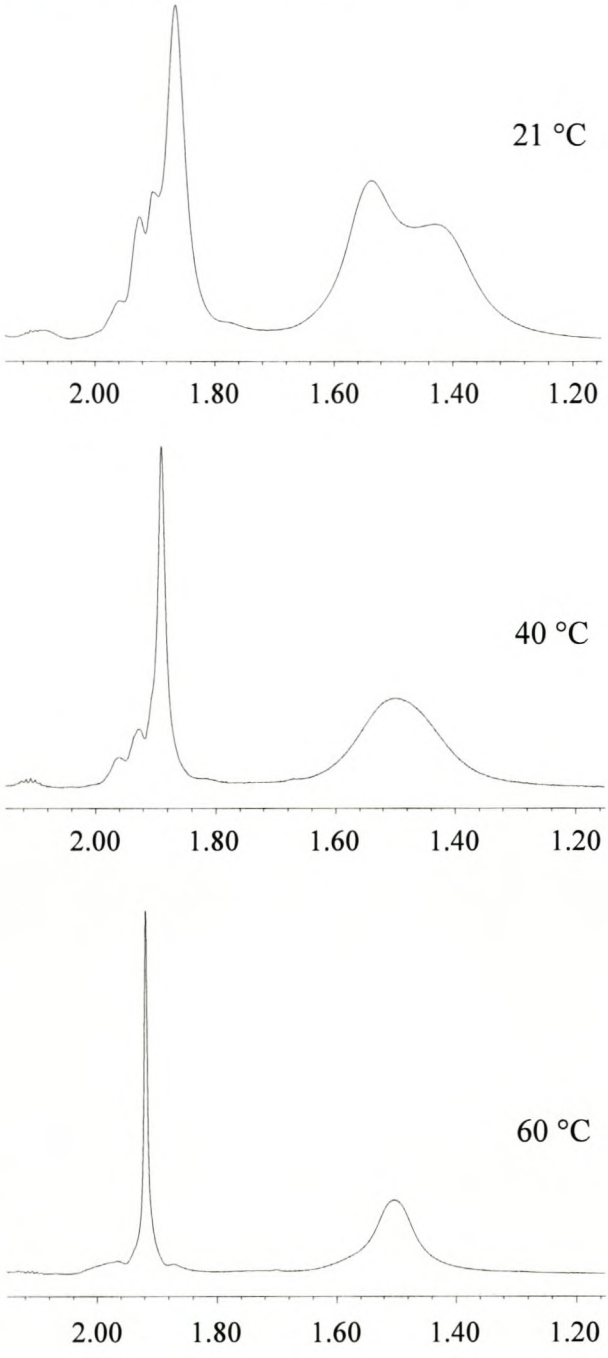

Figure 2.6.14 *^{1}H NMR spectra of complex **16** in toluene-d_8 at three different temperatures*

This information would suggest the presence of isomers caused by slowed inversion about the rhodium-coordinated sulfur atom. Abel and co-workers reported the occurrence of a rapid

ring-flipping process in rhodium complexes with sulfur ligands, indicated by variable temperature NMR studies.[123] The sulfur inversion will be slow on the NMR time scale, leading to the observation of both isomers at room temperature. At higher temperature this inversion happens too quickly to be observed as two different signals in the NMR spectra. However, sharp signals were observed in the NMR spectra of **13**, **14** and **15**. This is due to either an absence of ring-flipping because of sterical reasons or very quick sulfur inversions.

The difference in *trans* influences of the thione and chloride ligands is reflected in the different chemical shifts observed for the ^{1}H NMR signals of H^{14}/H^{15} (δ 4.33) and H^{18}/H^{19} (δ 3.82). This difference is smaller than that appearing in the ^{1}H NMR spectrum of **1** (δ 4.81 and δ 3.31), giving an indication that the *trans* influence of the carbene ligand is larger than that of the heterocyclic thione ligand in **16**.

Each of the carbon atoms of the thione ligand is responsible for two signals in the room temperature ^{13}C NMR spectrum of **16**, whereas none of the cyclooctadiene carbon atoms exhibit this phenomenon. High temperature NMR experiments performed in a deuterated toluene solution of **16**, showed that these double signals become one at higher temperatures. In Figure 2.6.15 an illustration of the two possible coordination positions of the thione ligand to the rhodium centre is given. The Rh-S-C^2 bond angle is smaller than 180° in the solid state structure of **17**, as will be discussed later.

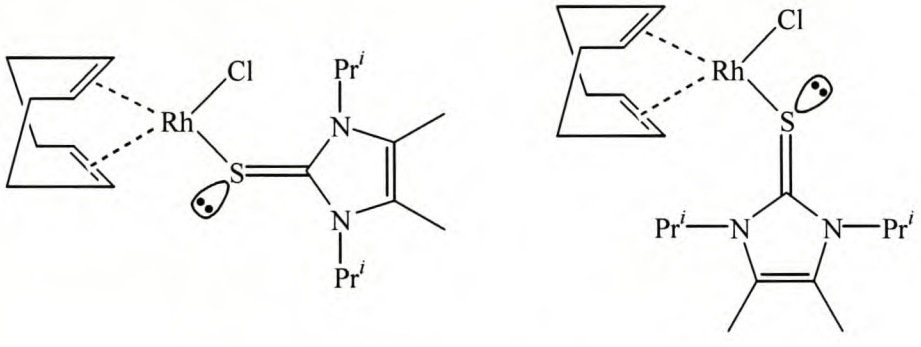

Figure 2.6.15 *Two possible isomers of* ***16***

The C^2 carbon atom resonates as two singlets (δ 155.6 and δ 155.4) in the ^{13}C NMR spectrum at room temperature. These peaks are further downfield than the signal observed in the spectrum of **14** (δ 152.9) and further upfield than the one observed for **13** (δ 157.2). The difference in the *trans* and *cis* influences of the carbene and chloride ligands is responsible for

these differences in chemical shifts. The strong *trans* influence of the carbene ligand is responsible for the chemical shift at lower field in **13**. The chemical shifts observed for the C^2 atom of **14** and **16** suggest that the chloride ligand has a stronger *cis* influence than the carbene ligand.

Table 2.6.22 *NMR data of complex* ***16*** *in CD_2Cl_2 (relative to internal TMS)*

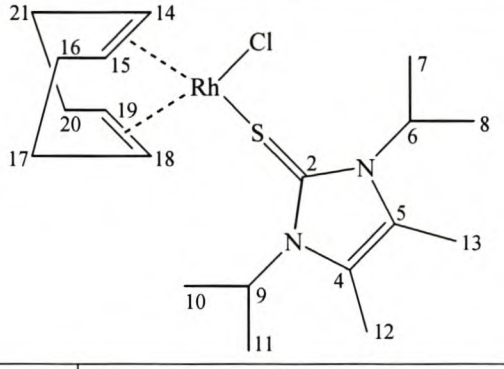

^{1}H NMR assignment	Chemical shift in ppm (number of protons, multiplicity, coupling constant)
H^6/H^9	5.63 (2H, broad signal)
H^{14}/H^{15}	4.33 (2H, m)
H^{18}/H^{19}	3.82 (2H, m)
H^{16}/H^{21}, H^{17}/H^{20} (equatorial)	2.35 (4H, m)
H^{12}/H^{13}	2.20 (3H, m) and 2.14 (3H, m)
H^{16}/H^{21}, H^{17}/H^{20} (axial)	1.75 (4H, m)
H^7/H^{10} and H^8/H^{11}	1.53 (6H, m) and 1.40 (6H, m)
^{13}C NMR assignment	Chemical shift in ppm (multiplicity, coupling constant)
C^2	155.6 (s) and 155.4 (s)
C^4/C^5	125.3 (s) and 122.3 (s)
C^{14}/C^{15}	83.7 (d, $^1J_{Rh\text{-}C}$ = 11.6 Hz)
C^{18}/C^{19}	74.4 (d, $^1J_{Rh\text{-}C}$ = 14.5 Hz)
C^6/C^9	51.9 (s) and 49.9 (s)
C^{16}/C^{21}	32.5 (s)
C^{17}/C^{20}	31.4 (s)
C^7/C^{10} and C^8/C^{11}	21.4 (s) and 21.1 (s)
C^{12}/C^{13}	11.0 (s) and 10.8 (s)

The magnitudes of the coupling constants observed for the doublets of the olefinic carbon atoms of the cyclooctadiene ligand are further proof that the *trans* influence of the thione ligand is smaller than the *trans* influence of the carbene ligand. The olefinic carbon atoms *trans* to the thione ligand are observed as a doublet at δ 83.7 with a coupling constant of 11.6 Hz, whereas the coupling constant for the same carbon atoms *trans* to the carbene ligand in **1** is only 7.4 Hz. The aliphatic carbon atoms are observed at their expected chemical shifts positions.

6.3.1.17 Chloro(η^4-1,5-cyclooctadiene)(1,3,4,5-tetramethyl-2,3-dihydro-1H-imidazol-2-thione)rhodium(I) (17)

The NMR chemical shifts of the proton and carbon atoms of **17** are summarised in Table 2.6.23. The two methyl protons H^6 and H^7 are observed as a broad signal at δ 3.62 in the ^1H NMR spectrum. C^6 and C^7 also appear as a broad signal (δ 33.6) in the ^{13}C NMR spectrum. The H^8 and H^9 protons are observed as more than one signal in the ^1H NMR spectrum, and C^8 and C^9 as a broad signal in the ^{13}C NMR spectrum. As in **16**, a probable reason is that the ring-flipping that takes place, is slow on the NMR timescale.

The signals of the protons of the cyclooctadiene ligand appear in the ^1H NMR spectrum at δ 4.28, δ 3.87, δ 2.35 and δ 1.72, similar to the signals observed at δ 4.33, δ 3.82, δ 2.35 and δ 1.75 for **16**. The signals for the cyclooctadiene ligand in the ^{13}C NMR spectrum are also at similar positions as those of **16**. The coupling constant of the doublet observed for the olefinic carbon atoms *trans* to the thione ligand is 11.9 Hz, almost the same as that observed for **16** ($^1J_{Rh\text{-}C}$ = 11.6 Hz). The olefinic carbon atoms *trans* to the chloride ligand also appear as a doublet with a coupling constant of 13.8 Hz, similar in magnitude to the coupling constant determined for **16** ($^1J_{Rh\text{-}C}$ = 14.5 Hz).

Table 2.6.23 *NMR data of complex* ***17*** *in CD_2Cl_2 (relative to internal TMS)*

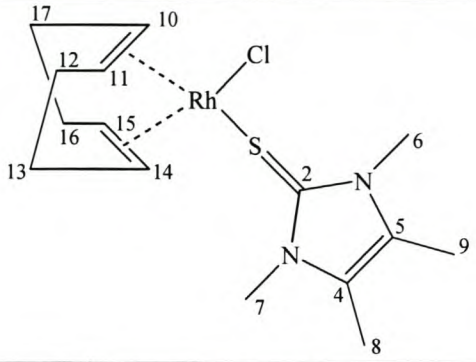

^{1}H NMR assignment	Chemical shift in ppm (number of protons, multiplicity, coupling constant)
H^{10}/H^{11}	4.28 (2H, m)
H^{14}/H^{15}	3.87 (2H, m)
H^{6}/H^{7}	3.62 (6H, m)
H^{12}/H^{17}, H^{13}/H^{16} (equatorial)	2.35 (4H, m)
H^{8}/H^{9}	2.09 (6H, m)
H^{12}/H^{17}, H^{13}/H^{16} (axial)	1.72 (4H, m)
^{13}C NMR assignment	Chemical shift in ppm (multiplicity, coupling constant)
C^2	156.3 (s)
C^4/C^5	124.4 (s)
C^{10}/C^{11}	83.6 (d, $^1J_{Rh\text{-}C}$ = 11.9 Hz)
C^{14}/C^{15}	74.8 (d, $^1J_{Rh\text{-}C}$ = 13.8 Hz)
C^6/C^7	33.6 (s)
C^{12}/C^{17}	32.4 (s)
C^{13}/C^{16}	31.3 (s)
C^8/C^9	9.7 (s)

6.3.1.18 Chloro(η^4-1,5-cyclooctadiene)(N,N-dimethylthioformamide)rhodium(I) (18)

The ^{1}H NMR data are summarised with the ^{13}C NMR data in Table 2.6.24. The only singlet in the proton NMR spectrum is observed for H^1 at δ 9.75. The same proton of the free ligand appears at δ 9.09. This downfield shift is probably due to the electron donation of the thione ligand to the rhodium metal *via* the sulfur atom. In the ^{13}C NMR spectrum C^1 is observed as a singlet at δ 191.6, close to the δ 188.8 observed for the same carbon atom of the free ligand.

Only one set of signals is observed for all the atoms in both NMR spectra, unlike the NMR spectra of **16** and **17**. The absence of isomers is probably due to a rapid inversion about the coordinated sulfur atom, not measurable on the NMR time-scale.

Table 2.6.24 *NMR data of complex* ***18*** *in CD_2Cl_2 (relative to internal TMS)*

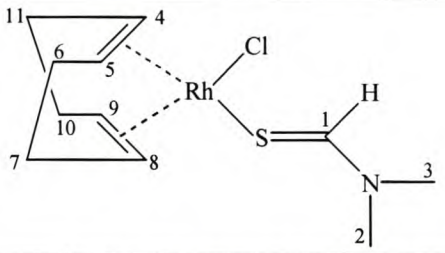

^{1}H NMR assignment	Chemical shift in ppm (number of protons, multiplicity, coupling constant)
H^1	9.75 (1H, s)
H^4/H^5	4.61 (2H, m)
H^8/H^9	3.85 (2H, m)
H^2 and H^3	3.33 (3H, m) and 3.23 (3H, m)
H^6/H^{11}, H^7/H^{10} (equatorial)	2.38 (4H, m)
H^6/H^{11}, H^7/H^{10} (axial)	1.83 (4H, m)
^{13}C NMR assignment	Chemical shift in ppm (multiplicity, coupling constant)
C^1	191.6 (s)
C^4/C^5	87.1 (m)
C^8/C^9	75.5 (m)
C^2 and C^3	47.5 (s) and 40.1 (s)
C^6/C^{11}	32.2 (m)
C^7/C^{10}	31.2 (m)

The protons of both the methyl groups are observed as multiplets (δ 3.33 and δ 3.23) in the ^{1}H NMR spectrum, similar to the signals for the free *N,N*-dimethylthioformamide ligand (δ 3.22 and δ 3.15). The carbon atoms C^2 and C^3 of the two methyl groups in **18**, are observed at δ 47.5 and δ 40.1. Two different signals (δ 45.6 and δ 37.4) are also observed for the two methyl carbons of the free ligand, the reason being the delocalisation of the S-C^1 double bond (see crystal structure determination of **18** in section 6.5), resulting in a partial C^1-N double

bond character and consequently restricted rotation about the C^1-N bond leading to the two methyl groups experiencing different chemical environments. The positions of the chemical shifts of the proton and carbon atoms of the cyclooctadiene ligand in **18** suggest that the bond between the *N,N*-dimethylthioformamide ligand and rhodium are similar to that of the heterocyclic thione ligands of **16** and **17**. The *trans* influence of *N,N*-dimethylthioformamide is thus also similar to that of the other thione ligands used in **16** and **17**.

6.3.1.19 Chloro(dicarbonyl)(1,3-diisopropyl-4,5-dimethyl-2,3-dihydro-1H-imidazol-2-thione)rhodium(I) (19)

Table 2.6.25 *NMR data of complex **19** in CD_2Cl_2 (relative to internal TMS)*

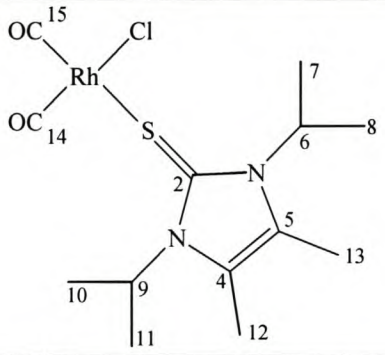

^{1}H NMR assignment	Chemical shift in ppm (number of protons, multiplicity, coupling constant)
H^6/H^9	5.52 (2H, broad peak)
H^{12}/H^{13}	2.23 (6H, s)
H^7/H^{10} and H^8/H^{11}	1.49 (12H, d, $^3J_{H\text{-}H}$ = 7.17 Hz)
^{13}C NMR assignment	Chemical shift in ppm (multiplicity, coupling constant)
C^{15} and C^{14}	184.6, 183.7, 183.6, 182.7 Two doublets – see discussion and figure
C^2	151.6 (s)
C^4/C^5	126.4 (s)
C^6/C^9	52.4 (s)
C^7/C^{10} and C^8/C^{11}	21.2 (s)
C^{12}/C^{13}	10.9 (s)

In contrast to the cyclooctadiene complex **16**, single peaks are observed for all the protons and carbons of the thione ligand in **19** (Table 2.6.25). Thus it can be deduced that the inversion of the thione ligand about the sulfur atom is too quick to be observed by NMR measurements, probably due to the absence of the sterically demanding cyclooctadiene ligand.

In the proton NMR spectrum the protons H^6 and H^9 appear as a broad peak similar to the peaks observed in the proton NMR spectra of the free ligand, **14**, **15** and **16**. All the other signals of the thione ligand in the ^1H NMR spectrum are sharp and appear at the normal positions.

Two sets of doublets are expected for the carbonyl carbons C^{14} and C^{15} in the ^{13}C NMR spectrum because of the difference between the *trans* influences caused by the thione ligand and the chloride. However, the four peaks of the two doublets are observed very close together (Figure 2.6.16), making definite assignment almost impossible. Two possibilities exist for assigning the signals to the carbonyl carbons, leading to two possible sets of coupling constants ($^1J_{C\text{-}Rh}$ = 76.91 and $^1J_{C\text{-}Rh}$ = 73.58 Hz or $^1J_{C\text{-}Rh}$ = 72.15 and $^1J_{C\text{-}Rh}$ = 68.81 Hz). From the results previously obtained for the reported carbene complexes, the doublet observed at the lowest chemical shift is expected to have a larger coupling constant than the other doublet; this is not found in the ^{13}C NMR spectrum of **19**. From the coupling constants it appears that the *trans* influences of the thione and chloride ligands are very similar.

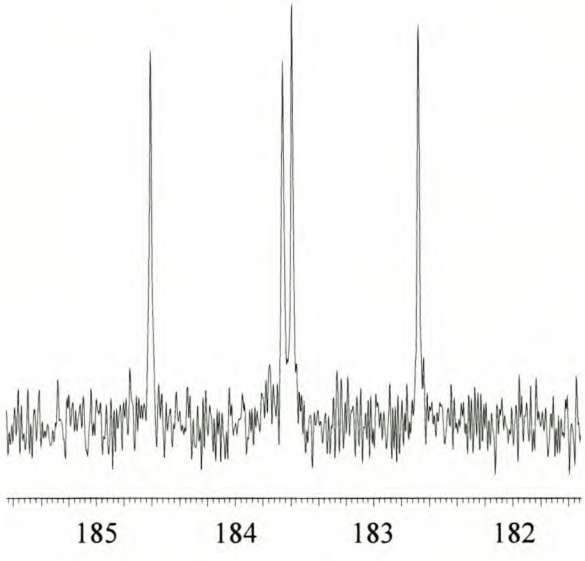

Figure 2.6.16 *The four signals representing the two CO carbon atoms of complex **19** in the ^{13}C NMR spectrum*

*6.3.1.20 Chloro(dicarbonyl)(1,3,4,5-tetramethyl-2,3-dihydro-1*H*-imidazol-2-thione)rhodium(I) (20)*

In the ^{1}H NMR spectrum of **20**, summarised with the ^{13}C NMR data in Table 2.6.26, two sharp signals are observed for the four methyl groups of the thione ligand. The carbon atoms of the thione ligand are also observed as very sharp singlets in the ^{13}C NMR spectrum. Sharp signals were expected after considering the NMR data of **19**, which has been discussed above.

Table 2.6.26 *NMR data of complex* ***20*** *in CD_2Cl_2 (relative to internal TMS)*

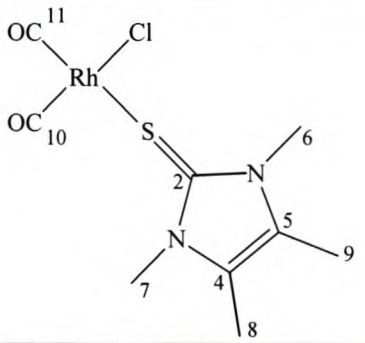

^{1}H NMR assignment	Chemical shift in ppm (number of protons, multiplicity, coupling constant)
H^6/H^7	3.65 (6H, s)
H^8/H^9	2.15 (6H, s)
^{13}C NMR assignment	Chemical shift in ppm (multiplicity, coupling constant)
C^{10} and C^{11}	182.9 (d, $^{1}J_{C\text{-}Rh}$ = 66.9 Hz)
C^2	152.3 (s)
C^4/C^5	125.6 (s)
C^6/C^7	34.0 (s)
C^8/C^9	9.8 (s)

In the ^{13}C NMR spectrum the chemical shifts of carbonyl carbons C^{10} and C^{11} appear as doublets with almost the same chemical shift, resulting in two broad signals. The coupling constant given in Table 2.6.26 was determined from these broad peaks and is not completely accurate. From this information it can be concluded that the less bulky 1,3,4,5-tetramethyl-2,3-dihydro-1*H*-imidazol-2-thione has a smaller *trans* influence than the 1,3-diisopropyl-4,5-dimethyl-2,3-dihydro-1*H*-imidazol-2-thione ligand of **19**, and a very similar *trans* influence than that of the chloride ligand.

6.3.1.21 Chloro(dicarbonyl)(N,N-dimethylthioformamide)rhodium(I) (21)

The NMR data of complex **21** are summarised in Table 2.6.27. In the ^{1}H NMR spectrum the H^{1} peak appears as a multiplet at δ 9.66. Both methyl groups appear as doublets, the one at δ 3.35 and the other at δ 3.43. The probable explanation is that both methyl group protons couple to the H^{1} proton.

In the ^{13}C NMR spectrum of **21** three singlets are observed for C^{1}, C^{2} and C^{3} at chemical shifts similar to those observed for **18**. One doublet is observed for the two carbonyl carbons C^{4} and C^{5} at δ 189.1. The absence of a second doublet probably indicates that, as in **20**, the *trans* influences of the thione ligand *N,N*-dimethylthioformamide and chloride are very similar.

Table 2.6.27 *NMR data of complex **21** in CD_2Cl_2 (relative to internal TMS)*

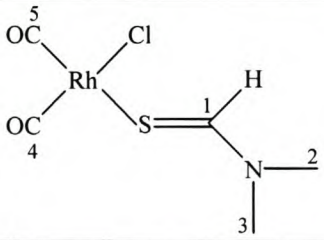

^{1}H NMR assignment	Chemical shift in ppm (number of protons, multiplicity, coupling constant)
H^{1}	9.66 (1H, m)
H^{2} and H^{3}	3.43 (3H, d, $J_{H\text{-}H}$ = 0.64 Hz) and 3.35 (3H, d, $J_{H\text{-}H}$ = 0.83 Hz)
^{13}C NMR assignment	Chemical shift in ppm (multiplicity, coupling constant)
C^{1}	189.1 (s)
C^{5} and C^{4}	182.5 (d, $^{1}J_{C\text{-}Rh}$ = 70.4 Hz)
C^{2} and C^{3}	48.4 (s) and 40.7 (s)

6.3.1.22 Chloro(carbonyl)-trans-(triphenylphosphine)(1,3-diisopropyl-4,5-dimethyl-2,3-dihydro-1H-imidazol-2-thione)rhodium(I) (22)

Table 2.6.28 *NMR data of complex* ***22*** *in CD_2Cl_2 (relative to internal TMS)*

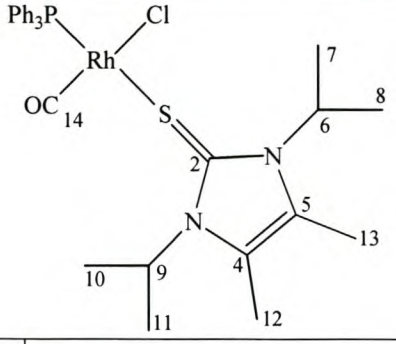

^{1}H NMR assignment	Chemical shift in ppm (number of protons, multiplicity, coupling constant)
H (Ph)	7.68 (6H, m) and 7.37 (9H, m)
H^6/H^9	5.87 (2H, broad signal)
H^{12}/H^{13}	2.19 (6H, s)
H^7/H^{10} and H^8/H^{11}	1.52 (12H, d, $^3J_{H\text{-}H}$ = 7.17 Hz)
^{13}C NMR assignment	Chemical shift in ppm (multiplicity, coupling constant)
C^{14}	188.5 (dd, $^1J_{C\text{-}Rh}$ = 75.5 Hz, $^2J_{C\text{-}P}$ = 16.2 Hz)
C^2	155.3 (s)
C_{ipso} (Ph)	135.6 (d, $^1J_{C\text{-}P}$ = 46.5 Hz)
C_{ortho} (Ph)	135.5 (d, $^2J_{C\text{-}P}$ = 11.6 Hz)
C_{meta} (Ph)	130.8 (d, $^3J_{C\text{-}P}$ = 1.8 Hz)
C_{para} (Ph)	128.8 (d, $^4J_{C\text{-}P}$ = 9.8 Hz)
C^4/C^5	125.4 (s)
C^6/C^9	51.9 (s)
C^7/C^{10} and C^8/C^{11}	21.2 (s)
C^{12}/C^{13}	10.9 (s)
^{31}P NMR assignment	Chemical shift in ppm (multiplicity, coupling constant)
P	32.5 (d, $^1J_{P\text{-}Rh}$ = 158.5 Hz)

The ^{1}H NMR spectrum of **22** is summarised in Table 2.6.28. No isomerisation is observable. All the signals observed for the thione ligand are sharp singlets, except for those of H^{6} and H^{9} that again appear as a broad peak. The phenyl groups are observed as two sets of multiplets.

In the ^{13}C NMR spectrum (Table 2.6.28) all the signals observed for the carbon atoms of the thione ligand and the phenyl groups have expected chemical shifts. All the carbon atoms of the thione ligand appear as singlets, while all the phenyl group carbon atoms appear as doublets as a result of carbon-phosphorus coupling. The signals of the *ortho*-, *meta*-, *para*- and *ipso*-carbon atoms appear at chemical shifts similar to those observed for **11**.

The carbonyl carbon C^{14} is observed as a doublet of doublets in the ^{13}C NMR spectrum. The chemical shift as well as the coupling constants are similar to those observed for complex **11** (δ 188.4, $^{1}J_{C\text{-}Rh}$ = 78.7 Hz, $^{2}J_{C\text{-}P}$ = 15.6 Hz). The phosphorus atom resonates at δ 32.5 in the ^{31}P NMR spectrum, almost at the same chemical shift (δ 32.8) as the phosphorus atom of complex **11**. The coupling constant of 158.5 Hz is larger than the value (116.3 Hz) observed for **11**, another indication that the thione ligand has a smaller *trans* influence than the carbene ligand.

6.3.1.23 Chloro(carbonyl)-trans-*(triphenylphosphine)*(N,N-*dimethylthioformamide)rhodium(I) (23)*

The NMR data of **23** are summarised in Table 2.6.29. The signals observed in the ^{13}C NMR spectrum for the *N,N*-dimethylthioformamide ligand show no significant difference from the signals observed for the same ligand in the dicarbonyl complex **21**, while the signals of the methyl groups in the proton NMR spectrum are much closer together for **23** than for **21**. The NMR data of the triphenylphosphine ligand also compares well to that of complex **22**, as do the doublet of doublets observed for the carbonyl carbon. The phosphorus atom appears as a doublet in the ^{31}P NMR spectrum. The chemical shift and coupling constant compare well to those observed for **22**. Although no impurities could be detected in the ^{1}H and ^{13}C NMR spectra, there are three signals in the ^{31}P NMR spectrum (δ 30.3, δ 29.3 and δ 27.8) which clearly shows that **23** was not completely pure. Many attempts were made to purify complex **23**, but all proved to be unsuccessful.

Table 2.6.29 *NMR data of complex* ***23*** *in CD_2Cl_2 (relative to internal TMS)*

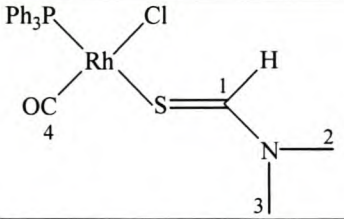

^{1}H NMR assignment	Chemical shift in ppm (number of protons, multiplicity, coupling constant)
H^1	9.71 (1H, s)
H (Ph)	7.70 (6H, m) and 7.40 (9H, m)
H^2/H^3	3.35 (3H, s) and 3.34 (3H, s)
^{13}C NMR assignment	Chemical shift in ppm (multiplicity, coupling constant)
C^1	189.7 (s)
C^4	186.7 (dd, $^1J_{C\text{-}Rh}$ = 75.0 Hz, $^2J_{C\text{-}P}$ = 16.7 Hz)
C_{ipso} (Ph)	135.1 (d, $^1J_{C\text{-}P}$ = 44.4 Hz)
C_{ortho} (Ph)	135.1 (d, $^2J_{C\text{-}P}$ = 11.1 Hz)
C_{meta} (Ph)	130.8 (d, $^3J_{C\text{-}P}$ = 2.8 Hz)
C_{para} (Ph)	128.6 (d, $^4J_{C\text{-}P}$ = 10.4 Hz)
C^2 and C^3	47.7 (s) and 40.2 (s)
^{31}P NMR assignment	Chemical shift in ppm (multiplicity, coupling constant)
P	38.8 (d, $^1J_{P\text{-}Rh}$ = 159.1 Hz)

*6.3.1.24 Chloro(carbonyl)-**trans**-bis(1,3-diisopropyl-4,5-dimethyl-2,3-dihydro-1**H**-imidazol-2-thione)rhodium(I) (24)*

From the NMR results for **24**, summarised in Table 2.6.30, it is clear that there is more than one complex in solution. All the signals in both the ^{1}H NMR and ^{13}C NMR spectra are multiplets. One set of signals stands out above the rest, indicating one predominant species. The only instance in which only one set of signals is observed is for the carbonyl carbon in the ^{13}C NMR spectrum. The doublet observed for this carbon at δ 187.1 is at a similar chemical shift to the signal for the carbonyl carbon in **22** (δ 188.5). The coupling constant is also of comparable magnitude ($^1J_{C\text{-}Rh}$ = 75.3 Hz for **24** and $^1J_{C\text{-}Rh}$ = 75.5 Hz for **22**).

Table 2.6.30 *NMR data of complex* ***24*** *in CD_2Cl_2 (relative to internal TMS)*

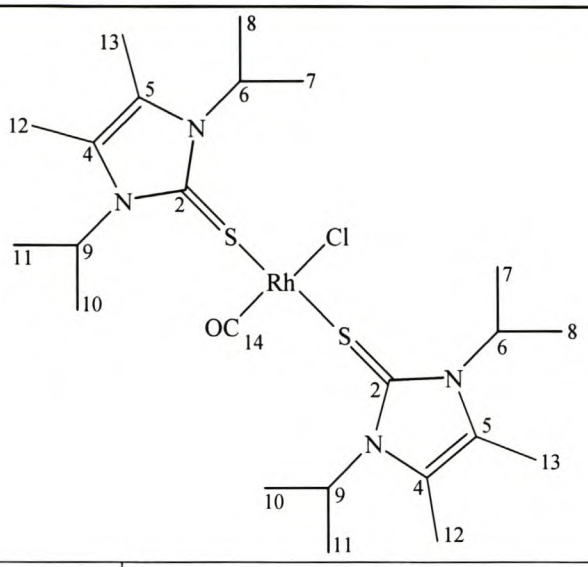

^{1}H NMR assignment	Chemical shift in ppm (number of protons, multiplicity, coupling constant)
H^6/H^9	5.91 (4H, broad signal)
H^{12}/H^{13}	2.18 (12H, m)
H^7/H^{10} and H^8/H^{11}	1.49 (24H, m)
^{13}C NMR assignment	Chemical shift in ppm (multiplicity, coupling constant)
C^{14}	187.1 (d, $^1J_{C\text{-}Rh}$ = 75.3 Hz)
C^2	153.5 (m)
C^4/C^5	125.9 (m)
C^6/C^9	51.9 (m)
C^7/C^{10} and C^8/C^{11}	21.7 (m)
C^{12}/C^{13}	11.1 (m)

As reported earlier the inversion about the sulfur atom can be responsible for the different signals observed in the NMR spectra. There are four possible ways that the two thione ligands can be bonded *via* the sulfur atom to the rhodium centre (Figure 2.6.17). The Rh-S-R angle is smaller than 120°, as shown in the crystal structure determination (Section 6.5) of **17**.

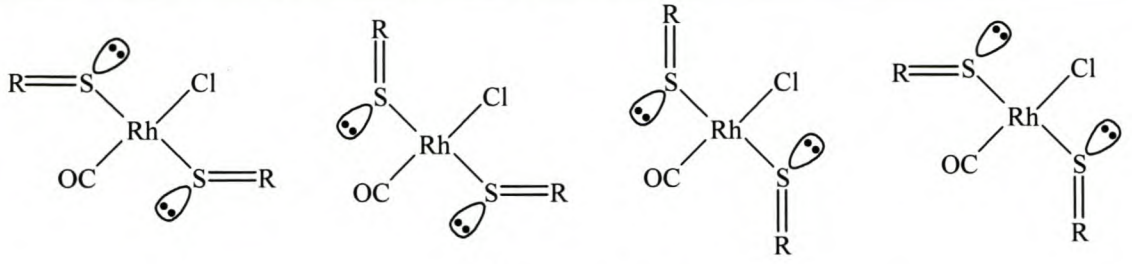

R = heterocyclic ring

Figure 2.6.17 *Three possible ways that the two thione ligands can be orientated*

*6.3.1.25 Chloro(carbonyl)-***trans-***bis(N,N-dimethylthioformamide)rhodium(I) (25)***

The same phenomenon occurring in **24** is observed for **25**. More than one signal appears for every proton and carbon atom of the two thione ligands. In Table 2.6.31 the strongest signals in the ^{1}H NMR spectrum observed for every proton are given along with the relative intensities. In the proton NMR spectrum there are two predominant sets of signals. A doublet appears for the carbonyl carbon at a chemical shift similar to that of **24**. The coupling constant is also comparable.

Table 2.6.31 *NMR data of the predominant species of complex* ***25*** *in CD_2Cl_2 (relative to internal TMS)*

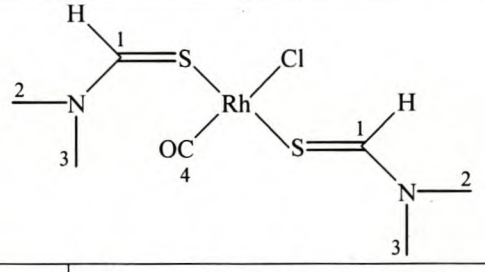

^{1}H NMR assignment	Chemical shift in ppm (number of protons, multiplicity, coupling constant)
H^1 H^2/H^3	9.51 (1H, m) and 9.19 (1H, m) 3.31 (3H, s) / 3.26 (3H, s) and 3.22 (3H, s) / 3.17 (3H, s)
^{13}C NMR assignment	Chemical shift in ppm (multiplicity, coupling constant)
C^1 C^4 C^2 and C^3	189.5 (m) 182.2 (d, $^1J_{C\text{-}Rh}$ = 70.8 Hz) 47.5 (m) and 43.5 (m)

*Cationic rhodium(I) complexes with thione ligands (**26** – **28**):*

6.3.1.26 [(η^4-1,5-Cyclooctadiene)bis(1,3-diisopropyl-4,5-dimethyl-2,3-dihydro-1H-imidazol-2-thione)rhodium(I)][tetrafluoroborate] (26)

Table 2.6.32 *Proton NMR data of complex **26** in CD_2Cl_2 (relative to internal TMS)*

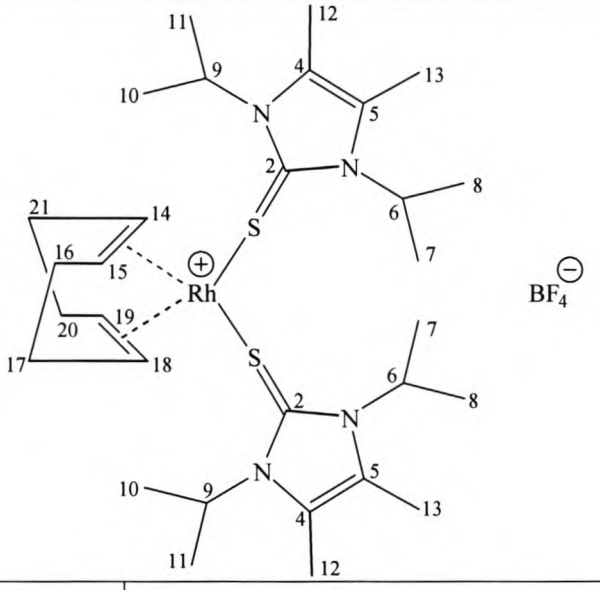

^{1}H NMR assignment	Chemical shift in ppm (number of protons, multiplicity, coupling constant)
H^6/H^9	5.44 (4H, broad signal)
H^{14}/H^{15} and H^{18}/H^{19}	3.76 (4H, m)
H^{16}/H^{21}, H^{17}/H^{20} (equatorial)	2.30 (4H, m)
H^{12}/H^{13}	2.21 (12H, s)
H^{16}/H^{21}, H^{17}/H^{20} (axial)	1.80 (4H, m)
H^7/H^{10} and H^8/H^{11}	1.49 (24H, d, $^3J_{H\text{-}H}$ = 7.17 Hz)

The four protons in the 6 and 9 positions are observed as a broad signal in the ^{1}H NMR spectrum of **26**. The same was observed for all the other thione complexes. The chemical shift of this signal (δ 5.44) is closer to that of the cationic complex **14** (δ 5.39) than to that of the cyclooctadiene complex **16** (δ 5.63). All the other protons of the thione ligand are observed at chemical shifts comparable to those of complexes **14** and **16** and are summarised in Table 2.6.32. All the signals are sharp signals similar to that observed for **14**, and unlike that observed for **16**. Steric bulk of the ligands is probably responsible for the prevention of ring-flipping in **26**.

Due to the symmetry of the complex (the thione ligands are perpendicular to the plane), all the olefinic protons of the cyclooctadiene ligand appear as a multiplet at δ 3.76, which is at a higher field than the δ 4.19 observed for the cationic biscarbene complex **5**. The axial and equatorial protons of the cyclooctadiene ligand appear at δ 1.80 and δ 2.30 respectively.

Table 2.6.33 *^{13}C NMR data of complex **26** in CD_2Cl_2 (relative to internal TMS)*

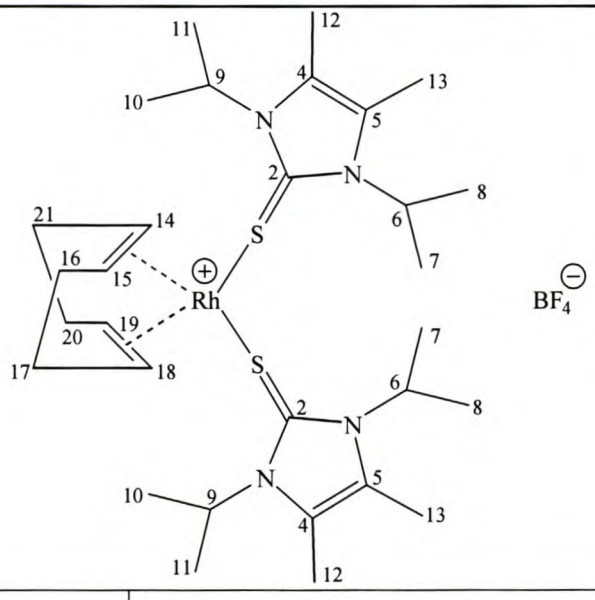

^{13}C NMR assignment	Chemical shift in ppm (multiplicity, coupling constant)
C^2	152.2 (s)
C^4/C^5	126.8 (s)
C^{14}/C^{15} and C^{18}/C^{19}	81.2 (d, $^1J_{C\text{-}Rh}$ = 11.6 Hz)
C^6/C^9	52.1 (s)
C^{16}/C^{21} and C^{17}/C^{20}	31.7 (s)
C^7/C^{10} and C^8/C^{11}	21.5 (s)
C^{12}/C^{13}	11.0 (s)

The ^{13}C NMR data are summarised in Table 2.6.33. The chemical shifts of the signals that are observed for the isopropyl and methyl groups of the thione ligands are similar to those found for all the other thione complexes discussed previously. The C^2 carbon atoms appear at δ 152.2, closer to the δ 152.9 observed for the cationic complex **14** than to the δ 155.5 observed for the cyclooctadiene complex **16**. The doublet observed for the olefinic carbon atoms of the cyclooctadiene ligand (δ 81.2) has a coupling constant of 11.6 Hz. This is 4.3 Hz

larger than the corresponding coupling constant of the doublet observed for the biscarbene complex **5** (δ 89.3), and 2.5 Hz less than the coupling constant observed for $[RhCl(cod)]_2$ (δ 79.5). This is further proof that the *trans* influence of the thione ligand is smaller than that of the carbene ligand, and greater than that of the chloride ligand.

*6.3.1.27 [(Dicarbonyl)*cis*-bis(1,3-diisopropyl-4,5-dimethyl-2,3-dihydro-1*H*-imidazol-2-thione)rhodium(I)][tetrafluoroborate] (27)*

Table 2.6.34 *NMR data of complex* ***27*** *in CD_2Cl_2 (relative to internal TMS)*

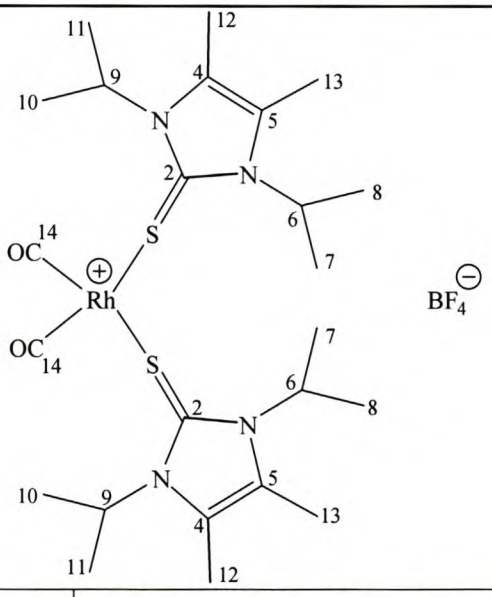

^{1}H NMR assignment	Chemical shift in ppm (number of protons, multiplicity, coupling constant)
H^6/H^9	5.45 (4H, broad signal)
H^{12}/H^{13}	2.27 (12H, s)
H^7/H^{10} and H^8/H^{11}	1.52 (24H, d, $^3J_{H\text{-}H}$ = 7.17 Hz)
^{13}C NMR assignment	Chemical shift in ppm (multiplicity, coupling constant)
C^{14}	184.3 (d, $^1J_{C\text{-}Rh}$ = 69.8 Hz)
C^2	149.9 (s)
C^4/C^5	127.5 (s)
C^6/C^9	52.6 (s)
C^7/C^{10} and C^8/C^{11}	21.2 (s)
C^{12}/C^{13}	10.9 (s)

All the signals of the thione ligands in the ^{1}H NMR spectrum (Table 2.6.34) appear at the expected values. The same is true for almost all the signals of the carbon atoms of the thione ligands in the ^{13}C NMR spectrum. The signal for C^{2} appears further upfield in the dicarbonyl complex **27** (δ 149.9) than in the cyclooctadiene complex **26** (δ 152.2).

The signal for the two equivalent carbonyl ligands appears as a doublet at δ 184.3 with a coupling constant of 69.8 Hz. The presence of only one doublet is confirmation that the two thione ligands are in a *cis* configuration. The coupling constant is larger than the 57.6 Hz coupling constant observed for the doublet which represents the two carbonyl ligands of the cationic biscarbene complex **9** at δ 189.9, and very similar to that of the cationic diimine complex $[Rh(CO)_2(Hbbtm)][BF_4]$ (δ 182.7, $^{1}J_{C\text{-}Rh}$ = 70.1 Hz).[102]

6.3.1.28 [(η^4-1,5-Cyclooctadiene)(4,5-dimethylthiazole)(1,3-diisopropyl-4,5-dimethyl-2,3-dihydro-1H-imidazol-2-thione)rhodium(I)][tetrafluoroborate] (28)

All the peaks in the proton NMR spectrum of **28** (Table 2.6.35) are observed as broad signals. This is expected from reported NMR results of various imine complexes[98] and the NMR results of the thione complex **16**, which has already been discussed. The most striking observation in the ^{1}H NMR spectrum is that only one broad signal appears for all four olefinic protons of the cyclooctadiene ligand, probably due to the similarities of the *trans* influences of the thione and imine ligands. The eight axial and equatorial aliphatic protons appear as four different multiplets.

In the ^{13}C NMR spectrum (Table 2.6.36) of **28**, the only significant observation is again for the signals of the cyclooctadiene ligand. Only one doublet at δ 85.5 is observed for the four olefinic carbon atoms. The coupling constant is 12.1 Hz, larger than the 11.6 Hz observed for complex **26**. The four aliphatic carbon atoms of the cyclooctadiene ligand surprisingly also appear as only one signal.

Table 2.6.35 *Proton NMR data of complex* ***28*** *in CD_2Cl_2 (relative to internal TMS)*

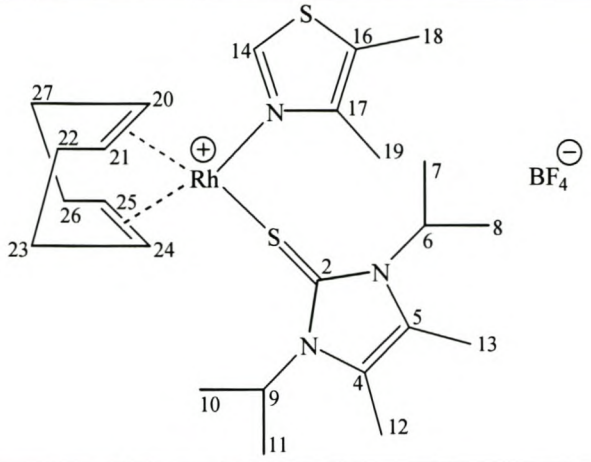

^{1}H NMR assignment	Chemical shift in ppm (number of protons, multiplicity, coupling constant)
H^{14}	8.95 (1H, s)
H^6/H^9	5.49 (2H, broad signal)
H^{20}/H^{21} and H^{24}/H^{25}	3.99 (4H, m)
H^{19}	2.86 (3H, s)
H^{22}/H^{27}, H^{23}/H^{26} (equatorial)	2.62 (2H, m) and 2.41 (2H, m)
H^{18}	2.28 (3H, s)
H^{12}/H^{13}	2.24 (12H, s)
H^{22}/H^{27}, H^{23}/H^{26} (axial)	2.13 (2H, m) and 1.97 (2H, m)
H^7/H^{10} and H^8/H^{11}	1.49 (12H, d, $^3J_{H\text{-}H}$ = 7.15 Hz)

Table 2.6.36 *^{13}C NMR data of complex **28** in CD_2Cl_2 (relative to internal TMS)*

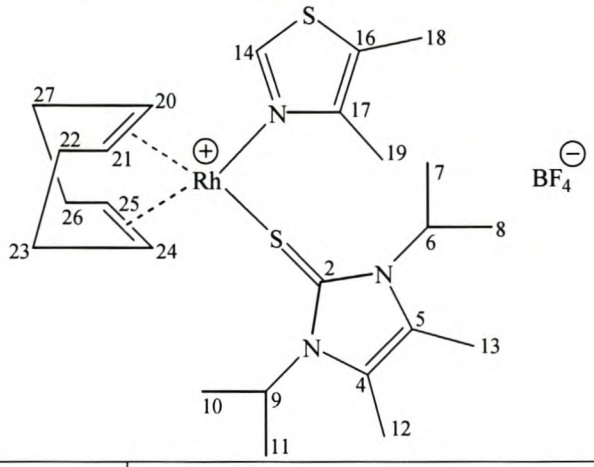

^{13}C NMR assignment	Chemical shift in ppm (multiplicity, coupling constant)
C^{2}	156.0 (s)
C^{17}	152.2 (s)
C^{14}	148.6 (s)
C^{16}	130.2 (s)
C^{14}/C^{15}	126.6 (s)
C^{20}/C^{21} and C^{24}/C^{25}	85.5 (d, $^{1}J_{C\text{-}Rh}$ = 12.1 Hz)
C^{6}/C^{9}	52.1 (s)
C^{22}/C^{27} and C^{23}/C^{26}	31.4 (s)
C^{7}/C^{10} and C^{8}/C^{11}	21.1 (s)
C^{19}	16.8 (s)
C^{12}/C^{13}	12.1 (s)
C^{18}	10.9 (s)

*Rhodium(I) complexes with imine ligands (**29 – 31**):*

6.3.1.29 Chloro(η^4-1,5-cyclooctadiene)(4,5-dimethylthiazole)rhodium(I) (29)

Broadening and coalescence of signals are observed in both the proton and ^{13}C NMR spectra of the thiazole complex **29**, summarised in Table 2.6.37. This is in accordance with the results obtained by Müller and Stock for other imine complexes, as well as the NMR results reported for **16** and **17**.

Table 2.6.37 *NMR data of complex* ***29*** *in CD_2Cl_2 (relative to internal TMS)*

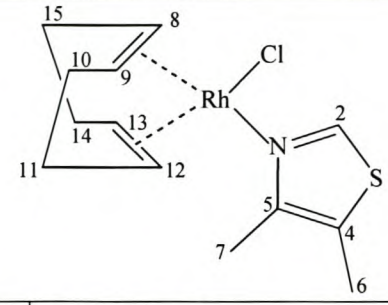

^{1}H NMR assignment	Chemical shift in ppm (number of protons, multiplicity, coupling constant)
H^2	8.63 (1H, s)
H^8/H^9	4.56 (2H, m)
H^{12}/H^{13}	3.49 (2H, m)
H^7	2.89 (3H, s)
H^{10}/H^{15}, H^{11}/H^{14} (equatorial)	2.46 (4H, m)
H^6	2.33 (3H, d, $J_{H\text{-}H}$ = 0.83 Hz)
H^{10}/H^{15}, H^{11}/H^{14} (axial)	1.79 (4H, m)
^{13}C NMR assignment	Chemical shift in ppm (multiplicity, coupling constant)
C^2	150.0 (s)
C^5	149.7 (s)
C^4	128.5 (m)
C^8/C^9	85.1 (d, $^1J_{C\text{-}Rh}$ = 8.4 Hz)
C^{12}/C^{13}	76.3 (d, $^1J_{C\text{-}Rh}$ = 11.1 Hz)
C^{10}/C^{15}	32.2 (s)
C^{11}/C^{14}	31.1 (s)
C^7	16.9 (m)
C^6	12.1 (m)

The only exception in the ^{1}H NMR spectrum is the sharp doublet observed for the three H^6 protons. The signals remained broad when the spectra were measured at a temperature of –30 °C, though not as broad when the spectra were measured at 25 °C. This is a possible indication that at lower temperatures the complex assumes a more rigid structure, resulting in slightly narrower signals.

A comparison between the chemical shifts observed for the free thiazole and the thiazole bonded to the rhodium in **29** shows that all the proton and carbon atoms are observed further downfield for the bonded ligand. The observed deshielding can be attributed to a delocalising of electron density to the metal centre *via* the Rh-N bond. The most significant changes are observed for the signals of the two methyl groups. The two methyl groups of the free ligand are observed at δ 2.34 and δ 2.33 in the ^{1}H NMR spectrum, whereas the same methyl signals are observed at δ 2.89 and δ 2.33 for the complex. The H^6 protons (δ 2.33) do not experience the deshielding as much as the other protons of the thiazole ligand because it is situated far away from the rhodium metal.

The chemical shifts of the olefinic proton and carbon atoms give an indication of the relative *trans* influence of the imine ligand. The coupling constant of the doublet observed for C^8 and C^9 *trans* to the thiazole ligand is 8.4 Hz. The coupling constant observed for the same olefinic carbon atoms of the carbene complex **1** is 7.4 Hz, but it is 11.6 Hz for the thione complex **16**. This confirms that the *trans* influence of the thiazole imine ligand is smaller than that of the carbene ligand, and greater than that of the thione ligand. The coupling constant measured for the C^{12} and C^{13} doublet *trans* to the chloride ligand is smaller than the corresponding coupling constant in **1** and **16** (Table 2.6.38). A probable reason for this observation is that the thiazole ligand has a stronger *cis* influence than the carbene and thione ligands.

Table 2.6.38 *Comparative NMR data of complex **1**, **16** and **29** in CD_2Cl_2 (relative to internal TMS)*

Assignment	**1**	**16**	**29**
H *trans* to L[a]	4.81 (m)	4.33 (m)	4.56 (m)
H *trans* to Cl	3.31 (m)	3.82 (m)	3.49 (m)
C *trans* to L[a]	97.4 (d, ^1J = 7.4 Hz)	83.7 (d, ^1J = 11.6 Hz)	85.1 (d, ^1J = 8.4 Hz)
C *trans* to Cl	68.1 (d, ^1J = 14.7 Hz)	74.4 (d, ^1J = 14.5 Hz)	76.3 (d, ^1J = 11.1 Hz)

[a] *L = a carbene ligand in **1**, a thione ligand in **16** and an imine ligand in **29***

A comparison between an imine *N*-donor ligand and a halide is found in the crystal structure of [RhCl(cod)(CTZ)] (CTZ = 1-[(2-chlorophenyl)diphenylmethyl]-1*H*-imidazole).[124] The crystal structure of this molecule, which was used in the study of metal complexes in the medicinal treatment of tropical diseases, shows that the imine ligand has a stronger *trans*

influence than the halide. The average Rh-$C_{olefinic\ cod}$ bond length *trans* to the chloride are 2.107(6) Å, while the average bond length *trans* to the imine ligand is 2.125(6) Å.

6.3.1.30 Chloro(η^4-1,5-cyclooctadiene)(4-methylthiazole)rhodium(I) (30)

All the ^{1}H NMR signals of complex **30** are summarised in Table 2.6.39, and the ^{13}C NMR spectrum in Table 2.6.40. All the signals in both the proton and ^{13}C NMR spectra exhibit the same broadening observed in the spectra of complex **28**. Determination of coupling constants is not possible due to the broadening. The signals of the cyclooctadiene ligand are observed at chemical shifts resembling those of **29**.

Table 2.6.39 *NMR data of complex **30** in CD_2Cl_2 (relative to internal TMS)*

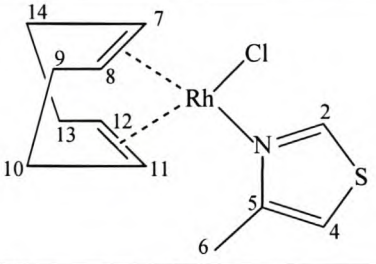

^{1}H NMR assignment	Chemical shift in ppm (number of protons, multiplicity, coupling constant)
H^2	8.85 (1H, s)
H^4	7.06 (1H, s)
H^7/H^8	4.57 (2H, m)
H^{11}/H^{12}	3.49 (2H, m)
H^6	2.93 (3H, s)
H^9/H^{14}, H^{10}/H^{13} (equatorial)	2.46 (4H, m)
H^9/H^{14}, H^{10}/H^{13} (axial)	1.78 (4H, m)

As with **29**, a comparison between the chemical shifts observed for the free thiazole and the thiazole bonded to the rhodium shows that all the proton and carbon atoms, except C^2, are observed further downfield for the bonded ligand.

Table 2.6.40 *NMR data of complex* ***30*** *in CD_2Cl_2 (relative to internal TMS)*

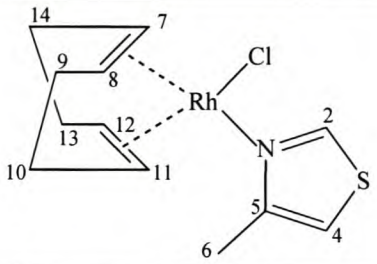

^{13}C NMR assignment	Chemical shift in ppm (multiplicity, coupling constant)
C^2	154.3 (s)
C^5	153.4 (s)
C^4	115.5 (s)
C^7/C^8	85.3 (m)
C^{11}/C^{12}	76.4 (m)
C^9/C^{14}	32.0 (m)
C^{10}/C^{13}	31.3 (m)
C^6	18.5 (s)

6.3.1.31 Chloro(dicarbonyl)(4-methylthiazole)rhodium(I) (31)

The proton NMR data of **31** are summarised with the ^{13}C NMR data in Table 2.6.41. Unlike the cyclooctadiene complexes **29** and **30**, all the signals that appear in the proton NMR spectrum are sharp signals. The signals all appear at a lower field compared to the free ligand. The deshielding of the protons can be attributed to delocalising of electron density to the metal centre. H^2 and H^6 are observed as doublets at δ 9.05 and δ 2.69 (δ 8.11 and δ 2.43 for the free ligand) while H^4 is observed as a doublet of quartets at δ 7.21 (δ 6.92 for the free ligand). The coupling constants for the H^4 signal ($^4J_{H\text{-}H6}$ = 0.96 Hz, $^4J_{H\text{-}H2}$ = 2.47 Hz) are similar to those observed for the free ligand ($^4J_{H\text{-}H6}$ = 1.01 Hz, $^4J_{H\text{-}H2}$ = 2.01 Hz).

All the carbon atoms of the thiazole ligand are also deshielded when it is bonded to the rhodium metal. C^2, C^4, C^5 and C^6 of the thiazole ligand appear as sharp signals in the ^{13}C spectrum, but the two carbonyl carbons are observed as broad doublets. A highly concentrated solution is needed to observe these two doublets, even if an extended NMR experiment is performed with a pulse delay of one second. The magnitude of the coupling constants (70.1 Hz and 72.9 Hz) are further proof of the weaker *trans* influence of the imine ligand in

comparison to the carbene ligand in **6** (54.3 Hz *trans* to the carbene ligand and 75.4 Hz *trans* to the chloride ligand).

Table 2.6.41 *NMR data of complex* ***31*** *in CD_2Cl_2 (relative to internal TMS)*

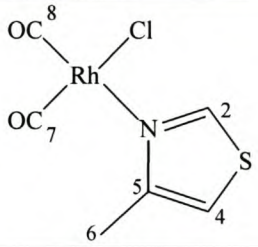

^{1}H NMR assignment	Chemical shift in ppm (number of protons, multiplicity, coupling constant)
H^2	9.05 (1H, d, $^4J_{H\text{-}H}$ = 2.47 Hz)
H^4	7.21 (1H, dq, $^4J_{H\text{-}H6}$ = 0.96 Hz, $^4J_{H\text{-}H2}$ = 2.47 Hz)
H^6	2.69 (3H, d, $^4J_{H\text{-}H}$ = 0.96 Hz)
^{13}C NMR assignment	Chemical shift in ppm (multiplicity, coupling constant)
C^8	184.1 (d, $^1J_{Rh\text{-}C}$ = 70.1 Hz)
C^7	180.8 (d, $^1J_{Rh\text{-}C}$ = 72.9 Hz)
C^5	157.8 (s)
C^2	153.8 (s)
C^4	116.3 (s)
C^6	19.0 (s)

6.3.2 Mass spectrometry

Electron impact (EI) mass spectra (MS) was recorded on an AMD 604 spectrometer at the Department of Chemistry at the University of Stellenbosch. Electro spray (ES) MS were recorded on a VG Quattro mass spectrometer at the Department of Biochemistry at the University of Stellenbosch with acetonitrile as solvent. Fast atom bombardment (FAB) MS were recorded on a Micromass DG 70/70E mass spectrometer at the University of Potchefstroom, South Africa, using xenon gas as bombardment atoms and *m*-nitrobenzylalcohol as matrix.

In 1982 Müller and Stock[98] reported that imine rhodium complexes decompose to the starting compounds when EI MS is performed. The free ligand as well as fragments of the rhodium starting complexes were observed. These fragments also recombined to give the starting complex, either $[RhCl(cod)]_2$ or $[RhCl(CO)_2]_2$. The same problem was observed with many of the 31 complexes prepared in this study. ES MS and FAB MS techniques were also employed in order to characterise some of the complexes. Fragmentation was observed in both these two techniques, and in the case of ES MS the solvent, acetonitrile, also coordinated to the fragments.

The $Rh\text{-}C_{carbene}$ bond is not broken as easily as the Rh-N bond in the imine complexes, meaning that EI MS is a good technique to observe the molecular ion of the carbene complex **1** (Table 2.6.42). The molecular ion of **1** was observed at m/z 426. The peak at m/z 282 shows that the halide and cyclooctadiene ligands dissociate from the metal centre before the carbene ligand.

Table 2.6.42 *Mass spectrometry of complex **1** (EI)*

m/z	I (%)	Fragment
426	26	$[M]^{+\,a}$
282	24	$[M - cod - Cl]^+$
240	8	$[Rh{=}\overline{CN(Pr)C(Me)C(Me)N}]^+$
198	12	$[Rh{=}\overline{CNC(Me)C(Me)N}]^+$
180	86	$[carbene\ ligand]^+$

[a] *M = molecular ion*

The molecular ion of **2** was also observed in the EI MS spectrum (Table 2.6.42). The consecutive loss of the 5 carbonyl ligands and the free carbene ligand are observed. The many isotopes of tungsten were clearly visible.

Table 2.6.43 *Mass spectrometry of complex **2** (EI)*

m/z	I (%)	Fragment
502	11	$[M]^+$
474	7	$[M - CO]^+$
446	32	$[M - 2CO]^+$
418	27	$[M - 3CO]^+$
390	24	$[M - 4CO]^+$
362	35	$[M - 5CO]^+$
180	12	[carbene ligand]$^+$

As with **1** and **2**, the molecular ion of **3** was observed with EI MS (Table 2.6.44). The loss of the chloride ligand is followed by the loss of the cyclooctadiene ligand. The carbene ligand form the base peak.

Table 2.6.44 *Mass spectrometry of complex **3** (EI)*

m/z	I (%)	Fragment
384	12	$[M]^+$
348	9	$[M - Cl]^+$
238	11	$[M - Cl - cod]^+$
139	74	[carbene ligand]$^+$

The molecular ion of complex **4** is observed by FAB MS (Table 2.6.45) and ES MS (Table 2.6.46). In the FAB MS the molecular ion gives a strong peak, as does the peak signifying the loss of the cyclooctadiene ligand.

Table 2.6.45 *Mass spectrometry of complex **4** (FAB)*

m/z	I (%)	Fragment
415	55	$[M]^+$
307	32	$[M - cod]^+$

The peak of the molecular ion is the base peak in the ES MS spectrum, with the loss of the cyclooctadiene ligand also giving a reasonably prominent peak.

Table 2.6.46 *Mass spectrometry of complex* ***4*** *(ES)*

m/z	I (%)	Fragment
415	100	$[M]^+$
307	16	$[M - cod]^+$
252	4	$[Rh(cod) + CH_3CN]^+$
211	8	$[Rh(cod)]^+$

In the ES MS spectrum of the cationic biscarbene complex **5** only the molecular ion is observed (Table 2.6.47).

Table 2.6.47 *Mass spectrometry of complex* ***5*** *(ES)*

m/z	I (%)	Fragment
459	100	$[M]^+$

The base peak observed in the EI MS spectrum of **6** (Table 2.6.48) is the peak signifying the loss of the two carbonyl ligands and the chloride ligand. The molecular ion is also observed as well as the loss of the first carbonyl ligand. No signal that indicates the loss of the second carbonyl ligand is seen. Other signals show the loss of the isopropyl substituents of the carbene ligand.

Table 2.6.48 *Mass spectrometry of complex* ***6*** *(EI)*

m/z	I (%)	Fragment
374	6	$[M]^+$
346	14	$[M - CO]^+$
282	100	$[M - 2CO - Cl]^+$
240	20	$[Rh{=}\overline{CN(Pr)C(Me)C(Me)N}]^+$
198	12	$[Rh{=}\overline{CNC(Me)C(Me)N}]^+$

The EI MS determination of **7** yielded only two peaks that can be identified as fragments of the dicarbonyl complex. The loss of the two carbonyl ligands and the chloride ligand is represented by the peak at m/z 239.

Table 2.6.49 *Mass spectrometry of complex 7 (EI)*

m/z	I (%)	Fragment
239	8	$[M - 2CO - Cl]^+$
139	36	$[\text{carbene ligand}]^+$

The EI MS spectrum of **8** is summarised in Table 2.6.50. The loss of both the two carbonyl ligands is observed at m/z 310, and is followed by the loss of the chloride ligand. The free carbene ligand is also observed in the spectrum.

Table 2.6.50 *Mass spectrometry of complex **8** (EI)*

m/z	I (%)	Fragment
310	22	$[M - 2CO]^+$
275	9	$[M - 2CO - Cl]^+$
171	19	$[\text{carbene ligand}]^+$

Both the ES MS (Table 2.6.51) and FAB MS (Table 2.6.52) of **9** were determined. The molecular ion was observed as the base peak in both spectra. The successive loss of the two carbonyl ligands was observed at m/z 335 and m/z 307, in both the ES MS and the FAB MS spectra. The peak at m/z 376 in the ES MS spectrum is a result of the coordination of acetonitrile to the rhodium metal after dissociation of the first carbonyl ligand.

Table 2.6.51 *Mass spectrometry of complex **9** (ES)*

m/z	I (%)	Fragment
376	36	$[M - CO + CH_3CN]^+$
363	100	$[M]^+$
335	49	$[M - CO]^+$
307	18	$[M - 2CO]^+$

Table 2.6.52 *Mass spectrometry of complex* ***9*** *(FAB)*

m/z	I (%)	Fragment
363	100	$[M]^+$
335	12	$[M - CO]^+$
307	52	$[M - 2CO]^+$

The molecular ion of **10** is observed at m/z 414 in the EI MS spectrum (Table 2.6.53). Signals representing the loss of the carbonyl ligand followed by the loss of the chloride ligand are also observed. The strongest peak observed represents the mass of the fragment equal to that of the free carbene ligand.

Table 2.6.53 *Mass spectrometry of complex* ***10*** *(EI)*

m/z	I (%)	Fragment
414	6	$[M]^+$
386	41	$[M - CO]^+$
351	2	$[M - CO - Cl]^+$
124	72	$[\text{carbene ligand}]^+$

In the ES MS spectrum of **11** (Table 2.6.54) a peak is observed at m/z 573, indicating the loss of the chloride ligand. Acetonitrile coordinates to this fragment resulting in the peak at m/z 614.

Table 2.6.54 *Mass spectrometry of complex* ***11*** *(ES)*

m/z	I (%)	Fragment
614	100	$[M - Cl + CH_3CN]^+$
573	57	$[M - Cl]^+$

The EI MS data of **12** are summarised in Table 2.6.55. The loss of the carbonyl ligand is observed at m/z 602. The phosphine ligand easily loses a thiazole group as indicated by the base peak at m/z 199. In addition to the fragments of the phosphine ligand, fragments for the free carbene ligand as well as the carbene ligand bonded to the rhodium metal are observed.

Table 2.6.55 *Mass spectrometry of complex* ***12*** *(EI)*

m/z	I (%)	Fragment
602	2	$[M - CO]^+$
421	17	$[Rh(Cl)(P\{\overline{CNCHCHS}\}_3)]^+$
283	19	$[Rh{=}\overline{CN(Pr)C(Me)C(Me)N(Pr)}]^+$ and $[P\{\overline{CNCHCHS}\}_3]^+$
199	100	$[P\{\overline{CNCHCHS}\}_2]^+$
180	46	[carbene ligand]$^+$

Due to the loss of the chloride ligand, the molecular ion is not observed in the ES MS spectrum of **13** (Table 2.6.56), as was the case for **11**. The peak indicating the loss of the chloride ligand is observed at m/z 523. Acetonitrile and 1,3-diisopropyl-4,5-dimethyl-2,3-dihydro-1*H*-imidazol-2-thione coordinate to this fragment resulting in peaks at m/z 564 and m/z 735 respectively. The loss of the carbonyl and thione ligands followed by acetonitrile coordination gives rise to the base peak at m/z 324. The peaks observed at m/z 495 and m/z 311 indicate that there is no sequence in the loss of the thione and carbonyl ligands.

Table 2.6.56 *Mass spectrometry of complex* ***13*** *(ES)*

m/z	I (%)	Fragment
735	4	$[M - Cl + thione]^+$
564	4	$[M - Cl + CH_3CN]^+$
523	62	$[M - Cl]^+$
495	15	$[M - Cl - CO]^+$
352	14	$[(CO)Rh{=}\overline{CN(Pr)C(Me)C(Me)N(Pr)} + CH_3CN]^+$
324	100	$[Rh{=}\overline{CN(Pr)C(Me)C(Me)N(Pr)} + CH_3CN]^+$
311	7	$[(CO)Rh{=}\overline{CN(Pr)C(Me)C(Me)N(Pr)}]^+$
283	41	$[Rh{=}\overline{CN(Pr)C(Me)C(Me)N(Pr)}]^+$
212	6	[thione ligand]$^+$
180	46	[carbene ligand]$^+$

The molecular ion of **14** is observed as a strong peak in the ES MS spectrum. The loss of the thione ligand gives the base peak at m/z 391. Acetonitrile coordination to this fragment is observed at m/z 432. The peak at m/z 349 is probably due to the loss of an isopropyl group from the carbene ligand.

Table 2.6.57 *Mass spectrometry of complex* ***14*** *(ES)*

m/z	I (%)	Fragment
603	45	$[M]^+$
432	15	$[(cod)Rh{=}\overline{CN(Pr)C(Me)C(Me)N}(Pr) + CH_3CN]^+$
391	100	$[(cod)Rh{=}\overline{CN(Pr)C(Me)C(Me)N}(Pr)]^+$
349	93	$[(cod)Rh{=}\overline{CN(Pr)C(Me)C(Me)N}]^+$
212	46	$[thione\ ligand]^+$
180	40	$[carbene\ ligand]^+$

The ES MS spectrum of **15** (Table 2.6.58) is very similar to that of **13**. However, the molecular ion is observed for **15**, which was not the case for **13**. The successive loss of the two carbonyl ligands is observed at m/z 523 and m/z 495. The peak resulting from the loss of the thione ligand as well as the two carbonyl ligands, followed by the coordination of acetonitrile is observed as the base peak.

Table 2.6.58 *Mass spectrometry of complex* ***15*** *(ES)*

m/z	I (%)	Fragment
551	81	$[M]^+$
523	67	$[M - CO]^+$
495	17	$[M - 2CO]^+$
352	10	$[(CO)Rh{=}\overline{CN(Pr)C(Me)C(Me)N}(Pr) + CH_3CN]^+$
324	100	$[Rh{=}\overline{CN(Pr)C(Me)C(Me)N}(Pr) + CH_3CN]^+$
311	7	$[(CO)Rh{=}\overline{CN(Pr)C(Me)C(Me)N}(Pr)]^+$
283	53	$[Rh{=}\overline{CN(Pr)C(Me)C(Me)N}(Pr)]^+$
212	11	$[thione\ ligand]^+$
180	22	$[carbene\ ligand]^+$

The molecular ion of **16** is observed as a very small peak in the ES MS spectrum. The peak at m/z 423 shows the loss of the chloride ligand. Coordination of a thione ligand to this fragment results in the base peak.

Table 2.6.59 *Mass spectrometry of complex **16** (ES)*

m/z	I (%)	Fragment
635	100	$[M - Cl + thione]^+$
458	1	$[M]^+$
423	8	$[M - Cl]^+$
212	14	$[thione\ ligand]^+$
180	20	$[\overline{CN(Pr)C(Me)C(Me)N}(Pr)]^+$

In the ES MS spectrum of **17** the molecular ion is observed as a peak with very low intensity at m/z 402. The fragment resulting from the loss of the chloride ligand gives rise to a peak that is stronger than the peak for the molecular ion, just as was observed in the spectrum of **16**. Coordination of acetonitrile and the thione ligand to the [M – Cl] fragment gives rise to the two peaks with the highest intensities.

Table 2.6.60 *Mass spectrometry of complex **17** (ES)*

m/z	I (%)	Fragment
523	87	$[M - Cl + thione]^+$
408	100	$[M - Cl + CH_3CN]^+$
402	3	$[M]^+$
367	82	$[M - Cl]^+$
156	30	$[thione\ ligand]^+$
124	16	$[\overline{CN(Me)C(Me)C(Me)N}(Me)]^+$

Complex **18**, with a similar structure to **16** and **17**, also has a similar ES MS spectrum. The only significant observation is that the peak at m/z 546 is probably due to the formation of a bimetallic fragment.

Table 2.6.61 *Mass spectrometry of complex* ***18*** *(ES)*

m/z	I (%)	Fragment
546	46	$[(cod)Rh(Cl)S{=}C(H)N(Me)_2Rh(cod)]^+$
389	58	$[M + thione]^+$
341	9	$[M - Cl + CH_3CN]^+$
335	1	$[M]^+$
300	100	$[M - Cl]^+$

The molecular ion of **19** is observed in the EI MS spectrum of the complex. The loss of the first carbonyl ligand is also observed, but not the loss of both the carbonyl ligands. The thione ligand is observed as a strong peak, indicating that the thione ligand easily dissociates from the rhodium metal in the EI MS environment.

Table 2.6.62 *Mass spectrometry of complex* ***19*** *(EI)*

m/z	I (%)	Fragment
406	3	$[M]^+$
378	2	$[M - CO]^+$
314	5	$[M - 2CO - Cl]^+$
212	87	$[thione\ ligand]^+$

Dissociation of the chloride ligand, followed by coordination of another thione ligand results in the base peak of **20** at m/z 471. The consecutive loss of the two carbonyl ligands from the [M – Cl + thione] ion is also observed.

Table 2.6.63 *Mass spectrometry of complex* ***20*** *(ES)*

m/z	I (%)	Fragment
471	100	$[M - Cl + thione]^+$
443	30	$[M - Cl - CO + thione]^+$
415	35	$[M - Cl - 2CO + thione]^+$
156	43	$[thione\ ligand]^+$
124	26	$[\overline{CN(Me)C(Me)C(Me)N}(Me)]^+$

In the EI MS spectrum of **21** (Table 2.6.64) the molecular ion is observed as a very weak peak, while the thione ligand is observed as the base peak. Dissociation of the thione ligand from the complex gives rise to the formation of the starting complex $[RhCl(CO)_2]_2$ which subsequently fragments.

Table 2.6.64 *Mass spectrometry of complex **21** (EI)*

m/z	I (%)	Fragment
283	1	$[M]^+$
103	14	$[Rh]^+$
89	100	$[thione\ ligand]^+$

As in the spectrum of **20**, the chloride ligand is easily lost from **22**, resulting in the peak at m/z 605. Coordination of a thione ligand to this fragment is observed as the base peak at m/z 817.

Table 2.6.65 *Mass spectrometry of complex **22** (ES)*

m/z	I (%)	Fragment
817	100	$[M - Cl + thione]^+$
605	17	$[M - Cl]^+$
180	7	$[\overline{CN(Pr)C(Me)C(Me)N}(Pr)]^+$

In the EI MS spectrum of **23** only the starting compounds are observed. Fragments of the triphenylphosphine ligand are also observed.

In the EI MS spectrum of **24** only the thione ligand is observed. However, in the ES MS spectrum of **24**, summarised in Table 2.6.66, it is seen that the loss of the chloride ligand is followed by the coordination of acetonitrile, as observed in the ES MS spectra of **11**, **13**, **16**, **17**, **18** and **20**. The signal at m/z 808 is probably due to the coordination of another thione ligand after the loss of the chloride ligand and acetonitrile coordination.

Table 2.6.66 *Mass spectrometry of complex* ***24*** *(ES)*

m/z	I (%)	Fragment
808	53	$[M - Cl + thione + CH_3CN]^+$
596	10	$[M - Cl + CH_3CN]^+$
212	22	$[thione\ ligand]^+$
180	100	$[\overline{CN(Pr)C(Me)C(Me)N}(Pr)]^+$

Like the NMR data, the ES MS spectrum of **25** is not perfectly clear and thus difficult to analyse. A bimetallic complex is probably observed, similar to the peaks observed in the mass spectrum of **18**. The peaks at m/z 281 and m/z 192 are also observed in the FAB MS spectrum of **25**.

Table 2.6.67 *Mass spectrometry of complex* ***25*** *(ES)*

m/z	I (%)	Fragment
529	13	$[\{(CO)(S{=}CHN\{Me\}_2)Rh\}_2(S{=}CHN\{Me\}_2)]^+$
281	40	$[M - Cl - CO]^+$
279	100	$[M - Cl - CO - 2H]^+$
233	71	$[Rh(S{=}CHN\{Me\}_2)_2 + CH_3CN]^+$
192	32	$[Rh(S{=}CHN\{Me\}_2)_2]^+$

The molecular ion of **26** is observed as a very strong peak in its ES MS spectrum (Table 2.6.68). The loss of one thione ligand leads to the base peak at m/z 423, which after acetonitrile coordination forms the fragment at m/z 464.

Table 2.6.68 *Mass spectrometry of complex* ***26*** *(ES)*

m/z	I (%)	Fragment
635	74	$[M]^+$
464	81	$[M - thione + CH_3CN]^+$
423	100	$[M - thione]^+$
212	17	$[thione\ ligand]^+$
180	21	$[\overline{CN(Pr)C(Me)C(Me)N}(Pr)]^+$

The molecular ion of **27** is the base peak in its ES MS spectrum (Table 2.6.69). The successive loss of the two carbonyl ligands is very clear. The two peaks with the highest m/z values are due to the respective coordination of acetonitrile and a third thione ligand to the [M – CO] fragment.

Table 2.6.69 *Mass spectrometry of complex* ***27*** *(ES)*

m/z	I (%)	Fragment
767	6	$[M - CO + thione]^+$
596	4	$[M - CO + CH_3CN]^+$
583	100	$[M]^+$
555	39	$[M - CO]^+$
527	18	$[M - 2CO]^+$
212	63	$[thione\ ligand]^+$

In the FAB MS of **28**, the molecular ion is not observed as expected at m/z 536, but a strong peak is present at m/z 533. The loss of protons on the ligands could result in this peak. The peaks with the highest intensity represent the loss of the thiazole ligand at m/z 423 and the free thiazole ligand at m/z 113.

Table 2.6.70 *Mass spectrometry of complex* ***28*** *(FAB)*

m/z	I (%)	Fragment
423	65	$[M - thiazole]^+$
212	32	$[thione\ ligand]^+$
180	34	$[\overline{CN(Pr)C(Me)C(Me)N}(Pr)]^+$
113	68	$[thiazole\ ligand]^+$

The molecular ion of **29** is observed in its FAB MS spectrum (Table 2.6.71). The loss of the chloride ligand and a proton leads to as a stronger fragment peak at m/z 323. The presence of the molecular ion is significant because the MS experiments carried out on similar imidazole complexes were reportedly unsuccessful.[98] In the ES MS spectrum of **29** the molecular ion was not observed, but the loss of the chloride ligand led to the base peak at m/z 324, and acetonitrile coordination to this fragment to the peak at m/z 365.

Table 2.6.71 *Mass spectrometry of complex* ***29*** *(FAB)*

m/z	I (%)	Fragment
359	11	$[M]^+$
323	53	$[M - Cl - H]^+$
211	38	$[Rh(cod)]^+$

A very weak peak is observed for the molecular ion in the FAB MS spectrum of **30** (Table 2.6.72). As with **29** the loss of the chloride ligand is also observed. In the ES MS spectrum of **30** the peak at m/z 310 signifies the loss of the chloride ligand, but unlike in the spectrum of **29**, this peak is very weak.

Table 2.6.72 *Mass spectrometry of complex* ***30*** *(FAB)*

m/z	I (%)	Fragment
346	7	$[M]^+$
310	10	$[M - Cl]^+$
211	16	$[Rh(cod)]^+$

Unexpectedly the molecular ion of **31** was observed in the EI MS spectrum. The easy dissociation of the thiazole ligand in the EI MS environment is indicated by the strength of the peak representing the thiazole ligand. The dissociation of the thiazole ligand also led to the reformation of the starting compound $[RhCl(CO)_2]_2$ and its fragments.

Table 2.6.73 *Mass spectrometry of complex* ***31*** *(EI)*

m/z	I (%)	Fragment
293	1	$[M]^+$
99	100	[thiazole ligand]$^+$

6.3.3 IR spectroscopy

IR spectra (4000 to 400 cm^{-1}, resolution 4 cm^{-1}) were recorded on a Perkin-Elmer 1600 series FTIR spectrometer. The rhodium complexes discussed in this chapter containing carbonyl ligands can be classified into three different groups with the general formulae $[RhCl(CO)_2L]$,

$[Rh(CO)_2L^1L^2]^+[X]^-$ and $[RhCl(CO)L^1L^2]$. The infrared vibrations of the first two types of complexes are summarised in Table 2.6.74, and those for the series of complexes of the type $[RhCl(CO)L^1L^2]$ in Table 2.6.75. All the complexes were dissolved in dichloromethane in order to be able to directly compare the recorded spectra.

Table 2.6.74 *IR-data of complex types $[RhCl(CO)_2L]$ and trans-$[Rh(CO)_2L^1L^2]^+[X]^-$ in CH_2Cl_2*

Complex	ν(CO) / cm^{-1}	
6 (L = $\overline{CN^iPrCMeCMeN^iPr}$)	1996.1	2076.2
7 (L = $\overline{CN^nBuCHCHNMe}$)	2024.7	2082.3
8 (L = $\overline{CN(CH_2Ph)CHCHNMe}$)	2000.5	2081.1
9 (L^1L^2 = $\overline{CNMeCHCHN}(CH_2)_3\overline{NCHCHNMeC}$)	2028.3	2084.9
15 (L^1 = $\overline{CN^iPrCMeCMeN^iPr}$, L^2 = S=$\overline{CN^iPrCMeCMeN^iPr}$)	2008.6	2070.0
19 (L = S=$\overline{CN^iPrCMeCMeN^iPr}$)	1994.4	2068.9
20 (L = S=$\overline{CNMeCMeCMeNMe}$)	1997.5	2070.9
21 (L = S=$CHNMe_2$)	2009.2	2081.3
27 (L^1 = L^2 = S=$\overline{CN^iPrCMeCMeN^iPr}$)	2001.1	2066.4
31 (L = 4-methylthiazole)	2013.6	2088.3

The $\sigma_{donor}/\pi_{acceptor}$-ratio of the ligand L plays an important role in determining the vibration frequencies observed for the CO-ligands of the different complexes. A large $\sigma_{donor}/\pi_{acceptor}$-ratio leads to a higher electron density on the metal that will be distributed to the carbonyl ligands *via* π-backbonding. It is clear that the *N*-substituents have an influence on the σ-donating properties of the carbene ligands, as seen in the difference of the vibration frequencies of the three carbene complexes **6**, **7** and **8**. These values are similar to the IR spectrum of the known carbene complex chloro(dicarbonyl)(1,3-dimethyl-2,3-dihydro-1*H*-imidazol-2-ylidene)rhodium(I) which shows strong peaks at 2006 and 2076 cm^{-1}.[63] The vibration frequencies of the thione complexes (**19**, **20** and **21**) are similarly affected as those of the carbene complexes with the isopropyl group placing the most negative charge on the metal moiety. The published thiourea complex $[RhCl(CO)_2(Hbztu)]$ has two bands in its IR spectrum at 2087 and 2018 cm^{-1}.[85]

The square planar complexes containing only one carbonyl ligand show only one strong vibration in the ν(CO) infrared region. The complexes and the observed bands are collected in Table 2.6.75 along with the values for a known complex. The strong σ-donor properties combined with the weak π-accepting properties of the carbene ligands result in a higher electron density on the rhodium metal than with, for example, phosphine ligands. This in turn results in greater π-backbonding to the CO ligand, observed in the infrared spectrum as a shift in vibration frequency. Complex **10**, which has two carbene ligands, shows this very clearly. A strong vibration frequency at 1924 cm^{-1} has been reported for an analogous biscarbene complex chloro(carbonyl)-*trans*-bis(1,3-dimethyl-2,3-dihydro-1*H*-imidazol-2-ylidene)rhodium(I).[74]

Table 2.6.75 *IR-data of complex type trans-[RhCl(CO)L^{1}L^2] in CH_2Cl_2*

Complex	ν(CO) / cm^{-1}
10 ($L^1 = L^2 = \overline{CN^iPrCMeCMeN^iPr}$)	1934.3 (s)
11 ($L^1 = \overline{CN^iPrCMeCMeN^iPr}$, $L^2 = PPh_3$)	1958.1 (s)
12 ($L^1 = \overline{CN^iPrCMeCMeN^iPr}$, $L^2 = P\{\overline{CNCHCHS}\}_3$)	1981.3 (s)
13 ($L^1 = \overline{CN^iPrCMeCMeN^iPr}$, $L^2 = S=\overline{CN^iPrCMeCMeN^iPr}$)	1934.3 (s)
22 ($L^1 = S=\overline{CN^iPrCMeCMeN^iPr}$, $L^2 = PPh_3$)	1958.8 (s)
23 ($L^1 = S=CHNMe_2$, $L^2 = PPh_3$)	1973.2 (s)
24 ($L^1 = L^2 = S=\overline{CN^iPrCMeCMeN^iPr}$)	1930.6 (s)
25 ($L^1 = L^2 = S=CHNMe_2$)	1960.8 (s)
$[RhCl(CO)(PPh_3)_2]$[125]	1965 (s)

From the infrared data of **13** and **24** it seems that the heterocyclic thione ligands have the same $\sigma_{donor}/\pi_{acceptor}$-ratio than carbene ligands, with **11** and **22** having almost identical vibration frequencies. The difference in ν(CO) for **11** and **12** can be attributed to better delocalisation of electron density in the thiazole rings compared to the phenyl rings, lowering the σ-donor properties of the phosphine ligand, tri{2′*H*-thiazol}phosphine.

For the sake of completeness the appropriate infrared vibrations of **2** are given in Table 2.6.76. The infrared spectra of similar complexes have been determined in THF. Only two vibration frequencies of the possible three IR active vibration frequencies for a complex with C_{4v} local symmetry were observed for the complexes *R*- and *S*-pentacarbonyl(1,3-bis{(*S*)-1′-

phenylethyl}-2,3-dihydro-1*H*-imidazol-2-ylidene)tungsten(0) (2060 and 1927 cm^{-1}),[71,72] while three frequencies were reported for pentacarbonyl(1,3-bis{(R)-1′-naphthylethyl}-2,3-dihydro-1*H*-imidazol-2-ylidene)tungsten(0) (2061, 1927 and 1909 cm^{-1})[71]. Four IR active bands with similar values for the CO vibration frequencies were observed for **2**. As complex **2** does not have exact C_{4v} symmetry, the B_2 vibration (which is normally only Raman active) also becomes IR active.

Table 2.6.76 *Infrared vibrations of* ***2*** *in* CH_2Cl_2

Complex	ν(CO) / cm^{-1}	
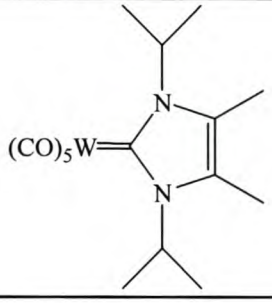	$A_1^{(1)}$	2059.7 (m)
	B_2	1958.1 (w)
	E	1915.8 (vs)
	$A_1^{(2)}$	1887.5 (sh)

6.4 Hydroformylation results

Most of the rhodium(I) complexes synthesised were used as precursor catalysts for the hydroformylation of 1-hexene in toluene. Synthesis gas with a carbon monoxide to hydrogen ratio of 1:1 was used. A set of standard conditions (8 MPa and 80 °C) was chosen within the safety features of the reactor system used. Most catalysts gave 100 % conversion after 16 hours and, therefore, this time was chosen as the reference reaction time for the hydroformylation reactions. Most experiments were performed in duplicate and the results obtained showed an error factor of less than 5 %.

A non-polar GC column (PS 255, FS 66, 1.2 mm x 40 m x 0.32 mm) was used to separate products on the basis of boiling points. This column is not suitable for the separation of the possible hydrogenation product hexane (b.p. 69 °C) and the two formed hexene isomers, 2-hexene (b.p. 67 – 69 °C) and 3-hexene (b.p. 69 °C). After a reaction time of 6 hours, the presence of one or more of these three molecules was detected. However, after reaction times of 16 hours no hexane or any hexene was present with 100 % conversion to aldehydes. The initial isomerisation of hexene, that probably occurred *via* a parallel conversion, was not further investigated.

Table 2.6.77 *Catalytic hydroformylation of 1-hexene performed in toluene under chosen conditions (80 °C, 8 MPa) for 16 h and with a catalyst : substrate ratio of 1:1000*

Catalyst	Conversion (%)	Yield of aldehyde (%)	Yield of hexane or 2-hexene or 3-hexene (%)[a]	*n:i* ratio[b]	Isomerisation[c]	Number of different aldehydes[d]
1	100	100	0	1 : 0.9	6	3
1 + 4 PPh_3[e]	100	100	0	1 : 0.4	0	2
3	100	100	0	1 : 1	9	3
4	100	100	0	1 : 1.1	10	3
5	29	21	0	1 : 0.6	0	2
6	100	100	0	1 : 1.1	9	3
6 + 4 PPh_3	32	32	0	1 : 0.4	0	2
9	64	53	11	1 : 0.6	0	2
10	20	16	4	1 : 0.6	0	2
11	100	100	0	1 : 0.6	0	2
11 + 4 PPh_3	100	100	0	1 : 0.9	8	3
12	52	45	7	1 : 0.4	0	2
13	21	16	5	1 : 0.5	0	2
14	100	100	0	1 : 1	8	3
15	100	100	0	1 : 1.1	11	3
16	100	100	0	1 : 1	9	3
17	100	100	0	1 : 0.9	6	3
18	100	100	0	1 : 1	7	3
19	100	100	0	1 : 1.1	7	3
20	100	100	0	1 : 1.2	10	3
21	100	100	0	1 : 1	8	3
22	100	100	0	1 : 0.7	5	3
22 + 4 PPh_3	100	100	0	1 : 0.4	0	2
22 + 4 thione[f]	100	100	0	1 : 0.7	5	3
24	0	-	-	-	-	-
26	100	100	0	1 : 1.3	11	3
27	100	100	0	1 : 1.3	11	3
31	100	100	0	1 : 1	7	3
Wilkinson cat.	100	100	0	1 : 0.8	7	3
$[RhCl(cod)]_2$	100	100	0	1 : 1.3	10	3

[a] *No distinction between 2-hexene, 3-hexene and hexane was possible with the polar GC column that was used;*

[b] *n:i = n-aldehyde : all iso-aldehydes;* [c] *Amount of all 3-aldehydes/amount of all aldehydes x 100;*

[d] *The number of different aldehydes formed;* [e] *4 denotes four mole equivalents;*

[f] *thione = 1,3-diisopropyl-4,5-dimethyl-2,3-dihydro-1H-imidazol-2-thione.*

All the data for the catalytic hydroformylation experiments conducted under the chosen conditions are summarised in Table 2.6.77. Conversion of the alkene to aldehyde is quantitative in almost all the experiments. Only seven of the precursor catalysts do not give a 100 % conversion to aldehydes after a reaction time of 16 hours. For example, when using complex **6** with 4 mole equivalents of triphenylphosphine, only 32 % conversion is achieved, but no hexane or hexene isomers other than 1-hexene are observed. Complex **24** gave no conversion whatsoever. In the five other experiments with incomplete conversion to aldehydes, some of the 1-hexene has been converted to 2-hexene and 3-hexene and possibly hexane. Catalyst decomposition was only observed for complex **12**. No evidence of Rh(0) deposition, that could result in a heterogeneous reaction was, however, found. The decomposition of this complex is probably the reason for the low rate of conversion.

Of the four biscarbene complexes **4**, **5**, **9** and **10**, only **4** gives a 100 % yield of aldehyde. The result for **4** is somewhat unexpected as complexes with two carbene ligands bonded to the rhodium centre were expected to donate too much electron density to the metal, leading to a lower activity of the catalyst.

The other complexes that produced lower yields are **13** that contains a carbene and a thione ligand, and **24**, with two thione ligands. It appears as if the thione ligands lead to an increase in electron density at the rhodium centre, as was also indicated in the IR spectra. This effect is similar to that of an *N*-heterocyclic carbene ligand when it is bonded to the rhodium along with another *N*-heterocyclic carbene or another heterocyclic thione ligand. Another interesting observation is that when **6** is used as a catalyst precursor, a 100 % yield of aldehyde is obtained, but with 4 equivalents of triphenylphosphine added, only a 32 % conversion is achieved.

It is clear from Table 2.6.77 that an important discrimination occurs depending on the chosen ligands: carbene complexes **5**, **9**, **10**, **11**, **12** and **13** afford only the n-aldehyde (heptaldehyde) and 2-aldehyde (2-methyl-1-hexanal) as hydroformylation products; carbene complexes **1**, **3**, **4** and **6** also yield the 3-aldehyde (2-ethyl-1-pentanal) as product, unless triphenylphosphine is added to the reaction mixtures of **1** or **6**, when only the n-aldehyde and 2-aldehyde forms; the hydroformylation reactions using the thione complexes as precursor catalysts produce

three aldehydes as products; the latter result is again achieved with the imine complex **31**, $[RhCl(PPh_3)_3]$ and the bimetallic compound $[RhCl(cod)]_2$.

The observed *n:i* ratios vary significantly from 1:0.4 to 1:1.3 throughout Table 2.6.77. In industrial hydroformylation processes an excess of ligand is usually added to the catalyst (see Chapter 1) and, therefore, a few randomly chosen complexes were used as pre-catalysts with an additional amount of triphenylphosphine or thione. The addition of 4 mole equivalents of triphenylphosphine to **11**, leads to a lower *n:i* ratio as well as substrate isomerisation by an unknown mechanism. The opposite happens when four mole equivalents of triphenylphosphine are added to complexes **1**, **6** and **22**. In all these three instances a linear to branched ratio of 1:0.4, the best for all the experiments, is observed as well as no isomerisation products. Complex **11**, that contains a carbene and a phosphine ligand, proves to be the best catalyst precursor of all when used alone, yielding aldehydes in a *n:i* ratio of 1:0.6 and in a 100 % yield. In addition the *iso*-aldehyde formed from isomerised 1-hexene is not detected.

In order to assess the ability of the carbene complexes to be used more than once, a solution of complex **1** was used in two consecutive hydroformylation reactions, giving the same products in the same ratios for both reactions.

The reaction mixtures of complexes **1**, **3**, **6**, **14**, **15**, **18** and **21** were red in colour after completion of the hydroformylation reaction. The red colour changed to yellow after a few minutes at room temperature. This colour change is probably an indication that the active hydroformylation catalyst does not exist at room temperature and in the absence of synthesis gas. Other types of complexes such as **11** and Wilkinson's catalyst produced intense orange solutions after completion of the hydroformylation.

Table 2.6.78 *Catalytic hydroformylation of 1-hexene performed in toluene under chosen conditions (80 °C, 8 MPa) for 16 h and with a catalyst : substrate ratio of 1:1000*

Catalyst	Conversion (%)	Yield of aldehyde (%)	Yield of hexane or 2-hexene or 3-hexene (%)	*n:i* ratio	Isomerisation	Number of different aldehydes
$[Rh(cod)(Hbbtm)]BF_4$	100	100	0	1 : 1.2	9	3
$[Rh(CO)_2(Hbbtm)]BF_4$	100	100	0	1 : 1.2	10	3

Two recently reported imine complexes were also investigated. The two cationic imine compounds $[Rh(cod)(Hbbtm)]BF_4$ and $[Rh(CO)_2(Hbbtm)]BF_4$ (Hbbtm = bis{benzothiazol-2-yl}methane)[102] were utilised under the same conditions as all the carbene and thione complexes discussed previously. The results are very similar to those obtained for $[RhCl(cod)]_2$ and are shown in Table 2.6.78.

Other solvent systems were also investigated. The ionic liquid $[BMIM]BF_4$ was used along with the catalyst precursors $[RhCl(cod)(\overline{CNMeCHCHN^nBu})]$, **3**, $[RhCl(CO)_2(\overline{CN^iPrCMeCMeN^iPr})]$, **6**, $[RhCl(CO)(PPh_3)(\overline{CN^iPrCMeCMeN^iPr})]$, **11**, $[RhCl(CO)_2(S{=}\overline{CN^iPrCMeCMeN^iPr})]$, **19**, and $[RhCl(CO)(PPh_3)(S{=}\overline{CN^iPrCMeCMeN^iPr})]$, **22** (Table 2.6.79). The organic product was extracted from the ionic liquid with ether. For **3**, **6** and **19** no measurable amount of aldehyde or higher alkenes were detected, the substrate 1-hexene remained unchanged. Several extractions of the reaction mixtures remained colourless throughout. Immobilisation of the rhodium complexes in the ionic liquid most probably led to their complete inactivity. Ether extractions of the reaction mixtures of complexes **11** and **22** were yellow and contained aldehydes, an indication of at least some catalyst activity. After performing multiple ether extractions on the reaction mixture of **11**, the yellow ionic liquid was again used in a hydroformylation reaction. The second hydroformylation reaction yielded only 29 % aldehyde and no detectable isomerised hexene or hexane. The *n:i* ratio for this second reaction (1:0.6) was not as good as for the first reaction. As with the first reaction, the ether layer was yellow even after the third extraction was performed.

Table 2.6.79 *Catalytic hydroformylation of 1-hexene performed in $[BMIM]BF_4$ under chosen conditions (80 °C, 8 MPa) for 16 h and with a catalyst : substrate ratio of 1:1000*

Catalyst	Conversion (%)	Yield of aldehyde (%)	Yield of hexane or 2-hexene or 3-hexene (%)	*n:i* ratio	Isomerisation	Number of different aldehydes
3	0	-	-	-	-	-
6	0	-	-	-	-	-
11	100	100	0	1 : 0.4	0	2
19	0	-	-	-	-	-
22	100	100	0	1 : 0.5	0	2

The four complexes **6**, **11**, **19** and **22** were used in the rest of the experiments. One carbene complex, **11**, contains PPh_3 as ligand, as does the thione complex **22**. Apart from [BMIM]BF_4, dodecane was also used as a solvent in a series of hydroformylation reactions (Table 2.6.80). In addition to the four complexes **6**, **11**, **19** and **22**, Wilkinson's catalyst was also investigated as a pre-catalyst in dodecane. No conversion to aldehydes was detected with Wilkinson's catalyst, a 91 % conversion with **6**, and a 100 % conversion with **11**, **19** and **22**. Although **6** produced a lower aldehyde yield in dodecane than in toluene, the amount of *iso*-aldehyde formed from isomerised 1-hexene was lower. The three other complexes yielded aldehydes with a similar or higher degree of isomerisation (amount of *iso*-aldehyde formed from isomerised 1-hexene) than the products obtained in toluene, with the only significant positive change in *n:i* ratio being observed for **6** (1:1.1 in toluene and 1:0.6 in dodecane)

Table 2.6.80 *Catalytic hydroformylation of 1-hexene performed in dodecane under chosen conditions (80 °C, 8 MPa) for 16 h and with a catalyst : substrate ratio of 1:1000*

Catalyst	Conversion (%)	Yield of aldehyde (%)	Yield of hexane or 2-hexene or 3-hexene (%)	*n:i* ratio	Isomerisation	Number of different aldehydes
6	91	74	17	1 : 0.6	0	2
11	100	100	0	1 : 0.5	2	3
19	100	100	0	1 : 1	8	3
22	100	100	0	1 : 1	8	3
Wilkinson cat.	0	-	-	-	-	-

Table 2.6.81 *Catalytic hydroformylation of 1-hexene performed in toluene under chosen conditions (80 °C, 8 MPa) for 16 h and with a catalyst : substrate ratio of 1:5000*

Catalyst	Conversion (%)	Yield of aldehyde (%)	Yield of hexane or 2-hexene or 3-hexene (%)	*n:i* ratio	Isomerisation	Number of different aldehydes
6	100	100	0	1 : 1	8	3
11	61	52	9	1 : 0.6	0	2
19	100	100	0	1 : 1	9	3
22	100	100	0	1 : 0.9	8	3

The influence of catalyst concentration on the hydroformylation reaction was also investigated (Table 2.6.81). Four catalyst precursors (**6**, **11**, **19** and **22**) were used in toluene

under the same conditions as in the earlier experiments with a catalyst to substrate ratio of 1:5000. The only significant change was found for **11**, where the conversion to aldehyde was not completed. The degree of isomerisation (amount of *iso*-aldehyde formed from isomerised 1-hexene) and *n:i* ratios observed for all 4 complexes were similar to the ratios observed previously.

Experiments were carried out to determine if the pressure of the syngas has a significant effect on the products of the hydroformylation reaction. The same four complexes **6**, **11**, **19** and **22** were used. The reactions were done at 4 MPa (Table 2.6.82) and 10 MPa (Table 2.6.83). At 4 MPa the carbene complexes exhibit a lower TOF than at 8 MPa, but the two thione complexes **19** and **22** still gave a 100 % conversion after 16 hours. At lower pressure the *n:i* ratios for **6**, **11** and **22** improved by a significant amount, especially for **6**. The degree of isomerisation (amount of *iso*-aldehyde formed from isomerised 1-hexene) for **6** and **22** were also considerably lower and remained zero for **11**. The results at the higher pressure of 10 MPa closely resemble those obtained at 8 MPa (Table 2.6.77).

Table 2.6.82 *Catalytic hydroformylation of 1-hexene performed in toluene at 80 °C and 4 MPa for 16 h and with a catalyst : substrate ratio of 1:1000*

Catalyst	Conversion (%)	Yield of aldehyde (%)	Yield of hexane or 2-hexene or 3-hexene (%)	*n:i* ratio	Isomerisation	Number of different aldehydes
6	100	62	38	1 : 0.5	2	3
11	100	56	44	1 : 0.4	0	2
19	100	100	0	1 : 1.6	12	3
22	100	100	0	1 : 0.5	3	3

Table 2.6.83 *Catalytic hydroformylation of 1-hexene performed in toluene at 80 °C and 10 MPa for 16 h and with a catalyst : substrate ratio of 1:1000*

Catalyst	Conversion (%)	Yield of aldehyde (%)	Yield of hexane or 2-hexene or 3-hexene (%)	*n:i* ratio	Isomerisation	Number of different aldehydes
6	100	100	0	1 : 1	7	3
11	100	100	0	1 : 0.6	0	2
19	100	100	0	1 : 1	10	3
22	100	100	0	1 : 0.6	4	3

Complexes **6**, **11**, **19** and **22** were used in tests where the reaction times were varied (Tables 2.6.84 and Table 2.6.85). With a reaction time of three hours only **6** and **19** proved to be active, whereas all four complexes are active after six hours. Wilkinson's catalyst was also used for the six hour period, and also proved to be active. These results show that the active catalytic species is only formed after some time. An important observation is that the *n:i* ratios are higher for the uncompleted hydroformylation reactions than for the completed reactions previously investigated (Table 2.6.77). It appears that the linear aldehydes are formed early in the process, followed by the formation of the branched aldehydes towards the end of the observation period. In addition, the amount of isomerised hexene observed after a certain time differs for the four complexes used, indicating that the rate of isomerisation of the substrate depends on the nature of the catalyst.

Table 2.6.84 *Catalytic hydroformylation of 1-hexene performed in toluene at 80 °C and 8 MPa for 3 h and with a catalyst : substrate ratio of 1:1000*

Catalyst	Conversion (%)	Yield of aldehyde (%)	Yield of hexane or 2-hexene or 3-hexene (%)	*n:i* ratio	Isomerisation	Number of different aldehydes	TOF[a]
6	3	3	0	1 : 0.5	0	2	10
11	0	-	-	-	-	-	-
19	31	22	9	1 : 0.6	0	2	103
22	0	-	-	-	-	-	-

[a] *TOF = (mol aldehydes formed/mol catalyst) per hour*

Table 2.6.85 *Catalytic hydroformylation of 1-hexene performed in toluene at 80 °C and 8 MPa for 6 h and with a catalyst : substrate ratio of 1:1000*

Catalyst	Conversion (%)	Yield of aldehyde (%)	Yield of hexane or 2-hexene or 3-hexene (%)	*n:i* ratio	Isomerisation	Number of different aldehydes	TOF
6	71	62	9	1 : 0.6	0	2	118
11	30	30	0	1 : 0.4	0	2	50
19	100	100	0	1 : 1	9	3	167
22	14	14	0	1 : 0.4	0	2	23
Wilkinson cat.	19	19	0	1 : 1.9	0	2	32

Complex **19** had a TOF of 103 h^{-1} after three hours and a 100 % conversion after a reaction time of six hours – now with a TOF of 167 h^{-1}. A reaction time of five hours (Table 2.6.86) yielded a conversion of 63 % and a TOF of 126 h^{-1}.

Table 2.6.86 *Catalytic hydroformylation of 1-hexene performed in toluene at 80 °C and 8 MPa with* ***19*** *at a catalyst : substrate ratio of 1:1000*

Hours	Conversion (%)	Yield of aldehyde (%)	Yield of hexane or 2-hexene or 3-hexene (%)	*n:i* ratio	Isomerisation	Number of different aldehydes	TOF
3	31	22	9	1 : 0.6	0	2	103
5	63	42	21	1 : 0.6	0	2	126
6	100	100	0	1 : 1	9	3	167

The graph in Figure 2.6.18 shows the sharp increase in 1-hexene conversion to other hexene isomers and aldehydes, as well as the formation of all the aldehyde products by catalyst **19** during six hours of reaction time, exhibiting an average TOF of 167 h^{-1}. Complex **11** also produced a 100 % conversion to aldehydes, but only after a reaction time of nine hours. An average TOF of 111 h^{-1} after nine hours of reaction time is due to a large increase in activity in the last three hours of the reaction. The hydroformylation of styrene carried out by Tiripicchio *et al.* using a thione complex, also yielded a 100 % conversion to aldehyde after reaction times of 10 to12 hours.[86]

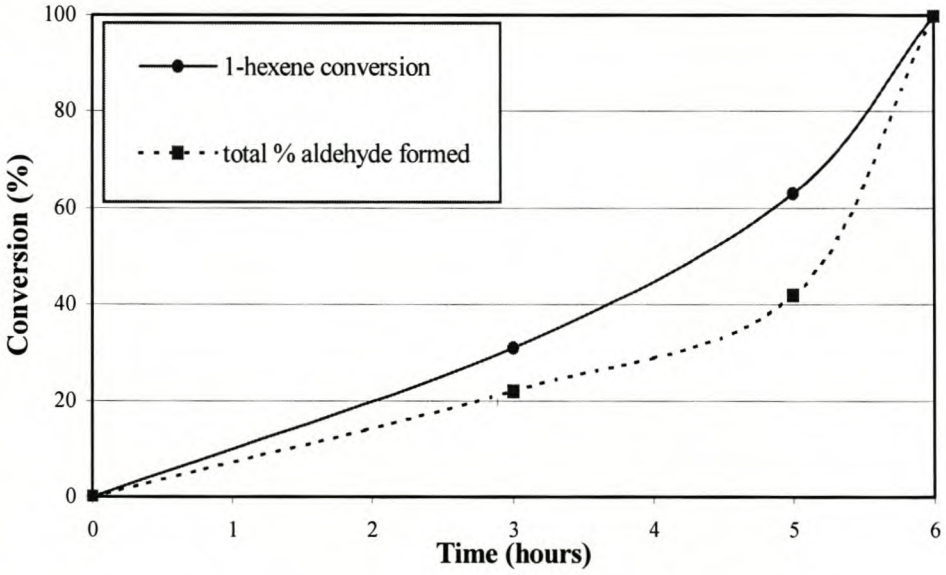

Figure 2.6.18 *1-Hexene conversion to aldehydes by complex* ***19***

No mechanistic studies have been undertaken. It is, however, reasonable to assume that the active rhodium hydride species are formed in two ways:

i. with Cl-containing pre-catalysts (*e.g.* **1**, **6**, **11**, **19**, **22**): oxidative addition of hydrogen followed by reductive elimination of HCl, and
ii. with cationic pre-catalysts (*e.g.* **4**, **5**, **9**, **14**, **15**, **26**, **27**): oxidative addition of hydrogen followed by H^+ loss to BF_4^-.

The carbene and thione ligands gave very good results and do show promise as ligands in the hydroformylation of α-olefins. The wide variety of results are briefly summarised below:

i. Initial 1-hexene isomerisation occurs, but the formed isomers are in general quantitatively hydroformylated.
ii. Incomplete reactions (after 16 hours) are only found for the biscarbene (cyclooctadiene) complex, **5**, the biscarbene(carbonyl) complex, **9**, the *trans*(carbene)(phosphine) complex, **12**, the *trans*(carbene)(thione) complex, **13**, and the *trans*(bisthione) complex, **24** (that does not catalyse the reaction at all).
iii. The carbene complexes, except the carbene(cyclooctadiene) complexes, **1** and **3**, the biscarbene complex, **4**, and the carbene(carbonyl) complex, **6**, produce both *n*- and *iso*-aldehydes where no isomerisation of 1-hexene occurred previously, whereas all the thione and imine complexes produce *iso*-aldehyde derived from isomerised 1-hexene as well.
iv. The addition of phosphine to the carbene(carbonyl) complex, **6**, retards the reaction significantly, whereas no retardation occurs with the carbene(cyclooctadiene) complex, **1**, the *trans*(carbene)(phosphine) complex, **11**, and the *trans*(phosphine)(thione) complex, **22**.
v. A higher linearity of aldehydes is obtained when additional phosphine is added to the carbene(cyclooctadiene) complex, **1**, the carbene(carbonyl) complex, **6**, and the *trans*(phosphine)(thione) complex, **22**. The opposite occurred when using the *trans*(carbene)(phosphine) complex, **11**.
vi. Hydroformylation reactions in the ionic liquid [BMIM]BF_4 are disappointing. The carbene(cyclooctadiene) complex, **3**, the carbene(carbonyl) complex, **6**, and the carbonyl(thione) complex, **19**, are too well immobilised in the ionic liquid, resulting in

no observable hydroformylation, while the *trans*(carbene)(phosphine) complex, **11**, and the *trans*(phosphine)(thione) complex, **22**, leach into the organic phase.

vii. The catalyst activity is solvent dependant. Wilkinson's catalyst is completely inactive in dodecane, the carbene(carbonyl) complex, **6**, is less active (conversion 91 % in dodecane and 100 % in toluene). The *n:i* ratio and the percentage of *iso*-aldehyde formed from the isomerised 1-hexene produced with the carbene(carbonyl) complex, **6**, the *trans*(carbene)(phosphine) complex, **11**, the carbonyl(thione) complex, **19**, and the *trans*(phosphine)(thione) complex, **22**, in dodecane differs significantly from the results obtained in toluene.

viii. At the lower pressure of 4 MPa the catalytic activity of the carbene(carbonyl) complex, **6**, and the *trans*(carbene)(phosphine) complex, **11**, are less than at 8 MPa, whereas the carbonyl(thione) complex, **19**, and the *trans* (phosphine)(thione) complex, **22**, still yield a 100 % conversion to aldehydes.

ix. The active catalytic species forms only after a certain period of time (depending on the catalyst) under hydroformylation conditions.

x. The carbonyl(thione) complex, **19**, is by far the most active catalyst.

Table 2.6.87 *Selected bond distances (Å) and bond angles (°) for complex* ***4***

Bond lengths (Å)		Bond angles (°)	
Rh1-C60	2.021(4)		
Rh1-C610	2.039(4)		
Rh1-C51	2.218(4)	C60-Rh1-C610	83.73(15)
Rh1-C54	2.210(4)	N5-C60-N6	103.6(3)
Rh1-C55	2.179(4)	N3-C610-N4	104.3(3)
Rh1-C58	2.218(4)	C60-N5-C63	111.0(4)
C60-N5	1.362(5)	C60-N6-C62	110.6(4)
C60-N6	1.360(5)	C610-N3-C67	111.0(4)
C610-N3	1.350(5)	C610-N3-C68	110.4(4)
C610-N4	1.350(5)	C62-C63-N5	107.6(4)
C62-N6	1.394(5)	C63-C62-N6	107.2(4)
C63-N5	1.379(5)	C67-C68-N4	107.4(4)
C67-N3	1.388(6)	C68-C67-N3	106.9(4)
C68-N4	1.393(6)	C60-N5-C64	124.2(3)
C64-N5	1.460(5)	C610-N3-C66	125.1(4)
C66-N3	1.454(5)	C64-C65-C66	116.4(4)
C64-C65	1.531(7)	C60-Rh1-C54	94.50(15)
C65-C66	1.525(7)	C60-Rh1-C55	92.74(15)
C62-C63	1.309(6)	C610-Rh1-C51	95.47(16)
C67-C68	1.313(7)	C610-Rh1-C58	96.59(17)
C51-C58	1.372(6)		
C54-C55	1.367(5)		

The two Rh-$C_{carbene}$ bond lengths are 2.021(4) Å and 2.039(4) Å, shorter than the two metal-carbene distances (2.053(8) Å and 2.059(8) Å) reported for *cis*-[(η^4-1,5-cyclooctadiene)bis(1,3-dimethyl-2,3-dihydro-1*H*-imidazol-2-ylidene)rhodium(I)]chloride and similar to the bond lengths reported for the monocarbene complexes with the general formula [RhX(cod)(NHC)] (2.021(4) Å for X = Cl and NHC = 1,3-dicyclohexyl-2,3-dihydro-1*H*-imidazol-2-ylidene,[64] 2.021(3) Å for X = Br and NHC = 1,3-dimethoxycarbonylmethyl-2,3-dihydro-1*H*-imidazol-2-ylidene,[77] 2.029(4) Å for X = Cl and NHC = 1-(2-{6-

The central rhodium atom resides in a square planar environment defined by the two carbene carbon atoms and the centres of the two double bonds of the cyclooctadiene ligand. Selected bond lengths and bond angles are summarised in Table 2.6.88.

Table 2.6.88 *Selected bond distances (Å) and bond angles (°) for complex* ***5***

Bond lengths (Å)		Bond angles (°)	
Rh1-C11	2.059(3)	C11-Rh1-C21	88.43(13)
Rh1-C21	2.051(4)	N11-C11-N12	104.0(3)
Rh1-C31	2.192(3)	N21-C21-N22	103.6(3)
Rh1-C32	2.174(4)	C11-N11-C12	111.5(3)
Rh1-C35	2.202(4)	C11-N12-C13	111.6(3)
Rh1-C36	2.175(4)	C21-N21-C22	112.0(3)
C11-N11	1.349(4)	C21-N22-C23	111.6(3)
C11-N12	1.361(4)	C13-C12-N11	106.5(3)
C21-N21	1.345(5)	C12-C13-N12	106.4(3)
C21-N22	1.363(4)	C23-C22-N21	106.5(3)
C12-N11	1.402(4)	C22-C23-N22	106.3(3)
C13-N12	1.392(4)	C11-Rh1-C35	93.79(14)
C22-N21	1.399(5)	C11-Rh1-C36	89.94(14)
C23-N22	1.398(5)	C21-Rh1-C31	93.93(14)
C12-C13	1.345(5)	C21-Rh1-C32	91.60(15)
C22-C23	1.341(6)	C31-Rh1-C36	81.68(15)
C31-C32	1.373(6)	C32-Rh1-C35	81.31(15)
C35-C36	1.374(5)		

The two Rh-$C_{carbene}$ bond distances, 2.059(3) Å and 2.051(4) Å, are similar to the bond lengths (2.053(8) Å and 2.059(8) Å) reported for *cis*-[(η^4-1,5-cyclooctadiene)bis(1,3-dimethyl-2,3-dihydro-1*H*-imidazol-2-ylidene)rhodium(I)]chloride.[63] These Rh-$C_{carbene}$ bond distances are longer than those in **4** (2.021(4) Å and 2.039(4) Å) and those observed for published monocarbene complexes with the general formula [RhX(cod)(NHC)] (2.021(4) Å for X = Cl and NHC = 1,3-dicyclohexyl-2,3-dihydro-1*H*-imidazol-2-ylidene,[64] 2.021(3) Å for X = Br and NHC = 1,3-dimethoxycarbonylmethyl-2,3-dihydro-1*H*-imidazol-2-ylidene,[77] 2.029(4) Å for X = Cl and NHC = 1-(2-{6-trimethylsilyl}pyridyl)-3-(2,6-diisopropyl)-2,3-

Rh1-S-C9 of 108.81(7)° is smaller than those reported for [RhCl(cod)(Hbztu)] (115.9(9)°) and [RhCl(cod)(Phtu)] (118.1(5)°), indicating that the S atom in the heterocyclic thione ligand has more sp^2 character than the S atom of the two reported complexes. In addition to this, the Rh-S bond distance in **17** (2.3602(7) Å) is somewhat shorter than those observed in [RhCl(cod)(Hbztu)] (2.382(1) Å) and [RhCl(cod)(Phtu)] (2.397(4) Å).

The bond lengths between the central rhodium atom and the four olefinic carbon atoms are 2.111(2) Å, 2.126(2) Å, 2.115(2) Å and 2.132(2) Å, a further indication that the thione ligand and the chloride atom have similar *trans* influences. These bond lengths are shorter than those reported for the carbene complex *cis*-[(η^4-1,5-cyclooctadiene)bis(1,3-dimethyl-2,3-dihydro-1*H*-imidazol-2-ylidene)rhodium(I)]chloride[63] (2.203(9) Å, 2.181(9) Å, 2.195(9) and 2.178(9) Å), thus providing an indication of the relative *trans* influences of the carbene and thione ligands.

Table 2.6.89 *Selected bond distances (Å) and bond angles (°) for complex* ***17***

Bond lengths (Å)		Bond angles (°)	
Rh1-Cl1	2.3783(9)		
Rh1-S	2.3602(7)	Cl2-Rh1-S	92.95(2)
Rh1-C1	2.111(2)	C9-S-Rh1	108.81(7)
Rh1-C2	2.126(2)	N1-C9-N2	106.30(18)
Rh1-C5	2.115(2)	C9-N1-C11	110.05(18)
Rh1-C6	2.132(2)	C9-N2-C13	110.16(17)
C9-S	1.725(2)	C11-C13-N2	106.62(18)
C9-N1	1.344(3)	C13-C11-N1	106.87(18)
C9-N2	1.346(3)	C1-Rh1-S	88.42(7)
C11-N1	1.389(3)	C2-Rh1-S	90.17(6)
C12-N2	1.389(2)	C5-Rh1-Cl2	89.44(7)
C11-C13	1.353(3)	C6-Rh1-Cl2	91.07(6)
C1-C2	1.397(3)		
C5-C6	1.391(3)		

thione ligand does not have as strong a *trans* influence as the carbene and phosphine ligands. The P-Rh-S bond angle is almost 180° at 179.38(2)°, corresponding to the P-Rh-P angle in the diphosphine complex (176.0(1)°), the N-Rh-P bond angle of the amine complex (174.6(2) Å) and the C-Rh-P bond angle in the carbene complex (174.46(12) Å). The Rh-$C_{carbonyl}$ bond length is 1.805(2) Å, the same as the 1.810(7) Å of the diphosphine complex and the 1.783(8) Å of the amine complex but longer than the 1.704(15) Å of the carbene complex.

Table 2.6.91 *Selected bond distances (Å) and bond angles (°) for complex* ***22***

Bond lengths (Å)		Bond angles (°)	
		Cl(chloride)-Rh-S	90.25(2)
		C1-Rh-S	86.16(7)
		P1-Rh-S	179.38(2)
Rh1-Cl(chloride)	2.3700(6)	Cl(chloride)-Rh-P1	89.84(2)
Rh1-S	2.4067(6)	C1-Rh-P1	93.79(7)
Rh1-P1	2.2653(5)	Rh-S-C41	106.85(7)
Rh1-C1	1.805(2)	Rh-C1-O1	175.6(2)
C41-S1	1.723(2)	Rh-P1-C11	113.13(7)
C41-N1	1.351(3)	Rh-P1-C21	118.98(7)
C41-N2	1.354(3)	Rh-P1-C31	113.53(7)
C42-N1	1.395(3)	N1-C41-S	126.28(17)
C43-N2	1.389(3)	N2-C41-S	126.36(17)
C42-C43	1.350(3)	N1-C41-N2	107.04(18)
C1-O1	1.147(3)	C41-N1-C42	109.18(18)
C11-P1	1.826(2)	C41-N2-C43	109.31(17)
C21-P1	1.832(2)	C43-C42-N1	107.13(19)
C31-P1	1.833(2)	C42-C43-N2	107.33(18)
		C11-P1-C21	104.17(10)
		C11-P1-C31	102.96(9)
		C21-P1-C31	102.36(10)

The Rh-Cl bond length of 2.3700(6) Å is similar to the Rh-Cl bond distance in **17**. The Rh-S bond length observed in **22** (2.4067(6) Å) is longer than the Rh-S bond length in **17** (2.3602(7) Å). This can be attributed to the *trans* influence of the PPh_3 ligand.

signals. These results provided proof that rotation about the Rh-$C_{carbene}$ bond is restricted. The use of very low or very high reaction temperatures during the preparation of the carbene complexes could possibly result in the formation of only one molecular structure of each complex. Such experiments should be exploited in a future investigation in order to understand the nature of these complexes completely. The thione complexes, **16** and **17**, were also present as isomers caused by slow inversion about the rhodium-coordinated sulfur atom.

Based on the physical data of the different complexes, the ligands used in this study can be arranged in decreasing order of their *trans* influences:

carbene > phosphine > imine > thione ≥ halide

Hydroformylation reactions of 1-hexene using the new rhodium(I) complexes as pre-catalysts were successfully performed. High conversions and variation in *n:i* ratios were observed. A 100 % conversion to aldehydes was obtained with most of the complexes, and the TOF observed for the carbene complex **11** was fairly high. The thione complex **19** also produced a 100 % conversion and an even higher TOF, the best of the investigated complexes. The experiments indicate that the active catalytic species forms after a certain period of time (depending on the catalyst) under hydroformylation conditions. Ionic liquids could not be successfully used as reaction media. The lack of activity is probably due to the immobilisation of the rhodium complexes in the ionic liquid phase and thus no real catalyst formation.

Further experiments are necessary to optimise the hydroformylation reaction conditions and fully investigate the formation of the active species and the mechanism involved. A higher synthesis gas pressure is probably necessary to optimise the activity and selectivity of the formed catalysts. The system at our disposal was not suitable to conduct tests at much higher pressures.

This study has demonstrated that rhodium complexes with thione ligands are useful and promising hydroformylation catalysts. Further research should fully explore these results by varying the conditions as suggested. The synthesis and coordination of novel thione ligands (Figure 2.7.1) to rhodium can yield complexes which could be successfully exploited in biphasic hydroformylation reactions.

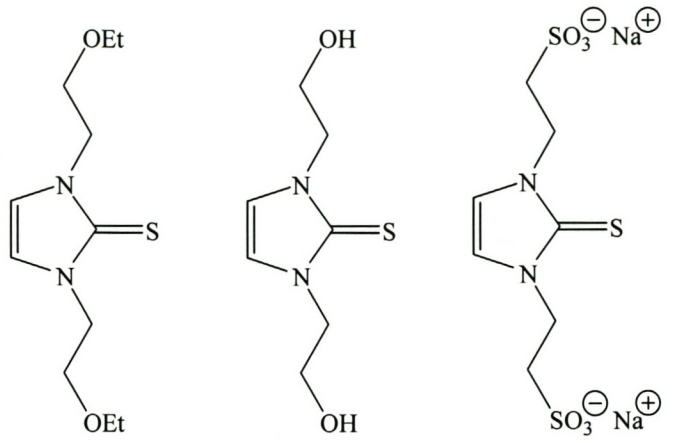

Figure 2.7.1 *Thione ligands for biphasic hydroformylation reactions*

8 Experimental procedure

8.1 General information

All reactions and manipulations were carried out under a dry argon atmosphere using standard Schlenk and vacuum-line techniques. All solvents were dried and purified by conventional methods and freshly distilled under nitrogen shortly before use. Flash column chromatography was performed with "flash grade" SiO_2 (SDS 230-400 mesh). All the common reagents, including *N*,*N*-dimethylthioformamide and KO^{t}Bu, were used as obtained from commercial suppliers without further purification.

The two easily accessible starting materials, $[RhCl(cod)]_2$ and $[RhCl(CO)_2]_2$, were prepared using published methods.[103] 1,3-Diisopropyl-4,5-dimethyl-2,3-dihydro-1*H*-imidazol-2-thione, 1,3-diisopropyl-4,5-dimethyl-2,3-dihydro-1*H*-imidazol-2-ylidene, 1,3,4,5-tetramethyl-2,3-dihydro-1*H*-imidazol-2-thione and 1,3,4,5-tetramethyl-2,3-dihydro-1*H*-imidazol-2-ylidene were prepared using the methods published by Kuhn and Kratz.[65] All compounds are stable in air and in solution unless otherwise stated.

8.2 Synthesis

8.2.1 Chloro(η^4-1,5-cyclooctadiene)(1,3-diisopropyl-4,5-dimethyl-2,3-dihydro-1*H*-imidazol-2-ylidene)rhodium(I) (1)

The reaction of 0.843g (4.676 mmol) 1,3-diisopropyl-4,5-dimethyl-2,3-dihydro-1*H*-imidazol-2-ylidene with 1.207g (2.448 mmol) $[RhCl(cod)]_2$ in THF (40 ml) yielded the monocarbene complex **1** as a yellow solid. An excess of $[RhCl(cod)]_2$ was used to prevent the formation of a biscarbene complex. Complex **1** was purified by flash chromatography on a short column (2 cm diameter) of silica (2 cm). Firstly, the excess $[RhCl(cod)]_2$ that remained after the reaction was removed on the column with dichloromethane, followed by the isolation of complex **1** from the column with ether. Complex **1** is a yellow microcrystalline solid that is soluble in THF and methylene chloride, slightly soluble in ether and insoluble in pentane and hexane.

Yield: 1.743 g (85 %)

Melting point: 192.8 °C (decomposition)

8.2.2 Pentacarbonyl(1,3-diisopropyl-4,5-dimethyl-2,3-dihydro-1*H*-imidazol-2-ylidene)tungsten(0) (2)

A solution of 1,3-diisopropyl-4,5-dimethyl-2,3-dihydro-1*H*-imidazol-2-ylidene (1.080 g, 5.990 mmol) in THF (30 ml) was added dropwise to a solution of $W(CO)_6$ (2.109 g, 5.993 mmol) also in THF (15 ml).The yellow solution was stirred overnight, filtered through celite (2 cm) and dried *in vacuo*. The remaining yellow powder obtained was washed 5 times with 20 ml of pentane. Complex **2** was purified by flash chromatography with SiO_2 and a 1:1 mixture of pentane and methylene chloride and then dried *in vacuo*. Complex **2** is a lime-yellow microcrystalline solid, soluble in ether, THF and methylene chloride, and insoluble in pentane.

Yield: 2.186 g (72 %)
Melting point: 194.8 °C

8.2.3 Chloro(η^4-1,5-cyclooctadiene)(1-butyl-3-methyl-2,3-dihydro-1*H*-imidazol-2-ylidene)rhodium(I) (3)

[BMIM]BF_4 (0.195 g, 0.863 mmol) in 5 ml of THF was treated with KO^{t}Bu (0.150 g, 1.337 mmol). After stirring this mixture for 2 hours, $[RhCl(cod)]_2$ (0.222g, 0.450 mmol) was added. The reaction mixture was stirred for a further 2 hours at room temperature, filtered through celite and dried *in vacuo*. Excess $[RhCl(cod)]_2$ was removed by the addition of 15 ml of ether and removing the formed orange ether solution. Complex **3** was purified by flash chromatography on a short column (2cm diameter) of silica (2 cm). The last traces of $[RhCl(cod)]_2$ were removed with methylene chloride, after which complex **3** was removed from the column using THF and then dried *in vacuo* to yield a yellow powder that is soluble in THF and methylene chloride, slightly soluble in ether and insoluble in pentane.

Yield: 0.105 g (61 %)
Melting point: 130.8 – 132.8 °C

8.2.4 [(η^4-1,5-Cyclooctadiene)-*cis*-(1,1′-propylene-3,3′-dimethyl-2,3,2′,3′-tetrahydro-1,1′*H*-diimidazol-2,2′-diylidene)rhodium(I)][hexafluorophosphate] (4)

$[RhCl(cod)]_2$ (0.172 g, 0.349 mmol) was added to a suspension of [1,1'-propylene-3,3'-dimethyl-1,1′*H*-diimidazole][dihexafluorophosphate][132] (0.157 g, 0.379 mmol) in 15 ml THF. The addition of KO^{t}Bu (0.128 g, 1.141 mmol) yielded a dark yellow solution. This solution was stirred for 4 hours before the solvent was removed *in vacuo*. The remaining yellow powder was washed 5 times with 30 ml of ether. Complex **4** was extracted with THF (five times with 30 ml) and filtered through anhydrous $MgSO_4$. Complex **4** was isolated using THF from a short column after removal of the last traces of $[RhCl(cod)]_2$ with methylene chloride. Complex **4** is a yellow microcrystalline powder which is stable in solution and in air, soluble in dichloromethane and THF, and insoluble in ether and pentane.

Yield: 0.112 g (56 %)
Melting point: 215.0 – 217.1 °C

8.2.5 *Cis*-[(η^4-1,5-cyclooctadiene)bis(1,3,4,5-tetramethyl-2,3-dihydro-1*H*-imidazol-2-ylidene)rhodium(I)]chloride (5)

$[RhCl(cod)]_2$ (0.215 g, 0.436 mmol) dissolved in 5 ml of THF was treated with a freshly prepared solution of the carbene ligand in THF (10 ml, 9 mmol). A yellow precipitate formed immediately. Stirring was continued for 2 hours. The suspension was filtered over a porosity 4 filter and the light yellow precipitate was then washed with ether (20 ml). Complex **5** was recrystallised from methylene chloride and pentane. The yellow product is soluble in methylene chloride, slightly soluble in THF and insoluble in ether and pentane.

Yield: 0.120 g (56 %)
Melting point: 159.2 °C (decomposition)

8.2.6 Chloro(dicarbonyl)(1,3-diisopropyl-4,5-dimethyl-2,3-dihydro-1*H*-imidazol-2-ylidene)rhodium(I) (6)

Carbon monoxide was bubbled through a yellow solution of **1** (0.269 g, 0.630 mmol) in 20 ml of methylene chloride. The reaction mixture turned orange within moments. After 5 minutes the reaction mixture was dried *in vacuo* and washed with pentane (10 ml). The remaining yellow powder was again dissolved in methylene chloride (20 ml) after which carbon monoxide was bubbled through the solution for 10 minutes. The mixture was again reduced to dryness and washed with pentane. Complex **6** is a light yellow microcrystalline powder, soluble in methylene chloride, THF and ether and insoluble in pentane.

Yield: 0.220 g (93 %)
Melting point: 149.8 °C (decomposition)

8.2.7 Chloro(dicarbonyl)(1-butyl-3-methyl-2,3-dihydro-1*H*-imidazol-2-ylidene)rhodium(I) (7)

Following the same procedure as for **6**, **7** was prepared from **3** (0.070 g, 0.187 mmol). **7** is a sticky yellow product, soluble in methylene chloride and THF, but insoluble in ether and pentane.

Yield: 0.032 g (51 %)

8.2.8 Chloro(dicarbonyl)(1-benzyl-3methyl-2,3-dihydro-1*H*-imidazol-2-ylidene)rhodium(I) (8)

Complex **8** was prepared from chloro(η^4-1,5-cyclooctadiene)(1-benzyl-3-methyl-imidazoline-2-ylidene)rhodium(I)[133] (0.070g, 0.167 mmol) using the same method as for the preparation of **6** and **7**. Complex **8** is a yellow brown powder with the same solubility properties as **7**.

Yield: 0.038 g (62 %)
Melting point: 79.1 – 81.3 °C

8.2.9 [Dicarbonyl(*cis*-(1,1′-propylene-3,3′-dimethyl-2,3,2′,3′-tetrahydro-1,1′*H*-diimidazol-2,2′-diylidene)rhodium(I)][hexafluorophosphate] (9)

Complex **9** was prepared in the same way as **6**, using **4** (0.068g, 0.121 mmol). Complex **9**, a microcrystalline solid, has a light yellow colour, is soluble in methylene chloride and THF, and is insoluble in ether and pentane.

Yield: 0.054 g (88 %)

Melting point: 173.9 – 174.0 °C (decomposition)

8.2.10 Chloro(carbonyl)-*trans*-bis(1,3,4,5-tetramethyl-2,3-dihydro-1*H*-imidazol-2-ylidene)rhodium(I) (10)

Carbon monoxide was bubbled through a yellow solution of **5** (0.159 g, 0.322 mmol) in 25 ml of methylene chloride for 30 minutes. The reaction mixture was dried *in vacuo* and washed twice with pentane (50 ml) and twice with ether (50 ml). The yellow powder was dried *in vacuo*. Complex **10** is soluble in methylene chloride and THF, and insoluble in ether and pentane.

Yield: 0.120 g (90 %)

Melting point: 218.5 °C (decomposition)

8.2.11 Chloro(carbonyl)-*trans*-(triphenylphosphine)(1,3-diisopropyl-4,5-dimethyl-2,3-dihydro-1*H*-imidazol-2-ylidene)rhodium(I) (11)

Triphenylphosphine (0.090 g, 0.343 mmol) was added to a solution of **6** (0.128 g, 0.342 mmol) in 5 ml of THF. Carbon monoxide evolution was observed as the mixture was stirred at room temperature. After stirring for 30 minutes, the reaction mixture was dried *in vacuo* and washed four times with 20 ml ether. Complex **11** is a light yellow powder which is soluble in methylene chloride and THF, and insoluble in ether and pentane.

Yield: 0.203 g (97 %)

Melting point: 167.6 – 168.2 °C

8.2.12 Chloro(carbonyl)-*trans*-(tri{2'H-thiazol}phosphine)(1,3-diisopropyl-4,5-dimethyl-2,3-dihydro-1*H*-imidazol-2-ylidene)rhodium(I) (12)

Complex **12** was prepared in the same way as **11**, starting from **6** (0.077 g, 0.206 mmol) and tri{2*H*-thiazol}phosphine[104] (0.057 g, 0.201 mmol). Complex **12** is a powder with a cream colour that dissolves in methylene chloride and THF, but is insoluble in ether and pentane.

Yield: 0.107 g (82 %)
Melting point: 168.3 – 171.1 °C

8.2.13 Chloro(carbonyl)-*trans*-(1,3-diisopropyl-4,5-dimethyl-2,3-dihydro-1*H*-imidazol-2-thione)(1,3-diisopropyl-4,5-dimethyl-2,3-dihydro-1*H*-imidazol-2-ylidene)rhodium(I) (13)

Complex **6** (0.164 g, 0.439 mmol) was added to a suspension of trimethylamine oxide (0.033 g, 0.438 mmol) in 30 ml of THF. After stirring for 30 minutes, 1,3-diisopropyl-4,5-dimethyl-2,3-dihydro-1*H*-imidazol-2-thione (0.092 g, 0.433 mmol) was added to the light yellow solution. The reaction mixture was stirred for two weeks and then dried *in vacuo*. Complex **13** was purified by flash chromatography on a short column. Firstly excess **6** that remained after the reaction was separated from **13** by column chromatography and elution with ether, and **13** was then isolated from the column with THF. The yellow solution was dried *in vacuo* to yield a yellow powder which is soluble in methylene chloride and THF, slightly soluble in ether and insoluble in pentane.

Yield: 0.138 g (56 %)
Melting point: 171.8 – 173.0 °C

8.2.14 [(η^4-1,5-Cyclooctadiene)(1,3-diisopropyl-4,5-dimethyl-2,3-dihydro-1*H*-imidazol-2-thione)(1,3-diisopropyl-4,5-dimethyl-2,3-dihydro-1*H*-imidazol-2-ylidene)rhodium(I)][tetrafluoroborate] (14)

A solution of **1** (0.188 g, 0.440 mmol) and 1,3-diisopropyl-4,5-dimethyl-2,3-dihydro-1*H*-imidazol-2-thione (0.094 g, 0.443 mmol) in 5 ml of THF was added to a suspension of $AgBF_4$ (0.100 g, 0.514 mmol) in THF (5 ml). AgCl, a white precipitate, was observed almost

immediately. Stirring was continued for 1 hour. The reaction mixture was filtered over celite and dried *in vacuo*. The yellow powder was washed twice with ether (20 ml) and dried *in vacuo*. The final product is soluble in THF and methylene chloride, and insoluble in ether and pentane.

Yield: 0.275 g (91 %)
Melting point: 141.0 °C (decomposition)

8.2.15 [(Dicarbonyl)-*cis*-(1,3-diisopropyl-4,5-dimethyl-2,3-dihydro-1*H*-imidazol-2-thione)(1,3-diisopropyl-4,5-dimethyl-2,3-dihydro-1*H*-imidazol-2-ylidene)rhodium(I)][tetrafluoroborate] (15)

Carbon monoxide was bubbled through a solution of **14** (0.100g, 0.145 mmol) in methylene chloride (30 ml) for 30 minutes. The reaction mixture was dried *in vacuo* to yield a green microcrystalline solid. The product was dissolved in dichloromethane (15 ml) and filtered over celite, dried *in vacuo* and washed with pentane (20 ml). Complex **15** was purified using short column chromatography similar to the method used for **1**. It was isolated with THF after removal of all the other products from the column with methylene chloride. Complex **15** was dried *in vacuo* and washed with pentane (10 ml) and ether (10 ml). The yellow microcrystalline solid is insoluble in ether and pentane, and soluble in THF and methylene chloride.

Yield: 0.068 g (74 %)
Melting point: 122.5 – 124.0 °C

8.2.16 Chloro(η^4-1,5-cyclooctadiene)(1,3-diisopropyl-4,5-dimethyl-2,3-dihydro-1*H*-imidazol-2-thione)rhodium(I) (16)

1,3-Diisopropyl-4,5-dimethyl-2,3-dihydro-1*H*-imidazol-2-thione (0.179 g, 0.843 mmol) and $[RhCl(cod)]_2$ (0.209 g, 0.424 mmol) were mixed together in THF (25 ml). A precipitate formed within seconds of combining the starting materials. Stirring was continued for 90 minutes and then the solvent was stripped *in vacuo*. Complex **16** was purified by flash chromatography on a short column. The excess $[RhCl(cod)]_2$ that remained after the reaction was first eluted from the column with methylene chloride. Complex **16** was then isolated from

the column with ether and dried *in vacuo*. Complex **16** is soluble in methylene chloride, THF and ether, and is insoluble in pentane and hexane.

Yield: 0.338 g (88 %)
Melting point: 139.7 – 140.6 °C

8.2.17 Chloro(η^4-1,5-cyclooctadiene)(1,3,4,5-tetramethyl-2,3-dihydro-1*H*-imidazol-2-thione)rhodium(I) (17)

Complex **17** was prepared in the same way as **16**, using $[RhCl(cod)]_2$ (0.179 g, 0.493 mmol) and 1,3,4,5-tetramethyl-2,3-dihydro-1*H*-imidazol-2-thione (0.113 g, 0.723 mmol). Complex **17** is a yellow microcrystalline solid that dissolves in methylene chloride, ether and THF, but is insoluble in pentane.

Yield: 0.357 g (90 %)
Melting point: 199.2 – 200.2 °C

8.2.18 Chloro(η^4-1,5-cyclooctadiene)(*N*,*N*-dimethylthioformamide)rhodium(I) (18)

N,*N*-dimethylthioformamide (0.065 ml, 0.751 mmol) was added to a solution of $[RhCl(cod)]_2$ (0.185 g, 0.375 mmol) in THF (30 ml). A yellow suspension formed within 2 minutes. Stirring was continued for another hour after which the solvent was removed. The microcrystalline yellow solid was washed three times with ether (50 ml) and dried *in vacuo*. The yellow product is soluble in methylene chloride, slightly soluble in THF, and insoluble in ether and pentane.

Yield: 0.245 g (97 %)
Melting point: 209.2 °C (decomposition)

8.2.19 Chloro(dicarbonyl)(1,3-diisopropyl-4,5-dimethyl-2,3-dihydro-1*H*-imidazol-2-thione)rhodium(I) (19)

A solution of $[RhCl(CO)_2]_2$ (0.179 g, 0.460 mmol) in THF (10 ml) was treated with 1,3-diisopropyl-4,5-dimethyl-2,3-dihydro-1*H*-imidazol-2-thione (0.196 g, 0.923 mmol). The

orange solution turned light yellow. After stirring the reaction mixture for one hour the solvent was removed *in vacuo*. The remaining solid was washed three times with pentane (10 ml) to yield **19** as a pale yellow microcrystalline solid which is soluble in methylene chloride, THF and ether, and is insoluble in pentane.

Yield: 0.319 g (85 %)
Melting point: 87.9 – 90.1 °C

8.2.20 Chloro(dicarbonyl)(1,3,4,5-tetramethyl-2,3-dihydro-1*H*-imidazol-2-thione)rhodium(I) (20)

The same procedure as for **19** was followed for the preparation of **20** from $[RhCl(CO)_2]_2$ (0.095 g, 0.244 mmol) and 1,3,4,5-tetramethyl-2,3-dihydro-1*H*-imidazol-2-thione (0.073 g, 0.467 mmol). Complex **20** is a yellow-brown microcrystalline solid, soluble in methylene chloride, THF and ether, and insoluble in pentane.

Yield: 0.146 g (85 %)
Melting point: 88.5 – 89.0 °C (decomposition)

8.2.21 Chloro(dicarbonyl)(*N*,*N*-dimethylthioformamide)rhodium(I) (21)

Complex **21** was prepared in the same way as **19** from $[RhCl(CO)_2]_2$ (0.224 g, 0.576 mmol) and *N*,*N*-dimethylthioformamide (0.10 ml, 1.174 mmol). In addition to washing the solid product with pentane (20 ml), the product was washed twice with ether (20 ml). Complex **21** is a brown-yellow microcrystalline solid which dissolves in methylene chloride and THF, is slightly soluble in ether and insoluble in pentane. Complex **21** is slightly hygroscopic and cannot be stored indefinitely.

Yield: 0.272 g (83 %)
Melting point: 52.3 °C

8.2.22 Chloro(carbonyl)-*trans*-(triphenylphosphine)(1,3-diisopropyl-4,5-dimethyl-2,3-dihydro-1*H*-imidazol-2-thione)rhodium(I) (22)

Triphenylphosphine (0.263 g, 1.003 mmol) was added to a solution of **19** (0.408 g, 1.003 mmol) in THF (10 ml). Carbon monoxide evolution was observed as the mixture was stirred at room temperature. After 30 minutes, the reaction mixture was dried *in vacuo* and washed four times with 20 ml of ether. Complex **22** is a yellow microcrystalline solid that is soluble in methylene chloride and THF, and insoluble in ether and pentane.

Yield: 0.524 g (82 %)
Melting point: 177.4 – 179.7 °C

8.2.23 Chloro(carbonyl)-*trans*-(triphenylphosphine)(*N*,*N*-dimethylthioformamide)rhodium(I) (23)

Complex **23** was prepared from **21** (0.132 g, 0.466 mmol) and triphenylphosphine (0.122 g, 0.465 mmol) using the same method as for the preparation of **22**. Complex **23** is a yellow-brown powder with the same solubility properties as **22**. Complex **23** is not as stable as the other complexes prepared in this study and decomposes in air.

Yield: 0.130 g (54 %)
Melting point: 123.7 – 126.7 °C

8.2.24 Chloro(carbonyl)-*trans*-bis(1,3-diisopropyl-4,5-dimethyl-2,3-dihydro-1*H*-imidazol-2-thione)rhodium(I) (24)

Complex **19** (0.162 g, 0.396 mmol) was added to a suspension of trimethylamine oxide (0.030 g, 0.399 mmol) in 30 ml of THF. After stirring for 30 minutes, 1,3-diisopropyl-4,5-dimethyl -2,3-dihydro-1*H*-imidazol-2-thione (0.084 g, 0.396 mmol) was added to the orange solution. The reaction mixture was stirred for two weeks and then dried *in vacuo*. The solid was washed 5 times with pentane (20 ml), dissolved in ether (100 ml), filtered over anhydrous $MgSO_4$ (2 cm on a filter with a 2 cm diameter) and dried *in vacuo*. Complex **24** is an orange microcrystalline solid, soluble in methylene chloride, ether and THF, and insoluble in pentane.

Yield: 0.100 g (43 %)

Melting point: 130.5 – 131.7 °C

8.2.25 Chloro(carbonyl)-*trans*-bis(*N*,*N*-dimethylthioformamide)rhodium(I) (25)

N,*N*-dimethylthioformamide (0.11 ml, 1.29 mmol) was added to a solution of $[RhCl(CO)_2]_2$ (0.119 g, 0.306 mmol) in THF (5 ml). After stirring for one hour, the orange reaction mixture was dried *in vacuo* to yield an orange solid. Complex **25** was washed four times with pentane (20 ml) and four times with ether (20 ml) and dried *in vacuo*. Complex **25** is a yellow-brown microcrystalline solid that turns brown upon exposure to air. It is soluble in methylene chloride and THF, and insoluble in ether and pentane. Complex **25** is slightly hygroscopic and cannot be stored indefinitely.

Yield: 0.175 g (83 %)

Melting point: 105.7 – 107.5 °C

8.2.26 [(η^4-1,5-Cyclooctadiene)bis(1,3-diisopropyl-4,5-dimethyl-2,3-dihydro-1*H*-imidazol-2-thione)rhodium(I)][tetrafluoroborate] (26)

A solution of $[RhCl(cod)]_2$ (0.192 g, 0.389 mmol) and 1,3-diisopropyl-4,5-dimethyl -2,3-dihydro-1*H*-imidazol-2-imidazole-2(3*H*)-thione (0.332 g, 1.563 mmol) in THF (5 ml) was added to a suspension of $AgBF_4$ (0.158 g, 0.786 mmol) in THF (5 ml). The precipitation of AgCl was observed almost immediately. Stirring was continued for 2 hours. The reaction mixture was filtered over celite (2 cm) and the filtrate dried *in vacuo*. The yellow powder was washed three times with ether (20 ml) and dried *in vacuo*. The final product is soluble in THF and methylene chloride, and insoluble in ether and pentane.

Yield: 0.464 g (83 %)

Melting point: 181.5 – 182.0 °C

8.2.27 [(Dicarbonyl)cis-bis(1,3-diisopropyl-4,5-dimethyl-2,3-dihydro-1*H*-imidazol-2-thione)rhodium(I)][tetrafluoroborate] (27)

Using the same procedure as for the preparation of **6**, **27** was prepared from **26** (0.240 g, 0.332 mmol). Complex **27** is a yellow-orange microcrystalline product which is soluble in methylene chloride and THF and insoluble in ether and pentane. Complex **27** is slightly hygroscopic and cannot be stored indefinitely.

Yield: 0.213 g (95 %)
Melting point: 64.7 – 65.2 °C

8.2.28 [(η^4-1,5-Cyclooctadiene)(4,5-dimethylthiazole)(1,3-diisopropyl-4,5-dimethyl-2,3-dihydro-1*H*-imidazol-2-thione)rhodium(I)][tetrafluoroborate] (28)

Complex **28** was prepared from **19** (0.125 g, 0.275 mmol), 4,5-dimethylthiazole (0.054 ml, 0.511 mmol) and $AgBF_4$ (0.100 g, 0.514 mmol) using the same method as for **26**. Complex **28** is a yellow microcrystalline solid with the same solubility properties as **26**.

Yield: 0.070 g (41 %)
Melting point: 159.9 °C (decomposition)

8.2.29 Chloro(η^4-1,5-cyclooctadiene)(4,5-dimethylthiazole)rhodium(I) (29)

4,5-Dimethylthiazole (0.085 ml, 0.804 mmol) was added to a solution of $[RhCl(cod)]_2$ (0.190 g, 0.385 mmol) in THF (10 ml). A yellow suspension was observed after 30 minutes. Stirring was continued for another 3 days. Complex **29** was isolated from a short SiO_2 flash chromatography column with methylene chloride as eluant and dried *in vacuo*. The yellow microcrystalline solid is soluble in methylene chloride, THF and ether, and insoluble in pentane.

Yield: 0.187 g (67 %)
Melting point: 226.3 °C (decomposition)

8.2.30 Chloro(η^4-1,5-cyclooctadiene)(4-methylthiazole)rhodium(I) (30)

The procedure followed for **29** was used to prepare **30** from $[RhCl(cod)]_2$ (0.195 g, 0.395 mmol) and 4-methylthiazole (0.09 ml, 0.769 mmol). Complex **30** is a yellow microcrystalline solid with the same solubility properties as **29**.

Yield: 0.195 g (72 %)
Melting point: 231.6 – 232.7 °C (decomposition)

8.2.31 Chloro(dicarbonyl)(4-methylthiazole)rhodium(I) (31)

Following the same procedure as for **19**, **31** was prepared from $[RhCl(CO)_2]_2$ (0.095 g, 0.244 mmol) and 4-methylthiazole (0.04 ml, 0.44 mmol) in THF (5 ml). Complex **31** is a yellow-brown microcrystalline solid, soluble in methylene chloride, THF and ether, and insoluble in pentane.

Yield: 0.083 g (64 %)
Melting point: 57.0 – 57.6 °C (decomposition)

8.2.32 General procedure for the hydroformylation reactions

The catalyst precursor and a magnetic stirrer bar were placed inside a 300 ml stainless steel autoclave. The apparatus was sealed, all the air was removed by vacuum and the autoclave was filled with argon. The solvent and substrate were then added and the autoclave was charged with a 1:1 hydrogen/carbon monoxide mixture obtained from Afrox. The vessel was placed in an oil bath set at a constant temperature. After the chosen reaction time the apparatus was cooled, opened and the solution removed. A sample was injected into a gas chromatograph to determine the conversion and *n:i* ratio of the products using a non-polar column (PS 255, FS 66, 1.2 mm x 40 m x 0.32 mm).

For the standard set of conditions 0.016 mmol precursor catalyst, 2 ml substrate (1-hexene) and 10 ml solvent (toluene) were used. Upon use of the ionic liquids instead of toluene, the solvent was added before sealing of the autoclave. Isolation of the organic product was performed *via* extraction with ether from the ionic liquid.

8.2.33 X-ray crystal structure determinations of 4, 5, 16, 18 and 22

The crystal data collection and refinement details for complexes **4**, **5**, **17**, **18** and **22** are summarised in Table 2.8.1 and Table 2.8.2. Single crystals suitable for a structure of the complexes determination were obtained by crystallisation from concentrated dichloromethane solutions layered with pentane. Data were collected on an Enraf-Nonius KappaCCD diffractometer using graphite monochromated Mo-K_α radiation (λ = 0.71073 Å) and scaled and reduced using DENZO-SMN.[134] The structures were solved by the heavy atom method (SHELXS)[135] and refined anisotropically for all the non-hydrogen atoms by full-matrix least squares calculations (SHELXL-97)[135] on F^2. ORTEP-III for Windows[136] was used to generate the various figures of the five complexes at the 50% probability level.

Crystal structure data collection and correction procedures were performed by Dr J. Bacsa and Ms Hong Su at the Department of Chemistry, University of Cape Town. All structure solutions and refinements were carried out by Dr C. Esterhuysen and Mr M.W. Esterhuysen at the Department of Chemistry at the University of Stellenbosch.

Table 2.8.1 *Crystallographic data for complex* ***4*** *and complex* ***5***

Complex	**4**	**5**
Chemical Formula	$C_{39}H_{58}N_8P_2Cl_2F_{12}Rh_2$	$C_{22}H_{36}N_4Rh$
MW (g/mol)	1205.59	588.84
Crystal system	Orthorhombic	Monoclinic
Space group	P 21 21 21	C2/c
a (Å)	15.8475 (2)	26.8149 (4)
b (Å)	17.4778 (2)	13.2815 (3)
c (Å)	17.5446 (2)	18.8678 (5)
α (°)	90.00	90.00
β (°)	90.00	126.8510 (10)
γ (°)	90.00	90.00
Volume (Å^3)	4859.49 (10)	5377.0 (2)
Z	4	8
d_{calcd} (g/cm^3)	1.648	1.455
Temp (K)	203	173 (2)
μ (cm^{-1})	0.940	0.953
θ (°)	$1.02 \leq \theta \leq 27.48$	$1.02 \leq \theta \leq 27.48$
Radiation	Mo Kα, graphite monochromated	Mo Kα, graphite monochromated
Crystal size (mm)	0.23 × 0.12 × 0.1	0.22 × 0.21 × 0.17
Index range	$-19 \leq h \leq 19$ $-21 \leq k \leq 21$ $-21 \leq l \leq 19$	$-31 \leq h \leq 33$ $-16 \leq k \leq -15$ $-20 \leq l \leq 23$
Number of reflections collected	35432	11822
Number of reflections used	22001	5231
Refinement	Full matrix on F^2 (SHELXL)	Full matrix on F^2 (SHELXL)
Parameters	641	311
R_1 ($F_o > 2\sigma F_o$)	0.0325	0.0419
wR_2 (all data)	0.0632	0.1053

Table 2.8.2 *Crystallographic data for complex* ***16****, complex* ***18*** *and complex* ***22***

Complex	**16**	**18**	**22**
Chemical Formula	$C_{15}H_{24}N_2SRhCl$	$C_{11}H_{19}NSRhCl$	$C_{30}H_{35}N_2OPSRhCl$
MW (g/mol)	402.78	335.69	640.99
Crystal system	Monoclinic	Monoclinic	Monoclinic
Space group	P21/c	P21/c	P21/c
a (Å)	14.389 (3)	7.26030 (10)	9.04670 (10)
b (Å)	7.7020 (15)	15.2871 (2)	10.58750 (10)
c (Å)	14.993 (3)	11.67520 (10)	30.4334 (3)
α (°)	90.00	90.00	90.00
β (°)	100.79 (3)	90.0180 (10)	94.15
γ (°)	90.00	90.00	90.00
Volume (Å^3)	1632.2 (6)	1295.82 (3)	2907.34 (5)
Z	4	4	4
d_{calcd} (g/cm^3)	1.639	1.721	1.464
Temp (K)	173 (2)	193 (2)	193 (2)
μ (cm^{-1})	1.330	1.654	0.832
θ (°)	$1.4 \le \theta \le 27.5$	$1.02 \le \theta \le 29.58$	$1.02 \le \theta \le 28.7$
Radiation	Mo Kα, graphite monochromated	Mo Kα, graphite monochromated	Mo Kα, graphite monochromated
Crystal size (mm)	0.19 × 0.12 × 0.10	0.11 × 0.09 × 0.08	0.22 × 0.21 × 0.17
Index range	$-18 \le h \le 18$ $-9 \le k \le 10$ $-19 \le l \le 19$	$-9 \le h \le 9$ $-19 \le k \le 19$ $-14 \le l \le 14$	$-11 \le h \le 11$ $-13 \le k \le -13$ $-38 \le l \le 38$
Number of reflections collected	11509	9994	12308
Number of reflections used	3740	5983	7915
Refinement	Full matrix on F^2 (SHELXL)	Full matrix on F^2 (SHELXL)	Full matrix on F^2 (SHELXL)
Parameters	197	141	340
R_1 ($F_o > 2\sigma F_o$)	0.0247	0.0267	0.0271
wR_2 (all data)	0.0514	0.0788	0.0670

9 References

1 R. Whyman, in *Applied Organometallic Chemistry and Catalysis*, Oxford University Press, New York, 2001, p. 19.

2 *Rhodium Catalysed Hydroformylation*, Eds. P.W.N.M. van Leeuwen, C. Claver, Kluwer Academic Publishers, Dordrecht, 2000.

3 G. Schiller, German Patent 965,605, 1956, Chem. Verwertungsges. Oberhausen.

4 V.L. Hughes, British Patent 801,734, 1958, Esso Res. Eng. Comp.

5 D. Evans, J.A. Osborn, G. Wilkinson, *J. Chem. Soc., A*, 1968, 3133.

6 P.W.N.M. van Leeuwen, C.P. Casey, G.T. Whiteker, in *Rhodium Catalysed Hydroformylation*, Eds. P.W.N.M. van Leeuwen, C. Claver, Kluwer Academic Publishers, Dordrecht, 2000, p.63.

7 J.C. Bayón, C. Claver, A.M. Masdeu-Bultó, *Coord. Chem. Rev.*, 1999, **193-195**, 73.

8 C.D. Frohning, C.W. Kohlpainter, in *Applied Homogeneous Catalysis with Organometallic Compounds*, Eds. W.A. Herrmann, B. Cornils, Wiley-VCH, Weinheim, New York, 1996, Vol. 1, p. 48.

9 R.F. Heck, D.S. Breslow, *J. Am. Chem. Soc.*, 1961, **63**, 4023.

10 Ref. 8, p. 49.

11 M.E. Brousard, B. Juma, S.G. Train, W.-J. Peng, S.A. Laneman, G.G. Stanley, *Science*, 1993, **260**, 1784.

12 R.C. Matthews, D.K. Howell, W.-P. Peng, S.G. Train, W. Dale Treleaven, G.G. Stanley, *Angew. Chem., Int. Ed. Engl.*, 1996, **35**, 2253.

13 J.N.H. Reek, P.C.J. Kamer, P.W.N.M. van Leeuwen, in *Rhodium catalysed Hydroformylation*, Eds. P.W.N.M. van Leeuwen, C. Claver, Kluwer Academic Publishers, Dordrecht, 2000, p. 254.

14 A.M. Trzeciak, J.J.Ziólkowski, *Coord. Chem. Rev.*, 1999, **190-192**, 883.

15 Ref. 8, p. 85.

16 C. Bergounhou, D. Neibecker, R. Réau, *J. Chem. Soc., Chem. Comm.*, 1988, 1370.

17 D. Neibecker, R. Réau, *Angew. Chem., Int. Ed. Engl.*, 1989, **28**, 500.

18 D. Neibecker, R. Réau, S. Lecolier, *J. Org. Chem.*, 1989, **54**, 5208.

19 W.A. Herrmann, C.W. Kohlpainter, R.B. Manetsberger, H. Bahrmann, H. Kottmann, *J. Mol. Cat. A*, 1995, **97**, 65.

20 P. Suomalainen, H.K. Reinus, H. Riihimaki, R.H. Laitinen, S. Jaaskelainen, M. Haukka, J.T. Pursiainen, T.A. Pakkanen, A.O.I. Krause, *J. Mol. Cat. A*, 2001, **169**, 67.

21 H.K. Reinus, A.O.I. Krause, *Chem. Lett.*, 2001, **70**, 149.

22 P.Suomalainen, R. Laitinen, S. Jääskeläinen, M. Haukka, J.T. Pursiainen, T.A. Pakkanen, *J. Mol. Cat. A*, 2002, **179**, 93.

23 S. Rojas, J.L.G. Fierro, R. Fandos, A. Rodriquez, P. Terreros, *J. Chem. Soc., Dalton Trans.*, 2001, 2316.

24 B. Breit, *Chem. Comm.*, 1996, 2071.

25 F. Ungváry, *Coord. Chem. Rev.*, 1997, **167**, 233.

26 Ref. 8, p. 90.

27 Ref. 13, p. 256.

28 P. Wasserscheid, W. Keim, *Angew. Chem., Int. Ed. Engl.*, 2000, **39**, 3772.

29 T. Welton, *Chem. Rev.*, 1999, **99**, 2071.

30 D. Zhao, M. Wu, Y. Kou, E. Min, *Cat. Today*, 2002, **74**, 157.

31 G.W. Parshall, Du Pont, *U.S. Pat.*, 3565823, 1971.

32 G.W. Parshall, Du Pont, *U.S. Pat.*, 3657368, 1972.

33 J.F. Knifton, Texaco Inc., *U.S. Pat.*, 4013584, 1977.

34 H. Waffenschmidt, W. Keim, P. Wasserscheid, *DE Pat.*, 19901524, 2000.

35 B.E. Mann, M.H. Guzman, *Inorg. Chim. Acta*, 2002, **330**, 143.

36 G.W. Parshall, *J. Am. Chem. Soc.*, 1972, **94**, 8716.

37 P. Wasserscheid, H. Waffenschmidt, *J. Mol. Cat. A*, 2000, **164**, 61.

38 Y. Chauvin, L. Mussmann, H. Olivier, *Angew. Chem., Int. Ed. Engl.*, 1995, **34**, 2698.

39 N. Karodia, S. Guise, C. Newlands, J.-A. Anderson, *Chem. Comm.*, 1998, 2341.

40 W. Keim, D. Vogt, H. Waffenschmidt, P. Wasserscheid, *J. Cat.*, 1999, **186**, 481.

41 M.F. Sellin, P.B. Webb, D.J. Cole-Hamilton, *Chem. Comm.*, 2001, 781.

42 F. Favre, H. Olivier-Bourbigou, D. Commereuc, L. Saussine, *Chem. Comm.*, 2001, 1360.

43 P. Wasserscheid, H. Waffenschmidt, P. Machnitzki, K.W. Kottsieper, O. Stelzer, *Chem. Comm.*, 2001, 451.

44 C.C. Brasse, U. Englert, A. Salzer, H. Waffenschmidt, P. Wasserscheid, *Organometallics*, 2000, **19**, 3818.

45 D.J. Brauer, K.W. Kottsieper, C. Liek, O. Stelzer, H. Waffenschmidt, P. Wasserscheid, *J. Organomet. Chem.*, 2001, **630**, 177.

46 O. Stenzel, H.G. Raubenheimer, C. Esterhuysen, *J. Chem. Soc., Dalton Trans.*, 2002, 1132.

47 T. Weskamp, V.P.W. Böhm, W.A. Herrmann, *J. Organomet. Chem.*, 2000, **600**, 12.

48 D.J. Cardin, M.J. Doyle, M.F. Lappert, *J. Chem. Soc., Chem. Comm.*, 1972, 927.

49 D.J Cardin, M.J. Doyle, M.F. Lappert, *J. Organomet. Chem.*, 1974, **65**, C13.

50 M.J. Doyle, M.F. Lappert, *J. Chem. Soc., Chem. Comm.*, 1974, 679.

51 P.B. Hitchcock, M.F. Lappert, P. Terreros, K.P. Wainwright, *J. Chem. Soc., Chem. Comm.*, 1980, 1180.

52 A.W. Coleman, P.B. Hitchcock, M.F. Lappert, R.K. Maskell, J.H. Müller, *J. Organomet. Chem.*, 1983, **250**, C9.

53 J.E. Hill, T.E. Nile, *J. Organomet. Chem.*, 1977, **137**, 293.

54 M.J. Doyle, M.F. Lappert, P.L. Pye, P. Terreros, *J. Chem. Soc., Dalton Trans.*, 1984, 2355.

55 B. Cetinkaya, P.B. Hitchcock, M.F. Lappert, D.B. Shaw, K. Spyropoulos, N.J.W. Warhurst, *J. Organomet. Chem.*, 1993, **459**, 311.

56 B. Cetinkaya, I. Özdemir, P.H. Dixneuf, *J. Organomet. Chem.*, 1997, **534**, 153.

57 H.-W. Wanzlick, *Angew. Chem., Int. Ed. Engl.*, 1962, **2**, 75.

58 A.J. Arduengo, III, R.L. Harlow, M. Kline, *J. Am. Chem. Soc.*, 1991, **113**, 361.

59 A.J. Arduengo, III, H.V.R. Dias, R.L. Harlow, M. Kline, *J. Am. Chem. Soc.*, 1992, **114**, 5530.

60 M. Regitz, *Angew. Chem., Int. Ed. Engl.*, 1991, **30**, 674.

61 K.K. Irikura, W.A. Goddard, III, J.L. Beauchamp, *J. Am. Chem. Soc.*, 1992, **114**, 48.

62 A.J. Arduengo, III, H.V.R. Dias, D.A. Dixon, R.L. Harlow, W.T. Klooster, T.F. Koetzle, *J. Am. Chem. Soc.*, 1994, **116**, 6812.

63 W.A. Herrmann, M. Elison, J. Fischer, C. Köcher, G.R.J. Artus, *Chem. Eur. J.*, 1996, **2**, 772.

64 W.A. Herrmann, C. Köcher, L. Goossen, G.R.J. Artus, *Chem. Eur. J.*, 1996, **2**, 1627.

65 N. Kuhn, T. Kratz, *Synthesis*, 1993, 561.

66 D. Enders, K. Breuer, G. Raabe, J. Runsink, J.H. Teles, J.P. Melder, K. Ebel, S. Brode, *Angew. Chem., Int. Ed. Engl.*, 1995, **34**, 1021.

67 M. Regitz, *Angew. Chem., Int. Ed. Engl.*, 1996, **35**, 725.

68 W.A. Herrmann, C. Köcher, *Angew. Chem., Int. Ed. Engl.*, 1997, **36**, 2162.

69 D.Bourissou, O. Guerret, F.P. Gabbaï, G. Bertrand, *Chem. Rev.*, 2000, **100**, 39.

70 W.A. Herrmann, *Angew. Chem., Int. Ed. Engl.*, 2000, **41**, 1291.

71 W.A. Herrmann, L.J. Goossen, C. Köcher, G.R.J. Artus, *Angew. Chem., Int. Ed. Engl.*, 1996, **35**, 2805.

72 W.A. Herrmann, L.J. Goossen, G.R.J. Artus, C. Köcher, *Organometallics*, 1997, **16**, 2472.

73 C. Köcher, W.A. Herrmann, *J. Organomet. Chem*, 1997, **532**, 261.

74 W.A. Herrmann, J. Fischer, K. Öfele, G.R.J. Artus, *J. Organomet. Chem.*, 1997, **530**, 259.

75 A.C. Chen, L. Ren, A. Decken, C.M. Crudden, *Organometallics*, 2000, **19**, 3459.

76 H.-W. Wanzlick, H.-J. Schönherr, *Angew. Chem., Int. Ed. Engl.* 1968, **7**, 141.

77 W.A. Herrmann, L.J. Goossen, M. Speigler, *J. Organomet. Chem.*, 1997, **547**, 357.

78 S.-T. Liu, T.-Y. Hsieh, G.-H. Lee, S.-M. Peng, *Organometallics*, 1998, **17**, 993.

79 R.-Z. Ku, J.-C. Huang, J.-Y. Cho, F.-M. Kiang, K.R. Reddy, Y.-C. Chen, K.-J. Lee, J.-H. Lee, G.-H. Lee, S.-M. Peng, S.-T. Liu, *Organometallics*, 1999, **18**, 2145.

80 R.E. Douthwaite, D. Haüssinger, M.L.H. Green, P.J. Silcock, P.T. Gomes, A.M. Martins, A.A. Danopoulos, *Organometallics*, 1999, **18**, 4584.

81 K. Öfele, W.A. Herrmann, D. Mihalios, .M. Elison, E. Herdtweck, W. Scherer, J. Mink, *J. Organomet. Chem.*, 1993, **459**, 177.

82 A.A. Danopoulos, S. Winston, M.B. Hursthouse, *J. Chem. Soc., Dalton Trans.*, 2002, 3090.

83 R.G. Pearson, *J. Am. Chem. Soc.*, 1963, **85**, 3533.

84 S. Rojas, P. Terreros, J.L.G. Fierro, *J. Mol. Cat. A*, 2002, **184**, 19.

85 D. Cauzzi, M. Lanfranchi, G. Marzolini, G. Predieri, A. Tiripicchio, M. Costa, R. Zanoni, *J. Organomet. Chem.*, 1995, **488**, 115.

86 D. Cauzzi, M. Costa, L. Gonsalvi, M.A. Pellinghelli, G. Predieri, A. Tiripicchio, R. Zanoni, *J. Organomet. Chem.*, 1997, **541**, 377.

87 D. Cauzzi, M. Costa, N. Cucci, C. Graiff, F. Grandi, G. Predieri, A. Tiripicchio, R. Zanoni, *J. Organomet. Chem.*, 2000, **593-594**, 431.

88 J. Kramer, A. Scholten, W.L. Driessen, J. Reedijk, *Inorg. Chim. Acta*, 2001, **315**, 183.

89 F. Touchard, F. Fache, M. Lemaire, *Tetrahedron Assym.*, 1997, **8**, 3319.

90 F. Touchard, M. Bernard, F. Fache, M. Lemaire, *J. Mol. Cat. A*, 1999, **140**, 1.

91 M.L. Tommasino, M. Casalta, J.A.J. Breuzard, M. Lemaire, *Tetrahedron Assym.*, 2000, **11**, 4835.

92 M. Bernard, F. Delbecq, F. Fache, P. Sautet, M. Lemaire, *Eur. J. Org. Chem.*, 2001, 1589.

93 A. Togni, L.M. Venanzi, *Angew. Chem., Int. Ed. Engl.*, 1994, **33**, 497.

94 H. Schumann, H. Hemling, V. Ravindar, Y. Badrieh, J, Blum, *J. Organomet. Chem.*, 1994, **469**, 213.

95 R. Uson, L.A. Oro, M.T. Pinillos, M. Royo, E. Pastor, *J. Mol. Cat.*, 1982, **14**, 375.

96 P. Kalck, A. Thorez, M.T. Pinillos, L.A. Oro, *J. Mol. Cat.*, 1985, **31**, 311.

97 G. Zassinovich, G. Mestroni, A. Camus, *J. Organomet. Chem.*, 1975, **91**, 379.

98 J. Müller, R. Stock, *Angew. Chem., Int. Ed. Engl.*, 1983, **22**, 993.

99 A.R. Siedle, G. Filipovich, P.E. Toren, F.J. Palensky, E. Cook, R.A. Newmark, W.L. Stebbings, K. Melancon, H.E. Mismash, *J. Organomet. Chem.*, 1983, **246**, 83.

100 G. Clauti, G. Zassinovich, G. Mestroni, *Inorg. Chim. Acta*, 1986, **112**, 103.

101 F. Bonati, L.A. Oro, T. Pinillos, C. Tejel, M.C. Apreda, C. Foces-Foces, F.H. Cano, *J. Organomet. Chem.*, 1989, **369**, 253.

102 G.R. Julius, S. Cronje, A. Neveling, C. Esterhuysen, H.G. Raubenheimer, *Helv. Chim. Acta*, 2002, **85**, 3737.

103 J. Chatt, L.M. Venanzi, *J. Chem. Soc.*, 1957, 4735.

104 S.S. Moore, G.M. Whitesides, *J. Org. Chem.*, 1982, **47**, 1489.

105 T.-Y. Luh, *Coord. Chem. Rev.*, 1984, **60**, 255.

106 M. O. Albers, N.J. Coville, *Coord. Chem. Rev.*, 1984, **53**, 227.

107 D.St.C. Black, G.B. Deacon, N.C. Thomas, *Inorg. Chim. Acta*, 1982, **65**, L75.

108 Y.-K. Yan, W. Koh, C. Jiang, W.K. Leong, T.S.A. Hor, *Polyhedron*, 2000, **19**, 641.

109 G. Clauti, G. Zassinovich, G. Mestroni, *Inorg. Chim. Acta*, 1986, **112**, 103.

110 B.E. Mann, B.F. Taylor, in *^{13}C NMR Data for Organometallic Compounds*, Ed. P.M. Maitlis, F.G.A. Stone, R. West, Academic Press, London, 1981, p.16.

111 L. Manojlović-Muir, K.W. Muir, *J. Chem. Soc., Dalton. Trans.*, 1974, 2427.

112 E.M. Badley, K.W. Muir, G.A. Sim, *J. Chem. Soc., Dalton. Trans.*, 1976, 1930.

113 G.K. Anderson, R.J. Cross, L. Manojlović-Muir, K.W. Muir, R.A. Wales, *J. Chem. Soc., Dalton. Trans.*, 1979, 684.

114 D. Enders, H. Gielen, J. Runsink, K. Mreuer, S. Brode, K. Boehn, *Eur. J. Inorg. Chem.*, 1998, 913.

115 D.L. Pavia, G.M. Lampmann, G.S. Kriz, *Introduction to Spectroscopy, A Guide for Students in Organic Chemistry*, Second Edition, Saunders College Publishing, Fort Worth, 1996, p. 121.

116 A. Neveling, *M.Sc dissertation*, University of Stellenbosch, 1999, p. 85.

117 M. Iglesias, C. Del Pino, A. Corma, S. García-Blanco, M. Carrera, *Inorg. Chim. Acta*, 1987, **127**, 215.

118 A.S.C. Chan, C. Chen, R. Cao, *Organometallics*, 1997, **16**, 3469.

119 D.L. Pavia, G.M. Lampman, G.S. Kriz, *Introduction to Spectroscopy*, Third Edition, Harcourt College Publishers, United States of America, 2001, p. 125.

120 G. Julius, *M.Sc dissertation*, University of Stellenbosch, 2002, p. 74.

121 A. Pidcock, R.E. Richards, L.M. Venanzi, *J. Chem. Soc. A*, 1966, 1707.

122 T.G. Appleton, H.C. Clark, L.E. Manzer, *Coord. Chem. Rev.*, 1973, **10**, 335.

123 E.W. Abel, S.K. Bhargava, K.G. Orrell, *Prog. Inorg. Chem.*, 1984, **32**, 1.

124 R.A. Sánchez-Delgado, M. Navarro, K. Lazardi, R. Atencio, M. Capparelli, F. Vargas, J.A. Urbina, A. Bouillez, A.F. Noels, D. Masi, *Inorg. Chim. Acta.*, 1998, **275-276**, 528.

125 K.R. Dunbar, S.C. Haefner, *Inorg. Chem.*, 1992, **31**, 3676.

126 A.A. Danopoulos, S. Winston, M.B. Hursthouse, *J. Chem. Soc., Dalton Trans.*, 2002, 3090.

127 M.P. Anderson, L.H. Pignolet, *Inorg. Chem.*, 1981, **20**, 4101.

128 M.J. Burk, J.E. Feaster, W.A. Nugent, R.L. Harlow, *J. Am. Chem. Soc.*, 1993, **115**, 10125.

129 E.S. Raper, *Coord. Chem. Rev.*, 1985, **61**, 115.

130 A. Ceriotti, G. Ciani, A. Sironi, *J. Organomet. Chem.*, 1983, **247**, 345.

131 M.G.L. Petrucci, A.-M. Lebuis, A.K. Kakkar, *Organometallics*, 1998, **17**, 4966.

132 K.-M. Lee, J.C.C. Chen, I.J.B. Lin, *J. Organomet. Chem.*, 2001, **617 – 618**, 364.

133 G. Julius, *M.Sc dissertation*, University of Stellenbosch, 2001, p. 70.

134 Z. Otwinowski, W. Minor, *Methods Enzymol.*, 1997, **276**, 307.

135 G.M. Sheldrick, *SHELX-97*. Program for crystal structure analysis, University of Göttingen, Germany, 1997.

136 L.J. Farrugia, *J. Appl. Cryst.*, 1997, **30**, 565.

Chapter 3

Cobalt complexes as hydroformylation catalysts

1 Introduction

In the early years of hydroformylation the catalysts of choice were cobalt compounds. Subsequently research has revealed that rhodium complexes are much more active catalysts than cobalt complexes and can operate under milder reaction conditions. The technical and economic success of the homogeneous Union Carbide process in 1976 led to the substitution of cobalt complexes with rhodium complexes. In 1995 nearly 80 % of all oxo products were produced using rhodium catalysts, compared to less than 10 % in 1980.[1(See page 211)] Therefore, most of the research during the last two decades has focused on rhodium complexes as catalysts.

The production of detergent alcohols, however, is still catalysed by cobalt complexes because no good alternatives have been found for the hydroformylation of internal, higher alkenes. In recent studies platinum and palladium complexes have shown some promise in the hydroformylation of higher olefins.[2] With the bulk of research focussing on compounds of other metals such as rhodium, iridium, ruthenium, platinum and palladium, we decided to concentrate on cobalt compounds.

Recognising the importance of carbene ligands in catalytic processes today,[3] the preparation and isolation of novel stable cobalt carbene complexes as possible catalysts is one of the objectives of this study. *N*-heterocyclic carbene ligands are also of interest because they are related to ionic liquids that are still seen as promising reaction media for catalysis. The background to the methods used in our quest to prepare stable cobalt carbene complexes will be discussed, a quest that unfortunately proved to be unsuccessful.

2 Cobalt complexes as catalysts in hydroformylation

The technology of cobalt-based processes has remained almost unchanged and a significant amount of oxo products are still produced using cobalt catalysts. The reaction pathway for hydroformylation has still not been clarified in every detail, even after its industrial application for more than 50 years. In 1961 Heck and Breslow formulated the generally accepted hydroformylation cycle for unmodified cobalt catalysts (Figure 3.2.1).[4] Typically, the catalyst is prepared in the reactor by treating finely powdered cobalt or a cobalt(II) salt with synthesis gas.

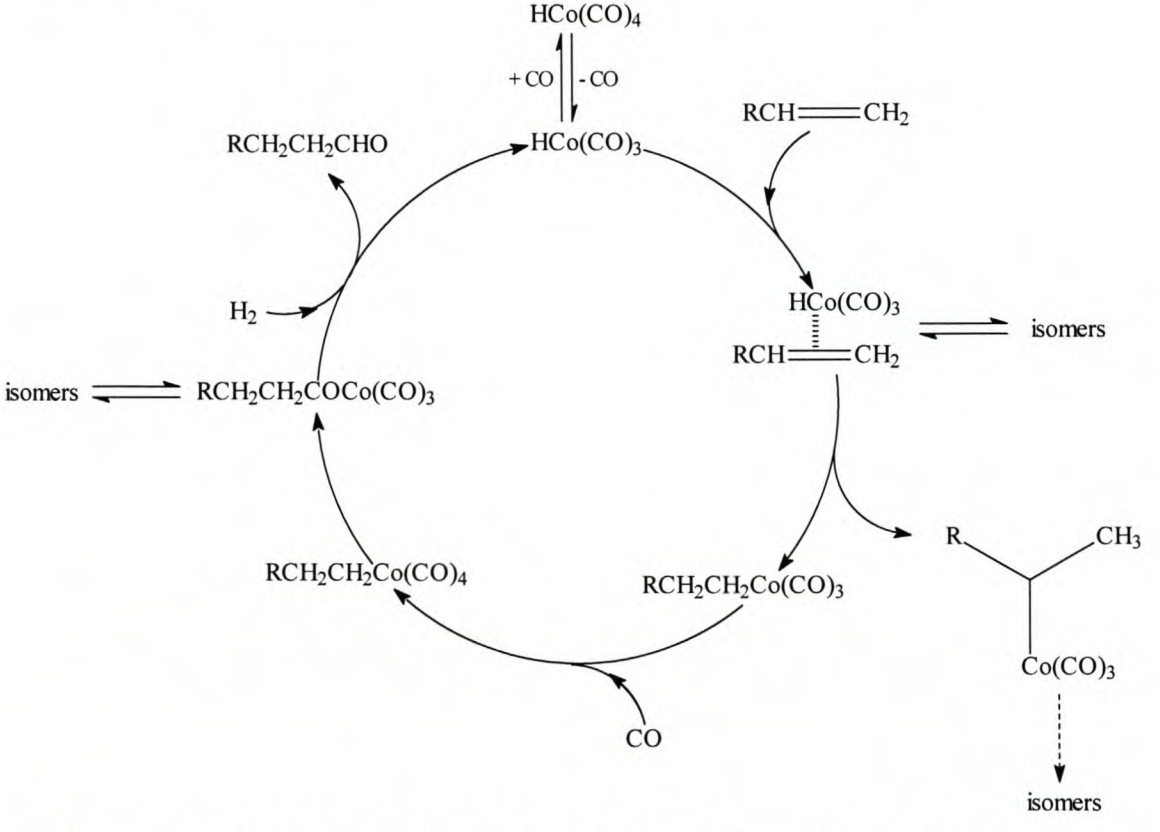

Figure 3.2.1 *Catalytic cycle of hydroformylation with unmodified cobalt catalysts*[5]

The addition of a phosphine ligand to the reaction mixture results in better product selectivity and allows lower pressures to be used.[6] Cobalt carbonyls are poor catalysts for aldehyde hydrogenation. Shell developed and reported the use of PBu_3 as ligand in a process where the alkene hydroformylation and aldehyde hydrogenation are combined.[7] With cobalt carbonyl catalysts, 1-octene is converted to nonanal which then has to be hydrogenated by a separate step using a heterogeneous catalyst. The addition of a trialkylphosphine ligand combines the hydroformylation and hydrogenation reactions satisfactorily. Even though the phosphine-modified catalyst is less active overall, there are various advantages in using these phosphine

pre-catalysts. The activity towards hydrogenation of aldehydes is much higher, the branched to linear ratio is almost twice as high (7:1 compared to 4:1), the catalyst can be used at a lower pressure (100 atmospheres compared to 200-300 atmospheres) and is more stable, thus simplifying catalyst recycling because the alcohols can be distilled from the catalyst.[8]

One aim of this study was to prepare potential cobalt catalysts for biphasic hydroformylation. Biphasic processes have considerable advantages in product separation and catalyst recovery and recycling. The process that was introduced by Ruhrchemie/Rhône-Poulenc (discussed in Chapter 1) and implemented in 1984 utilises a water-soluble rhodium catalyst. One major limitation of this system is the very low conversion rates achieved for branched and internal olefins.[9] The demand for the production of *n*-valeraldehyde is one example of why it is increasingly important to be able to hydroformylate internal olefins. This aldehyde is a precursor for *n*-valeric acid that is the basis of a new ester-type lubricant for CFC substituents in refrigerator systems.[10] Cobalt catalysts are known to hydroformylate internal olefins selectively to linear aldehydes. In 1999 Beller and Krauter reported the first study of cobalt-catalysed biphasic hydroformylation of internal olefins.[10]

A new option is to use ionic liquids in biphasic systems. The application of ionic liquids in hydroformylation reactions has been discussed in Chapter 2. In order for such a system to be successful, the catalyst should remain in the ionic liquid phase. This implies that the ligands must be very soluble in the ionic liquids. Heterocyclic carbene ligands have similar ring structures to the cations in ionic liquids and can provide the solution to the problem of catalyst leaching into the organic phase. Later, in section 4, a brief history of carbene complexes of cobalt is given before we look at other possible routes for preparing heterocyclic carbene complexes.

2.1 Recent application of cobalt in hydroformylation

When discussing homogeneous catalysis, the study of bi- and polymetallic catalysts cannot be ignored. Multinuclear hydroformylation catalysts have been thoroughly studied and some interesting results have been reported recently.[11,12,13,14]

In the previous section we proposed that ionic liquids and carbene ligands could be employed successfully in new biphasic catalytic processes. Recent work by Salzer *et al.* showed that

cobalt complexes like phosphine-substituted cobaltocenium can be used as ligands for rhodium-catalysed hydroformylation in ionic liquids.[15,16,17]

Metallocene derivatives have found widespread use as ligands with phosphine-substituted ferrocenes being used industrially as ligands in enantioselective hydrogenations.[18] The high solubility of cobaltocenium cations in polar solvents led Salzer and co-workers to investigate functionalised cobaltocenium salts as possible ligands for hydroformylation in ionic liquids. The solubility of the phosphinocobaltocenium salts in water was not high enough to allow biphasic catalytic reactions in aqueous systems, and 1-butyl-3-methylimidazolium hexafluorophosphate, [BMIM]PF_6, was chosen as an alternative.

Experiments were done with a variety of phosphine ligands in the rhodium-catalysed hydroformylation of 1-octene. Results obtained by Salzer are shown in Table 3.2.1. The conditions used were a ligand to Rh ratio of 1:2, CO to H_2 ratio of 1:1, stirring time of one hour, reaction temperature of 100 °C, pressure of 10 bar, and a 1-octene to Rh ratio of 1000:1. The catalyst was prepared *in situ* by mixing $Rh(CO)_2(acac)$ with the cobaltocenium ligand in 5 ml of [BMIM]PF_6 for one hour at room temperature thus yielding a rhodium carbene compound.

Table 3.2.1 *Comparison of different phosphine ligands in the hydroformylation of 1-octene*

Ligand	TOF (h^{-1})	*n/iso*	S (*n*-aldehyde) %[a]
PPh_3	426	2.6	72
TPPTS	98	2.6	72
dppe	35	3.0	75
dppf	828	3.8	79
cobaltocenium salt **1**[b]	66	2.6	73
cobaltocenium salt **2**[c]	810	16.2	94

[a] *S (n-aldehyde) % = selectivity to n-nonanal in the product*

[b,c] *Cobaltocenium salt **1** and **2** are shown in Figure 3.2.2*

The two different cobaltocenium salts that were used are shown in Figure 3.2.2. Only with these two ligands does the reaction take place exclusively in the ionic liquid phase. Quantitative rhodium analysis of the organic layer revealed rhodium leaching of less than

0.2 %. Furthermore, no rhodium or cobalt decomposition was found on the reactor walls when these ligands were used. This work demonstrates the importance of choosing the right ligands to prevent catalyst leaching.

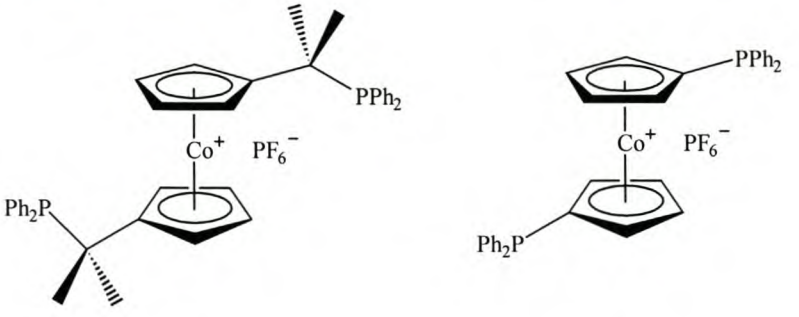

1 **2**

Figure 3.2.2 *1,1′-Bis(diphenylphosphino)cobaltocenium hexafluorophosphate*

3 Ligands in hydroformylation

As far as industrial application of hydroformylation with cobalt complexes are concerned, the only classes of ligands used are phosphines, triphenylphosphine oxide and, in some cases, phosphites.[19] Lower reaction rates in the oxo reaction are achieved by using nitrogen donor ligands, such as amines, amides and isonitriles, because of their stronger coordination to the metal centre. Other heteroatom-containing ligands have been tested for use in hydroformylation but their performances are without exception not as good as that of phosphines.[20] Carbene ligands were introduced into hydroformylation catalysts by Hermann in 1995,[21,22,23,24] but all the published results have been obtained with rhodium complexes. The different ligands currently in use for hydroformylation have been discussed in detail in Chapter 1.

4 The quest for a stable cobalt carbene complex

E.O. Fischer introduced carbenes to organometallic chemistry in 1964.[25] Since this discovery there has been an increasing interest in the preparation, structure and reactivity of transition metal carbene complexes. During the first decades after their introduction many structural and theoretical aspects of carbene complexes were investigated.[26] However, during the last ten years research has focussed very much on the possible applications of carbene complexes.[27,28] The similarity between *N*-heterocyclic carbenes and phosphines as ligands, discussed in

Chapters 1 and 2, and the importance of phosphine ligands in catalytic processes, makes the quest for stable cobalt carbene complexes a project with good potential. Unfortunately only relatively few cobalt carbene complexes are known. Therefore, new synthetic methods have to be developed to prepare novel cobalt carbene complexes.

4.1 Cobalt carbene complexes

The isolation and characterisation of the first cobalt carbene complex was reported by Darensbourg and Darensbourg in 1970.[29] These scientists used the same preparative method as the one introduced by Fischer in 1964.[25] The addition of phenyllithium to respectively $[(Ph_3Sn)Co(CO)_4]$ or $[(Ph_3Pb)Co(CO)_4]$ followed by alkylation led to the isolation of the Fischer-type carbene complex $[(Ph_3Sn)Co(CO)_3(C\{OEt\}Ph)]$ as a stable yellow solid with a relatively high melting point of 122 – 124 °C and the corresponding lead complex $[(Ph_3Pb)Co(CO)_3(C\{OEt\}Ph)]$ which is unstable when exposed to air or heat. A crystal structure of a similar tin-cobalt compound $[(Ph_3Sn)Co(CO)_2(PMe_3)(C\{OEt\}NPh_2)]$ was published in 1988, the yellow compound being obtained in a yield of 75 %.[30]

In these complexes the triphenyltin and triphenyllead ligands help to stabilise the Co-$C_{carbene}$ bond. At the latter part of the 1970's Corriu and co-workers published the synthesis and characterisation of Fischer-type cobalt carbene complexes with a triphenyl germyl ligand, employing similar preparative procedures to Darensbourg and Darensbourg.[31,32,33,34] The metal-metal interaction plays a significant role in stabilising the bond between the cobalt and the carbene carbon. The germyl ligand is not only a good σ-donor, but also a good π-acceptor, as demonstrated in the study of infrared spectra by Graham and co-workers. An increase in the π-backbonding to germanium occurs at the expense of π-backbonding to carbon monoxide.[35] This is shown schematically in Figure 3.4.1. As a result the carbon monoxide carbon is susceptible to nucleophilic attack. The metal-metal interaction between tin or lead and cobalt has the same effect.

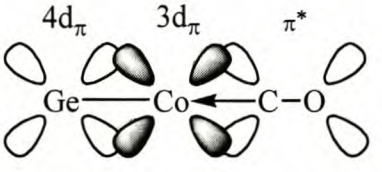

Figure 3.4.1 *Illustration showing the π-interactions of Ge and the carbonyl ligand with the central Co atom*

Work by E.O. Fischer and co-workers introduced the nitrosyl ligand to stabilise the metal-carbene bond.[36,37] The stoichiometric reaction between $[(CO)_3Co(NO)]$ and LiR (R = NHMe, NMe_2 or NEt_2) followed by alkylation yielded orange or red cobalt carbene complexes such as $[Co(CO)_2(NO)(C\{OEt\}NHMe)]$. However, the yields obtained were low, varying from 15 to 30 %.

Lappert and Pye reported the first cobalt carbene complexes with heterocyclic Öfele-type carbene ligands in 1977.[38] Electron-rich olefins such as $[:\overline{CN(R)CH_2CH_2NR}]_2$ (R = Me, Et) were used to replace one or two carbonyl ligands of $[(CO)_3Co(NO)]$ to obtain thermally stable neutral mono- and biscarbene complexes. The complexes were obtained in yields of 80 to 90 %, which are significantly higher than those reported by Fischer. Lappert extended this work and also published the crystal structure of $[Co(NO)(CO)\{=\overline{CN(Me)CH(Me)CH_2N}(Me)\}(PPh_3)]$ in 1983.[39,40]

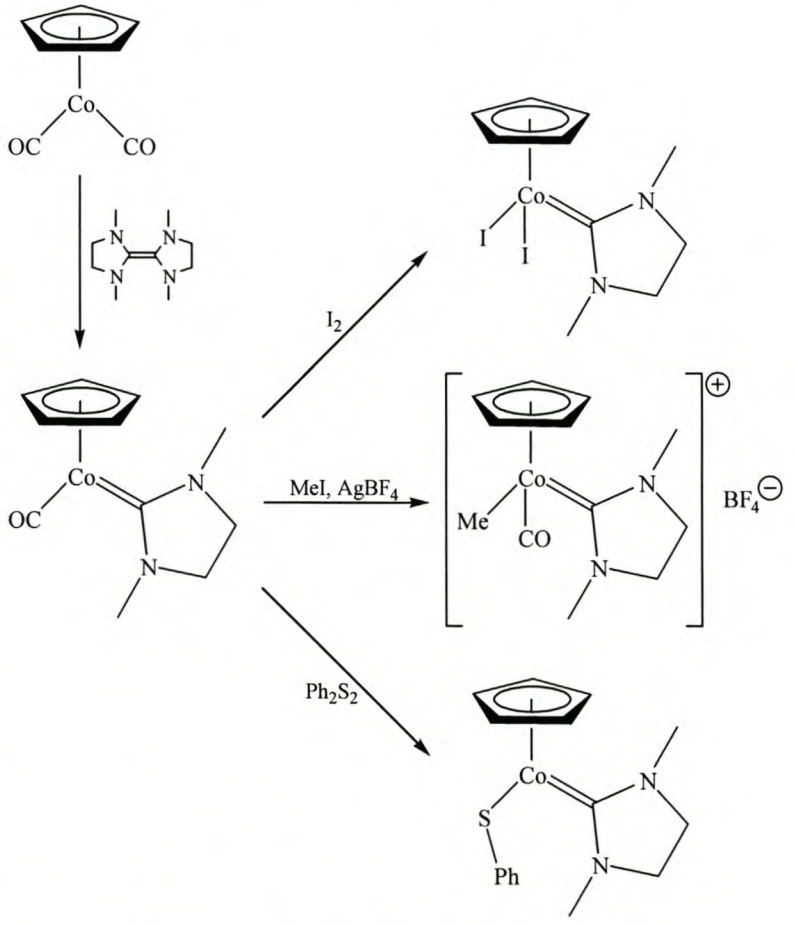

Figure 3.4.2 *Cyclopentadienyl cobalt carbene complexes prepared by Macomber and Rodgers*[41]

The cyclopentadienyl ligand can also play a significant role in stabilising a cobalt carbene complex due to the possibility of charge distribution onto the ring system. Macomber and Rodgers prepared the first mononuclear cyclopentadienyl cobalt carbene complexes.[41] A range of complexes were prepared by boiling a solution of $CpCo(CO)_2$ and the electron rich olefin bis(1,3-dimethyl-2,3,4,5-tetrahydro-1*H*-imidazol-2-ylidene) in methylcyclohexane and doing oxidative addition reactions with different substrates (Figure 3.4.2). Dinuclear cyclopentadienyl cobalt carbene complexes in which the carbene ligand is stabilised as a bridging ligand have also been reported.[42,43]

Other cobalt carbene complexes with cyclopentadienyl ligand systems have been prepared. One example is the coupling reaction of Cp_2Zr(butadiene) with $CpCo(CO)_2$ that yielded the metallacyclic Fischer-type carbene complex $[Cp_2\overline{Zr(C_4H_6)(OC=)}Co(CO)Cp]$.[44] A free *N*-heterocyclic carbene has been used recently to prepare a cyclopentadienyl cobalt carbene complex *via* a ligand exchange reaction.[45]

4.2 Possible preparation methods

A wide range of methods is known for the synthesis of transition metal carbene complexes. A variety of synthetic methods as well as structural data and reactivity information have been the subjects of recent reviews about stable carbene complexes.[46,47]

In this study the focus falls on *N*-heterocyclic carbene ligands because of our interest in ionic liquids as solvents for catalysis. The first researchers to report complexes with *N*-heterocyclic carbene ligands were Öfele[48] and Wanzlick.[49] During the course of this investigation Arduengo-type *N*-heterocyclic carbene ligands and transmetallation reactions were used in the pursuit of the synthesis of new cobalt carbene complexes. A brief discussion on possible synthetic methods appears in sections 4.2.1 and 4.2.2.

4.2.1 Arduengo-type carbenes

The isolation of stable free carbenes opened the way to facile synthetic methods in which transition metal carbene complexes could be prepared by substitution. From the earlier discussion in Chapter 1 it is known that the characteristics of free carbenes are very similar to those of phosphines. The similarity between these two types of ligands leads to the question

whether *N*-heterocyclic free carbenes can be used to prepare carbene compounds similar to the known catalytically active cobalt phosphine complexes.[50] Research by Herrmann *et al.* showed that 2,3-dihydro-1*H*-imidazol-2-ylidene ligands coordinate to transition metals of low and high oxidation states.[51,52,53] Nucleophilic *N*-heterocyclic carbenes can replace other ligands such as carbon monoxide,[54] phosphines[55] or halides[56] and show a high tendency toward complexation.[57,58] Free carbenes can substitute one or more carbon monoxide ligands in carbonyl complexes such as $Cr(CO)_6$, $W(CO)_6$, $Fe(CO)_5$, and $Ni(CO)_4$.[57,59,60,61]

In 1968 Manning published the preparation of a number of cobalt carbonyl derivatives of the type $[Co(CO)_3L]_2$ (L = PEt_3, PBu_3, PPh_3, PMe_2Ph, PEt_2Ph, $P(OMe)_3$, or $P(OPh)_3$).[62] These complexes, which reportedly decompose slowly in solution, were prepared by gently refluxing a benzene solution of $Co_2(CO)_8$ and the phosphine ligand. Toluene was used in later studies.[63]

Taking all this information into consideration it seemed feasible to prepare disubstituted carbene cobalt complexes, analogues of $Co_2(CO)_6(PR_3)_2$, by the reaction of free carbenes with $Co_2(CO)_8$.

4.2.2 Transmetallation reactions

Another method of synthesising carbene complexes is *via* a transmetallation of a lithiated thiazole followed by alkylation or protonation. Utilising this method we attempted to prepare Co(I) carbene complexes. Co(II) species are often used as precursor compounds in hydroformylation reactions. According to suggested reaction steps the Co(II) species is converted to a Co(I) species,[64] the precursor to the proposed active catalyst.

The synthesis of carbene complexes through transmetallation has been used extensively in our group for a variety of transition metals. Recently some manganese thiazolyl complexes were isolated and characterised.[65] The reaction scheme showing two different transmetallation reactions and the subsequent alkylation or protonation are shown in Figure 3.4.3.

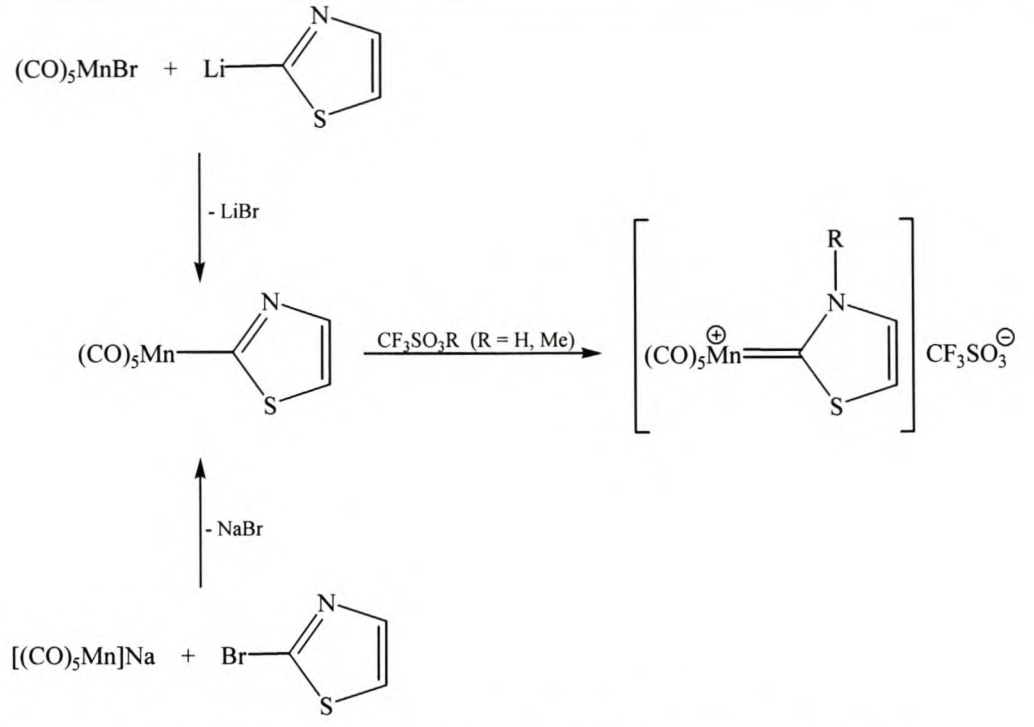

Figure 3.4.3 *Transmetallation followed by alkylation or protonation yields manganese carbene complexes*

During the last decade similar complexes of iron,[66,67,68] tungsten[69] and gold[70] were prepared. The formation of a lithium halide salt acts as the driving force for the transmetallation reactions. The azolyl intermediates of manganese, iron and gold were isolated.

It is also important to consider transmetallation reactions involving cobalt. Compounds similar to alkyltetracarbonylcobalt $[Co(CO)_4R]$ are important intermediates in the hydroformylation reaction. Therefore, many studies have been carried out on Co(I)-R compounds. Studies on the tetracarbonyl compounds are complicated by their general instability and tendency to transform to the acyl compounds $[Co(CO)_4(COR)]$.[71] These compounds are often characterised as the more stable phosphine substituted acyl complexes $[Co(CO)_3(COR)(PR_3)]$.[72]

More than one method for the preparation of alkyltetracarbonylcobalt compounds, and derivatives thereof, are known. Ligand exchange reactions also yield Co(I)-R complexes.[73] However, the focal point of our study was to use the transmetallation reaction. A few examples found in the literature are summarised in the Table 3.4.1.

An aryl cobalt complex has been synthesised and characterised, indicating that it is feasible to attempt the preparation of a pseudo-aromatic thiazolyl cobalt complex, an intermediate in the preparation of a carbene complex.

Table 3.4.1 *Preparation of some organocobalt(I) carbonyl compounds*

Compound	Preparation
$[CoMe(CO)_4]$[74]	MeI + $Na[Co(CO)_4]$
$[CoEt(CO)_4]$[74]	$Et_3O^+BF_4^-$ + $Na[Co(CO)_4)]$
$[Co(CH_2Ph)(CO)_3]$[74]	$PhCH_2Br$ + $Na[Co(CO)_4)]$
$[CoMe(CO)_3(PPh_3)]$[75]	MeI + $Na[Co(CO)_3(PPh_3)]$
$[CoMe(CO)_3\{P(OPh)_3\}]$[75]	MeI + $Na[Co(CO)_3\{P(OPh)_3\}]$
$[CoMe(CO)_3L]$[a, 76]	MeI + $Na[Co(CO)_3L]$
$[CoMe(CO)_2L_2]$[a, 76]	MeI + $Na[Co(CO)_2L_2]$
$[CoMe(CO)L_3]$[a, 76]	MeI + $Na[Co(CO)L_3]$
$[CoMe(CO)_2\{P(OMe)_3\}_2]$[76]	MeI + $Na[Co(CO)_2\{P(OMe)_2\}]$
$[Co(CH_2CN)(CO)_3(PPh_3)]$[77]	$ClCH_2CN$ + $Na[Co(CO)_4]$ + PPh_3
$[CoPh(CO)_3(PPh_3)]$[78]	$[CoBr(CO)_3(PPh_3)]$ + PhLi
$[Co\{p\text{-}(CH_3)_3CC_6H_4CH_2\}(CO)_3(PPh_3)]$[72]	$\{p\text{-}(CH_3)_3CC_6H_4CH_2\}Cl$ + $Na[Co(CO)_4]$ + PPh_3

[a] L = $MeCH_2C(CH_2O)_3P$

5 Aims of this study

The main aim of this part of the study was to prepare novel cobalt carbene complexes that could be used as possible catalysts in the hydroformylation of α-olefins. A secondary goal was to employ these complexes in ionic liquids and carry out biphasic hydroformylation reactions utilising such ionic liquid systems.

N-heterocyclic carbenes have properties similar to those of phosphines. Utilising Arduengo-type carbenes instead of phosphines, the aim was to prepare complexes of the type

$[Co(CO)_3(NHC)]_2$ (NHC = *N*-heterocyclic carbene), related to complexes prepared by Manning.[62]

Alkyl- and aryl complexes of cobalt can be prepared utilising transmetallation reactions. It has also been shown that carbene complexes of various transition metals can be isolated after consecutive transmetallation and alkylation. Such alternative preparation of carbene complexes of cobalt (*via* transmetallation) was also planned.

6 Results and discussion

In the following section the various synthetic methods used and the results that were obtained are described. The synthetic work mainly involved the two reaction routes mentioned above.

6.1 Utilisation of free Arduengo type carbenes instead of phosphines

Free carbenes were used in attempt to prepare biscarbene cobalt complexes similar to the dinuclear cobalt phosphine complexes which have been used as catalysts in hydroformylation reactions.

Depending on reaction conditions, the reaction between octacarbonyldicobalt and phosphine ligands gives either $[Co_2(CO)_7(PR_3)]$, $[Co(CO)PR_3]_2$ or $[Co(CO)_3(PR_3)_2][Co(CO)_4]$. During the course of this work the method used by Manning to prepare complexes of the type $[Co(CO)PR_3]_2$ was modified in an attempt to prepare complexes of the type $[Co(CO)_3(NHC)]_2$ (NHC = *N*-heterocyclic carbene).

In all the reactions a $Co_2(CO)_8$ to free carbene ratio of 1:2 was used for the reactions. Toluene, benzene or THF were used as solvents. Reactions were performed at either room temperature or at 0 °C. Very fast colour changes were observed for all the reactions. All the products obtained were oily substances. Efforts to purify the complexes by flash chromatography proved to be fruitless, as did extraction with different solvents. The products remained oily. The *N*-substituents on the carbene ligands can have an influence on the properties of the products. This is illustrated by the different properties of the rhodium complexes **6** and **7** (Chapter 2), the former being a microcrystalline solid and the latter an oil-like substance.

Therefore, a range of different free carbenes was used to prepare the cobalt carbene complexes (Figure 3.6.1). Complexes **32** to **36** were prepared by the reaction of $Co_2(CO)_8$ with carbenes **A**, **B**,[79] **C**, **D** or **E**[80] respectively.

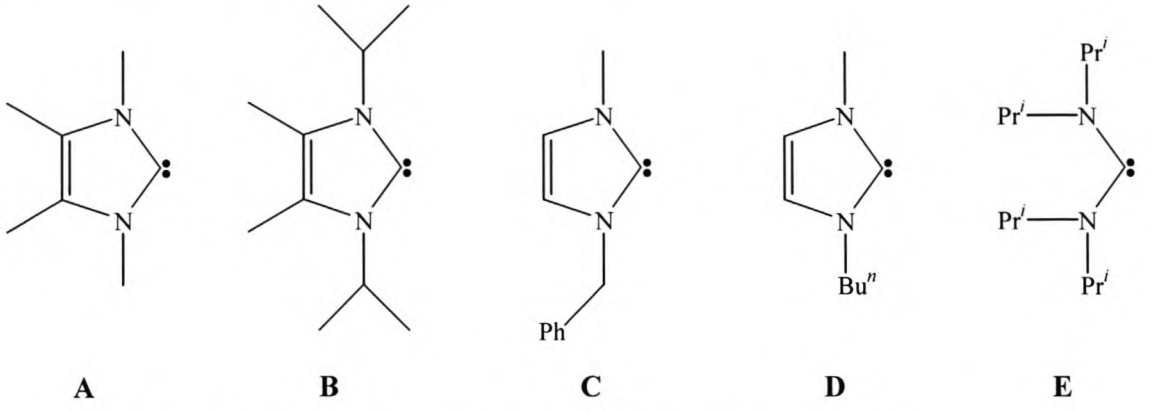

Figure 3.6.1 *The five free carbenes used to prepare Co carbene complexes*

IR studies of the products were very promising indicating that the desired complexes had formed. The complexes proved to be extremely unstable when exposed to air as well as in solution, rendering NMR studies almost impossible. The proton NMR spectrum of one complex (**36**) was obtained, but no ^{13}C NMR spectrum as the complex decomposed too quickly in solution. In Table 3.6.1 the IR absorption bands observed for known phosphine complexes of the type $[Co(CO)_3L]_2$ as well as those observed for complexes **32** to **36** are summarised.

Table 3.6.1 *IR absorption bands of $[Co(CO)_3L]_2$ complexes in solution*

Complex	ν(CO) / cm^{-1}
$[Co(CO)_3(PPh_3)]_2$	1957[a], 1955.1[b]
$[Co(CO)_3(PBu_3)]_2$	1951[a], 1941.9[b]
32	1888.3[b]
33	1888.8[b]
34	1888.8[b]
35	1889.7[b]
36	1888.3[b]

[a] *$CHCl_3$,* [b] *CH_2Cl_2*

All the carbene complexes showed one strong, broad band in the IR spectrum, which is similar to what is seen for the corresponding phosphine complexes. The difference in the frequencies can be attributed to less π-backbonding for the carbene ligands compared to the phosphine ligands, leading to a larger $\sigma_{donor}/\pi_{acceptor}$-ratio. Thus, the carbonyl ligands have to accommodate the extra electron density, which is indicated in the infrared spectrum by ν(CO) shifting to a lower value.

The peaks observed in the EI MS spectra were also not identifiable as fragments of carbene complexes of cobalt.

6.2 Transmetallation reactions

Two methods were used to prepare cobalt carbene complexes *via* transmetallation. In the first reaction route $[Co(CO)_4]Na$ was reacted with 2-bromothiazole, 2-chlorobenzothiazole or 2-bromopyridine. The second method involves the reaction of thiazolyllithium with one of three cobalt complexes: $[CoI(CO)_2(PPh_3)_2]$, $[CoI(PPh_3)_3]$ or $[CoI(CO)(PPh_3)_3]$.

$[Co(CO)_4]Na$ can be prepared by reducing $Co_2(CO)_8$ with Na/Hg in diethyl ether[72] or by reacting $Co_2(CO)_8$ with NaOH in a THF solution.[81] $[CoI(CO)_2(PPh_3)_2]$,[82,83] $[CoI(PPh_3)_3]$[84] and $[CoI(CO)(PPh_3)_3]$[85,86] were prepared using published procedures.

Attempts to isolate the intermediate thiazolyl complexes proved futile. Triphenylphosphine was added to the reaction mixture in an attempt to stabilise the intermediate complexes. Unfortunately this also proved to be fruitless. When it became clear that the intermediate complexes could not be isolated, *in situ* protonation or alkylation was attempted in an effort to prepare the carbene complex. Various different reaction routes and starting complexes were used under different reaction conditions; none of the isolated complexes were carbene complexes but rather completely different from what was expected. The reaction routes and isolated products of two such reactions are shown in Figure 3.6.2 and Figure 3.6.3. Only the complexes that were isolated as crystals from the reaction mixtures are shown in the figures. The crystal structures of these complexes are discussed later (section 6.4).

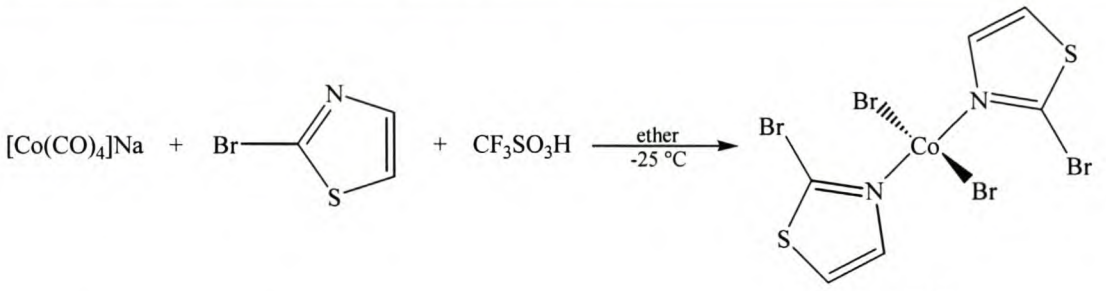

37

Figure 3.6.2 *Unexpected Co(II) complex isolated from the reaction mixture*

Complex **37** was formed from the reaction of $[Co(CO)_4]Na$ with bromothiazole in ether at room temperature. After three hours of stirring the mixture was cooled to –25 °C. The addition of the CF_3SO_3H led to the formation of a green precipitate. Continued bubbling signified the loss of the carbonyl ligands. This reaction mixture was then stirred overnight. The precipitate that formed was filtered off and the green solution dried *in vacuo* and then dissolved in methylene chloride. A second pink precipitate was also filtered off. Complex **37** crystallised as blue crystals from this green methylene chloride solution. In the EI MS spectrum of **37** the only fragments observed are cations of bromothiazole, bromine atoms and cobalt.

The addition of bromothiazole to $[Co(CO)_4]Na$ in THF, followed two hours later by the addition of triphenylphosphine and 16 hours later with CF_3SO_3H subsequently afforded **38** and **39** (Figure 3.6.3). The reaction mixture was filtered and the green solution dried *in vacuo*, dissolved in methylene chloride and layered with hexane. Complex **38** was isolated as blue crystals from this solution and complex **39** as pink crystals. In the EI MS spectrum of **38** only Br and $OPPh_3$ and its fragments are observed, while free thiazole, CF_3SO_3, and $OPPh_3$ and its fragments are observed in the EI MS spectrum of **39**.

Although stringent inert reaction conditions were employed, the isolated complexes show that sufficient water was still available to crystallise with the cobalt complexes.

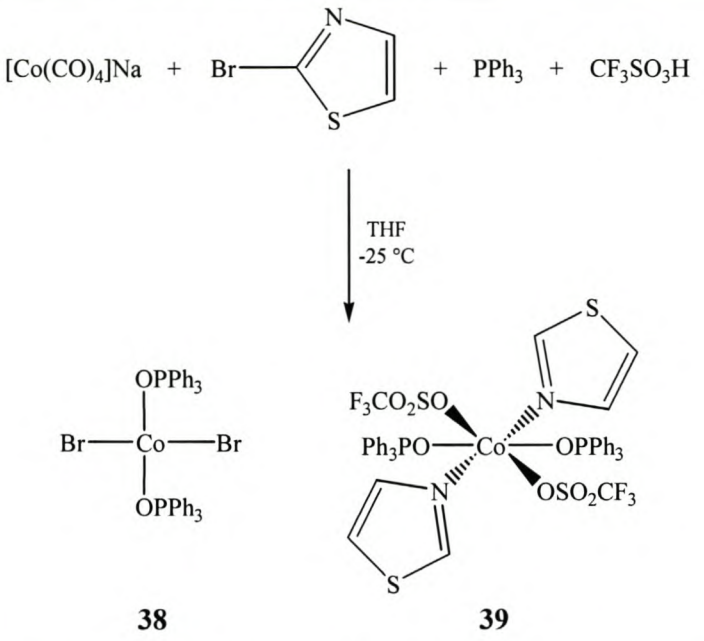

38 **39**

Figure 3.6.3 *Two different Co(II) complexes isolated from one reaction mixture*

6.3 Other

Other methods were also explored in the quest to prepare cobalt carbene complexes. Mestroni and co-workers prepared the active hydroformylation catalyst $[Co(bipyridine)(CO)_2]_2$ from $CoCl_2.6H_2O$, bipyridine and $NaBH_4$ in a CO atmosphere.[87] To establish whether such a method is viable for carbene synthesis, PPh_3 was used as substitution ligand. This led to the formation of $[CoH(CO)(PPh_3)_3]$ (**40**), despite the fact that much less $NaBH_4$ was used than in the published procedure.[88] Complex **40** was isolated as orange crystals from a diethyl ether solution layered with hexane. The hydride was clearly observed in the ^1H NMR spectrum at δ –12.52 (in CD_2Cl_2). Due to this result, the preparation of a carbene complex along the same route was abandoned.

angle reported in the abovementioned complexes. All the bond angles around the Co atom are close to 90° (see Table 3.6.4).

Table 3.6.4 *Selected bond distances (Å) and bond angles (°) for complex* ***39***

Bond lengths (Å)		Bond angles (°)	
		O1-Co1-O1′	180.000(1)
		O1-Co1-N1	90.83(11)
		O1-Co1-N1′	89.17(11)
		O1-Co1-O2	89.12(10)
		O1-Co1-O2′	90.88(10)
Co1-N1	2.114(3)	O1′-Co1-N1′	90.83(11)
Co1-O1	2.051(2)	O1′-Co1-N1	89.17(11)
Co1-O2	2.204(2)	O1′-Co1-O2	90.88(10)
O1-P1	1.498(3)	O1′-Co1-O2′	89.12(10)
O2-S1	1.456(3)	O2-Co1-O2′	180.000(1)
S1-O3	1.443(3)	O2-Co1-N1	88.78(11)
S1-O4	1.437(3)	O2-Co1-N1′	91.22(11)
		O2′-Co1-N1	88.78(11)
		O2′-Co1-N1′	91.22(11)
		N1-Co1-N1′	180.000(1)
		Co1-O1-P1	152.50(17)
		Co1-O2-S1	139.78(16)

6.4.4 *[CoH(CO)(PPh$_3$)$_3$]* (40)

The molecular structure of complex **40** is shown in Figure 3.6.9. Selected bond lengths and bond angles are summarised in Table 3.6.5. The central Co atom is surrounded by 5 ligands. The molecule has a trigonal bipyrimidal geometry. Two ether molecules crystallise with every molecule of **40**. A crystal structure determination of this compound has been carried out before,[88,93] but the packing of the molecules in the unit cell and the contents of the unit cell in the crystal is different from that in the reported complexes.

Table 3.6.5 *Selected bond distances (Å) and bond angles (°) for complex* ***40***

Bond lengths (Å)		Bond angles (°)	
Co1-C1	1.739(3)		
Co1-P1	2.1752(8)		
Co1-P2	2.1643(8)	C1-Co1-H1	174.1(11)
Co1-P3	2.1861(8)	C1-Co1-P1	97.83(10)
Co1-H1	1.31(2)	C1-Co1-P2	100.55(10)
C1-O1	1.163(3)	C1-Co1-P3	96.46(9)
P1-C111	1.843(3)	P1-Co1-H1	80.4(11)
P2-C121	1.841(3)	P1-Co1-P2	120.48(3)
P3-C131	1.849(3)	P1-Co1-P3	112.34(3)
P1-C211	1.843(3)	P2-Co1-H1	75.8(11)
P2-C221	1.850(3)	P2-Co1-P3	120.94(3)
P3-C231	1.837(3)	P3-Co1-H1	89.5(11)
P1-C311	1.848(3)	Co1-C1-O1	178.8(3)
P2-C321	1.847(3)		
P3-C331	1.848(3)		

Figure 3.6.10 shows the molecules of **40** in a unit cell. Two layers of cobalt molecules lie alternating with a layer of ether molecules sandwiched in between. There seems to be no pi-stacking between the two layers of cobalt molecules lying next to each other.

Table 3.6.6 *Crystallographic data for complex **37** and complex **38***

Complex	**37**	**38**
Chemical Formula	$C_6H_4Br_4CoN_2S_2$	$C_{36}H_{30}Br_2CoO_2P_2$, $2(C_1H_2Cl_2)$
MW (g/mol)	546.80	945.14
Crystal system	Orthorhombic	Orthorhombic
Space group	Pbcn	Pna
a (Å)	9.4010 (3)	16.6434 (5)
b (Å)	10.7737 (4)	16.5063 (3)
c (Å)	13.2321 (6)	14.7900 (3)
α (°)	90.00	90.00
β (°)	90.00	90.00
γ (°)	90.00	90.00
Volume (Å^3)	1340.19 (9)	4063.12 (15)
Z	4	4
d_{calcd} (g/cm^3)	2.260	0.687
Temp (K)	173 (2)	173 (2)
μ (cm^{-1})	4.634	0.594
θ (°)	$1.02 \leq \theta \leq 27.48$	$1.74 \leq \theta \leq 25.00$
Radiation	Mo Kα, graphite monochromated	Mo Kα, graphite monochromated
Crystal size (mm)	0.37 × 0.35 × 0.32	0.33 × 0.25 × 0.18
Index range	$-12 \leq h \leq 12$ $-13 \leq k \leq 13$ $-16 \leq l \leq 17$	$-19 \leq h \leq 12$ $-19 \leq k \leq -19$ $-17 \leq l \leq 17$
Number of reflections collected	5444	15327
Number of reflections used	1602	4033
Refinement	Full matrix on F^2 (SHELXL)	Full matrix on F^2 (SHELXL)
Parameters	70	470
R_1 ($F_o > 2\sigma F_o$)	0.0316	0.0467
wR_2 (all data)	0.0681	0.0950

Table 3.6.7 *Crystallographic data for complex* ***39*** *and complex* ***40***

Complex	**39**	**40**
Chemical Formula	-	$C_{118}H_{112}Co_2O_4P_6$
MW (g/mol)	-	1897.76
Crystal system	-	Monoclinic
Space group	-	C2/c
a (Å)	9.4465 (2)	41.6022 (12)
b (Å)	11.6083 (3)	11.2063 (3)
c (Å)	13.3543 (3)	21.8220 (7)
α (°)	112.5250 (10)	90.00
β (°)	101.1970 (1)	103.816 (2)
γ (°)	103.2820 (10)	90.00
Volume (Å^3)	1249.96 (5)	9879.2 (5)
Z	8	4
d_{calcd} (g/cm^3)	1.691	1.276
Temp (K)	293 (2)	173 (2)
μ (cm^{-1})	1.367	0.487
θ (°)	$1.74 \leq \theta \leq 25.00$	$1.00 \leq \theta \leq 25.35$
Radiation	Mo Kα, graphite monochromated	Mo Kα, graphite monochromated
Crystal size (mm)	-	$0.27 \times 0.24 \times 0.21$
Index range	$-11 \leq h \leq 9$ $-13 \leq k \leq 13$ $-15 \leq l \leq 15$	$-49 \leq h \leq 49$ $-13 \leq k \leq -13$ $-25 \leq l \leq 25$
Number of reflections collected	10624	24947
Number of reflections used	4321	9202
Refinement	Full matrix on F^2 (SHELXL)	Full matrix on F^2 (SHELXL)
Parameters	322	592
R_1 ($F_o > 2\sigma F_o$)	0.0523	0.0442
wR_2 (all data)	0.1493	0.0916

7 Summary and conclusion

The IR spectra of the bimetallic products seem to indicate that carbene complexes of cobalt compounds formed. They are, however, unstable and attempts to stabilise the complexes with alkyne or phosphine ligands were unsuccessful.

The attempted preparation of carbene complexes utilising the transmetallation reaction was also unsuccessful. It appears as if the inert conditions used were insufficient. The very stringent inert conditions used in lanthanide chemistry might provide a solution to the problems experienced during the attempts to isolate and characterise cobalt(I) carbene complexes. Another possible solution to the problems experienced is to use ligands like the germyl ligand (Ph_3Ge) as a stabilising ligand (Figure 3.4.1).

8 References

1 M. Beller, B. Cornils, C.D. Frohning, C.W. Kohlpainter, *J. Mol. Cat. A*, 1995, **104**, 17.

2 P.W.N.M. van Leeuwen, in *Rhodium catalysed Hydroformylation*, Eds. P.W.N.M. van Leeuwen, C. Claver, Kluwer Academic Publishers, Dordrecht, 2000, p. 7.

3 W.A. Herrmann, *Angew. Chem., Int. Ed. Engl.*, 2002, **41**, 1290.

4 R.F. Heck, D.S. Breslow, *J. Am. Chem. Soc.*, 1961, **83**, 4023.

5 C.D. Frohning, C.W. Kohlpainter, in *Applied Homogeneous Catalysis with Organometallic Compounds*, Eds. W.A. Herrmann, B. Cornils, Wiley-VCH, Weinheim, 1996, Vol. 1, p. 45.

6 F.E. Paulik, *Catal. Rev.*, 1972, **6**, 49.

7 L.H. Slaugh, R.D. Mullineaux, U.S. Patents 3,239,569 and 3,239,570, 1966, Shell.

8 G.W. Parshall, S.D. Ittel, in *Homogeneous Catalysis*, *Second Edition*, John Wiley & Sons, Inc., New York, 1992, p. 108.

9 H. Bahrmann, S. Bogdanovic, in *Aqueous-Phase Organometallic Catalysis – Concepts and Applications*, Eds. W.A. Herrmann, B. Cornils, Wiley-VCH, Weinheim, 1998, p. 306.

10 M. Beller, J.G.E. Krauter, *J. Mol. Cat. A*, 1999, **143**, 31.

11 S.A. Laneman, F.R. Fronczek, G.G. Stanley, *J. Am. Chem. Soc.*, 1988, **110**, 5585.

12 S.A. Laneman, G.G. Stanley, *Adv. Chem. Ser.*, 1992, **230**, 349.

13 M.E. Broussard, B. Juma, S.G. Train, W.-J. Peng, S.A. Laneman, G.G. Stanley, *Science*, 1993, **260**, 1784.

14 G. Süss-Fink, *Angew. Chem., Int. Ed. Engl.*, 1994, **106**, 71.

15 C.C. Brasse, U. Englert, A. Salzer, H. Waffenschmidt, P. Wasserscheid, *Organometallics*, 2000, **19**, 3818.

16 A. Salzer, B. C. Brasse, German patent DE 19742904 C, Celanese GMBH, 1999.

17 H. Bahrmann, S. Salzer, C. Brasse, German patent DE 19742907 A, Celanese GMBH, 1999

18 R.R. Bader, P. Baumeister, H.U. Blaser, *Chimia*, 1996, **50**, 99.

19 C.D. Frohning, C.W. Kohlpainter, in *Applied Homogeneous Catalysis with Organometallic Compounds*, Eds. W.A. Herrmann, B. Cornils, Wiley-VCH, Weinheim, 1996, Vol. 1, p. 34.

20 B. Cornils, in *New Synthesis with Carbon Monoxide*, Ed. J. Falbe, Springer, Berlin, 1980, Chapter 1.

21 W.A. Herrmann, M. Elison, C. Köcher, J. Fischer, K. Öfele, German Patent DE 4.447.066, 1995, Hoechst AG.

22 W.A. Herrmann, M. Elison, C. Köcher, J. Fischer, German Patent DE 4.447.067, 1995, Hoechst AG.

23 W.A. Herrmann, M. Elison, C. Köcher, J. Fischer, German Patent DE 4.447.068, 1995, Hoechst AG.

24 W.A. Herrmann, German Patent DE 4.447.070, 1995, Hoechst AG.

25 E.O. Fischer, A. Maasböl, *Angew. Chem., Int. Ed. Engl.*, 1964, **3**, 580.

26 H.W. Wanzlick, *Angew. Chem., Int. Ed. Engl.*, 1962, **2**, 75.

27 W.A. Herrmann, C. Köcher, *Angew. Chem., Int. Ed. Engl.*, 1997, **36**, 2162.

28 W.A. Herrmann, *Angew. Chem., Int. Ed.*, 2002, **41**, 1290.

29 D.J. Darensbourg, M.Y. Darensbourg, *Inorg. Chem.*, 1970, **9**, 1691.

30 A.C. Filippou, E. Herdtweck, H.G. Alt, *J. Organomet. Chem.*, 1988, **355**, 437.

31 E. Colomer, R.J.P. Corriu, *J. Chem. Soc., Chem. Comm.*, 1976, 176.

32 E. Colomer, R.J.P. Corriu, *J. Organomet. Chem.*, 1977, **133**, 159.

33 E. Colomer, R.J.P. Corriu, J.C. Young, *J. Chem. Soc., Chem. Comm.*, 1977, 73.

34 G. Cerveau, E. Colomer, R.J.P. Corriu, J.C. Young, *J. Organomet. Chem.*, 1981, **205**, 31.

35 D.J. Patmore, W.A.G. Graham, *Inorg. Chem.*, 1967, **6**, 981.

36 E.O. Fischer, F.R. Kreissl, E. Winkler, C.G. Kreiter, *Chem. Ber.*, 1972, **105**, 588.

37 F.R. Kreissl, *Ph.D Dissertation*, Technischen Universität München, 1972.

38 M.F. Lappert, P.L. Pye, *J. Chem. Soc., Dalton Trans.*, 1977, 2172.

39 A.W. Coleman, P.B. Hitchcock, M.F. Lappert, R.K. Maskell, J.H. Müller, *J. Organomet. Chem.*, 1983, **250**, C9.

40 A.W. Coleman, P.B. Hitchcock, M.F. Lappert, R.K. Maskell, J.H. Müller, *J. Organomet. Chem.*, 1985, **296**, 173.

41 D.W. Macomber, R.D. Rodgers, *Organometallics*, 1985, **4**, 1485.

42 W.A. Herrmann, *Chem. Ber.*, 1978, **111**, 1077.

43 W.A. Herrmann, I. Steff, M.L. Ziegler, K. Weidenhammer, *Chem. Ber.*, 1979, **112**, 1731.

44 G. Erker, R. Lecht, J.L. Petersen, H. Bönnemann, *Organometallics*, 1987, **6**, 1962.

45 J. Foerstner, A. Kakoschke, R. Goddard, J. Rust, R. Wartchow, H. Butenschön, *J. Organomet. Chem.*, 2001, **617-618**, 412.

46 D. Bourissou, O. Guerret, F.P. Gabbaï, G. Bertrand, *Chem. Rev.*, 2000, **100**, 39.

47 T. Weskamp, V.P.W. Böhm, W.A. Herrmann, *J. Organomet. Chem.*, 2000, **600**, 12.

48 K. Öfele, *J. Organomet. Chem.*, 1968, **12**, P42.

49 H.-W. Wanzlick, H.-J. Schönherr, *Angew. Chem., Int. Ed. Engl.*, 1968, **7**, 141.

50 Y.T. Vigranenko, *Kinet. Cat.*, 1999, **40**, 86.

51 K. Öfele, W.A. Herrmann, D. Mihalios, M. Elison, E. Herdtweck, W. Scherer, J. Mink, *J. Organomet. Chem.*, 1993, **459**, 177.

52 W.A. Herrmann, K. Öfele, M. Elison, F.E. Kuhn, P.W. Roesky, *J. Organomet. Chem.*, 1994, **480**, C7.

53 W.A. Herrmann, O. Runte, G.R.J. Artus, *J. Organomet. Chem.*, 1995, **501**, C1.

54 W.A. Herrmann, L.J. Goossen, C. Köcher, G.R.J. Artus, *Angew. Chem., Int. Ed. Engl.*, 1996, **35**, 2805.

55 T. Weskamp, W.C. Schattenmann, M. Spiegler, W.A. Herrmann, *Angew. Chem., Int. Ed. Engl.*, 1998, **110**, 2490.

56 W.A. Herrmann, J. Fischer, K. Öfele, G.R.J. Artus, *J. Organomet. Chem.*, 1997, **530**, 259.

57 K. Öfele, W.A. Herrmann, D. Mihalios, M. Elison, E. Herdtweck, E. Scherer, J. Mink, *J. Organomet. Chem.*, 1993, **459**, 177.

58 M. Regitz, *Angew. Chem., Int. Ed. Engl.*, 1996, **35**, 725.

59 W.A. Herrmann, C. Köcher, L.J. Goossen, G.R.J. Artus, *Chem. Eur. J.*, 1996, **2**, 1627.

60 W.A. Herrmann, L.J. Goossen, C. Köcher, G.R.J. Artus, *Angew. Chem., Int. Ed. Engl.*, 1996, **35**, 2805.

61 N. Kuhn, T. Kratz, R. Boese, D. Bläser, *J. Organomet. Chem.*, 1994, **470**, C8.

62 A.R. Manning, *J. Chem. Soc. (A)*, 1968, 1135.

63 K.W. Kramarz, R.J. Klinger, D.E. Fremgen, J.W. Rathke, *Cat. Today*, 1999, **49**, 339.

64 G.W. Parshall, S.D. Ittel, in *Homogeneous Catalysis*, *Second Edition*, John Wiley & Sons, Inc., New York, 1992, p. 107.

65 A. Neveling, H.G. Raubenheimer, D. Billing, S. Cronje, *Polyhedron*, 2001, **20**, 1089.

66 H.G. Raubenheimer, F. Scott, S. Cronje, P.H. van Rooyen, K. Psotta, *J. Chem. Soc., Dalton. Trans.*, 1992, 1009.

67 J.G. Toerien, M. Desmet, G.J. Kruger, H.G. Raubenheimer, *J. Organomet. Chem.*, 1994, **479**, C12.

68 H.G. Raubenhiemer, M. Desmet, P. Olivier, G.J. Kruger, *J. Chem. Soc., Dalton Trans.*, 1996, 4431.

69 H.G. Raubenheimer, M. Desmet, *J. Chem. Research (S)*, 1995, 30.

70 H.G. Raubenheimer, L. Lindeque, S. Cronje, *J. Organomet. Chem.*, 1996, **511**, 177.

71 C. Zucchi, G. Pályi, V. Galamb, E. Sámpár-Szerencsés, L. Márko, P. Li, H. Alper, *Organometallics*, 1996, **15**, 3222.

72 C. Zucchi, A. Cornia, R. Boese, E. Kleinpeter, H. Alper, G. Pályi, *J. Organomet. Chem.*, 1999, **586**, 61.

73 I. Omae, *Chem. Rev.*, 1979, **79**, 287.

74 R.F. Heck, *Adv. Organomet. Chem.*, 1966, **4**, 243.

75 R.B. King, *Adv. Organomet. Chem.*, 1964, **2**, 157.

76 R.F. Heck. *J. Am. Chem. Soc.*, 1963, **85**, 1220.

77 R.F. Heck, D.S. Breslow, *J. Am. Chem. Soc.*, 1962, **84**, 2499.

78 W. Hieber, E. Lindner, *Chem. Ber.*, 1962, **95**, 273.

79 N. Kuhn, T. Kratz, *Synthesis*, 1993, 561.

80 R.W. Alder, P.R. Allen, M. Murray, A.G. Orpen, *Angew. Chem., Int. Ed. Engl.*, 1996, **35**, 1121.

81 W.F. Edgell, J. Lyford, *Inorg. Chem.*, 1970, **9**, 1932.

82 M.Bressan, B. Corain, P. Rigo, A. Turco, *Inorg. Chem.*, 1970, **9**, 1733.

83 F.A. Cotton, O.D. Faut, D.M.L. Goodgame, R.H. Holm, *J. Am. Chem. Soc.*, 1961, **83**, 1780.

84 M.M. Brezinski, K.J. Klabunde, B.B. Anderson, in *Synthetic Methods of Organometallic and Inorganic Chemistry*, Ed. W.A. Herrmann, Georg Thieme Verlag Stuttgart, 1997, Vol. 8, p. 205.

85 R.F. Heck, *J. Am. Chem. Soc.*, 1964, **86**, 5138.

86 H.W. Sternberg, I. Wender, R.A. Friedel, M. Orchin, *J. Am. Chem. Soc.*, 1953, **75**, 2717.

87 G. Mestroni, A. Camus, E. Mestroni, *J. Organomet. Chem.*, 1970, **24**, 775.

88 J.M. Whitfield, S.F. Watkins, G.B. Tupper, W.H. Baddley, *J. Chem. Soc., Dalton Trans.*, 1977, 407.

89 M.R. Caira, L.R. Nassimbeni, *Acta. Cryst.*, 1974, **B30** ,2332.

90 P. Pérez-Lourido, J. Romero, J.A. García-Vázquez, A. Sousa, J. Zubieta, K. Maresca, *Polyhedron*, 1998, **17**, 4457.

91 S.J. Chadwell, S.J. Coles, P.G. Edwards, M.B. Hurthouse, *J. Chem. Soc., Dalton Trans.*, 1995, 3551.

92 M.-T. Youinou, R. Ziessel, J.-M. Lehn, *Inorg. Chem.*, 1991, **30**, 2144.

93 D.C. Moody, R.R. Ryan, *Cryst. Struct. Comm.*, 1981, **10**, 129.